BACTERIAL CHONDRONECROSIS AND OSTEOMYELITIS IN BROILER CHICKENS: DEVELOPMENT OF EXPERIMENTAL MODELS AND ANALYSIS OF DISEASE MECHANISMS

by

VENKATA SESHA REDDY CHOPPA

(Under the Direction of Woo Kyun Kim)

ABSTRACT

Bacterial Chondronecrosis and Osteomyelitis (BCO) is a leading cause of lameness in modern broiler chickens, imposing substantial welfare and economic concerns on the poultry industry. The pathophysiological mechanisms behind BCO and experimental models of the disease remain poorly defined. This thesis systematically investigates the multifactorial etiology of BCO besides highlighting pathogen-induced osteoimmune dysregulation, gut-bone axis, and possible mitigation strategies. To elucidate the roles of *Staphylococcus aureus* and lipopolysaccharides (LPS) in induction and progression of BCO, a series of in vivo and in vitro studies were conducted. Invitro and embryonic models using LPS exposure revealing disruption of osteogenic differentiation in chicken mesenchymal stem cells (MSCs). Furthermore, MSCs and macrophage -mediated osteoimmune signaling involving nuclear factor kappa B (NF-κB), tumor necrosis factor alpha (TNF-α), sclerostin (SOST) regulatory pathways which provides mechanistic insights into osteopathology. Moreover, in vivo studies were conducted to elucidate experimental challenge

models using both oral and intraperitoneal challenge with *S. aureus*. Findings revealed characteristic BCO lesions, disrupted bone mineralization, and increases trabecular parameters, confirmed with dual-energy X-ray absorptiometry (DEXA), micro-computed tomography (micro-CT), dynamic histomorphometry. Co-challenge with *Eimeria* spp. revealed intestinal barrier dysfunction and systemic endotoxemia represented by elevated plasma LPS concentrations. These findings were accompanied by gut microbiome changes and altered functional pathways related to inflammation and bone metabolism, providing the evidence on gut-bone axis in BCO pathogenesis. Additionally, dietary supplementation of curcumin demonstrated a positive role in mitigating *S. aureus* induced BCO reflected as improved bone microarchitecture, decreased bacterial colonization, and modulating systemic inflammatory responses besides preserving growth performance. The findings presented in this thesis establish reproducible experimental models for BCO, decipher the molecular and pathophysiological mechanisms, and mitigation strategy like dietary curcumin for alleviating BCO-associated lameness. These results contribute to the advancement of integrative approach for maintain skeletal integrity and welfare in commercial broiler production.

INDEX WORDS: broiler chickens, bacterial chondronecrosis and osteomyelitis, *Staphylococcus aureus*, lipopolysaccharides, *Eimeria* spp., gut-bone axis, osteoimmunology, curcumin, bone health

BACTERIAL CHONDRONECROSIS AND OSTEOMYELITIS IN BROILER CHICKENS: DEVELOPMENT OF EXPERIMENTAL MODELS AND ANALYSIS OF DISEASE MECHANISMS

by

VENKATA SESHA REDDY CHOPPA

B.V.Sc and A.H. (equivalent to DVM), Sri Venkateswara Veterinary University, India, 2019

A Dissertation Submitted to the Graduate Faculty of The University of Georgia in Partial Fulfillment of the Requirements for the Degree

DOCTOR OF PHILOSOPHY

ATHENS, GEORGIA

2025

BACTERIAL CHONDRONECROSIS AND OSTEOMYELITIS IN BROILER CHICKENS: DEVELOPMENT OF EXPERIMENTAL MODELS AND ANALYSIS OF DISEASE MECHANISMS

by

VENKATA SESHA REDDY CHOPPA

Major Professor: Woo Kyun Kim

Committee: Hector M. Cervantes

Charles L. Hofacre

Chongxiao Chen

Electronic Version Approved:

Ron Walcott

Vice Provost for Graduate Education and Dean of the Graduate School

The University of Georgia

December 2025

DEDICATION

I dedicate this thesis to my beloved parents, late Ramana Reddy and Venkata Subbamma, whose love and values have been my guiding light. I also wish to extend this dedication to my dear wife, Sujitha Bhumanapalli and my sisters, Dr. Vijaya Nirmala and Pallavi, for their unconditional love, sacrifice, support, and encouragement, without which this achievement would not have been possible. I would also like to express my heartfelt gratitude to my brothers-in-law, Dr. Vijay Kumar Reddy and Aravinda Reddy for their continuous support and motivation throughout this journey.

ACKNOWLEDGEMENTS

I would like to express my deepest gratitude to my major professor, **Dr. Woo Kyun Kim**, for his exceptional mentorship, patience, trust, and unwavering guidance throughout my Ph.D. journey. His trust, encouragement, and insights has shaped not only my academic and professional growth but also my approach to research and problem-solving ability. I am deeply indebted to Dr. Kim for his constant support to pursue excellence in every endeavor during this program. My heartful appreciation also goes to my advisory committee members- **Dr. Hector M. Cervantes**, **Dr. Charles L. Hofacre**, **Dr. Chongxiao Chen** for their invaluable advice, constructive feedback, and generosity in sharing their expertise. Intellectual contributions have greatly enriched the quality and depth of this work.

My heartfelt thanks are also due to everyone at the Department of Poultry Science and Poultry Research Center at the University of Georgia, who mentored, supported, and encouraged for my growth as a researcher. I am truly fortunate for having such a supportive group of people. I extend my deepest appreciation of your friendship, generosity, and tireless assistance both at lab and on the farm to my lab mates- **Milan, Guanchen, Coco, Brett, JC, Hanyi, Jinquan, Sudhir, Seshi, Hamid, Hemanth, Sai Kumar, Prathap, Doyun, Hanseo, Deependra, Fatemeh, Ishwari, Indira, and Jonah.**

I am profoundly grateful to my extended family (I would say God-gifted)- **Hemanth, Prathap, Akhila, Murali, Himanshu, Laharika, Seshi, Brunda, Manoj, Arjun, Umesh, Sai, Sujitha, Bharath, Bhargavi, Praveen, Rishitha, Tharun, Mohan, Ramadevi, Satwik, Nikitha, Surendra, Venkatesh, and Vamsi**- who made my Ph.D. journey the most memorable besides

providing constant encouragement in every obstacle and made this achievement possible. This accomplishment stands as a testament to your unwavering faith, and I dedicate it to everyone with all my heart.

TABLE OF CONTENTS

LIST OF TABLES

LIST OF FIGURES

CHAPTER 1

INTRODUCTION

Bacterial chondronecrosis and osteomyelitis (BCO) has emerged as a major cause of lameness and welfare concern in modern poultry production. Intensive genetic selection made broilers prone to subclinical bone microfractures due to outpaced rapid growth and high breast muscle yield compared to skeletal development (Wideman, 2016a; Choppa and Kim, 2023). Consequently, 30 % of broilers (approximately) in intensive systems show lameness or some skeletal disorder affecting hundreds of millions of birds (Szafraniec et al., 2020; Anthney et al., 2024). Furthermore, BCO alone accounts for roughly 17 % of lameness and 28 % of the flock culling in surveys of commercial flocks (Szafraniec et al., 2020). Surprisingly, annual losses from BCO through condemnations, mortality and under-performance are estimated to exceed 100 million USD (Anthney et al., 2024). These trends emphasize the economic and animal-welfare impact of BCO in fast-growing broilers and the need for uncovering the causes and mitigation strategies.

BCO is typically an opportunistic, multifactorial infection of the proximal femur which arises when bacteria colonize growth-plate microfractures. Among several opportunistic pathogens, *Staphylococcus aureus* is the most frequently isolated pathogen in BCO lesions and has ability to infiltrate bone since it can persist in quiescent small-colony variants and reactivate to induce osteomyelitis (Tuchscherr et al., 2011; Yang et al., 2018). *Enterococcus cecorum* and *Escherichia coli* are also isolated from BCO lesions, which reflects opportunistic nature of the disease (Wideman, 2016a). BCO in broilers occurs through hematogenous spread, where bacteria

originate from environment, respiratory or intestine which then translocate to rapidly growing bones from blood circulation (McNamee and Smyth, 2000; Wideman, 2016a). Immunosuppressive stressors like viral, bacterial or parasitic co infections or environmental stress exacerbate the above process by compromising host defenses (Mandal et al., 2020; Ferver - Ramser, 2020a). Once bacteria seed the highly vascular chondro-osseous junction of bone, they trigger osteonecrosis and an inflammatory cascade, with elevated cytokines, and inflammasome activity (Ramser et al., 2021; Choppa et al., 2023). Furthermore, compromised intestinal health is also recognized as a co-factor for BCO since intestinal damage caused by enteric pathogens and *Eimeria* spp. leads to break in barrier integrity. As a result of enterocyte injury and villus atrophy, luminal bacteria and endotoxins (lipopolysaccharides) can translocate into blood circulation (Nikaido and Vaara, 1985; Reisinger et al., 2020, 2024; Choi and Kim, 2022). Above findings strongly suggests gut-bone axis where coccidial enteritis and dysbiosis potentiate systemic inflammation which amplify the risk of opportunistic osteopathogens to induce and modulate the severity of BCO. Monitoring systemic markers of systemic inflammation and circulating endotoxin (LPS) serves as a key indicator of gut barrier dysfunction besides providing insight into BCO progression (Choppa and Kim, 2023; Perera et al., 2024). Cytokine storm originating from activation of nuclear factor kappa B (NF-κB) and mitogen activated protein kinase (MAPK) pathways favors osteoclastogenesis and suppress osteoblast differentiation (Huang et al., 2020; Zhou and Graves, 2022; Choppa et al., 2023). Concurrently, osteocytes respond to above triggers which upregulate sclerostin (SOST), a Wnt (Wingless integrated-1) inhibitory protein which blocks bone formation (Choppa and Kim, 2023; Dreyer et al., 2023). In challenged broilers, high SOST levels correlate with lower bone mineral density and increased trabecular porosity (Choppa et al., 2025).

Experimental models have been developed to mimic BCO pathogenesis like intravenous *S. aureus* injection to healthy birds and mechanical stress models, though each has limitations (Daum et al., 1990; Wideman Jr et al., 2012). Moreover, studies also used a combination of wire-flooring along with exposure of drinking water challenged with *S. aureus*, showed 50-80 % lameness (Al-Rubaye et al., 2017). These studies are hard to replicate in a commercial setting since the models rely on non-physiological routes. Recent studies on litter reared broilers exposed to repeated low-dose oral *S. aureus* challenge is better at inducing BCO compared to single exposure (Meroni et al., 2022). These studies confirmed that persistent bacteremia drives bone colonization, consistent with field conditions. Lacuna still remains to understand BCO since no model capture the complex interactions of intestinal health, bacterial challenge, and genetics (Choppa et al., 2025). This gap serves as motivation for development of integrated models which address the above limitations to better reproduce natural BCO pathogenesis.

To unravel BCO mechanisms, complementary models at various levels were employed. Invivo broiler challenges (oral or intraperitoneal *S. aureus*) with or without coccidia to reproduce host response and gross bone lesions. Furthermore, in ovo models exposed to LPS to study direct effects on ossification in the absence of confounding maternal factors. Moreover, invitro systems using primary mesenchymal stem cells and macrophages under osteogenic conditions to identify LPS dose-dependent mechanisms on bone formation. These integrated experimental models that couple microbial challenge, immune activation, and bone assessment provide a unified view on critical mechanisms behind BCO. Building on these insights and the limitations of existing models, this thesis develop and employ comprehensive experimental models linking intestinal challenge and systemic inflammation along with osteopathology and mitigation strategies.

REFERENCES

Al-Rubaye, A. A. K., N. S. Ekesi, S. Zaki, N. K. Emami, R. F. Wideman Jr, and D. D. Rhoads. 2017. Chondronecrosis with osteomyelitis in broilers: Further defining a bacterial challenge model using the wire flooring model. Poult Sci 96:332–340.

Anthney, A., A. D. T. Do, and A. A. K. Alrubaye. 2024. Bacterial chondronecrosis with osteomyelitis lameness in broiler chickens and its implications for welfare, meat safety, and quality: a review. Front Physiol 15:1452318.

Choi, J., and W. Kim. 2022. Interactions of microbiota and mucosal immunity in the ceca of broiler chickens infected with Eimeria tenella. Vaccines (Basel) 10:1941.

Choppa, V. S. R., and W. K. Kim. 2023. A Review on Pathophysiology, and Molecular Mechanisms of Bacterial Chondronecrosis and Osteomyelitis in Commercial Broilers. Biomolecules 13:1032.

Choppa, V. S. R., G. Liu, H. Shi, M. K. Sharma, D. Goo, and W. K. Kim. 2025. Effect of lipopolysaccharides and mixed Eimeria spp. challenge on performance and bone development in broilers. Poult Sci:105501.

Choppa, V. S. R., G. Liu, Y. H. Tompkins, and W. K. Kim. 2023. Altered Osteogenic Differentiation in Mesenchymal Stem Cells Isolated from Compact Bone of Chicken Treated with Varying Doses of Lipopolysaccharides. Biomolecules 13:1626.

Daum, R. S., W. H. Davis, K. B. Farris, R. J. Campeau, D. M. Mulvihill, and S. M. Shane. 1990. A model of Staphylococcus aureus bacteremia, septic arthritis, and osteomyelitis in chickens. Journal of orthopaedic research 8:804–813.

Dreyer, T. J., J. A. C. Keen, L. M. Wells, and S. J. Roberts. 2023. Novel insights on the effect of sclerostin on bone and other organs. Journal of Endocrinology 257.

Ferver - Ramser, A. 2020. Bacterial chondronecrosis with osteomyelitis (BCO) in modern broilers: Impacts, mechanisms, and perspectives. CAB Reviews: Perspectives in Agriculture, Veterinary Science, Nutrition and Natural Resources 15.

Huang, X., M. Xie, Y. Xie, F. Mei, X. Lu, X. Li, and L. Chen. 2020. The roles of osteocytes in alveolar bone destruction in periodontitis. J Transl Med 18:479.

Mandal, R. K., T. Jiang, R. F. Wideman, T. Lohrmann, and Y. M. Kwon. 2020. Microbiota Analysis of Chickens Raised Under Stressed Conditions . Frontiers in Veterinary Science 7:696 Available at https://www.frontiersin.org/article/10.3389/fvets.2020.482637.

McNamee, P. T., and J. A. Smyth. 2000. Bacterial chondronecrosis with osteomyelitis ('femoral head necrosis') of broiler chickens: A review. Avian Pathology 29:253–270 Available at https://doi.org/10.1080/03079450050118386.

Meroni, G., A. Tsikopoulos, K. Tsikopoulos, F. Allemanno, P. A. Martino, and J. F. Soares Filipe. 2022. A journey into animal models of human osteomyelitis: a review. Microorganisms 10:1135.

Nikaido, H., and M. Vaara. 1985. Molecular basis of bacterial outer membrane permeability. Microbiol Rev 49:1–32.

Perera, R., K. Alharbi, A. Hasan, A. Asnayanti, A. Do, A. Shwani, R. Murugesan, S. Ramirez, M. Kidd, and A. A. K. Alrubaye. 2024. Evaluating the Impact of the PoultryStar® Bro Probiotic on the Incidence of Bacterial Chondronecrosis with Osteomyelitis Using the Aerosol Transmission Challenge Model. Microorganisms 12:1630.

Ramser, A., E. Greene, R. Wideman, and S. Dridi. 2021. Local and systemic cytokine, chemokine, and FGF profile in bacterial chondronecrosis with osteomyelitis (BCO)-Affected broilers. Cells 10:3174.

Reisinger, N., B. Doupovec, T. Czabany, F. Van Immerseel, S. Croubels, and G. Antonissen. 2024. Endotoxin Translocation Is Increased in Broiler Chickens Fed a Fusarium Mycotoxin-Contaminated Diet. Toxins (Basel) 16:167.

Reisinger, N., C. Emsenhuber, B. Doupovec, E. Mayer, G. Schatzmayr, V. Nagl, and B. Grenier. 2020. Endotoxin translocation and gut inflammation are increased in broiler chickens receiving an oral lipopolysaccharide (LPS) bolus during heat stress. Toxins (Basel) 12:622.

Szafraniec, G. M., P. Szeleszczuk, and B. Dolka. 2020. A review of current knowledge on Staphylococcus agnetis in poultry. Animals 10:1421.

Tuchscherr, L., E. Medina, M. Hussain, W. Völker, V. Heitmann, S. Niemann, D. Holzinger, J. Roth, R. A. Proctor, and K. Becker. 2011. Staphylococcus aureus phenotype switching: an effective bacterial strategy to escape host immune response and establish a chronic infection. EMBO Mol Med 3:129–141.

Wideman, R. F. 2016. Bacterial chondronecrosis with osteomyelitis and lameness in broilers: a review. Poult Sci 95:325–344 Available at https://www.sciencedirect.com/science/article/pii/S0032579119321534.

Wideman Jr, R. F., K. R. Hamal, J. M. Stark, J. Blankenship, H. Lester, K. N. Mitchell, G. Lorenzoni, and I. Pevzner. 2012. A wire-flooring model for inducing lameness in broilers: evaluation of probiotics as a prophylactic treatment. Poult Sci 91:870–883.

Yang, D., A. R. Wijenayaka, L. B. Solomon, S. M. Pederson, D. M. Findlay, S. P. Kidd, and G. J. Atkins. 2018. Novel insights into Staphylococcus aureus deep bone infections: the involvement of osteocytes. mBio 9:10–1128.

Zhou, M., and D. T. Graves. 2022. Impact of the host response and osteoblast lineage cells on periodontal disease. Front Immunol 13:998244.

CHAPTER 2

LITERATURE REVIEW: A REVIEW ON PATHOPHYSIOLOGY, AND MOLECULAR MECHANISMS OF BACTERIAL CHONDRONECROSIS AND OSTEOMYELITIS IN COMMERCIAL BROILERS [1]

[1] Choppa, V. S. R., & Kim, W. K. (2023). Biomolecules, 13(7), 1032.

INTRODUCTION

An active tissue that experiences continual remodeling is the bone. Any changes in its regular turnover may lead to skeletal diseases characterized by bone loss (D'Amelio & Sassi, 2016). During the past few decades, commercial poultry production has increased dramatically in terms of feed efficiency and growth rate; however, this pattern has also shown some adverse implications such as Fatty-liver syndrome, pulmonary hypertension and skeletal problems (Cook, 2000; Havenstein et al., 2003; Julian, 2005; Packialakshmi et al., 2015). Furthermore, modern broilers are having the genetic potential to achieve higher body weights with high metabolic demands. This makes them prone to skeletal damage followed by opportunistic bacterial infection and later with Bacterial chondronecrosis and Osteomyelitis (BCO). The physiology of the bone and its turnover process is complex involving several pathways working coherently (Ferver & Dridi, 2020). A common skeletal disease condition that affects broilers worldwide is lameness and is associated with the factors including genetic traits, infectious agents, the center of gravity of the bird, body conformation, activity and nutrition (Bradshaw et al., 2002; Knowles et al., 2008; Rojas-Núñez et al., 2020). Important factors that contribute to lameness has been reviewed in Figure 1 (Kierończyk et al., 2017). Besides, the rate of culling at farm level due to lameness is 0.5% to 4 % which in turn reflects on the losses of approximately $100 million per year in United States alone (Perpetua T McNamee & Smyth, 2000; Rojas-Núñez et al., 2020). Moreover, BCO is considered as a common cause of lameness in Australia, Canada, Europe and the US (Bradshaw et al., 2002; Dinev, 2009; Jiang, Mandal, Wideman, et al., 2015; P T McNamee et al., 1998; Pattison, 1992). Additionally, BCO in broiler production would impact the poultry revenue through the culling and condemnation rates along with a lowered livability since the production is usually expressed as production costs, net profit per pound of a bird (Gocsik et al., 2017; Nääs et al., 2009). The above

impact would be considerably contributed by the incidence of lame birds in the farm, which causes higher feed conversion, lower weight gain, and higher condemnation rates in processing plant (Gocsik et al., 2017). The current review pivots on BCO which is the most common cause of leg disorders which raised concerns on animal welfare and economic losses.

INFLAMMATION AND BCO

BCO is commonly observed in femurs, tibia, and thoracic vertebrae (Perpetua T McNamee & Smyth, 2000; R. F. Wideman, 2016a). This occurs majorly due to formation of microfractures and clefts because of rapid growth of juvenile bones. Also, this is often associated with rapid increases in body weight leading to focal ischemia providing a convenient breeding ground for bacterial colonization (R. F. Wideman, 2016a; R. Wideman & Prisby, 2013). Post infection or injury, acute phase response (APR) is a key sequela affecting the nutrient requirements and metabolism and is usually initiated by local inflammatory response (Kirk C Klasing, 1998). The above response can be measured by observing the changes in acute phase proteins and cytokine profiles where the excessive levels indicates decreasing production traits and rise in pathology (Baumann & Gauldie, 1994; Kirk C Klasing, 1998; Koj, 1989; Kushner & Rzewnicki, 1994; Mireles et al., 2005). Cytokines (IL-1,6 and tumor necrosis factor) released as a result of APR hasten bone resorption (Mireles et al., 2005; Rath et al., 2000; Roux & Orcel, 2000) as well as muscle breakdown (Kirk C Klasing & Johnstone, 1991). A study involving the injection of lipopolysaccharide (LPS) to the birds has shown a severe disruption in bone homeostasis, production parameters including livability, bodyweight, and feed conversion (Mireles et al., 2005). This usually occurs due to macrophages and osteoclast like cells responding to LPS by release of cytokines and nitric oxide (Wiggers et al., 2011). Moreover, a study on RAW 264.7 cells in vitro

were not able to differentiate into mature osteoclasts in the presence of LPS. RANKL or LPS treated cells increased toll like receptor 4 (TLR4) levels in membrane (AlQranei et al., 2021). A TLR4 inhibitor, TAK-242 (resatorvid) reduced the osteoclast number as well as tumor necrosis factor (TNF)-α in LPS treated cells. In contrast, RANKL- induced cells were not affected by TAK-242 and secreted basal levels of TNF- α . This clearly shows that LPS associated bone resorption is associated with LPS/TLR4/ tumor necrosis factor receptor (TNFR)-2 axis but not with RANKL/RANK/OPG axis (AlQranei et al., 2021). Furthermore, osteoclasts and their activities are regulated by osteoblasts which in turn are altered by the bacteria and their products by means of apoptosis which occurs by activation of intrinsic and extrinsic cell death pathways leading to disruption in bone homeostasis (Marriott, 2013) **(Figure 2.1)**.

PATHOGENS AND BCO

Staphylococcus aureus is the most commonly reported organism found in BCO epiphyseal lesion, but septicemic pathogens like *Staphylococcus hyicus*, *S xylosus*, *S simulans*, *Mycocaterium avium*, *Salmonella* spp., *E. coli* and *Enterococcus* were also isolated (Dinev, 2009; Perpetua T McNamee & Smyth, 2000; Reece, 1992; Wijesurendra et al., 2017). Histological changes in epiphyseal region of growth plate due to BCO lead to transection of the capillaries and blood vessels within the highly vascularized epiphyseal region, which paves the way for decreased blood flow to the areas around that region(R. F. Wideman, 2016a). Furthermore, this allows the circulating bacteria to enter and proliferate, along with immunological response leading to tissue damage (Necrotic abscesses and voids) (Jiang, Mandal, Wideman, et al., 2015; Wideman Jr et al., 2012; R. F. Wideman, 2016a; R. Wideman & Prisby, 2013). Physiological stress also aids in heightened entry of opportunistic pathogens through the epithelial tight junctions, and the

pathogens finally arrive at osteochondrotic micro-fractures and clefts (Jiang, Mandal, Wideman, et al., 2015). BCO is also observed in clinically non-lame birds at higher incidences, but there are notable pathognomic lesions as seen in lame birds with BCO (Jiang, Mandal, Wideman, et al., 2015; Wideman Jr et al., 2012). Bacterial translocation through the damaged epithelium is reported to be one of the causes for higher incidence of BCO(Rojas-Núñez et al., 2020). In addition, young intestines have higher susceptibility to bacterial leakage than fully developed intestines in the presence of mucosal damage (Rojas-Núñez et al., 2020; Wideman Jr et al., 2012). Furthermore, Chicken anemia virus and Infectious bursal disease virus make the birds more prone to BCO as a result of immunosuppression (Perpetua T McNamee et al., 1999; Perpetua T McNamee & Smyth, 2000). An understanding of bacterial diversity, 3D structural alterations in bone and cartilage, bone remodeling marker gene expression, and omega 3 fatty acid and/or probiotic supplementation in BCO is being less focused topic till date, and this needs to be rationalized to identify precise etiology and treatment. Also, there is a limited information on extra intestinal bacteria which may induce the APR followed by BCO. In a study involving Linear discriminant analysis Effect Size (LEfSe) analysis showed that physiological stress will allow commensal and pathogenic bacteria to enter extra intestinal sites, indicating the need for exploring the novel taxa (Mandal et al., 2020; Segata et al., 2011). These extra intestinal sites would be circulating maternal blood microbiota in chick or In ovo colonies of microbes (Mandal et al., 2020). Apart from microbiota, some managemental practices like light intensity, drinking water, flooring may also affect the incidence of BCO (Alrubaye et al., 2020). Light intensity is directly related to the bird movement and activity which may affect the incidence of BCO (Alvino et al., 2009; Deep et al., 2012; Newberry et al., 1988; Rault et al., 2017), and a study showed that detecting surface temperatures of broiler leg regions with the help of non-invasive methods would also help in detecting lesions of BCO

(Weimer et al., 2019). In two different studies, provision of 25-OH vitamin D3, prophylactic administration of probiotics were reported to abate the incidence of BCO in wire flooring model which had been attributed to trigger the lameness in broilers (Wideman Jr et al., 2012, 2015) **(Figure 2.2, 2.3)**.

UNDERLYING ANATOMY AND PHYSIOLOGY BEHIND BCO AND ITS POTENTIAL BIOMARKERS

BCO and other bone problems usually occurs in the birds with higher growth rate and body gain which may be related to different breeds of commercial poultry (Kestin et al., 1992, 1999). Mostly the body gain is attributed to pectoral muscles resulting in a shift in center of gravity with a disproportionate development of femur, which makes them more prone to BCO (Applegate & Lilburn, 2002; Corr et al., 2003; Paxton et al., 2010, 2013; Tickle et al., 2014). Integrity of articular cartilage (AC) and growth plate cartilages are crucial because the disproportionate development of legs to the body predisposes to injury under strenuous conditions. These cartilages greatly differ in their histology and extracellular matrices. AC is made of mostly all collagens except type X collagen and proteoglycans with chondrocytes (Aspden & Hukins, 1981; Sophia Fox et al., 2009). Type X collagen appears in the growth plate usually when it undergoes endochondral ossification process which is assisted by adhesion molecules like cadherins and integrins, essential for regulating canonical signaling in Wnt pathway which is activated upon binding of Wnt ligands to LRP-5/6 co receptors and this can be inhibited when these receptors are bound to Wnt antagonists like sclerostin and Dkk -1 (Dickkopf proteins) (Houschyar et al., 2019; Kwan et al., 1989; Mackie et al., 2008). Among these adhesion molecules, cadherins mediate homotypic adhesion between bone cells, and integrins mediate adhesion between bone cells and its extracellular matrix (Mui et al., 2016). Usually, long bones will develop by endochondral ossification where mesenchymal

stem cells forms chondrogenic template through chondrogenic differentiation followed by hypertrophic differentiation resulting in blood supply and remodeling of chondrogenic template into bone through the release of angiogenic factors (Kronenberg, 2003). Furthermore, the gradient increase in oxygen levels is also important in modulating the endochondral ossification where chondrogenic differentiation takes place at low levels of oxygen and hypertrophic differentiation at higher levels of oxygen tension (Ma et al., 2009; Sheehy et al., 2019). The proximal tibial center is the only true secondary ossification center in the long bones of fowl during the rapid growth phase, leading to a reduced reinforcement of AC (Breugelmans et al., 2007; Hogg, 1980). Although there is no conclusive evidence, ischemia is presumed to be the cause of lowered blood supply, leading to poor reinforcement of AC (R. Wideman & Prisby, 2013) **(Figure 2.4)**.

Osteochondrotic crypts are developed from poor mineralization of chondrocytes, resulting in microfractures that allow the opportunistic bacteria to colonize in those crypts through hematogenous routes (Al-Rubaye et al., n.d.; Jiang, Mandal, Wideman Jr, et al., 2015; Mandal et al., 2016; Petry et al., 2018; Weimer et al., 2020; R. F. Wideman, 2016a; R. Wideman & Prisby, 2013). These bacteria may originated from broiler breeders, hatchery contamination, gastrointestinal tract, respiratory system, or integumentary system (Stalker et al., 2010; R. F. Wideman, 2016b; R. Wideman & Prisby, 2013). In an experimentally induced and spontaneous occurring study on BCO in broilers, dyslipidemia was reported to be a common feature (VIJAY Durairaj et al., 2009). Moreover, thrombospondin, interferon γ, and transforming growth factor-ß, and angiogenesis inhibitors was suggested to be the risk of avascular necrosis (El-Jawhari et al., 2021; H.W., 1954). In young chickens, arrest of angiogenesis and growth plate development due to reduction in plasma levels of vascular endothelial growth factor isoform-C and protochaderin-15 (adhesion molecule) occurs in glucocorticoid induced BCO, leading to apoptosis of

chondrocytes(Kerachian et al., 2009; Packialakshmi et al., 2015). Furthermore, reduced levels of fibroblast growth factor-2 and runt related transcription factor-2 (RUNX2) which are regulators of apoptosis and chondrocyte maturation, respectively, were suggestive of promoting BCO (P. F. Li et al., 2015; Paludo et al., 2014). In some studies, serum metabolites like lipids, lipoproteins, and apolipoprotein derived peptides have shown changes when chickens were induced with glucocorticoids and naturally occurring BCO (V Durairaj et al., 2012; VIJAY Durairaj et al., 2009; Packialakshmi et al., 2015). On the other hand, the use of these biomarkers for BCO needs further validation because they were significant in vascular diseases and osteoarthritis (Di Angelantonio et al., 2009; Fandridis et al., 2011).

An experimental model of chicken BCO for human osteomyelitis has identified a novel pathophysiological mechanism for this severe inflammatory condition which is described below (Greene et al., 2019). DICER1 (a highly conserved RNaseIII endoribonuclease), a multifaceted protein which is responsible for dsRNA cleavage and its dysregulation had been recognized in several human diseases and reported to have a critical role in osteogenesis (Bendre et al., 2018; J.-F. Chen et al., 2008; Hata & Kashima, 2016; Liu et al., 2016; Zheng et al., 2017; Zhou et al., 2016). DICER1 dysregulation alters cortical bone integrity and homeostasis which are usually associated with RUNX2 (Paludo et al., 2015). DICER1 dysregulation and infection exposure leads to increase in dsRNA levels (Greene et al., 2019). A study shows DICER1 dysregulation due to bacterial infection might induce dsRNA accumulation which in turn is related to IL-1β pathway which plays a key role in pathogenesis of human bone inflammation. DICER1 dysmetabolism acts as an upstream regulator of NACHT (Nucleotide-binding domain, LRR (Leucine-rich repeat) and PYD (Pyrin domain) domains containing protein (NLRP)3 inflammasome, upon activation of NLRP3 paves the way for break in bone homeostasis through the increased activity of neutrophils,

monocytes, macrophages, osteoblasts, and osteoclasts (Behera et al., 2022; Gurung et al., 2016; Y. Li et al., 2021; McCall et al., 2008; Sharma & Kanneganti, 2016). Although there is a potential positive impact from inflammasome activation through reduction of bacterial proliferation and removal of pathogen a from host, this decreases the osteoblastic activity. Additionally, NLRP3 levels tend to be higher in bone tissue affected by a pathogen than the one with fractures indicating that this inflammasome activation contributing to inflammatory bone loss(Greene et al., 2019; Y. Li et al., 2021)(**Figure 2.5**). MtDNA mutations are one form of mitochondrial dysfunction associated with alterations in mitochondrial biology(Exner et al., 2012; Tiku et al., 2020). This is usually associated with Alzheimer's disease, dementia, coronary heart disease, chronic fatigue syndrome, and ataxia (Exner et al., 2012; Genestier et al., 2005; López-Armada et al., 2013; Maassen, 2004; Pieczenik & Neustadt, 2007; Sivitz & Yorek, 2010; Tiku et al., 2020). This association with several diseases is due to the relation between its dysfunction to apoptotic and inflammatory pathways. Mitochondria are direct targets for some bacterial infections like *Staphylococcus aureus* (Genestier et al., 2005; Haden et al., 2007).

Peroxisome proliferator activated receptor coactivator-1 (PGC-1α and PGC-1β) targets transcription factors (transcription factor A mitochondrial) and gene expression in mitochondrial biogenesis pathways (Ventura-Clapier et al., 2008). Precisely, any changes in metabolism or cell growth will modulate the expression and upregulation of PGC-1α, leading to an increased mitochondrial biogenesis and respiration in inflammatory states (Cherry & Piantadosi, 2015; Hock & Kralli, 2009). Both mitochondrial biogenesis associated genes (PGC-1α and PGC-1β) are significantly upregulated in BCO affected tissue. In addition, the inflammatory response, associated reactive oxygen species accumulation, and metabolic shifts cause an increased need for mitochondria. On the other hand, during stress, mitochondrial fusion occurs, leading to formation

of a large network, and this is associated with an important components such as OPA1 (Mitochondrial Dynamin like GTPase) and Mitofusins (MFN1 and 2) (H. Chen et al., 2005; Cipolat et al., 2004). In ascites, OPA1 expression is decreased in the susceptible lines but not in ascites resistant selected line (Al-Zahrani et al., 2019). In contrast, BCO has shown a significant decrease in OPA1 but an upregulated MFN2(Ferver et al., 2021). The decrease in the former is coupled with a gradual increase in OMA1 that is a regulator of mitochondrial fission via cutting OPA1 at some sites and making it inactive. At high levels of cellular stress, fission causes removal of damaged mitochondria when complementation through fusion is not possible. The above shift from fusion to fission indicates mitochondrial turn-over in accordance to the high level of stress during BCO (Ferver et al., 2021). Besides, other potential and widely studied biomarkers are shown in **table 2.1**.

INFLUENCES OF GUT MICROBIOTA AND IMMUNE SYSTEM IN BCO

The commensal bacteria of the intestine that are acquired at perinatal stage are termed as gut microbiota (Diaz Carrasco et al., 2019). These bacteria composition will get stabilized by some period of time after birth; however it varies from individual to individual through their diet, antibiotics and infections (D'Amelio & Sassi, 2016). This symbiotic relationship with the host helps in offering many antigens for the immune system. Dysbiosis in the gastrointestinal tract will lead to weakened immune system, making the host prone several diseases (D'Amelio & Sassi, 2016). In addition, gut microbial niche plays a pivotal role in pathogenesis of several diseases (Peterson et al., 2015). A study on mice grown in germ free environment shown a sterile gut and unfledged gut mucosal immune system and that there is a reduction in T helper cells in spleen and peripheral blood, suggesting gut microbiota influence on systemic immunity development (Peterson et al., 2015). Furthermore, mice have been protected from ovariectomy induced bone

loss. In these animals, bone mass and density are more with decreased bone resorption and regular bone formation(Sjögren et al., 2012). This could be due to lesser number of T cells, Proinflammatory, and pro-osteoclastogenic cytokines such as Interleukin 6 (IL6) and Tumor necrosis factor α (TNFα) (Sjögren et al., 2012). Probiotic and prebiotic supplementation can enhance bone formation by upregulating SPARC (Osteonectin) and BMP-2 (Bome morphogenetic protein 2) genes involved in osteoblast formation(Parvaneh et al., 2015). In addition, Probiotics ferments the prebiotics to short chain fatty acids (SCFA) reducing gut pH and abating the formation of calcium phosphates. Also, SCFAs influence calcium absorption through signaling pathway modulation and butyrate controls the calcium uptake by non-gut cells(Weaver, 2015).b

MISCELLANEOUS PREDISPOSING FACTORS FOR BCO

Calcium and phosphorus levels that are optimal for chicken feeding is 2:1 and is usually kept up by using fodder phosphates, fodder chalk, and enzymes like phytase. Imbalance in this ratio due to excessive supplementation of either of these macro elements leads to altered assimilation of other element. Water containing higher levels (>75mg/L) of calcium affects the nutrient and medicine absorption(Kierończyk et al., 2017). Addition of 25-hydroxy vitamin D3 to water helps in alleviating calcium malabsorption (Pattison, 1992). In another study, supplementation of charcoal decreases the calcium bioavailability leading to increased bone disorders due to increased phosphorus content in tibia (Oso et al., 2011). In plants, there will be nearly 70% phosphorus in the form of phytic acid which can only be hydrolyzed by phytase (Kierończyk et al., 2017). Also, dietary supplementation of this enzyme enhances the tibial Mg and Fe concentration and also Zn utilization (Pintar et al., 2005; Yi et al., 1996). On the other hand, action of this enzyme is influenced by gut microflora and enzymes wherein fibrinolytic enzymes has a synergistic effect with phytase. Furthermore, microelements like fluorine and boron are

proven to be beneficial in attaining good bone density(Kierończyk et al., 2017). In contrast, suboptimal levels of copper in diet leads to shrinkage of collagen network and lowered bone mineral density. An increase in zinc to 100 mg/kg in feed leads to good bone strength and reduction of lameness in broiler chickens (Štofaníková et al., 2011). Also, vitamins like A, C, K apart from cholecalciferol affects maturation of chondrocytes, collagen synthesis, ossification process respectively. Additionally, supplementation of lysophospholipid had improved intestinal development along with gut and bone health(C Chen et al., 2019).

Moreover, feed quality especially with reference to mycotoxins possess a contradictory effect in terms of bird growth performance, health, and reproduction. Precisely, aflatoxin and ochratoxin have negative influence on bone properties and allows lameness problem to flourish from 2.3% to 25%(Okiki et al., 2010). Astonishingly, probiotic bacteria like *Bacillus licheniformis, B.subtilis, and Lactobacillus spp.* increased uptake of calcium, phosphorus, and bone inorganic substances thus increasing the bone mechanical strength. Furthermore, dietary supplementation of probiotic, prebiotic and synbiotics alleviate lameness concern.

Furthermore, bone development in poultry greatly rely on environmental conditions during incubation and production. Also, managerial factors like litter quality, lighting programme, stocking density, ventilation, drinking water quality, and supplements. During incubation, an increase in temperature and lowered oxygen levels in the final phase of incubation leads to poor development of bones and type X collagen leading to asymmetric skeleton in broilers. Now a days, embryos has high metabolic rate wherein the bone growth rate is higher in last phase of incubation which indicates nutrient deficiency in this phase turns out into incompletely developed skeletal system, digestive system(Applegate & Lilburn, 2002). Numerous physiological changes occurs

during heat stress leading to the production of glucocorticoids which is reported to induce BCO(Castro et al., 2019; Zhang et al., 2017).

A crucial factor in poultry production which correlated with bone pathologies is light intensity and ambient temperature. Intermittent lighting system is commonly reported to increase body mass and feed conversion. Also, there exists an interaction between lighting programme and sex of the bird. Male birds are more prone to leg health problems where a proper lighting schedule will be helpful. In addition, thermal stress is proved to reduce bone mass and its mechanical strength. And too low temperatures can decrease the mineral absorption. Furthermore, the presence of pathogenic bacteria is associated with temperatures. For instance, *E.coli and Enterococcus* has a highest prevalence in hot months compared to colder months. Also, Poor gait scores tend to be more in September but less in March (Kierończyk et al., 2017).

BACTERIAL DIVERSITY THROUGH CULTURE INDEPENDENT METHODS

Although some broilers would not exhibit clinical signs of lameness, there exists a progressive development of lesions that are pathognomic to BCO. Sometimes, routine culture methods possess some cons especially with respect to nonculturable species that remain undetected. Next generation sequencing which are culture independent would help in identifying the bacterial communities by deep profiling of their 16s rRNA gene sequences. In a study, there exists a great diversity within a bacterial community in initial days but trend decreased with aging and this trend is reversed in cecal samples(Danzeisen et al., 2011). *Staphylococcus aureus* has been detected in culture dependent and independent methods. Furthermore, ultrastructural studies shown that, this organism damages growth plate cartilage and proliferate within thick adherent glycocalyx. This doesn't allows the antibiotic penetration but presents the bacterial cell surface to host defense mechanisms(Speers & Nade, 1985). Furthermore, Enterobacter, Serratia, and

Nitrinicola are overpresented in BCO samples but these are not detectable through culture methods. Entrobacter and Serratia belongs to family Enterobacteriaceae and Nitrinicola is a alkaliphilic bacterium. Serratia marcescens, usually causes nosocomial infections and forms biofilms. Enterobacter strains are opportunistic pathogens. The same study indicated a great variability among individuals in the bacterial composition at various locations. Also, Principal Coordinate Analysis has shown the presence of individual specific selection pressures. In a study, bacterial communities that exists in blood of chicken were analyzed. Although blood is once considered to be sterile but they do have their immanent microbiota. In some studies, most abundant phylum in blood of chicken is *Proteobacteria*. Other abundant phyla in the chicken blood are *Bacteroidetes, Firmicutes, Actinobacteria, and Cyanobacteria*. Furthermore, most abundant phylum in chicken gut includes firmicutes followed by *Proteobacteria and Bacteroidetes*(Mandal et al., 2016). These studies in different species infer that blood may lodge selected microbiota and possess a unique habitat to maintain them stably. In contrast, blood microbiota dysbiosis in any means may lead to significant increase of other phyla which might be due to leakage of gut microbiota to it under stress. Analysis from the above study showed microbiota existence of 30 to 40 OTUs in blood of broiler chickens irrespective of the age, and host factors(Mandal et al., 2016). Several analyses like beta diversity, hierarchical clustering, and bacterial network analysis suggested the existence of distinctive bacterial communities in BCO affected birds from the healthy birds representing shift in these communities with certain selective pressures(Mandal et al., 2016).

MESENCHYMAL STEM CELL CULTURES- A POTENTIAL TOOL TO UNDERSTAND BCO

Mesenchymal stem cells (MSCs) are spindle-shaped, adherent, non- hemopoietic stem cells lodges in bone marrow. They are usually isolated after removal of non-adherent cells from whole bone marrow aspirates followed by culturing adherent mononuclear layer in Dulbecco's Modified Eagle Medium (DMEM) supplemented with 10% fetal bovine serum. MSCs can be retrieved from umblical cord wall, blood, adipose tissue, liver, and skin(Assis-Ribas et al., 2018). In addition, characterization can be done using positive markers like CD44, Sca-1, CD71, CD73, CD90, and CD105. Negative markers include hematopoietic, and endothelial markers like CD45, CD34, CD19, CD11b, CD11c, CD79a, and CD31) along with co-stimulatory molecules like CD80, CD86, and CD40(Assis-Ribas et al., 2018; Dominici et al., 2006). Tissue specific phenotypes of MSCs is regulated by molecular signature linked to MSCs habitat. These are capable of differenting into various cell types of mesodermal and non-mesodermal origin like chondrocytes, osteocytes, adipocytes, endothelial cells, cardiomyocytes, hepatocytes, and neural cells (Talaei-Khozani et al., 2015; Ziadlou et al., 2015). On the top, there are no standardized methods to isolate and identify differential populations since they vary in basic and fundamental properties which are critical for differentiation. In an experimental design, even though 1,25-Dihydroxyvitamin D3 showed some inhibitory effects in initial stages of differentiation (1-2 days), but latter stages were shown with stimulatory effects (3-7 days). This could be due to inhibition of RUNX2 and BMP2 expression in former stages(Chongxiao Chen et al., 2021; J. H. Kim et al., 2016).

A better way to understand BCO through culture models is by harboring MSCs. This can applied for several applications and aids in understanding mechanism of osteogenic, myogenic, and adipogenic pathways along with the compounds involved in driving them(Adhikari et al.,

2019). Furthermore, MSCs in culture conditions can adhere to a plastic surface and have multilineage differentiation property, and unveil the surface antigens(Dominici et al., 2006). Isolation of MSCs involves several purification steps since there are chances of contamination with blood cells and hematopoietic stem cells. In addition, purification, and enrichment of MSCs can be done by several methods like use of ficole, antibody-based cell sorting, density-based culture techniques. In contrast, isolation of MSCs from compact bones of day-old chickens could be an economical and easy. Also, they demonstrated multilineage differentiation potential when provided with respective differentiation conditions. A study has shown that MSCs and pericytes are developmentally related and shares common phenotypic markers like CD146, NG2, PDF-Rβ. CD146 expression attributes to osteogenic and immunomodulatory potential along with hematopoietic control, and therapeutic efficacy. In a rat model of acute inflammation of synovial membrane, intra-articular injection of POS cells promoted M2 macrophages polarization indicative of anti-inflammatory and healing mechanisms of synovium(Bowles et al., 2020). 20(S)-Hydroxycholesterol supplementation stimulates osteogenic differentiation accompanied with HES-1 and HEY-1 (Notch target genes) expression of MSCs through positive regulation of RUNX2. This occurs through hedgehog signaling pathway which is reported to be a key for bone homeostasis through coordinating maintenance of mesenchymal cell progenitors. LXR (Liver X receptor) signaling also plays a key role in HEY-1 expression in MSCs(W.-K. Kim et al., 2010).

CONCLUSION

BCO is turned out to be a major concern in poultry production and animal welfare. Understanding the underlying mechanisms involved in the incidence is very crucial in restraining this problem. Several studies can enhance our knowledge on BCO. however, some studies are not precise in tracing this knot. Through some experimental models like the flooring models that can

induce BCO lesions and cell culture models can help in divulging novel BCO mechanisms which further could help arriving at precise etiology along with diagnosis and treatment. Although there are several studies related to BCO, but there is a huge lacuna in finding precise biomarkers, pathophysiological mechanisms, and treatment alternatives. This would help in building a productive poultry industry which can resist challenges from genetic improvements like heavy body weights.

REFERENCES

Adhikari, R., Chen, C., Waters, E., West, F. D., & Kim, W. K. (2019). Isolation and differentiation of mesenchymal stem cells from broiler chicken compact bones. *Frontiers in Physiology*, *9*, 1892.

Al-Rubaye, A. A. K., Couger, M. B., Ojha, S., Pummill, J. F., & Koon, J. A. (n.d.). II, Wideman RF Jr, Rhoads DD. 2015. *Genome Analysis of Staphylococcus Agnetis, an Agent of Lameness in Broiler Chickens. PLoS One*, *10*, e0143336.

Al-Zahrani, K., Licknack, T., Watson, D. L., Anthony, N. B., & Rhoads, D. D. (2019). Further investigation of mitochondrial biogenesis and gene expression of key regulators in ascites-susceptible and ascites-resistant broiler research lines. *Plos One*, *14*(3), e0205480.

AlQranei, M. S., Senbanjo, L. T., Aljohani, H., Hamza, T., & Chellaiah, M. A. (2021). Lipopolysaccharide- TLR-4 Axis regulates Osteoclastogenesis independent of RANKL/RANK signaling. *BMC Immunology*, *22*(1), 23. https://doi.org/10.1186/s12865-021-00409-9

Alrubaye, A. A. K., Ekesi, N. S., Hasan, A., Elkins, E., Ojha, S., Zaki, S., Dridi, S., Wideman, R. F., Rebollo, M. A., & Rhoads, D. D. (2020). Chondronecrosis with osteomyelitis in broilers: further defining lameness-inducing models with wire or litter flooring to evaluate protection with organic

trace minerals. *Poultry Science*, *99*(11), 5422–5429. https://doi.org/https://doi.org/10.1016/j.psj.2020.08.027

Alvino, G. M., Archer, G. S., & Mench, J. A. (2009). Behavioural time budgets of broiler chickens reared in varying light intensities. *Applied Animal Behaviour Science*, *118*(1–2), 54–61.

Applegate, T. J., & Lilburn, M. S. (2002). Growth of the femur and tibia of a commercial broiler line. *Poultry Science*, *81*(9), 1289–1294.

Aspden, R. M., & Hukins, D. W. L. (1981). Collagen organization in articular cartilage, determined by X-ray diffraction, and its relationship to tissue function. *Proceedings of the Royal Society of London. Series B. Biological Sciences*, *212*(1188), 299–304.

Assis-Ribas, T., Forni, M. F., Winnischofer, S. M. B., Sogayar, M. C., & Trombetta-Lima, M. (2018). Extracellular matrix dynamics during mesenchymal stem cells differentiation. *Developmental Biology*, *437*(2), 63–74. https://doi.org/https://doi.org/10.1016/j.ydbio.2018.03.002

Baumann, H., & Gauldie, J. (1994). The acute phase response. *Immunology Today*, *15*(2), 74–80.

Behera, J., Ison, J., Voor, M. J., & Tyagi, N. (2022). Exercise-linked skeletal irisin ameliorates diabetes-associated osteoporosis by inhibiting the oxidative damage–dependent miR-150-FNDC5/pyroptosis axis. *Diabetes*, *71*(12), 2777–2792.

Bendre, A., Moritz, N., Väänänen, V., & Määttä, J. A. (2018). Dicer1 ablation in osterix positive bone forming cells affects cortical bone homeostasis. *Bone*, *106*, 139–147.

Bowles, A. C., Kouroupis, D., Willman, M. A., Perucca Orfei, C., Agarwal, A., & Correa, D. (2020). Signature quality attributes of CD146+ mesenchymal stem/stromal cells correlate with high therapeutic and secretory potency. *Stem Cells*, *38*(8), 1034–1049.

Bradshaw, R. H., Kirkden, R. D., & Broom, D. M. (2002). A review of the aetiology and pathology of leg weakness in broilers in relation to welfare. *Avian and Poultry Biology Reviews*, *13*(2), 45–104.

Breugelmans, S., Muylle, S., Cornillie, P., Saunders, J., & Simoens, P. (2007). Age determination of poultry: a challenge for customs. *Vlaams Diergeneeskundig Tijdschrift*, *76*(6), 423–430.

Castro, F. L. S., Kim, H. Y., Hong, Y. G., & Kim, W. K. (2019). The effect of total sulfur amino acid levels on growth performance, egg quality, and bone metabolism in laying hens subjected to high environmental temperature. *Poultry Science*, *98*(10), 4982–4993. https://doi.org/https://doi.org/10.3382/ps/pez275

Chen, C, Jung, B., & Kim, W. K. (2019). Effects of lysophospholipid on growth performance, carcass yield, intestinal development, and bone quality in broilers. *Poultry Science*, *98*(9), 3902–3913. https://doi.org/https://doi.org/10.3382/ps/pez111

Chen, Chongxiao, Adhikari, R., White, D. L., & Kim, W. K. (2021). Role of 1,25-Dihydroxyvitamin D(3) on Osteogenic Differentiation and Mineralization of Chicken Mesenchymal Stem Cells. *Frontiers in Physiology*, *12*, 479596. https://doi.org/10.3389/fphys.2021.479596

Chen, H., Chomyn, A., & Chan, D. C. (2005). Disruption of fusion results in mitochondrial heterogeneity and dysfunction. *Journal of Biological Chemistry*, *280*(28), 26185–26192.

Chen, J.-F., Murchison, E. P., Tang, R., Callis, T. E., Tatsuguchi, M., Deng, Z., Rojas, M., Hammond, S. M., Schneider, M. D., & Selzman, C. H. (2008). Targeted deletion of Dicer in the heart leads to dilated cardiomyopathy and heart failure. *Proceedings of the National Academy of Sciences*, *105*(6), 2111–2116.

Cherry, A. D., & Piantadosi, C. A. (2015). Regulation of mitochondrial biogenesis and its intersection with inflammatory responses. *Antioxidants & Redox Signaling*, *22*(12), 965–976.

Cipolat, S., de Brito, O. M., Dal Zilio, B., & Scorrano, L. (2004). OPA1 requires mitofusin 1 to promote mitochondrial fusion. *Proceedings of the National Academy of Sciences*, *101*(45), 15927–15932.

Cook, M. E. (2000). Skeletal deformities and their causes: introduction. *Poultry Science*, *79*(7), 982–984. https://doi.org/10.1093/ps/79.7.982

Corr, S. A., Gentle, M. J., McCorquodale, C. C., & Bennett, D. (2003). The effect of morphology on walking ability in the modern broiler: a gait analysis study. *Animal Welfare*, *12*(2), 159–171.

D'Amelio, P., & Sassi, F. (2016). Osteoimmunology: from mice to humans. *Bonekey Reports*, *5*, 802. https://doi.org/10.1038/bonekey.2016.29

Danzeisen, J. L., Kim, H. B., Isaacson, R. E., Tu, Z. J., & Johnson, T. J. (2011). Modulations of the chicken cecal microbiome and metagenome in response to anticoccidial and growth promoter treatment. *PloS One*, *6*(11), e27949.

Deep, A., Schwean-Lardner, K., Crowe, T. G., Fancher, B. I., & Classen, H. L. (2012). Effect of light intensity on broiler behaviour and diurnal rhythms. *Applied Animal Behaviour Science*, *136*(1), 50–56.

Di Angelantonio, E., Sarwar, N., Perry, P., Kaptoge, S., Ray, K. K., Thompson, A., Wood, A. M., Lewington, S., Sattar, N., & Packard, C. J. (2009). Emerging Risk Factors collaboration. *Major Lipids, Apolipoproteins, and Risk of Vascular Disease. JAMA*, *302*, 1993–2000.

Diaz Carrasco, J. M., Casanova, N. A., & Fernández Miyakawa, M. E. (2019). Microbiota, Gut Health and Chicken Productivity: What Is the Connection? In *Microorganisms* (Vol. 7, Issue 10). https://doi.org/10.3390/microorganisms7100374

Dinev, I. (2009). Clinical and morphological investigations on the prevalence of lameness associated with femoral head necrosis in broilers. *British Poultry Science*, *50*(3), 284–290.

Dominici, M., Le Blanc, K., Mueller, I., Slaper-Cortenbach, I., Marini, F. C., Krause, D. S., Deans, R. J., Keating, A., Prockop, D. J., & Horwitz, E. M. (2006). Minimal criteria for defining multipotent mesenchymal stromal cells. The International Society for Cellular Therapy position statement. *Cytotherapy*, *8*(4), 315–317.

Durairaj, V, Clark, F. D., Coon, C. C., Huff, W. E., Okimoto, R., Huff, G. R., & Rath, N. C. (2012). Effects of high fat diets or prednisolone treatment on femoral head separation in chickens. *British Poultry Science*, *53*(2), 198–203.

Durairaj, VIJAY, Okimoto, R., Rasaputra, K., Clark, F. D., & Rath, N. C. (2009). Histopathology and serum clinical chemistry evaluation of broilers with femoral head separation disorder. *Avian Diseases*, *53*(1), 21–25.

El-Jawhari, J. J., Ganguly, P., Jones, E., & Giannoudis, P. V. (2021). Bone Marrow Multipotent Mesenchymal Stromal Cells as Autologous Therapy for Osteonecrosis: Effects of Age and Underlying Causes. In *Bioengineering* (Vol. 8, Issue 5). https://doi.org/10.3390/bioengineering8050069

Exner, N., Lutz, A. K., Haass, C., & Winklhofer, K. F. (2012). Mitochondrial dysfunction in Parkinson's disease: molecular mechanisms and pathophysiological consequences. *The EMBO Journal*, *31*(14), 3038–3062. https://doi.org/10.1038/emboj.2012.170

Fandridis, E., Apergis, G., Korres, D. S., Nikolopoulos, K., Zoubos, A. B., Papassideri, I., & Trougakos, I. P. (2011). Increased expression levels of apolipoprotein J/clusterin during primary osteoarthritis. *In Vivo*, *25*(5), 745–749.

Ferver, A., & Dridi, S. (2020). Bacterial chondronecrosis with osteomyelitis (BCO) in modern broilers: impacts, mechanisms, and perspectives. *CABI Reviews*, *2020*.

Ferver, A., Greene, E., Wideman, R., & Dridi, S. (2021). Evidence of Mitochondrial Dysfunction in Bacterial Chondronecrosis With Osteomyelitis–Affected Broilers. *Frontiers in Veterinary Science*, *8*(February), 1–8. https://doi.org/10.3389/fvets.2021.640901

Genestier, A.-L., Michallet, M.-C., Prévost, G., Bellot, G., Chalabreysse, L., Peyrol, S., Thivolet, F., Etienne, J., Lina, G., & Vallette, F. M. (2005). Staphylococcus aureus Panton-Valentine leukocidin directly targets mitochondria and induces Bax-independent apoptosis of human neutrophils. *The Journal of Clinical Investigation*, *115*(11), 3117–3127.

Gocsik, É., Silvera, A. M., Hansson, H., Saatkamp, H. W., & Blokhuis, H. J. (2017). Exploring the economic potential of reducing broiler lameness. *British Poultry Science*, *58*(4), 337–347.

Greene, E., Flees, J., Dhamad, A., Alrubaye, A., Hennigan, S., Pleimann, J., Smeltzer, M., Murray, S., Kugel, J., Goodrich, J., Robertson, A., Wideman, R., Rhoads, D., & Dridi, S. (2019). Double-Stranded RNA Is a Novel Molecular Target in Osteomyelitis Pathogenesis: A Translational Avian Model for Human Bacterial Chondronecrosis with Osteomyelitis. *American Journal of Pathology*, *189*(10), 2077–2089. https://doi.org/10.1016/j.ajpath.2019.06.013

Gurung, P., Burton, A., & Kanneganti, T.-D. (2016). NLRP3 inflammasome plays a redundant role with caspase 8 to promote IL-1β–mediated osteomyelitis. *Proceedings of the National Academy of Sciences*, *113*(16), 4452–4457.

H.W., S. (1954). Experimental staphylococcal infections in chickens. *Journal of Pathology and Bacteriology*, *47*, 81.

Haden, D. W., Suliman, H. B., Carraway, M. S., Welty-Wolf, K. E., Ali, A. S., Shitara, H., Yonekawa, H., & Piantadosi, C. A. (2007). Mitochondrial biogenesis restores oxidative metabolism during Staphylococcus aureus sepsis. *American Journal of Respiratory and Critical Care Medicine*, *176*(8), 768–777.

Hata, A., & Kashima, R. (2016). Dysregulation of microRNA biogenesis machinery in cancer. *Critical Reviews in Biochemistry and Molecular Biology*, *51*(3), 121–134. https://doi.org/10.3109/10409238.2015.1117054

Havenstein, G. B., Ferket, P. R., & Qureshi, M. A. (2003). Growth, livability, and feed conversion of 1957 versus 2001 broilers when fed representative 1957 and 2001 broiler diets. *Poultry Science*, *82*(10), 1500–1508. https://doi.org/10.1093/ps/82.10.1500

Hock, M. B., & Kralli, A. (2009). Transcriptional control of mitochondrial biogenesis and function. *Annual Review of Physiology*, *71*, 177–203.

Hogg, D. A. (1980). A re-investigation of the centres of ossification in the avian skeleton at and after hatching. *Journal of Anatomy*, *130*(Pt 4), 725–743. https://pubmed.ncbi.nlm.nih.gov/7429964

Houschyar, K. S., Tapking, C., Borrelli, M. R., Popp, D., Duscher, D., Maan, Z. N., Chelliah, M. P., Li, J., Harati, K., & Wallner, C. (2019). Wnt pathway in bone repair and regeneration–what do we know so far. *Frontiers in Cell and Developmental Biology*, *6*, 170.

Jiang, T., Mandal, R. K., Wideman Jr, R. F., Khatiwara, A., Pevzner, I., & Min Kwon, Y. (2015). Molecular survey of bacterial communities associated with bacterial chondronecrosis with osteomyelitis (BCO) in broilers. *PLoS One*, *10*(4), e0124403.

Jiang, T., Mandal, R. K., Wideman, R. F., Khatiwara, A., Pevzner, I., & Kwon, Y. M. (2015). Molecular survey of bacterial communities associated with bacterial chondronecrosis with osteomyelitis (BCO) in broilers. *PLoS ONE*, *10*(4). https://doi.org/10.1371/journal.pone.0124403

Julian, R. (2005). Production and growth related disorders and other metabolic diseases of poultry - A review. *Veterinary Journal (London, England : 1997)*, *169*, 350–369. https://doi.org/10.1016/j.tvjl.2004.04.015

Kerachian, M. A., Séguin, C., & Harvey, E. J. (2009). Glucocorticoids in osteonecrosis of the femoral head: a new understanding of the mechanisms of action. *The Journal of Steroid Biochemistry and Molecular Biology*, *114*(3–5), 121–128.

Kestin, S. C., Knowles, T. G., Tinch, A. E., & Gregory, N. G. (1992). Prevalence of leg weakness in broiler chickens and its relationship with genotype. *The Veterinary Record*, *131*(9), 190–194.

Kestin, S. C., Su, G., & Sorensen, P. (1999). Different commercial broiler crosses have different susceptibilities to leg weakness. *Poultry Science*, *78*(8), 1085–1090.

Kierończyk, B., Rawski, M., Józefiak, D., & Świątkiewicz, S. (2017). Infectious and non-infectious factors associated with leg disorders in poultry-a review. *Annals of Animal Science*, *17*(3), 645.

Kim, J. H., Seong, S., Kim, K., Kim, I., Jeong, B.-C., & Kim, N. (2016). Downregulation of Runx2 by 1, 25-dihydroxyvitamin D3 induces the transdifferentiation of osteoblasts to adipocytes. *International Journal of Molecular Sciences*, *17*(5), 770.

Kim, W.-K., Meliton, V., Tetradis, S., Weinmaster, G., Hahn, T. J., Carlson, M., Nelson, S. F., & Parhami, F. (2010). Osteogenic oxysterol, 20(S)-hydroxycholesterol, induces notch target gene expression in bone marrow stromal cells. *Journal of Bone and Mineral Research*, *25*(4), 782–795. https://doi.org/https://doi.org/10.1359/jbmr.091024

Klasing, KIRK C. (1998). Avian macrophages: regulators of local and systemic immune responses. *Poultry Science*, *77*(7), 983–989.

Klasing, Kirk C, & Johnstone, B. J. (1991). Monokines in growth and development. *Poultry Science*, *70*(8), 1781–1789.

Knowles, T. G., Kestin, S. C., Haslam, S. M., Brown, S. N., Green, L. E., Butterworth, A., Pope, S. J., Pfeiffer, D., & Nicol, C. J. (2008). Leg Disorders in Broiler Chickens: Prevalence, Risk Factors and Prevention. *PLOS ONE*, *3*(2), e1545. https://doi.org/10.1371/journal.pone.0001545

Koj, A. (1989). The Role of Interleukin-6 as the Hepatocyte Stimulating Factor in the Network of Inflammatory Cytokines a. *Annals of the New York Academy of Sciences*, *557*(1), 1–8.

Kronenberg, H. M. (2003). Developmental regulation of the growth plate. *Nature*, *423*(6937), 332–336.

Kushner, I., & Rzewnicki, D. L. (1994). The acute phase response: general aspects. *Bailliere's Clinical Rheumatology*, *8*(3), 513–530.

Kwan, A. P., Dickson, I. R., Freemont, A. J., & Grant, M. E. (1989). Comparative studies of type X collagen expression in normal and rachitic chicken epiphyseal cartilage. *The Journal of Cell Biology*, *109*(4), 1849–1856.

Li, P. F., Zhou, Z. L., Shi, C. Y., & Hou, J. F. (2015). Downregulation of basic fibroblast growth factor is associated with femoral head necrosis in broilers. *Poultry Science*, *94*(5), 1052–1059.

Li, Y., Ling, J., & Jiang, Q. (2021). Inflammasomes in alveolar bone loss. *Frontiers in Immunology*, *12*, 691013.

Liu, P., Baumgart, M., Groth, M., Wittmann, J., Jäck, H.-M., Platzer, M., Tuckermann, J. P., & Baschant, U. (2016). Dicer ablation in osteoblasts by Runx2 driven cre-loxP recombination affects bone integrity, but not glucocorticoid-induced suppression of bone formation. *Scientific Reports*, *6*(1), 1–10.

López-Armada, M. J., Riveiro-Naveira, R. R., Vaamonde-García, C., & Valcárcel-Ares, M. N. (2013). Mitochondrial dysfunction and the inflammatory response. *Mitochondrion*, *13*(2), 106–118.

Lowder, B. V, Guinane, C. M., Zakour, N. L. Ben, Weinert, L. A., Conway-Morris, A., Cartwright, R. A., Simpson, A. J., Rambaut, A., Nübel, U., & Fitzgerald, J. R. (2009). Recent human-to-poultry host jump, adaptation, and pandemic spread of Staphylococcus aureus. *Proceedings of the National Academy of Sciences*, *106*(46), 19545–19550.

Ma, T., Grayson, W. L., Fröhlich, M., & Vunjak-Novakovic, G. (2009). Hypoxia and stem cell-based engineering of mesenchymal tissues. *Biotechnology Progress*, *25*(1), 32–42.

Maassen, J. A. (2004). 't Hart LM, van Essen E, Heine RJ, Nijpels G, Jahangir Tafrechi RS, Raap AK, Janssen GM, Lemkes HH: Mitochondrial diabetes: molecular mechanisms and clinical presentation. *Diabetes*, *53*(Suppl 1), S103–S109.

Mackie, E., Ahmed, Y. A., Tatarczuch, L., Chen, K.-S., & Mirams, M. (2008). Endochondral ossification: how cartilage is converted into bone in the developing skeleton. *The International Journal of Biochemistry & Cell Biology*, *40*(1), 46–62.

Mandal, R. K., Jiang, T., Al-Rubaye, A. A., Rhoads, D. D., Wideman, R. F., Zhao, J., Pevzner, I., & Kwon, Y. M. (2016). An investigation into blood microbiota and its potential association with Bacterial Chondronecrosis with Osteomyelitis (BCO) in Broilers. In *Scientific reports* (Vol. 6, p. 25882). https://doi.org/10.1038/srep25882

Mandal, R. K., Jiang, T., Wideman, R. F., Lohrmann, T., & Kwon, Y. M. (2020). Microbiota Analysis of Chickens Raised Under Stressed Conditions . In *Frontiers in Veterinary Science* (Vol. 7, p. 696). https://www.frontiersin.org/article/10.3389/fvets.2020.482637

Marriott, I. (2013). Apoptosis-associated uncoupling of bone formation and resorption in osteomyelitis. In *Frontiers in Cellular and Infection Microbiology* (Vol. 3, Issue DEC). https://doi.org/10.3389/fcimb.2013.00101

McCall, S. H., Sahraei, M., Young, A. B., Worley, C. S., Duncan, J. A., Ting, J. P., & Marriott, I. (2008). Osteoblasts express NLRP3, a nucleotide-binding domain and leucine-rich repeat region containing receptor implicated in bacterially induced cell death. *Journal of Bone and Mineral Research*, *23*(1), 30–40.

McNamee, P T, McCullagh, J. J., Thorp, B. H., Ball, H. J., Graham, D., McCullough, S. J., McConaghy, D., & Smyth, J. A. (1998). Study of leg weakness in two commercial broiler flocks. *Veterinary Record*, *143*(5), 131–135.

McNamee, Perpetua T, McCullagh, J. J., Rodgers, J. D., Thorp, B. H., Ball, H. J., Connor, T. J., McConaghy, D., & Smyth, J. A. (1999). Development of an experimental model of bacterial chondronecrosis with osteomyelitis in broilers following exposure to Staphylococcus aureus by aerosol, and inoculation with chicken anaemia and infectious bursal disease viruses. *Avian Pathology*, *28*(1), 26–35.

McNamee, Perpetua T, & Smyth, J. A. (2000). Bacterial chondronecrosis with osteomyelitis ('femoral head necrosis') of broiler chickens: A review. *Avian Pathology*, *29*(4), 253–270. https://doi.org/10.1080/03079450050118386

Mireles, A. J., Kim, S. M., & Klasing, K. C. (2005). An Acute Inflammatory Response Alters Bone Homeostasis, Body Composition, and the Humoral Immune Response of Broiler Chickens. *Poultry Science*, *84*(4), 553–560. https://academic.oup.com/ps/article-abstract/84/4/553/1562224

Mui, K. L., Chen, C. S., & Assoian, R. K. (2016). The mechanical regulation of integrin–cadherin crosstalk organizes cells, signaling and forces. *Journal of Cell Science*, *129*(6), 1093–1100.

Nääs, I. A., Paz, I. C. L. A., Baracho, M. S., Menezes, A. G., Bueno, L. G. F., Almeida, I. C. L., & Moura, D. J. (2009). Impact of lameness on broiler well-being. *Journal of Applied Poultry Research*, *18*(3), 432–439.

Newberry, R. C., Hunt, J. R., & Gardiner, E. E. (1988). Influence of light intensity on behavior and performance of broiler chickens. *Poultry Science*, *67*(7), 1020–1025.

Okiki, P. A., Ojeizeh, T. I., & Ogbimi, A. O. (2010). Effects of feeding diet rich in mycotoxins on the health and growth performances of broiler chicken. *International Journal of Poultry Science*, *9*(12), 1136–1139.

Oso, A. O., Idowu, A. A., & Niameh, O. T. (2011). Growth response, nutrient and mineral retention, bone mineralisation and walking ability of broiler chickens fed with dietary inclusion of various unconventional mineral sources. *Journal of Animal Physiology and Animal Nutrition*, *95*(4), 461–467.

Packialakshmi, B., Liyanage, R., Lay Jr, J. O., Okimoto, R., & Rath, N. C. (2015). Prednisolone-induced predisposition to femoral head separation and the accompanying plasma protein changes in chickens. *Biomarker Insights*, *10*, BMI-S20268.

Paludo, E., Ibelli, A. M. G., PEIXOTO, J. de O., TAVERNARI, F. de C., Zanella, R., Pandolfi, J. R. C., COUTNHO, L. L., Lima-Rosa, C. A. V, & Ledur, M. C. (2014). RUNX2 plays an essential role in the manifestation of femoral head necrosis in broilers. *Embrapa Suínos e Aves-Artigo Em Anais de Congresso (ALICE)*.

Paludo, E., Ibelli, A. M. G., Peixoto, J. O., Tavernari, F. C., Lima-Rosa, C. A. V, Pandolfi, J. R. C., Ledur, M. C., Elgheznawy, A., Shi, L., Hu, J., Wittig, I., Laban, H., Pircher, J., Mann, A., Provost, P., Randriamboavonjy, V., & Fleming, I. (2015). The involvement of RUNX2 and SPARC genes in the bacterial chondronecrosis with osteomyelitis in broilers. *Animal*, *117*(2), 157–165.

Parvaneh, K., Ebrahimi, M., Sabran, M. R., Karimi, G., Hwei, A. N. M., Abdul-Majeed, S., Ahmad, Z., Ibrahim, Z., & Jamaluddin, R. (2015). Probiotics (Bifidobacterium longum) increase bone mass density and upregulate Sparc and Bmp-2 genes in rats with bone loss resulting from ovariectomy. *BioMed Research International*, *2015*.

Pattison, M. (1992). Impacts of bone problems on the poultry meat industry. *Poultry Science Symposium*.

Paxton, H., Anthony, N. B., Corr, S. A., & Hutchinson, J. R. (2010). The effects of selective breeding on the architectural properties of the pelvic limb in broiler chickens: a comparative study across modern and ancestral populations. *Journal of Anatomy*, *217*(2), 153–166.

Paxton, H., Daley, M. A., Corr, S. A., & Hutchinson, J. R. (2013). The gait dynamics of the modern broiler chicken: a cautionary tale of selective breeding. *Journal of Experimental Biology*, *216*(17), 3237–3248.

Peterson, C. T., Sharma, V., Elmén, L., & Peterson, S. N. (2015). Immune homeostasis, dysbiosis and therapeutic modulation of the gut microbiota. *Clinical & Experimental Immunology*, *179*(3), 363–377.

Petry, B., Savoldi, I. R., Ibelli, A. M. G., Paludo, E., de Oliveira Peixoto, J., Jaenisch, F. R. F., de Córdova Cucco, D., & Ledur, M. C. (2018). New genes involved in the Bacterial Chondronecrosis with Osteomyelitis in commercial broilers. *Livestock Science*, *208*, 33–39.

Pieczenik, S. R., & Neustadt, J. (2007). Mitochondrial dysfunction and molecular pathways of disease. *Experimental and Molecular Pathology*, *83*(1), 84–92.

Pintar, J., Bujan, M., Homen, B., Gazic, K., Sikiric, M., & Cerny, T. (2005). Effects of supplemental phytase on the mineral content in tibia of broilers fed different cereal based diets. *Czech J. Anim. Sci*, *50*, 68–73.

Rath, N. C., Huff, G. R., Huff, W. E., & Balog, J. M. (2000). Factors regulating bone maturity and strength in poultry. *Poultry Science*, *79*(7), 1024–1032.

Rault, J.-L., Clark, K., Groves, P. J., & Cronin, G. M. (2017). Light intensity of 5 or 20 lux on broiler behavior, welfare and productivity. *Poultry Science*, *96*(4), 779–787.

Reece, R. L. (1992). role of infectious agents in leg abnormalities in growing birds. *Poultry Science Symposium*.

Rojas-Núñez, I., Moore, A. F., & Gino Lorenzoni, A. (2020). Incidence of bacterial chondronecrosis with osteomyelitis (Femoral head necrosis) induced by a model of skeletal stress and its correlation with subclinical necrotic enteritis. *Microorganisms*, *8*(2), 205. https://doi.org/10.3390/microorganisms8020205

Roux, S., & Orcel, P. (2000). Bone loss: Factors that regulate osteoclast differentiation-an update. *Arthritis Research & Therapy*, *2*(6), 1–6.

Segata, N., Izard, J., Waldron, L., Gevers, D., Miropolsky, L., Garrett, W. S., & Huttenhower, C. (2011). Metagenomic biomarker discovery and explanation. *Genome Biology*, *12*(6), 1–18.

Sharma, D., & Kanneganti, T.-D. (2016). The cell biology of inflammasomes: Mechanisms of inflammasome activation and regulation. *Journal of Cell Biology*, *213*(6), 617–629.

Sheehy, E. J., Kelly, D. J., & O'Brien, F. J. (2019). Biomaterial-based endochondral bone regeneration: a shift from traditional tissue engineering paradigms to developmentally inspired strategies. *Materials Today Bio*, *3*, 100009. https://doi.org/https://doi.org/10.1016/j.mtbio.2019.100009

Sivitz, W. I., & Yorek, M. A. (2010). Mitochondrial dysfunction in diabetes: from molecular mechanisms to functional significance and therapeutic opportunities. *Antioxidants & Redox Signaling*, *12*(4), 537–577.

Sjögren, K., Engdahl, C., Henning, P., Lerner, U. H., Tremaroli, V., Lagerquist, M. K., Bäckhed, F., & Ohlsson, C. (2012). The gut microbiota regulates bone mass in mice. *Journal of Bone and Mineral Research*, *27*(6), 1357–1367.

Sophia Fox, A. J., Bedi, A., & Rodeo, S. A. (2009). The basic science of articular cartilage: structure, composition, and function. *Sports Health*, *1*(6), 461–468.

Speers, D. J., & Nade, S. M. (1985). Ultrastructural studies of adherence of Staphylococcus aureus in experimental acute hematogenous osteomyelitis. *Infection and Immunity*, *49*(2), 443–446.

Stalker, M. J., Brash, M. L., Weisz, A., Ouckama, R. M., & Slavic, D. (2010). Arthritis and osteomyelitis associated with Enterococcus cecorum infection in broiler and broiler breeder chickens in Ontario, Canada. *Journal of Veterinary Diagnostic Investigation*, *22*(4), 643–645.

Štofaníková, J., Šály, J., Molnar, L., Sesztáková, E., & Bilek, J. (2011). The influence of dietary zinc content on mechanical properties of chicken tibiotarsal bone. *Acta Veterinaria*, *61*(5–6), 531–541.

Talaei-Khozani, T., Borhani-Haghighi, M., Ayatollahi, M., & Vojdani, Z. (2015). An in vitro model for hepatocyte-like cell differentiation from Wharton's jelly derived-mesenchymal stem cells by cell-base aggregates. *Gastroenterology and Hepatology from Bed to Bench*, *8*(3), 188.

Tickle, P. G., Paxton, H., Rankin, J. W., Hutchinson, J. R., & Codd, J. R. (2014). Anatomical and biomechanical traits of broiler chickens across ontogeny. Part I. Anatomy of the musculoskeletal respiratory apparatus and changes in organ size. *PeerJ*, *2*, e432.

Tiku, V., Tan, M.-W., & Dikic, I. (2020). Mitochondrial functions in infection and immunity. *Trends in Cell Biology*, *30*(4), 263–275.

Ventura-Clapier, R., Garnier, A., & Veksler, V. (2008). Transcriptional control of mitochondrial biogenesis: the central role of PGC-1α. *Cardiovascular Research*, *79*(2), 208–217.

Weaver, C. M. (2015). Diet, gut microbiome, and bone health. *Current Osteoporosis Reports*, *13*(2), 125–130.

Weimer, S. L., Wideman, R. F., Scanes, C. G., Mauromoustakos, A., Christensen, K. D., & Vizzier-Thaxton, Y. (2019). The utility of infrared thermography for evaluating lameness attributable to bacterial chondronecrosis with osteomyelitis. *Poultry Science*, *98*(4), 1575–1588.

Weimer, S. L., Wideman, R. F., Scanes, C. G., Mauromoustakos, A., Christensen, K. D., & Vizzier-Thaxton, Y. (2020). Broiler stress responses to light intensity, flooring type, and leg weakness as assessed by heterophil-to-lymphocyte ratios, serum corticosterone, infrared thermography, and latency to lie. *Poultry Science*, *99*(7), 3301–3311.

Wideman Jr, R. F., Blankenship, J., Pevzner, I. Y., & Turner, B. J. (2015). Efficacy of 25-OH vitamin D3 prophylactic administration for reducing lameness in broilers grown on wire flooring. *Poultry Science*, *94*(8), 1821–1827.

Wideman Jr, R. F., Hamal, K. R., Stark, J. M., Blankenship, J., Lester, H., Mitchell, K. N., Lorenzoni, G., & Pevzner, I. (2012). A wire-flooring model for inducing lameness in broilers: evaluation of probiotics as a prophylactic treatment. *Poultry Science*, *91*(4), 870–883.

Wideman, R. F. (2016a). Bacterial chondronecrosis with osteomyelitis and lameness in broilers: a review. *Poultry Science*, *95*(2), 325–344. https://doi.org/https://doi.org/10.3382/ps/pev320

Wideman, R. F. (2016b). Bacterial chondronecrosis with osteomyelitis and lameness in broilers: A review. In *Poultry Science* (Vol. 95, Issue 2, pp. 325–344). Oxford University Press. https://doi.org/10.3382/ps/pev320

Wideman, R., & Prisby, R. (2013). Bone Circulatory Disturbances in the Development of Spontaneous Bacterial Chondronecrosis with Osteomyelitis: A Translational Model for the Pathogenesis of Femoral Head Necrosis . In *Frontiers in Endocrinology* (Vol. 3, p. 183). https://www.frontiersin.org/article/10.3389/fendo.2012.00183

Wiggers, E. C., Johnson, W., Tucci, M., & Benghuzzi, H. (2011). Biochemical and morphological changes associated with macrophages and osteoclasts when challenged with infection-biomed 2011. *Biomedical Sciences Instrumentation*, *47*, 183–188.

Wijesurendra, D. S., Chamings, A. N., Bushell, R. N., Rourke, D. O., Stevenson, M., Marenda, M. S., Noormohammadi, A. H., & Stent, A. (2017). Pathological and microbiological investigations into cases of bacterial chondronecrosis and osteomyelitis in broiler poultry. *Avian Pathology*, *46*(6), 683–694. https://doi.org/10.1080/03079457.2017.1349872

Yi, Z., Kornegay, E. T., & Denbow, D. M. (1996). Supplemental microbial phytase improves zinc utilization in broilers. *Poultry Science*, *75*(4), 540–546.

Zhang, M., Shi, C. Y., Zhou, Z. L., & Hou, J. F. (2017). Bone characteristics, histopathology, and chondrocyte apoptosis in femoral head necrosis induced by glucocorticoid in broilers. *Poultry Science*, *96*(6), 1609–1614. https://doi.org/https://doi.org/10.3382/ps/pew466

Zheng, L., Tu, Q., Meng, S., Zhang, L., Yu, L., Song, J., Hu, Y., Sui, L., Zhang, J., & Dard, M. (2017). Runx2/DICER/miRNA pathway in regulating osteogenesis. *Journal of Cellular Physiology*, *232*(1), 182–191.

Zhou, J., Hu, Y., Chen, Y., Yang, L., Song, J., Tang, Y., Deng, F., & Zheng, L. (2016). Dicer-dependent pathway contribute to the osteogenesis mediated by regulation of Runx2. *American Journal of Translational Research*, *8*(12), 5354.

Ziadlou, R., Shahhoseini, M., Safari, F., Sayahpour, F.-A., Nemati, S., & Eslaminejad, M. B. (2015). Comparative analysis of neural differentiation potential in human mesenchymal stem cells derived from chorion and adult bone marrow. *Cell and Tissue Research*, *362*(2), 367–377.

Table 2.1 Represents the potential biomarkers involved in the incidence of BCO

Biomarkers	Function and Correlation	References
Serum Calcium	Bone density and mineralization along with bone breaking strength	(Williams et al., 2004; Zhang et al., 2017)
IL-17, IL-6, TNF-α, NLRP-3	Pyroptosis of osteoblasts, and Pro-inflammatory factors stimulates osteoclastogenesis or inhibits osteoblastogenesis	(Ferver - Ramser, 2020b; Ferver et al., 2021)
Peroxisome proliferator activated receptor coactivator (PGC-1α, 1β)	Repress the transcriptional activity of NF-κB, Mitochondrial biogenesis	(Packialakshmi et al.,; Ferver et al., 2021; Tompkins et al., 2023b)
Mitofusins	Increased ROS production,	(Ferver et al., 2021)
Matrix metalloproteases	Tissue remodeling, angiogenesis, Extracellular matrix degradation	(Zhang et al., 2017; Cui et al., 2022)
Osteocalcin	Secreted by differentiating osteoblasts	(Oso et al., 2011; Li et al., 2015; Jiang et al., 2015a)

RANKL and OPG	Crtitical cytokine produced by osteoblasts and OPG is an decoy receptor for RANKL	(Li et al., 2014; Matsumoto et al., 2017; Zheng et al., 2017)
Alkaline phosphatase	Involved in Ca and P deposition during the bone mineralization and formation	(Rojas-Núñez et al., 2020; Chen et al., 2021a; Tompkins et al., 2023b)
Sclerostin, DICKKOPF protein	Inhibit Wnt/β-catenin signalling pathway	(Glass et al., 2005; Zhong et al., 2012; Gao et al., 2013; Shi et al., 2016)
Tartarate resistant Acid Phosphatase	Activity of osteoclasts	(Wideman and Prisby, 2013; Ferver - Ramser, 2020b; Tompkins et al., 2023b)
Thrombospondin, Interferon-γ, Transforming growth factor-β, Vascular endothelial growth factor	Associated with the risk of avascular necrosis seen in BCO	(Wideman and Prisby, 2013; Wideman, 2016b; Rojas-Núñez et al., 2020; Ekesi et al., 2021)

isoform-C, and Protocadherin-15		
Fibroblast growth factor-2, BMP, SMAD1 and RUNX-2	Essential in osteoblast activity, bone mineralization, and osteoclast differentiation	("haematogenous osteomyelitis and septic arthritis - a single disease,"; Cook, 2000; Wijesurendra et al., 2017)

Figure 2.1 Response of lipopolysaccharides to various factors (A) Response of lipopolysaccharides (LPS) with respect to TNFα (Tumor necrosis factor), and osteoclastic activity (B) TNFα, and osteoclastic activity in the presence LPS under the influence of TLR4 blockers (C) TNFα, and osteoclastic activity in the presence of RANKL under the influence of TLR4 blockers

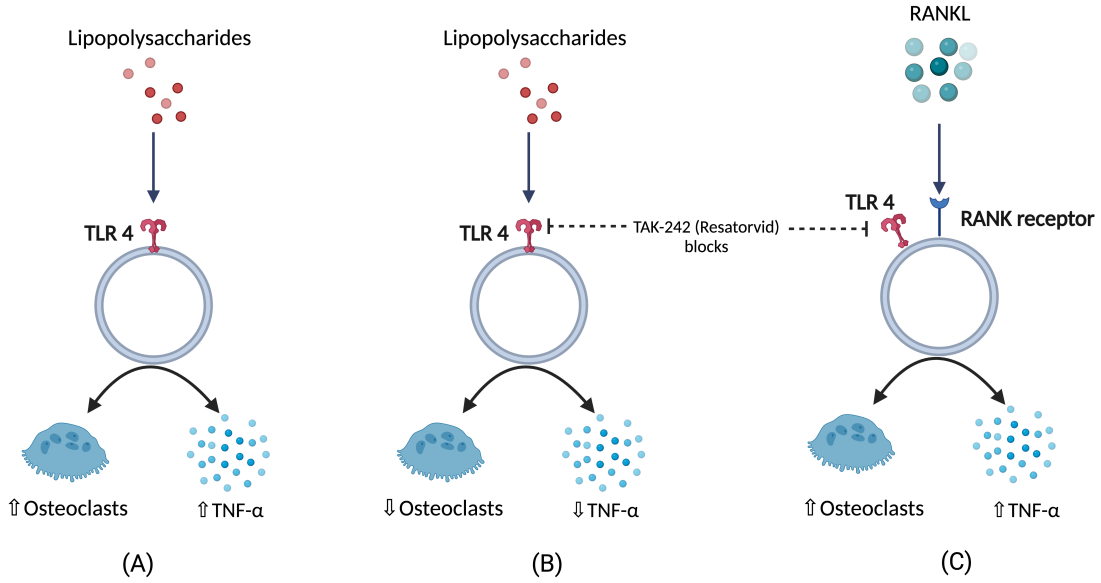

Figure 2.2 Known pathways through which Bacterial Chondronecrosis and Osteomyelitis (BCO) is observed in modern day broilers.

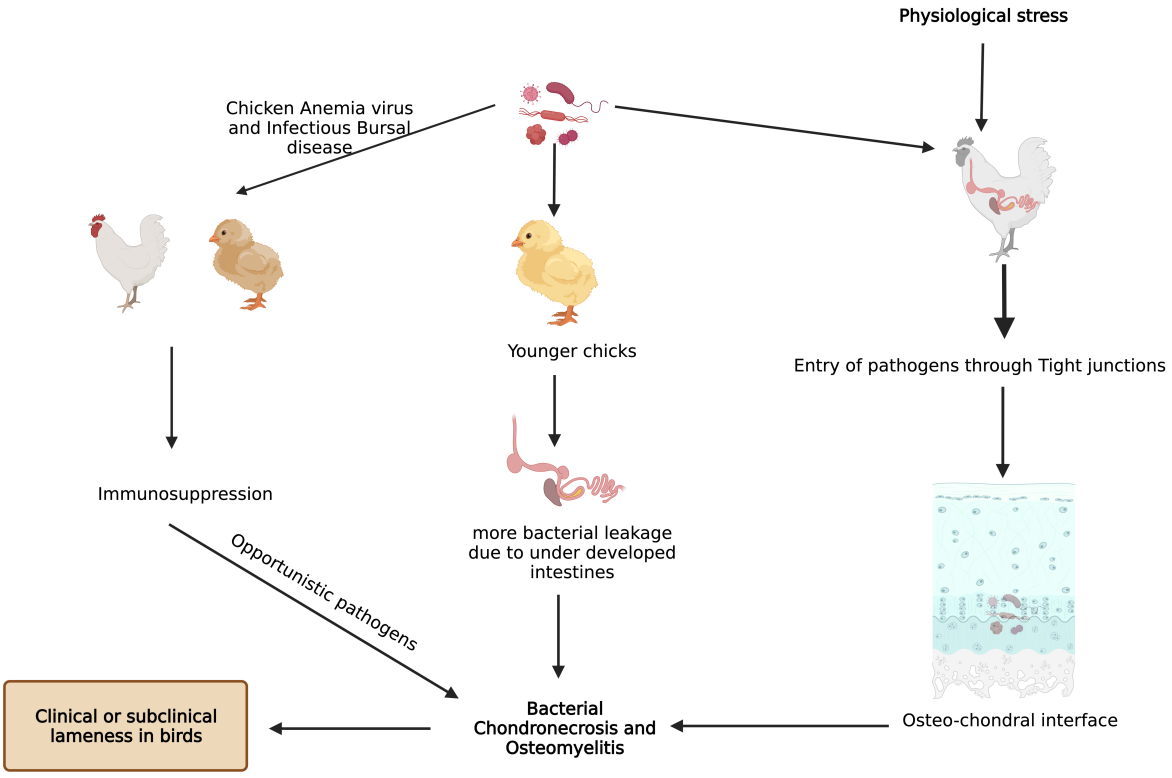

Figure 2.3. Factors affecting incidence of lameness.

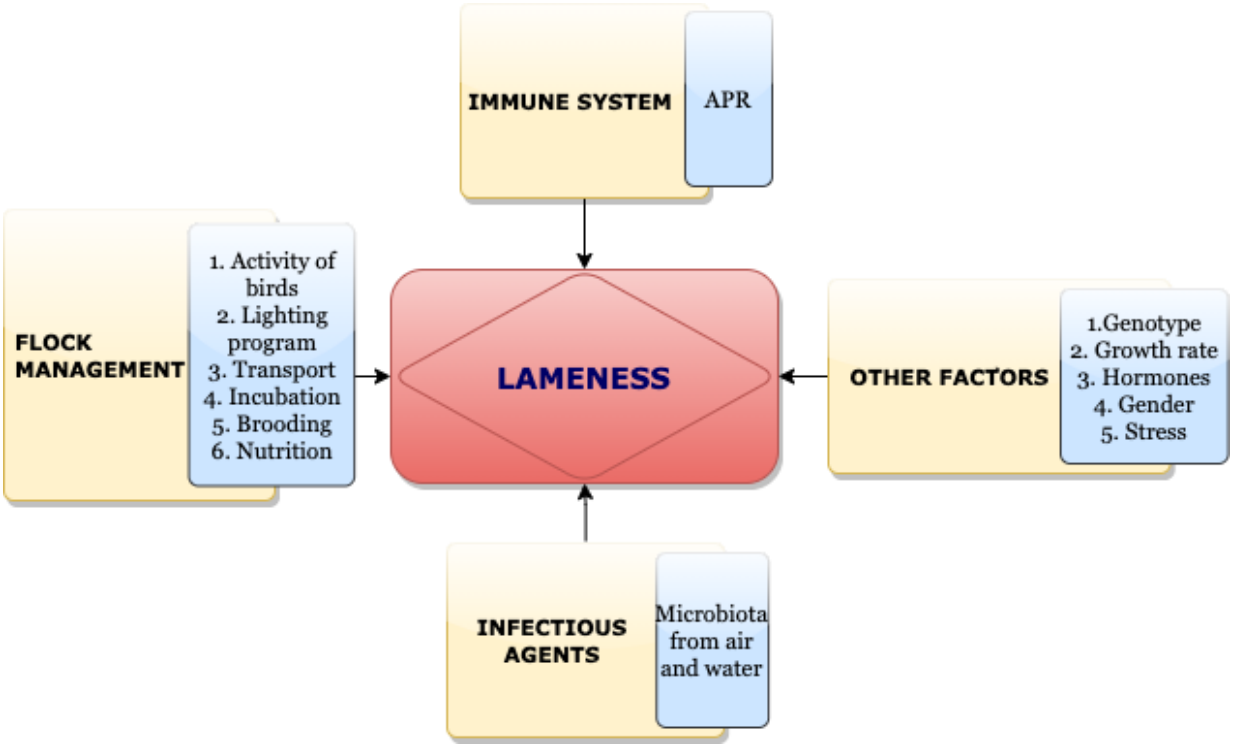

Figure 2.4 Mechanisms during pre and postnatal development of chicken increasing incidence of BCO

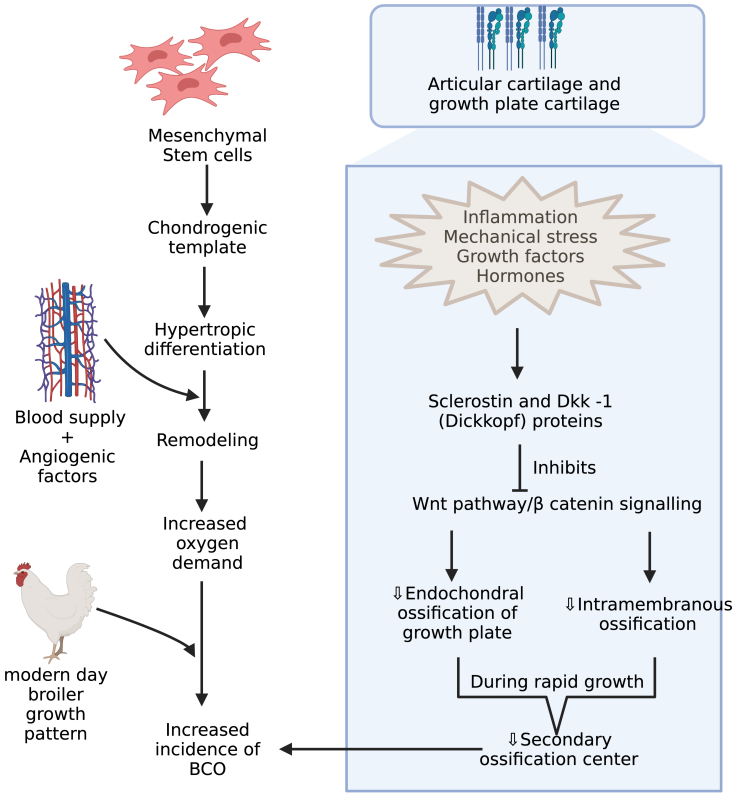

Figure 2.5 DICER 1 dysregulation in the presence of bacteria causing break in bone homeostasis.

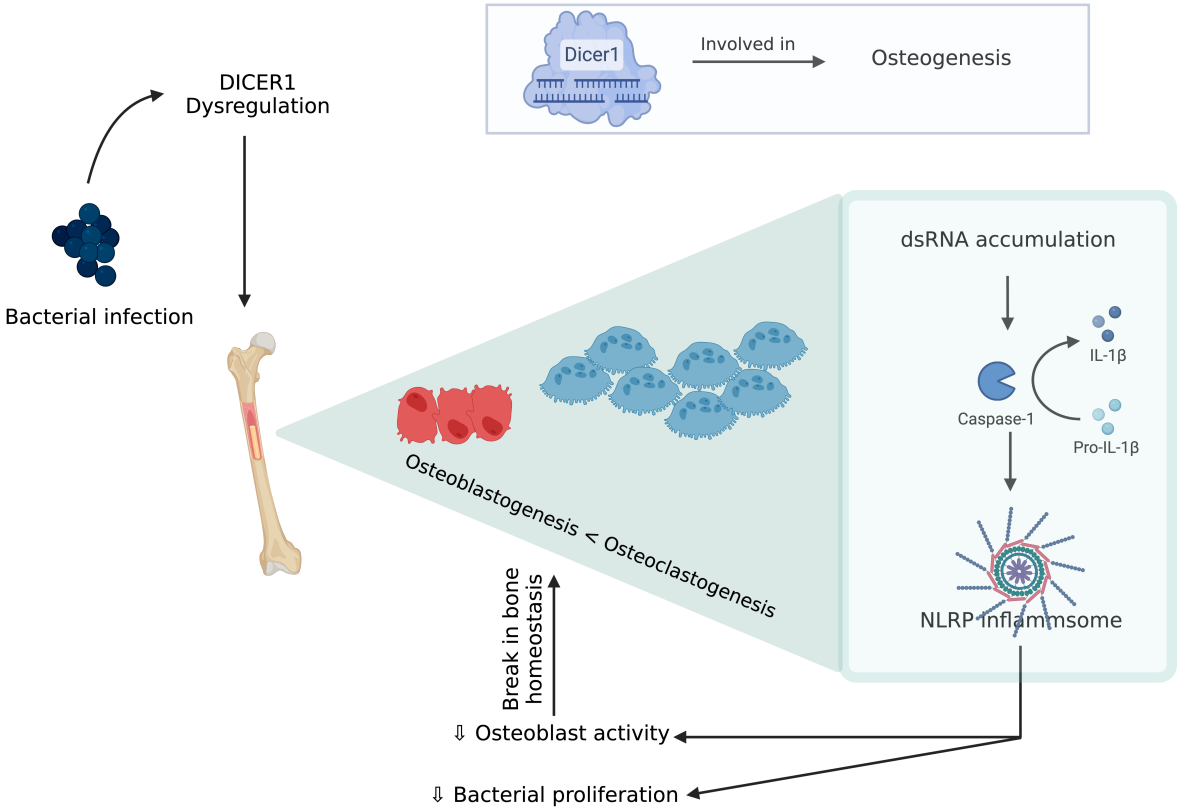

CHAPTER 3

ALTERED OSTEOGENIC DIFFERENTIATION IN MESENCHYMAL STEM CELLS ISOLATED FROM COMPACT BONE OF CHICKEN TREATED WITH VARYING DOSES OF LIPOPOLYSACCHARIDES [1]

[1]Choppa, V. S. R., Liu, G., Tompkins, Y. H., & Kim, W. K. (2023). *Biomolecules*, *13*(11), 1626.

Reprinted here with permission of publisher.

ABSTRACT

Persistent inflammation biologically alters signaling molecules and ultimately affects osteogenic differentiation including modern-day broilers with unique physiology. Lipopolysaccharides (LPS) are gram-negative bacterial components that activate cells through transmembrane receptor activation and other molecules. Previous studies have shown several pathways associated with osteogenic inductive ability, but the pathway has yet to be deciphered, and the data related to the dose-dependent effect is limited. Primary Mesenchymal Stem Cells (MSCs) were isolated from the bones of day-old broiler chickens, and the current study focused on the dose-dependent variation (3.125 micrograms/ml to 50 micrograms/ml) on osteogenic differentiation and associated biomarkers in primary MSCs. The doses in this study were determined using the cell viability (MTT) assay. Study revealed that, osteogenic differentiation varied with dose, and the cells exposed to higher LPS were viable but lacked differentiating ability. However, this effect became transient with lower doses, and this phenotypic character was observed with differential staining methods like Alizarin red, Von Kossa, and Alkaline phosphatase. The data from this study revealed that LPS at varying doses had a varying effect on osteogenic differentiation through several pathways acting simultaneously during bone development.

INTRODUCTION

Genetic potential of chicken has increased with a need of global production of chicken meat, making the chicken more prone to skeletal disorders (Fornari et al. 2014; Mir et al. 2017; Weimer et al. 2019). These issues can only be alleviated by novel methods which can be achieved by the studies on mesenchymal stem cells (MSCs) to provide crucial insights for optimal skeletal development (Tompkins et al. 2023). This can be achieved by exploiting the ability of MSCs to

study mechanisms like tissue repair, homing potential for understanding the biology, as well as defining therapeutic targets (Melo et al. 2017; Sohni and Verfaillie 2013). Bone MSCs have strong self-renewal ability and multilineage differentiation potential with an important role in bone turnover and metabolism. In contrast, this will be affected by acute or chronic inflammatory mediators such as lipopolysaccharides (LPS). LPS is a gram-negative bacterial component that stimulates the immune system leading to systemic inflammation. These are usually released into circulation during dysbiosis and abundant gram-negative bacterial proliferation, which leads to strong inflammatory reactions even at low concentrations inducing sepsis in the host when translocated (Wassenaar and Zimmermann 2018). On the other hand, LPS activates TLR4-MD2 complex which further activates the NF-κB pathway, ultimately leading to production of cytokines and chemokines. Additionally, intracellular LPS can trigger cytokine release through LPS binding protein (LBP) which is independent of the former (Leimer et al. 2016; Page, Kell, and Pretorius 2022). Studies on osteogenic potential is limited to none in chicken isolated MSCs, but human MSCs studies revealed that TLR4 activation by LPS activates NF-κB and increases the proliferation and osteogenic differentiation (Herzmann et al. 2017). In congruity, similar studies have shown the effect of inflammatory mediators on proliferation, migration, and differentiation of MSCs (Croes et al. 2015). In contrast, Toll like receptor (TLR) 4 generates osteoclast activating cytokine when triggered by LPS stimulation besides having inhibitory effects on osteoblast differentiation (Bandow et al. 2010; Li et al. 2014). Besides, there are other important pathways which are involved in MSCs proliferation and differentiation like Wnt (Wingless Int) pathway and Dicer 1 (Endoribonuclease III) signaling (X.-J. Chen et al. 2019; Greene et al. 2019; Houschyar et al. 2019). As a strong activator of immune system through their release into circulation during septicemia, LPS must be investigated in terms of dose dependent and prolonged response of MSCs

in their osteogenic potential and immunological responses. This study was focused on effects of varying LPS doses on osteogenic differentiation and pathways affecting this process. The objective **(Figure 3.1)** of this study was to establish an invitro model for inflammation associated with bone diseases besides understanding the pathways being involved which will assist the researchers in application of compounds targeting them.

MATERIALS AND METHODS

Animal use and ethics statement

The investigation was conducted according to the ARRIVE guidelines, and all experimental procedures and animal utilization were authorized by the Institutional Animal Care and Use Committee at the University of Georgia, Athens, GA

Isolation of MSCs

MSCs isolation was carried out using previously described methods (Adhikari et al. 2019a). After cervical dislocation, bones from the day-old chicks' femurs and tibias from both legs were taken. Following cervical dislocation, the birds were immersed in alcohol for two minutes. Legs were taken off the metacarpal and hip joints. Dissected legs were kept in DMEM (Corning, NY, USA) containing 10% Fetal Bovine Serum (FBS), 100 U/mL penicillin, 100 g/mL streptomycin, and 0.292 mg/mL L-glutamine (Thermo Fisher Scientific, MA, USA) until connective tissues and muscles were completely removed. A scalpel and micro-dissecting scissors were used in a bio-safety cabinet to immediately remove the muscles and connective tissues surrounding the tibia and femurs. The process involved preparing tibia and femur bones by washing them with a buffer solution containing Phosphate-Buffer Saline (PBS) (Corning) and 2% FBS (Hyclone laboratories Inc., Logan, UT). The bones were then cracked open to remove the

bone marrow, which was flushed out with the same buffer solution. The bones were washed again to ensure all bone marrow cells were removed and were then transferred to a cell culture dish containing a digestion medium composed of DMEM, penicillin, streptomycin, collagenase (Sigma-Aldrich, St. Louis, MO, USA), and FBS. The bones were chopped into smaller fragments and digested in a shaking water bath at 37°C for 60 minutes. The resulting mixture was filtered, and the bone fragments were rinsed with 10% DMEM before being centrifuged. The supernatant was discarded, and the remaining cells were suspended in 10% DMEM and plated in two 100-mm cell culture dishes. The cells were cultured in a humidified incubator containing 5% CO2 (NuAire, Plymouth, MN, USA), with the media being changed every 2-3 days. Once the cells reached 95% confluency, they were washed and subcultured at a ratio of 25,000 cells/cm2 in new 100-mm cell culture dishes, which were marked as P1. Subsequent cultures were named P2, P3, P4, and so on. P4 cells were used for the MSC differentiation experiments. The procedure followed in this study was summarized and depicted in the **Figure 3.2** below.

Cell viability Assay

Cell viability was assessed using cellular 3-(4,5-dimethylthiazol-2-yl)-2,5-diphenyltetrazolium bromide (MTT) kits (Cayman Chemical in Ann Arbor, MI, USA). The cells were planted in 96-well black well culture plates containing differentiation medium at a concentration of 5×10^4 cells/100 μL. In the current study, the impact of treating MSCs with various concentrations of LPS (3.25, 6.25, 12.5, 25, 50, 100, and 200 μg/ml, Sigma-Aldrich) was analyzed during the culture period. Cells were exposed to different LPS treatments for 24 and 48 hours in the dark, but the MTT viability assay was not performed for longer periods due to high cell density, which led to high absorbance readings that impeded detection accuracy. DMEM with 10% MTT was added and incubated for 4 hours, after which the culture medium was removed

completely. The generated formazan was dissolved using 100 µl dimethyl sulfoxide (DMSO; Sigma-Aldrich) to create a purple color, and the plates were positioned on an orbital shaker (VWR) set at a low-speed setting for 5 minutes. The microplate reader (BioTek, Winooski, VT, United States) was used to measure the absorbance at 570 nm.

Osteogenic differentiation

The cMSCs that were at P4 were put into 24-well plates at a density of 20,000 cells/cm2 for Alizarin Red S (AZ), Alkaline Phosphate (ALP), and Von Kossa (VK) stain, and in 6-well plates to measure osteogenic gene regulation. These cells were cultured in basal media that contained DMEM, 10% FBS, 100 IU/ml penicillin, and 100 µg/ml streptomycin until they reached 90% confluency. Once they were confluent, they were treated with osteogenic media that contained DMEM with 10^{-7}M dexamethasone (DXA), 10 mM β-glycerophosphate, 50 µg/ml ascorbate, and 5% FBS to induce osteogenesis. Cells cultured in DMEM basal media with 10% FBS were used as a negative control. Fresh media were replaced with the old media in the culture plate every 3 days. The cells were stained with AR and VK for detection of mineralization and for ALP to measure osteogenic differentiation on days 7 and 14 of treatment.

Alizarin red S staining (AZ) and Mineral deposit quantification

In this study, the level of mineralization in chicken MSCs was measured using a technique called Alizarin red S staining(Adhikari et al. 2019b; Tompkins et al. 2023). The cells were initially cultured in 24-well plates coated with gelatin and incubated in a growth medium until they reached full confluency. Next, the cells were exposed to LPS in osteogenic differentiation medium for 7 and 14 days. On each day of staining, the cells were fixed with neutral buffered formalin and then stained with Alizarin red S (Sigma-Aldrich, St. Louis, MO). Mineralized nodules were identified

as dark red spots which were captured in 4X magnification using a microscope (Keyence BZ-X800, Keyence corp, Itasca, IL).

Alkaline phosphatase expression assay

Alkaline phosphatase (ALP) expression was used in conjunction with the SIGMAFAST BCIP/NBT substrate (Sigma Aldrich, St. Louis, MO) to identify osteoblast differentiation(Adhikari et al. 2019b; Tompkins et al. 2023). A successful differentiation of MSC into osteoblasts is indicated by ALP activity(Adhikari et al. 2019b; C. Chen et al. 2021). When given BCIP/NBT as a substrate, differentiated osteoblasts were stained in blue violet while undifferentiated MSCs had less intense color which indicated weak alkaline phosphatase (ALP) activity. Cells were cleaned in PBS before being fixed in pre-cooled methanol for five minutes at -20°C. After that, the sample was rinsed with distilled H2O before being incubated with dissolved SIGMAFAST BCIP/NBT substrate for 10 min at room temperature with steady agitation on a plate shaker. The cells were washed with distilled H2O after the stain solution was withdrawn, and images were taken right away using a microscope (Keyence BZ-X800, Keyence corp, Itasca, IL) while the cells were kept wet.

Von Kossa staining

The cells in the culture plates were washed with PBS and fixed with 0.1% glutaraldehyde in PBS for 15 minutes at room temperature at different time points(C. Chen et al. 2021; Tompkins et al. 2023). Then, the cells were washed with distilled water and exposed to 5% silver nitrate for 30 minutes. After washing the cells with distilled water and air-drying, they were exposed to bright light until black color appeared in the calcified areas. Images of the cell culture plates were taken using a microscope with a camera at 4x magnification (Keyence BZ-X800, Keyence corp, Itasca, IL).

Cellular ROS assay

Intracellular ROS formation was evaluated using DCFDA/H2DCFDA-Cellular ROS Assay kits (ab113852, ABCAM, USA). Manufacturer's instructions were followed to perform this assay at 1, 2.5, and 4 hr after treatments.

Gene Expression

Cells plated in 6-well plates were harvested from 6, 12, 24, and 48 hours to analyze gene expression of bone formation and resorption markers using Quantitative Reverse Transcription Polymerase Chain Reaction (qRT-PCR). To detect osteogenic differentiation of cMSCs, mRNA expression of Runt-related transcription factor 2 (RUNX2) and Bone Morphogenetic Protein (BMP2) was analyzed. RNA was isolated from the cells using QIAzol lysis reagents, and the quantity of RNA was determined using a Nano-Drop 1000 Spectrophotometer. The high-capacity cDNA reverse transcription kits were used to synthesize cDNA from 2000 ng of total RNA. mRNA expression was measured using qRT-PCR with primers designed using the Primer-BLAST program. The specificity of the primers was validated by PCR product sequencing. The qRT-PCR was performed in an Applied Biosystems StepOnePlus™ using iTaq™ universal SYBR Green Supermix with melting curve analysis and gel electrophoresis used to verify primer quality. The qRT-PCR conditions were the same for all genes. These conditions included an initial denaturation at 95°C for 10 min, followed by 40 cycles at 95°C for 15 s, annealing temperature for 20 s, and extending at 72°C for 1 min. The primers used in this study are listed in the **Table 3.1**.

Statistical Analysis

Statistical analysis was performed using the ANOVA of the JMP® Pro 16 software (SAS institute, Cary, NC, 2023). Mean separation test was conducted using Tukey test. and $P \leq 0.05$ was considered as statistically significant among the groups.

RESULTS

Cell viability, Osteogenic differentiation, and ROS production

The LPS doses in this study were decided based on the results obtained from MTT assay (cell viability assay) **(Figure 3.3)**. Chicken MSCs were treated with doses starting from 3.125 to 200 μg/ml in osteogenic medium for 6, 12, and 24 h. The trend in this assay was similar at all the time points. Precisely, when compared with growth media the viability percentage for DM was nearly 165 and the viability for 3.125, 6.125, 12.5, 25, 50, 100, and 200 μg/ml dose of LPS at 6 h time point was nearly 190, 180, 145, 131, 133, 108, and 56 respectively. Additionally, for 12 h time point viability for the above doses were 239, 407, 377, 310, 278, 229, 228, 112 % respectively but these values at 24 h was 107.5, 96, 111, 108, 105, 95, 48, 19 % respectively. By the end of 24 h and 48 h, 200 μg/ml showed significant reduction in cell viability by less than 25% and 50 % ($p < 0.05$; **Figure 3.3**). Varying statistically significant differences were observed between the remaining doses but not much among 3.125, 6.25, 12.5, 25 and 50 μg/ml. Hence the above doses were considered for the current study. Seeded mesenchymal stem cells were then subjected to osteogenic differentiation and stained for Alizarin Red, Von Kossa, and Alkaline Phosphatase. From these staining methods, a decrease in osteogenic differentiation was observed from 3.125 μg/ml to 50 μg/ml on day 7 (Figure not shown) and day 14 **(Figure 3.4)**. Furthermore, the relation between intracellular ROS and the osteogenic differentiation was evaluated by cellular DCFDA

assay, and images are presented in **Figure 3.5.** ROS response was observed at 2.5 h, 12.5 μg/ml shown a significant increase compared to DM and this was significantly lower for 50 μg/ml compared to 12.5 and 25 μg/ml (p <0.05) at 12.5 μg/ml but not at the higher doses (25 and 50 μg/ml). At 4 h of treatment with varying doses observable changes are seen in **Figure 3.5**, showing that ROS response was higher in 12.5 and 25 μg/ml but not much significant differences in quantified data. In contrast, there are significant differences with 12.5 μg/ml compared to 6.25 and 50 μg/ml.

mRNA expression of CASP8 (pro-apoptotic marker) and transcription factor Nrf2 (major regulator of antioxidant and cellular protective genes) were observed at 24 and 48 h from the addition of treatments. The data indicated that the dose dependent decrease in CASP8 gene expression at 24 h, but this was significantly (p value <0.05) upregulated at 3.125 μg/ml **(Figure 3.6)**. Furthermore, NRF2 was significantly upregulated by lower doses (3.125 and 6.25 μg/ml) at 24 h (p value <0.05) but controls and other treatments were not significant but there was an increase in gene expression in treatments compared to controls.

Inflammatory pathways

Pro inflammatory cytokine, IL-1β (Interleukin 1β) was upregulated with 3000 and 6000-fold increase in gene expression at 25 and 50 μg/ml doses respectively in both 24 h (p value <0.05) and greater than 100-fold increase at 48 h (p value <0.05) **(Figure 3.7)**. Moreover, Toll-Like Receptor 4 (TLR4) signal pathway plays a key role in triggering the innate immune response and this is responsible for acute and chronic inflammatory disorders which is due to the activation of early phase nuclear factor-κB (NF-κB) which further leads to production of inflammatory cytokines. The current study shown a significant upregulation (nearly 50-fold increase) of TLR4

at 3.125 μg/ml compared to 50 μg/ml of LPS (p value <0.05) **(Figure 3.7)**. Additionally, NF-κB expression was not significant (data not shown). DICER 1, endoribonuclease that regulates miRNA maturation has shown greater than 100-fold increase with 3.125 μg/ml and nearly 150-fold increase at 24 h (p value <0.05) **(Figure 3.7)**.

Wnt signaling and bone homeostasis

Canonical Wnt signaling pathway is associated with osteoblast early and ultimate differentiation stages, but the physiological balance should be met to positively promote osteoblastogenesis. Dysregulated elevation of LRP5 – Wnt signaling is associated with the more bone synthesis with normal resorption, but deficiency leads to inhibition of canonical Wnt signaling. The Lipoprotein receptor protein (LRP5) gene expression was significantly upregulated with nearly 80-fold and 70-fold at 3.125 and 6.25 μg/ml respectively (p value <0.05). Similarly, this study showed that beta catenin at 24 h was significantly upregulated nearly 20-fold and 13-fold at 3.125 and 6.25 μg/ml respectively (p value <0.05) **(Figure 3.8)**. In contrast, Sclerostin (SOST) which is inhibitor of Wnt signaling pathway was significantly upregulated at nearly 250-fold with 3.125 μg/ml of LPS and 180-fold increase in gene expression with 6.25 μg/ml and followed by decrease in expression with increasing LPS doses (p value <0.05) **(Figure 3.8)**. In view of osteogenesis, Runx2 (runt-related transcription factors) is an upstream transcription factor (master regulator of osteogenesis) involved in osteoblast differentiation. This gene expression was not significant in MSCs subjected to LPS doses (data not shown). BMP2 is an upstream to RUNX2 and are potent osteogenic agents responsible for maturation of mesenchymal osteoprogenitor cells to osteoblasts. BMP signaling is responsible for RUNX2 transcriptional activity. Treatments have not shown significant differences with all LPS doses at 24 and 48 h (data not shown) (p value =0.3580, 0.5316). BMP's osteogenic role is activating SMAD1 and mediating Runx2 expression,

this study shown an upregulation of SMAD1 signaling at 3.125 μg/ml LPS (nearly 70-fold) (*p* value <0.05) and 80-fold increase with 6.25 μg/ml **(Figure 3.9)**. Osteoprotegerin (OPG), which is a decoy receptor for RANKL to inhibit osteoclastogenesis and osteoclast activation, was not significant (data not shown) (*p* value =0.0615). In contrast, RANKL expression was significantly upregulated at 3.125 (100-fold increase) and 6.25 μg/ml (40-fold) at 24 h (*p* value <0.05) but not significant at 48 h treatment (data not shown) (*p* value =0.7545) **(Figure 3.9)** which indicates higher expression of RANKL favoring osteoclastogenesis. These results indicate the potential roles of LPS on bone formation and bone resorption by regulating Wnt signaling and osteoclastogenesis; LPS potentially reduces osteogenic differentiation and increase osteoclastogenesis.

DISCUSSION

The interaction between the immune system and bone development were confirmed by several researchers and by previous studies which provided a great insight in developing new mitigating strategies against inflammatory bone homeostasis dysregulation (Sharma et al. 2022; Tompkins et al. 2023). Surprisingly, limited or none of the studies provided the dose dependent effect of bacterial LPS on chicken MSCs or human derived MSCs which would help in alleviating the issues associated with this pathogenic factor at different doses. In this study, dose dependent variation of osteogenic differentiation was observed, and the data revealed that the immune and differentiation response greatly varies with nidus of inflammatory stimulus. Higher doses in this study (50 μg/ml) of LPS have affected the osteogenic differentiation greatly with mere mineralization on days 7 and 14 without affecting the cell viability. Moreover, there is decreased osteogenic potential with subsequent lowering of LPS doses. Cell viability was not affected by the LPS dosing from 3.125 μg/ml to 50 μg/ml, indicating their potential to be a valuable tool to conduct such as inflammation research, and the current finding agrees with a study conducted on

human bone marrow derived MSCs. Osteogenic differentiation staining revealed that higher doses of LPS affected MSCs lowering their osteogenic potential but shown a dose dependent increase in mineralization with decreasing doses of LPS. LPS at 10 μg/ml on human periodontal ligament stem cells impaired the osteogenic differentiation ability but not with human bone marrow MSCs (Li et al. 2014). This study revealed the underlying mechanisms behind the effect of LPS on osteogenic differentiation when treated with various doses.

Inflammatory pathways

The current study shown increased gene expression of IL-1β with increase in LPS dose which might be due to dysregulation of DICER 1 even in the presence of higher doses of LPS which leads to accumulation of double stranded RNA (dsRNA) which trigger the formation of IL-1β from pro- IL-1β. In contrast, lower doses of LPS have shown an increased gene expression which could have provided some protective effect preventing the dsRNA accumulation which further prevent IL-1β formation (Greene et al. 2019; Zheng et al. 2017; Zhou et al. 2016). This mechanism was reported to play key role in osteogenesis and shown dysregulation in several human diseases thus leading to break in bone homeostasis (J.-F. Chen et al. 2008; Choppa and Kim 2023; Greene et al. 2019). TLR4, a transmembrane receptor was upregulated in lower doses but not at higher doses indicates that the effect of high doses might be transient and follows a different pathway like DICER dysregulation leading to elevated gene expression with higher LPS doses. Furthermore, the literature related to transient effect of LPS was not found but a study on rats in liver mRNA expression at higher and lower LPS doses was elevated (Al-Aalim, Al-Iedani, and Hamad 2021). Additionally, mRNA expression of pro-inflammatory cytokines was limited in muscle compared to liver, spleen, and kidney in rats injected with LPS intraperitoneally indicating that the TLR4 activation varies based on type of tissue and origin of cells although dose dependent

relation was also limited to none (Lang et al. 2003). The data from the current study revealed the role of DICER 1 dysregulation in higher gene expression of pro inflammatory cytokine (IL-1β) but a contrasting observation with respect to TLR4 mRNA expression which reveals the effect of LPS at higher doses would be transient but dysregulates DICER1 signaling.

Some studies reported the increase in superoxide production in mitochondria along with decrease in osteogenic differentiation which is due to activation of inflammasome and IL-1β release (Ma et al. 2018). In contrast, the current study found that the ROS response has increased at 12.5 μg/ml but not at higher doses or other doses with 2.5 and 4 h treatments. This indicates that ROS generation at higher doses would be momentary and would release greater amounts of IL-1β which was observed in the current data along with the release of this cytokine at relatively very scarce amounts even though there was ROS generation at 3.125, 6.25, and 12.5 μg/ml. These findings are different from the other studies because those studies found ROS generation will activate inflammasome and induce NF-κB pathway activation. This hold true in this study since the NF-κB along with NLRP inflammasome gene expression was insignificant (Data not shown) which revealed that the DICER 1 pathway takes upper hand when compared with other pathways leading to higher IL-1β gene expression and thus a reduction in osteogenic differentiation of MSCs. On the other hand, findings in this study could be because ROS assay was analyzed at 2.5 and 4 h, but IL-1β was observed at 24 and 48 h (Smeekens et al. 2014; van de Veerdonk et al. 2010). Microenvironment surrounding MSCs can alter the physiology and osteogenic differentiation like regulating the polarization of macrophages and enhanced immunosuppressive effects but this is still undeciphered (Fan et al. 2012; Ti et al. 2015). Evidence shows, upregulation of pro-inflammatory cytokines is to enhance the cell plasticity along with immune regulatory characteristics but this depends on the concentration of cytokines (Barrachina et al. 2017). The

current study found the upregulation of IL-1β, which may affect the microenvironment, thus affecting the osteogenic differentiation by downregulating the SMAD1 which agrees with the previous statement.

Wnt signaling pathway

Wnt signaling is an important pathway in tissue homeostasis and abnormal signaling leads to degenerative diseases. Furthermore, activation of this pathway stimulated by the pathogens reduce several molecular inflammatory processes (Shi et al. 2016). Current study shown that the Wnt signaling was also compromised which was observed with LRP5 and beta catenin downregulation by increasing LPS doses in all treatments. Studies shown that Wnt/beta catenin cascade activation results in mesenchymal precursors to osteoblast differentiation where the inhibition leads to impaired growth (Gao et al. 2013; Glass et al. 2005; Zhong et al. 2012). At lower LPS doses like 3.125, 6.25, 12.5 μg/ml there was upregulation of beta catenin and LRP5 Receptor gene expression which reveals that lower doses of LPS should be able to trigger the osteogenic differentiation but this is in contrast to findings from other studies (Choppa and Kim 2023; Houschyar et al. 2019; Shi et al. 2016). In contrast, the data shown that the sclerostin mRNA expression was upregulated with lower LPS doses (3.125, 6.25, 12.5 μg/ml), which indicates the inhibitory role in Wnt signaling pathway by creating a negative feedback loop of osteogenesis by binding to LRP5 receptor which reveals that the trigger from LRP5 and beta catenin activation which supports the osteogenic differentiation will be inhibited due to significantly higher gene expression of sclerostin. Furthermore, this leads to decreased mineralization compared to the solely differentiation media treated MSCs conclusively affecting the proliferation and differentiation of MSCs (Gao et al. 2013; Zhong et al. 2012). Finally, the current study shows that several pathways which are illustrated in Figure19 are synergistic and linked to each other in

causing the decrease in osteogenic potential, but this varies with dose of LPS. This evidently indicates the role of role of Wnt signaling pathway in regulating the bone formation along with role of sclerostin in countering the Wnt pathway at lower doses of LPS coupled with DICER1 dysregulation affecting bone formation at higher doses of LPS.

Bone formation and resorption

Bone formation and remodeling are key processes involved to aid the cells like MSCs to adapt to the microenvironment and external stimuli. This homeostasis in bone remodeling is maintained through bone resorption by osteoclast and bone formation through osteoblasts which are maintained by RANKL, Smad1, DICER1 and Wnt signaling pathways which were described in the current study. Smad is an intracellular signaling protein which phosphorylates Transforming growth factor(TGF)-β and bone morphogenic proteins (BMPs) which acts on transcription factors like RunX2 and Osx which crucial in osteogenic differentiation of MSCs (C. Chen et al. 2021; Choppa and Kim 2023; Subramaniam et al. 2023). The current study has shown higher mRNA expression of Smad1 with lower doses of LPS (3.125, 6.25, 12.5 μg/ml) indicating the increase in bone formation but RUNX2 which is key transcription factor was insignificant which shows incongruity of this factor with the intracellular signaling molecule (Smad1). These findings indicates that, even with the increase in gene expression of Smad1 RUNX2 recruitment was not in synchrony thus leading relatively lesser mineralization compared to the positive control (DM). Furthermore, some studies proved the relation between Smad and RUNX2 along the higher expression of the latter in inducing osteogenic potential (Bai et al. 2020). The current study revealed that the Smad1 mRNA expression would not necessarily lead to transcription of downstream regulators like RUNX2. Additionally, this also might be linked to Wnt signaling and other inflammatory triggers to promote osteogenesis.

Secondly, the other important component of remodeling is bone resorption. RANKL (receptor activator of nuclear factor-κB), an important gene expression marker and primary regulator involved in bone resorption (Choppa and Kim 2023; Matsumoto et al. 2017). The gene expression of RANKL was significantly upregulated with lower doses (3.125, and 6.25 μg/ml) indicating the potential activation of resorbing cells at these doses which would represent the turnover with respect to bone homeostasis. This statement was supported by the gene expression of Smad1 which was shown the former paragraph. This increased gene expression of Smad1 and RANKL represents heightened scope for bone formation and resorption respectively, but this trend was similar in other doses of LPS with gene expression weakening with increase in LPS. In contrast to the statements supporting the ability of RANKL to resorb a bone, anabolic effect was observed from vesicular RANK and RANKL binding peptides but less in RANKL deficient osteoblasts (Ikebuchi et al. 2018). The data from the current study revealed the RANKL is lenient towards the resorption or would also be supporting the bone formation (anabolic effect) in lower doses of LPS (3.125, and 6.25 μg/ml) compared to other.

CONCLUSION

MSCs, which have potential to differentiate into osteoblasts, can be an excellent model to provides valuable insight in resolving the issues in the bone related diseases besides concerns in poultry industry, especially bacterial chondronecrosis and osteomyelitis. This study suggests that these pathways discussed in the current study are all linked to each other in the MSCs microenvironment which significantly affects the osteogenic differentiation. Additionally, the varied response with different doses of LPS showed the synchronized mechanisms in altering the bone homeostasis. Furthermore, these varied at higher and lower levels of LPS. Precisely, lower doses of LPS affected bone homeostasis through the inhibition of Wnt signaling from Sclerostin

and higher levels of LPS were affected from IL-1β pathway which could be related to DICER1 dysregulation. Although there are limitations in deciphering some issues, the data obtained in this study have provided the potential therapeutic targets at various levels of LPS which can be related with inflammatory bone diseases in several fields including poultry industry.

REFERENCES

Adhikari, Roshan et al. 2019a. "Isolation and Differentiation of Mesenchymal Stem Cells from Broiler Chicken Compact Bones." *Frontiers in Physiology* 10(JAN).

———. 2019b. "Isolation and Differentiation of Mesenchymal Stem Cells from Broiler Chicken Compact Bones." *Frontiers in physiology* 9: 1892.

Al-Aalim, Ammar M, Ali A Al-Iedani, and Mohammad A Hamad. 2021. "Study of the Effects of Escherichia Coli Lipopolysaccharide on Innate Immunity: The Expression Profile of TLR4 and CD14 Genes in Rat Liver." *Open Veterinary Journal* 11(4): 771–79.

Bai, Jiaxiang et al. 2020. "Biomimetic Osteogenic Peptide with Mussel Adhesion and Osteoimmunomodulatory Functions to Ameliorate Interfacial Osseointegration under Chronic Inflammation." *Biomaterials* 255: 120197.

Bandow, Kenjiro et al. 2010. "Molecular Mechanisms of the Inhibitory Effect of Lipopolysaccharide (LPS) on Osteoblast Differentiation." *Biochemical and biophysical research communications* 402(4): 755–61.

Barrachina, Laura et al. 2017. "Inflammation Affects the Viability and Plasticity of Equine Mesenchymal Stem Cells: Possible Implications in Intra-Articular Treatments." *Journal of Veterinary Science* 18(1): 39–49.

Chen, Chongxiao, Roshan Adhikari, Dima Lynn White, and Woo Kyun Kim. 2021. “Role of 1,25-Dihydroxyvitamin D(3) on Osteogenic Differentiation and Mineralization of Chicken Mesenchymal Stem Cells.” *Frontiers in physiology* 12: 479596. https://pubmed.ncbi.nlm.nih.gov/33597893.

Chen, Jian-Fu et al. 2008. “Targeted Deletion of Dicer in the Heart Leads to Dilated Cardiomyopathy and Heart Failure.” *Proceedings of the National Academy of Sciences* 105(6): 2111–16.

Chen, Xiao-Jun et al. 2019. “Polydatin Promotes the Osteogenic Differentiation of Human Bone Mesenchymal Stem Cells by Activating the BMP2-Wnt/β-Catenin Signaling Pathway.” *Biomedicine & Pharmacotherapy* 112: 108746.

Choppa, Venkata Sesha Reddy, and Woo Kyun Kim. 2023. “A Review on Pathophysiology, and Molecular Mechanisms of Bacterial Chondronecrosis and Osteomyelitis in Commercial Broilers.” *Biomolecules* 13(7): 1032.

Croes, Michiel et al. 2015. “Proinflammatory Mediators Enhance the Osteogenesis of Human Mesenchymal Stem Cells after Lineage Commitment.” *PloS one* 10(7): e0132781.

Fan, Hongye et al. 2012. “Pre-Treatment with IL-1β Enhances the Efficacy of MSC Transplantation in DSS-Induced Colitis.” *Cellular & molecular immunology* 9(6): 473–81.

Fornari, Marcelo B et al. 2014. “Unraveling the Associations of Osteoprotegerin Gene with Production Traits in a Paternal Broiler Line.” *SpringerPlus* 3: 1–8.

Gao, Yanhong et al. 2013. “Crosstalk between Wnt/β-Catenin and Estrogen Receptor Signaling Synergistically Promotes Osteogenic Differentiation of Mesenchymal Progenitor Cells.” *PloS one* 8(12): e82436.

Glass, Donald A et al. 2005. “Canonical Wnt Signaling in Differentiated Osteoblasts Controls Osteoclast Differentiation.” *Developmental cell* 8(5): 751–64.

Greene, Elizabeth et al. 2019. “Double-Stranded RNA Is a Novel Molecular Target in Osteomyelitis Pathogenesis: A Translational Avian Model for Human Bacterial Chondronecrosis with Osteomyelitis.” *American Journal of Pathology* 189(10): 2077–89.

Herzmann, Nicole, Achim Salamon, Tomas Fiedler, and Kirsten Peters. 2017. “Lipopolysaccharide Induces Proliferation and Osteogenic Differentiation of Adipose-Derived Mesenchymal Stromal Cells in Vitro via TLR4 Activation.” *Experimental cell research* 350(1): 115–22.

Houschyar, Khosrow S et al. 2019. “Wnt Pathway in Bone Repair and Regeneration–What Do We Know so Far.” *Frontiers in cell and developmental biology* 6: 170.

Ikebuchi, Yuki et al. 2018. “Coupling of Bone Resorption and Formation by RANKL Reverse Signalling.” *Nature* 561(7722): 195–200.

Lang, Charles H et al. 2003. “Endotoxin Stimulates in Vivo Expression of Inflammatory Cytokines Tumor Necrosis Factor Alpha, Interleukin-1β,-6, and High-Mobility-Group Protein-1 in Skeletal Muscle.” *Shock* 19(6): 538–46.

Leimer, Nadja et al. 2016. “Nonstable Staphylococcus Aureus Small-Colony Variants Are Induced by Low PH and Sensitized to Antimicrobial Therapy by Phagolysosomal Alkalinization.” *The Journal of infectious diseases* 213(2): 305–13.

Li, Chenghua et al. 2014. "Lipopolysaccharide Differentially Affects the Osteogenic Differentiation of Periodontal Ligament Stem Cells and Bone Marrow Mesenchymal Stem Cells through Toll-like Receptor 4 Mediated Nuclear Factor KB Pathway." *Stem cell research & therapy* 5(3): 1–13.

Ma, Jun et al. 2018. "Resveratrol Attenuates Lipopolysaccharides (LPS)-Induced Inhibition of Osteoblast Differentiation in MC3T3-E1 Cells." *Medical Science Monitor: International Medical Journal of Experimental and Clinical Research* 24: 2045.

Matsumoto, Yoshinori et al. 2017. "RANKL Coordinates Multiple Osteoclastogenic Pathways by Regulating Expression of Ubiquitin Ligase RNF146." *The Journal of clinical investigation* 127(4): 1303–15.

Melo, Fernanda Rosene et al. 2017. "Transplantation of Human Skin-Derived Mesenchymal Stromal Cells Improves Locomotor Recovery after Spinal Cord Injury in Rats." *Cellular and molecular neurobiology* 37: 941–47.

Mir, Nasir Akbar et al. 2017. "Determinants of Broiler Chicken Meat Quality and Factors Affecting Them: A Review." *Journal of food science and technology* 54: 2997–3009.

Page, Martin J, Douglas B Kell, and Etheresia Pretorius. 2022. "The Role of Lipopolysaccharide-Induced Cell Signalling in Chronic Inflammation." *Chronic Stress* 6: 24705470221076390.

Sharma, Milan K et al. 2022. "Effects of Mixed Eimeria Challenge on Performance, Body Composition, Intestinal Health, and Expression of Nutrient Transporter Genes of Hy-Line W-36 Pullets (0-6 Wks of Age)." *Poultry Science* 101(11): 102083.

Shi, Juan et al. 2016. “Emerging Role and Therapeutic Implication of Wnt Signaling Pathways in Autoimmune Diseases.” *Journal of immunology research* 2016.

Smeekens, Sanne P et al. 2014. “Reactive Oxygen Species-Independent Activation of the Interleukin-1β Inflammasome in Cells from Patients with Chronic Granulomatous Disease.” *Immunological and genetic components of the anti-Candida host immune response*: 157.

Sohni, Abhishek, and Catherine M Verfaillie. 2013. “Mesenchymal Stem Cells Migration Homing and Tracking.” *Stem cells international* 2013.

Subramaniam, Revatyambigai et al. 2023. “The Role and Mechanism of MicroRNA 21 in Osteogenesis: An Update.” *International journal of molecular sciences* 24(14): 11330.

Ti, Dongdong et al. 2015. “LPS-Preconditioned Mesenchymal Stromal Cells Modify Macrophage Polarization for Resolution of Chronic Inflammation via Exosome-Shuttled Let-7b.” *Journal of translational medicine* 13: 1–14.

Tompkins, Yuguo et al. 2023. “Effect of Hydrogen Oxide-Induced Oxidative Stress on Bone Formation in the Early Embryonic Development Stage of Chicken.” *Biomolecules* 13(1): 154.

van de Veerdonk, Frank L et al. 2010. “Reactive Oxygen Species–Independent Activation of the IL-1β Inflammasome in Cells from Patients with Chronic Granulomatous Disease.” *Proceedings of the National Academy of Sciences* 107(7): 3030–33.

Wassenaar, Trudy M, and Kurt Zimmermann. 2018. “Lipopolysaccharides in Food, Food Supplements, and Probiotics: Should We Be Worried?” *European Journal of Microbiology and Immunology* 8(3): 63–69.

Weimer, Shawna L et al. 2019. “The Utility of Infrared Thermography for Evaluating Lameness Attributable to Bacterial Chondronecrosis with Osteomyelitis.” *Poultry science* 98(4): 1575–88.

Zheng, Leilei et al. 2017. “Runx2/DICER/MiRNA Pathway in Regulating Osteogenesis.” *Journal of cellular physiology* 232(1): 182–91.

Zhong, Zhendong et al. 2012. “Wntless Functions in Mature Osteoblasts to Regulate Bone Mass.” *Proceedings of the National Academy of Sciences* 109(33): E2197–2204.

Zhou, Jie et al. 2016. “Dicer-Dependent Pathway Contribute to the Osteogenesis Mediated by Regulation of Runx2.” *American journal of translational research* 8(12): 5354.

Table 3.1 represents all the primers used in this study with their respective gene names, forward, reverse primers, and accession numbers.

Gene name	Accession number	F primer sequence	R primer sequence
BMP 2	NM_001398170.1	CCCCTACATGTTGGACCTC	CCCACTTGTTTCTGGCAGT
RUNX2	NM_204128.2	GTGGCCAGATTCAATGACCT	CCATCCACCGTCACCTTTAT
CTSK (Cathepsin K)	NM_204971.3	AGTCTGCCCTCCTTCCAGTT	CTTGATGATCCAGTGCTTGG
TNFSF11 (RANKL)	NM_001083361.2	GTCCAGCGTATTCTGGGAAA	GCAAAAGGTTGCTTCTCTGG
LRP5	NM_001012897.2	GGTGCCCCCTTATATGACAG	GATCAGTAGCTGGGGATGGA
TLR4	NM_001030693.2	ACTCTTGGGGTGCTGCTG	TGTCCTGTGCATCTGAAAG
Beta catenin (CTNNB1)	NM_205081.3	AGGGTGCTGAAGGTGTTGTC	GCTGGCTTGGATCTGTAAGG
DICER1 (ribonuclease 3)	NM_001040465.2	GACCTGACCAATCTCAACCAG	TTTGCCTTCCTCTTCTCAGC

		CCACGTCACCAAGAAG	GGTCCATCACCTTCT
NFKB2	NM_204413.2	AACA	TCAGC
NFE2L2		ATGCAGCTCTTGGCAGA	CTGGGTGGCTGAGT
(NRF-2)	NM_205117.2	AG	TTGATT
	NM_0010336	ACGCTTGTGCTCTTGGA	CAGCGTAGTACTGG
OPG	41.1	CAT	TCTGGG
	XM_0152974	TGCCTGCAGAAGAAGC	GACGGGCTCAAAAA
IL-1B	69.2	CTCG	CCTCCT
	XM_0049485	ATCCCACCTCCTGCCCA	GGTTCGGTTTGCTG
SOST	51	ACTCCATC	CTCCTGGCTC
		F-	R-
	XM_0406987	GTTTTGTAAAGGGTTGG	AATGCAGGAGCTTG
SMAD1	19.1	GGAGC	GGACCTTA
		CAACACAGTGCTGTCTG	ATCGTACTCCTGCTT
Beta actin	NM_205518.2	GTGGTA	GCTGATCC

Figure 3.1 illustrates the objective of the current study representing the source of LPS along with their effect hypothesized to establish an invitro model for understanding inflammatory bone diseases.

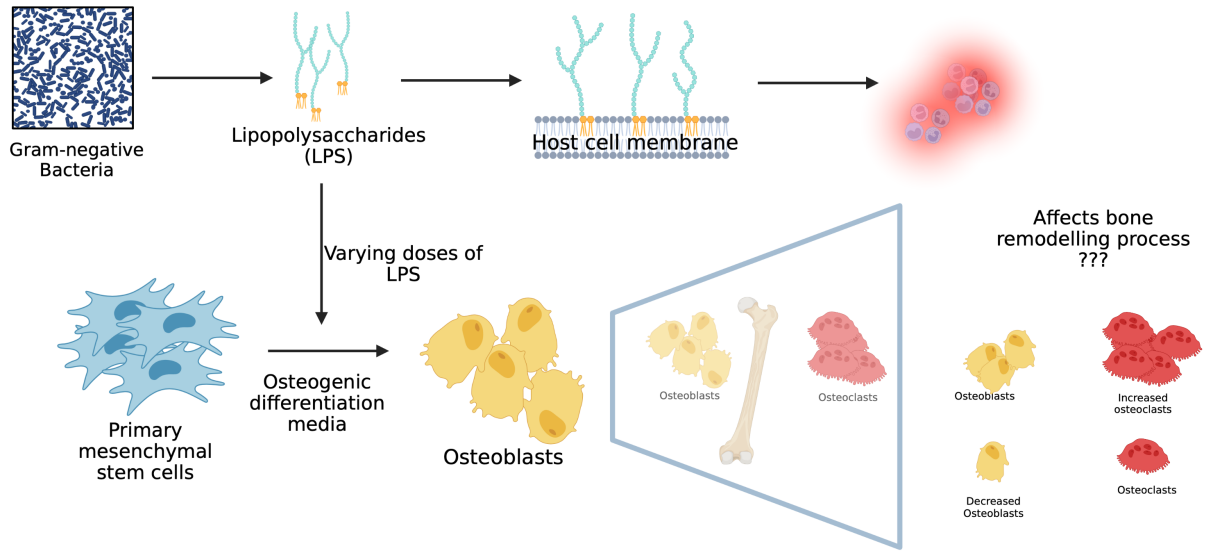

Figure 3.2 represents the protocol for isolating MSCS (Mesenchymal stem cells) from the compact bones of chicken.

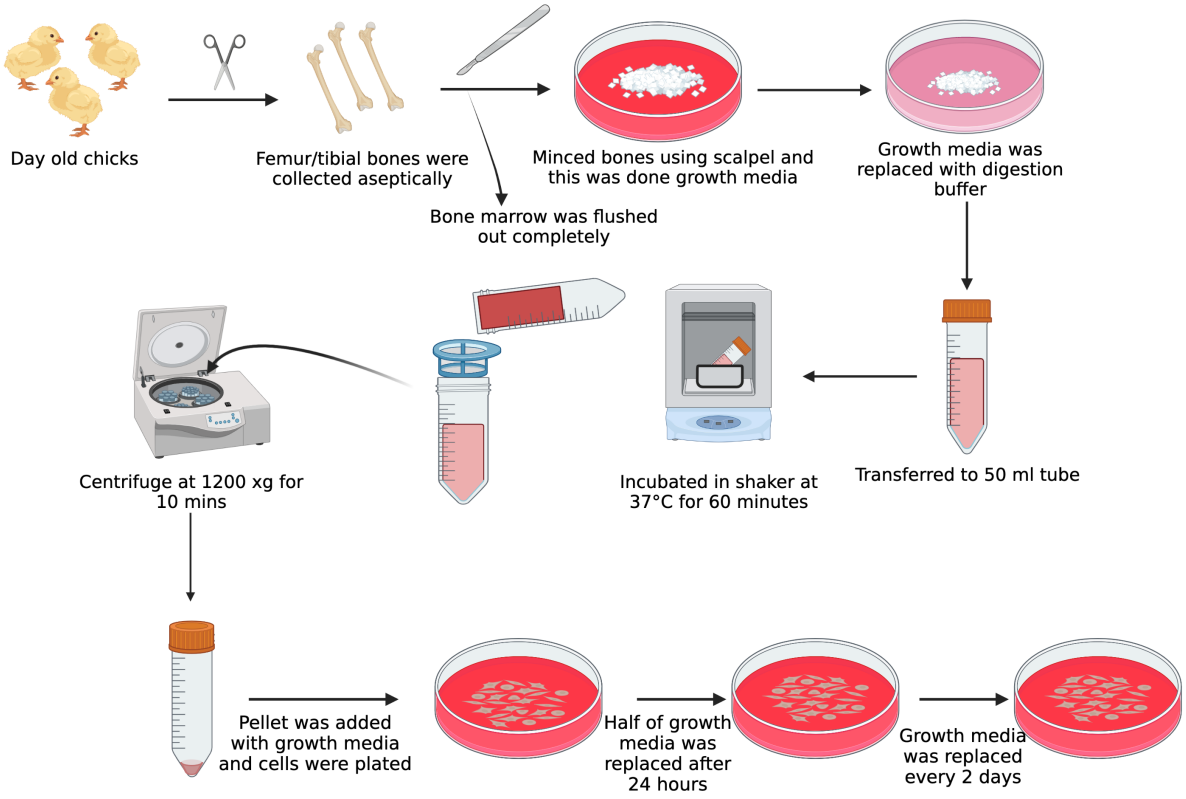

Figure 3.3 represents the cell viability assay when MSCs were treated with LPS conducted at 6, 12, 24, and 48 h. GM and DM are negative and positive controls respectively. Treatments with different letters indicate significant difference between treatments using Tukey's HSD test, $p < 0.05$. data shown includes mean ± SEM of 6 individual replicates (n=6).

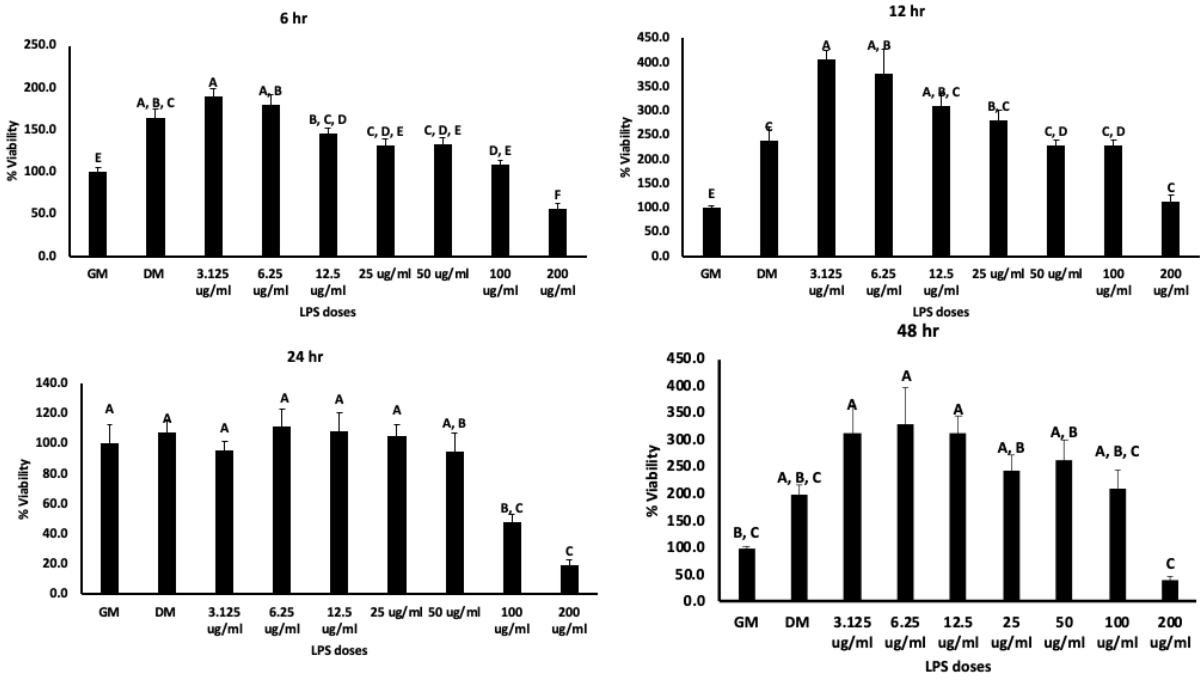

Figure 3.4 represents the osteogenic differentiation staining at day 14 which revealed the decrease in differentiation (A, C) and alkaline phosphatase activity (B) with increase in dose of lipopolysaccharide (LPS). GM and DM are negative and positive controls respectively.

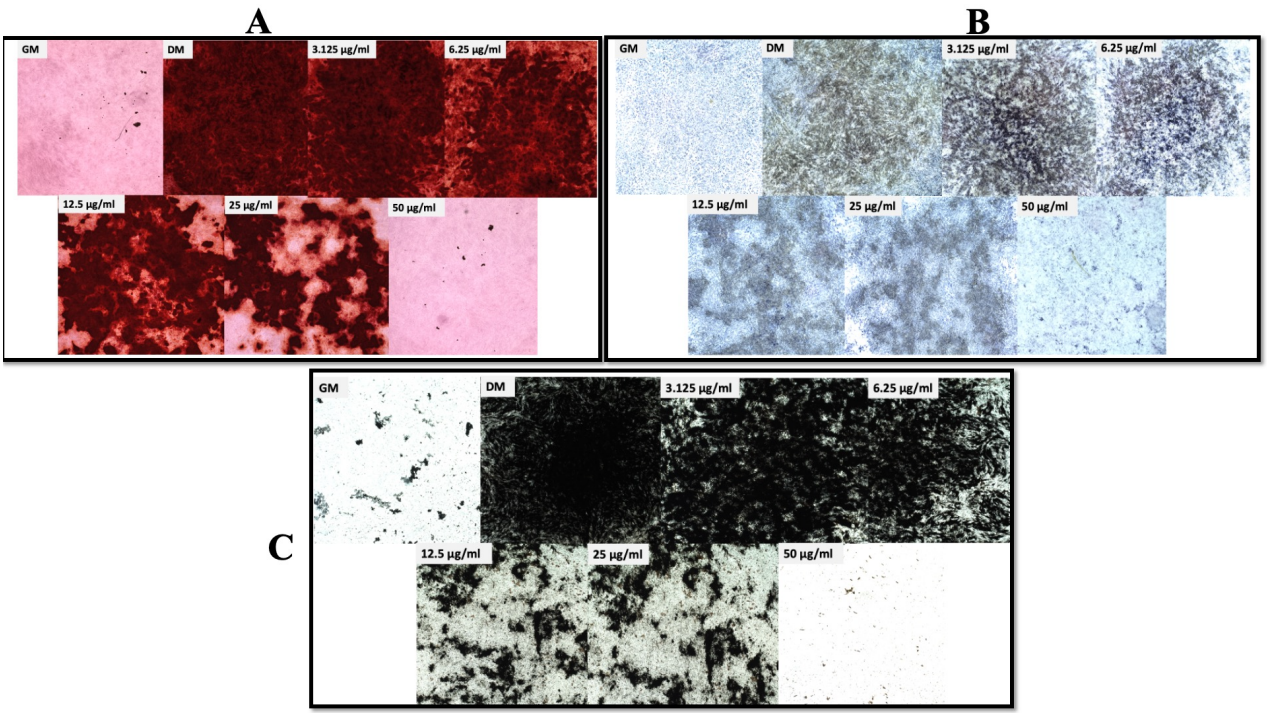

Figure 3.5 represents the ROS production in chicken MSCs at 2.5 and 4 h of treatment. Treatments with different letters indicate significant difference between treatments using Tukey's HSD test, $p < 0.05$. data shown includes mean ± SEM of 5 individual replicates (n=5).

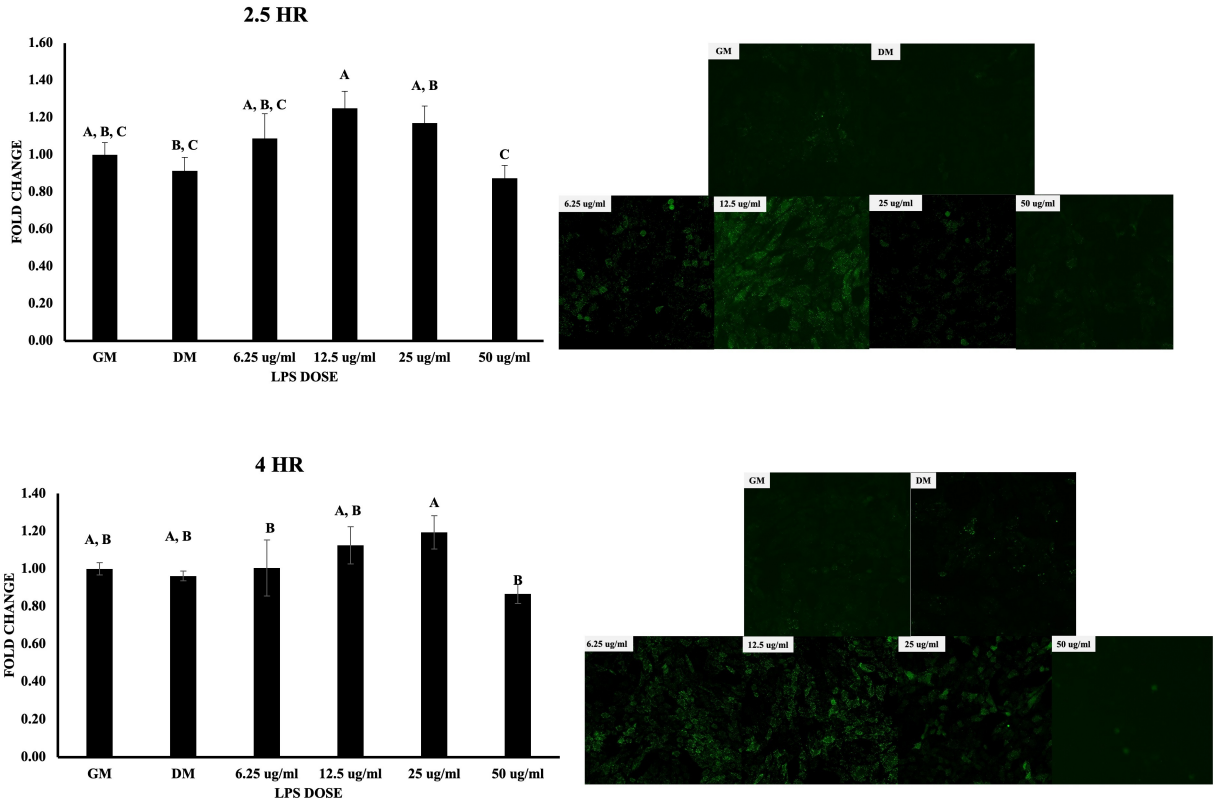

Figure 3.6 represents the effect of LPS on chicken MSCs in CASP8, NRF2 gene expression at 24 h of treatment. Treatments with different letters indicate significant difference between treatments using Tukey's HSD test, $p < 0.05$. data shown includes mean ± SEM of 3 individual replicates (n=3).

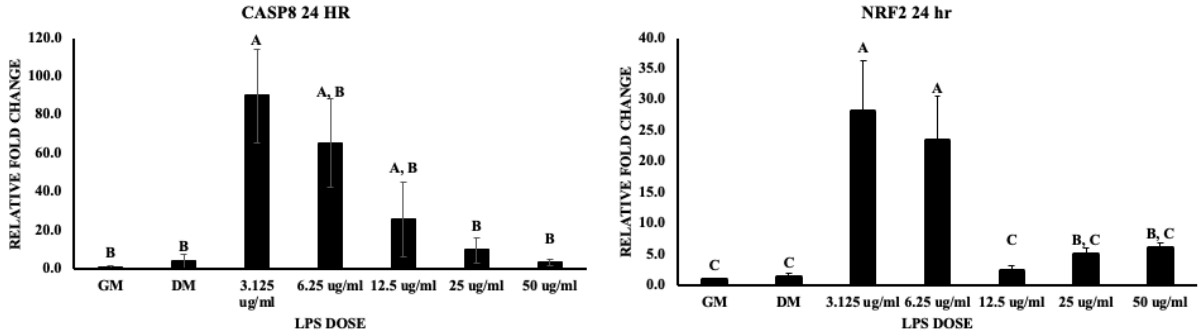

Figure 3.7 represents the effect of LPS on chicken MSCs in IL-1β, TLR4, and DICER1 gene expression at 24 h of treatment (48 h treatment for IL-1β). Treatments with different letters indicate significant difference between treatments using Tukey's HSD test, $p < 0.05$. data shown includes mean ± SEM of 3 individual replicates (n=3).

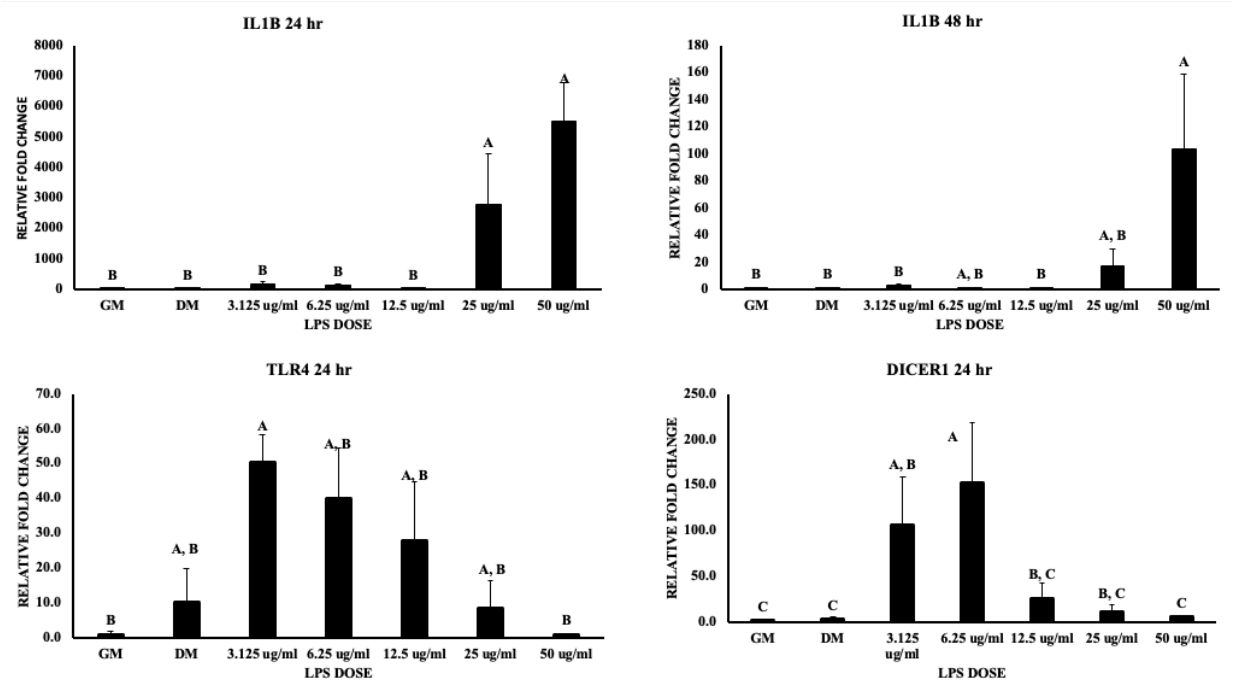

Figure 3.8 represents the effect of LPS on chicken MSCs in LRP5, CTNNB1, and SOST gene expression at 24 h of treatment. Treatments with different letters indicate significant difference between treatments using Tukey's HSD test, $p < 0.05$. data shown includes mean ± SEM of 3 individual replicates (n=3).

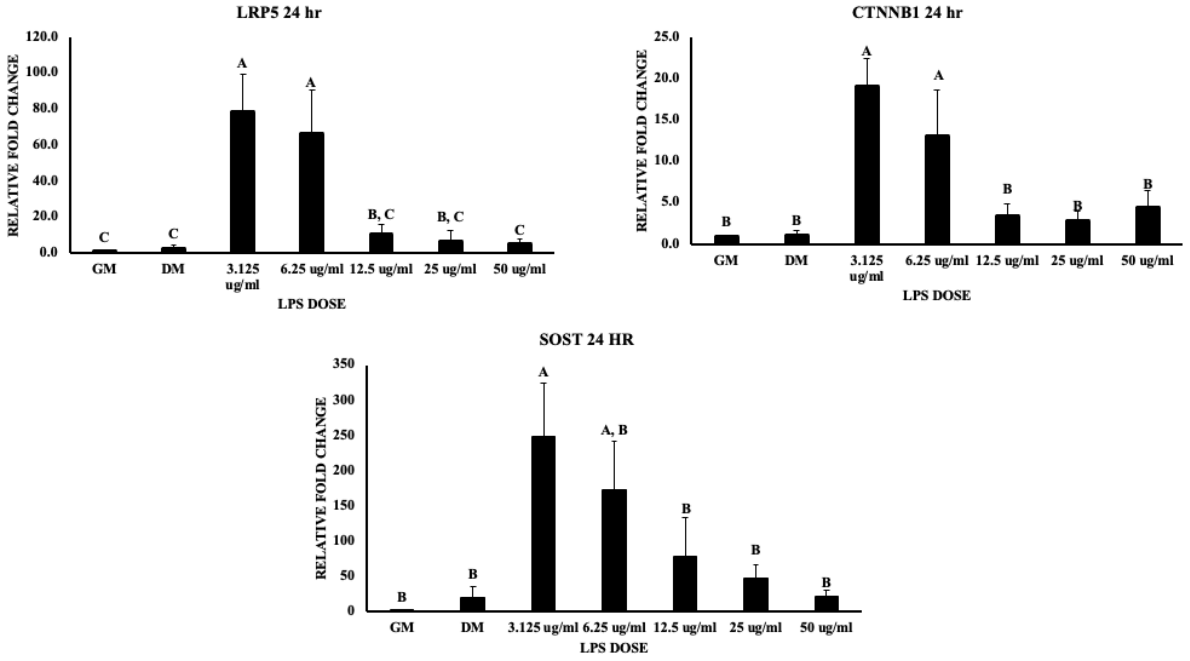

Figure 3.9 represents the effect of LPS on chicken MSCs in SMAD1 and RANKL gene expression at 24 h of treatment. Treatments with different letters indicate significant difference between treatments using Tukey's HSD test, $p < 0.05$. data shown includes mean ± SEM of 3 individual replicates (n=3).

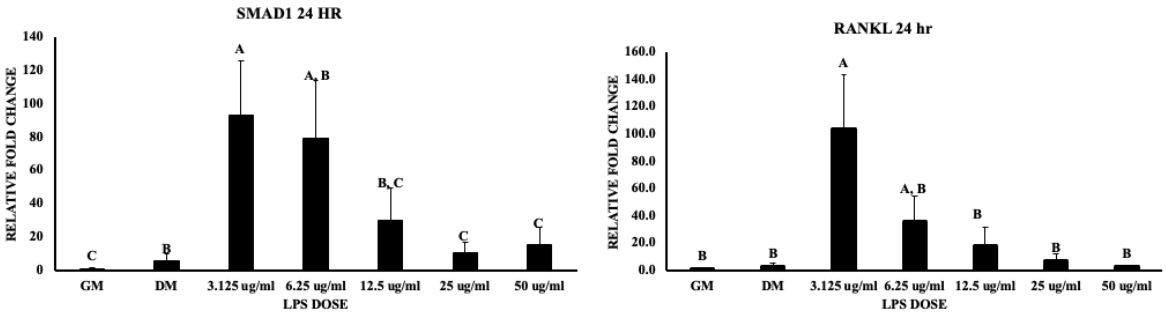

Figure 3.10 summarizes the possible pathways affecting the osteogenic differentiation in the current study at lower (3.125 µg/ml and 6.25 µg/ml and higher (25 µg/ml and 50 µg/ml doses.

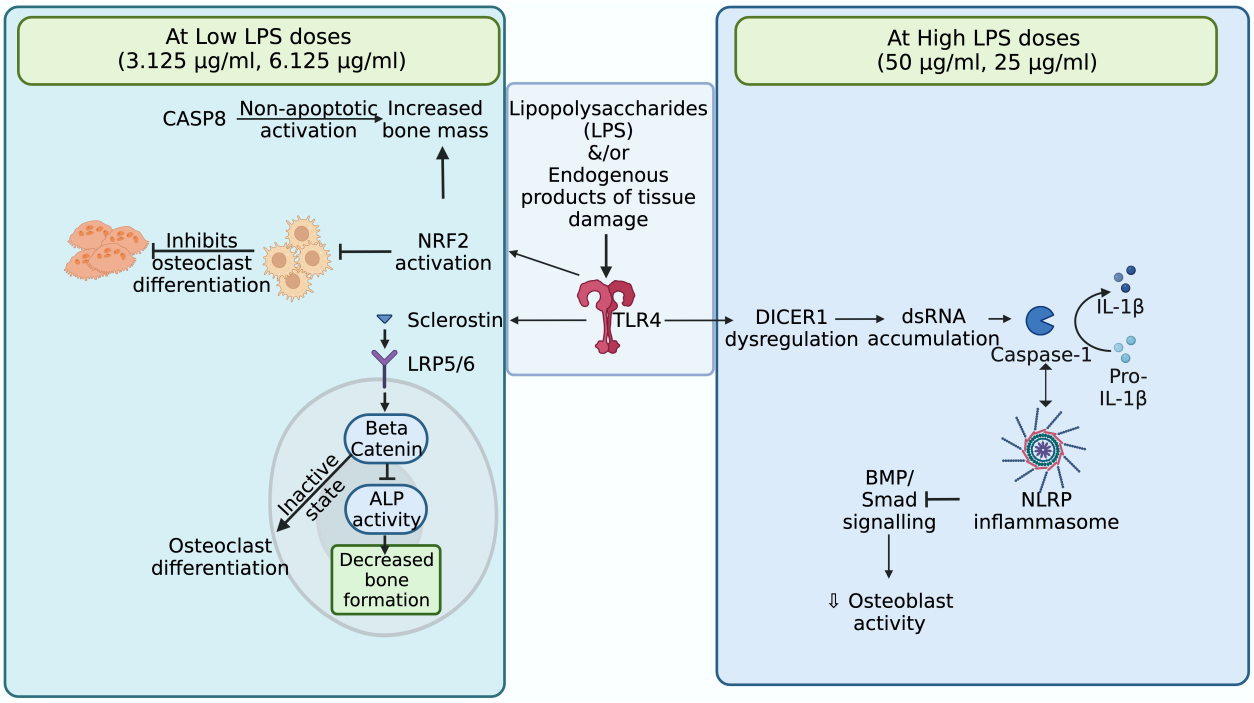

CHAPTER 4

EFFECT OF LIPOPOLYSACCHARIDES ON MACROPHAGES COCULTURED WITH MESENCHYMAL STEM CELLS, DAY 3, AND DAY 18 CHICKEN EMBRYOS [1]

[1]Venkata Sesha Reddy Choppa, Venkata Prathap Reddy K, Seshidhar Reddy Gudidoddi, Hemanth Reddy Katha, and Woo Kyun Kim. 2025.

To be submitted to Poultry Science.

ABSTRACT

Bacteremia and Endotoxemia plays key role in pathogenesis of Bacterial Chondronecrosis and osteomyelitis (BCO) in broilers with immune-suppressed state allowing dominance of opportunistic pathogens. This study integrated three complementary experimental models to unveil effects of Lipopolysaccharide (LPS) on bone. Firstly, primary chicken mesenchymal stem cell-macrophage coculture under osteogenic conditions with LPS (3.125 and 25 μg). Furthermore, day 3 embryos challenged with LPS (3.125 and 25 μg) and day 13 embryos challenged with LPS (1.5, 3.125, and 6.25 μg) sampled on day 18. Gene expression of osteogenic markers (BMP2, LRP5), osteoclast/osteocyte markers (CTSK, SOST), innate inflammatory markers (TNFA, NFKB, TLR4), NRF2, and DICER1 were assessed. To understand changes in bone microarchitecture and bone growth, micro-CT and mineral apposition rate (MAR)(calcein labeling) were used respectively. In coculture model, LPS challenge revealed an upregulated TNFA, SOST, LRP5, and CTSK for higher doses besides a significantly higher LRP5/CTSK/SOST ratios for 3.125 μg LPS. Similarly, LPS challenge on day 3 primed inflammatory signaling (NFKB/TNFA) and bone dyshomeostasis for 25 μg. Moreover, LRP5/SOST and LRP5/CTSK ratios for 3.125 μg indicating mild pro-osteogenic counter-response. Late embryonic changes with day 13 LPS challenge when sampled on day 18 revealed a dose-dependent effects on bone volume and porosity parameters, where higher LPS doses (3.125 and 6.25 μg) shown a bone volume of 5860-6094 mm^3, 35-37 % BV/TV, 63-64 % open porosity. MAR width increased from lower to higher LPS doses (51.8, 125.7, 188.7, 192.2 μm). Furthermore, late-stage gene expression for TNFA and DICER1 were high for high LPS dose. In conclusion, LPS disrupted osteoimmune homeostasis coupled with heightened osteoclast to osteoblast signals with dose and stage dependent osteogenic suppression

reflected as structural fragility at high LPS exposures. These findings mechanistically suggest a link for endotoxemia to BCO pathology in broilers.

INTRODUCTION

Bacterial chondronecrosis and osteomyelitis (BCO) has become a leading cause of lameness in fast growing broiler chicken which typically is associated with bacteremia (Mandal et al., 2016). The bacteremia arises from translocation of opportunistic pathogens from intestinal or respiratory tract into circulation during stress/disease associated immunosuppression (Jiang et al., 2015b; Mandal et al., 2016, 2020; Choppa and Kim, 2023; Anthney et al., 2024). This is followed by seeding of femur head's micro clefts formed in rapidly growing bones (Wideman, 2016a). This pathogenesis can be related to hematogenous osteomyelitis seen in other species (including humans), where bacteria colonize highly vascular growth plate leading to osteomyelitis. The interplay between entry, infection, systemic inflammatory responses and changes with respect to bone pathology or turnover, needs to be understood. Additionally, role of endotoxemia including response to lipopolysaccharides needs an active investigation to understand BCO.

Lipopolysaccharides (LPS) are endotoxins from gram-negative bacterial outer cell membranes that trigger innate immune system. Moreover, LPS from the bloodstream trigger systemic inflammatory response characterized by cytokine storm and sepsis. These changes are seen when LPS binds to toll like receptor 4 (TLR4) on immune cells especially monocytes or macrophages thereby activating MyD88/NFKB (Myeloid differentiation primary response 88/ nuclear factor kappa B) signaling pathway (Muralidharan and Mandrekar, 2013; Page et al., 2022). This activation leads to production of pro-inflammatory cytokines like TNFα (tumor necrosis factor alpha) and interleukins (IL-1β, IL-6) which mediate inflammation with profound effects on

bone metabolism (Lang et al., 2003; Redlich and Smolen, 2012; Li et al., 2021). This primarily seen due to ability of these cytokines to promote osteoclastogenesis and suppress differentiations of osteoblasts (Huang et al., 2014; Zhou and Graves, 2022; Choppa et al., 2023). Furthermore, inflammatory signals induce osteocytes to release sclerostin and DKK-1 which binds to LRP5/6 co-receptor present on osteoblasts which inhibit pro-osteogenic Wnt signaling (Zhou and Graves, 2022; Choppa and Kim, 2023). This phenomenon is extensively documented in mammalian experimental models for periodontitis, arthritis, alveolar or joint bone loss (Muralidharan and Mandrekar, 2013; Zhou and Graves, 2022). Effect of LPS on bone cells and progenitors (Stem Cells) will play a key role in understanding BCO. Osteoblast lineage cells possess TLR4 which respond to LPS and alters differentiation (mineralization potential) (Huang et al., 2014). Altered mineralization potential has been attributed to NFKB cross talk in suppressing BMP2/Smad signaling which in turn block pro-osteogenic effects.

Mesenchymal stem cells could be isolated from various tissues like bone, bone marrow, umbilical tissue, adipose tissue, and placental tissue and possess ability to differentiate into cartilage, osteoblasts, and adipocytes (Pittenger et al., 1999; Meirelles et al., 2006). Additionally, these cells could regulate inflammatory and immune response in a particular microenvironment in response to innate immune cells, like macrophages, monocytes, dendritic cells, natural killer cells, etc. (Li et al., 2010; Chiesa et al., 2011; Cahill et al., 2015). Specialized phagocytic cells of the innate immune system that involve in equilibrating the immune responses are macrophages. Furthermore, macrophage activation is greatly influenced based on the responses to immune system which is further supported by its phenotypes obtained through classic (M1 phenotype) and alternative activation (M2 phenotype) (Gordon, 2003; Aggarwal et al., 2014). In macrophage cultures, LPS upregulates bone resorptive marker genes like tartrate-resistant acid phosphatase

(TRAP) and Cathepsin (CTSK) (Hou et al., 2013). Current study uniquely applies early and late embryonic stages and macrophage and MSCs co-culture models in understanding BCO-related bone changes. Study employs two In-Ovo models, 3-day-old (prior to ossification) and 18-day-old chicken embryos (when skeleton is well ossified). These models aim at examining distinct developmental stages of bone formation when treated with various LPS doses. Furthermore, sterile, controlled environment for all these stages with minimal to zero influence of maternal immunity helps in isolating direct effects of LPS on developing tissues. We hypothesize, LPS exposure disrupts usual osteogenic potential and immune homeostasis in dose-dependent manner to reflect changes in bone affected by BCO.

MATERIALS AND METHODS

Ethics statement

All experiments in this study were conducted in research facility at Department of Poultry Science, University of Georgia, Athens, GA, USA, based on guidelines from Institutional Animal Care and Use Committee (A2024 06-021-Y1-A0).

Primary Mesenchymal Stem Cells isolation

Mesenchymal Stem Cells were isolated basing on previously established methods from our lab (Choppa et al., 2023; Tompkins et al., 2023a). Following cervical dislocation of day-old broiler chicks, femur and tibia were taken and immersed in 70 % ethanol for a brief period. This was followed by keeping them in growth media made from Dulbecco's Modified Essential Media (Corning, NY, USA) added with 10% fetal bovine serum (FBS) (Cytiva Hyclone™ FBS, Cytiva life Sciences, MA, USA), 100 U/mL penicillin, 100 g/mL, 100 g/mL streptomycin, and 0.292 mg/mL L-glutamine (Thermofisher Scientific, Waltham, MA, USA). All the tissues other than

bones were removed carefully with scalpel and scissors followed by washing the bones with 2 % FBS containing Phosphate buffered saline (Corning, NY, USA). The bones were chopped into small pieces to allow digestion in digestion buffer made with DMEM, 20% FBS, and 0.25 % collagenase (Sigma-Aldrich, St. Louis, MO, USA). To allow digestion, the fragments along with digestion buffer were kept in shaker at 37^{o}C for 60 minutes which was then filtered using 40 μm sterile strainer (Corning, NY, USA). The cells strained were cultured in 100 mm cell culture plates using growth media prepared earlier and incubated in humidified incubator with 5 % CO_2 (VWR® water jacketed CO_2 incubator, Radnor, PA, USA). Once the cells reach 95 % confluency following media changes for every 2-3 days, cells were subcultured into new culture plates.

Primary Chicken Macrophages isolation

The protocol used in the current study was partially based on previous literature (Davies and Gordon, 2005). Bone marrow was isolated form the long bones of chicken tibia or femur of approximately 2-week-old broiler chickens. Bone marrow cell suspensions were recovered using 70 μm sterile cell strainer (Corning, NY, USA) while making gentle pestle movements using sterile syringe plunger in DMEM medium (serum free). Media containing cells was added with an equal volume of histo-paque (Sigma-Aldrich, St. Louis, MO, USA) carefully below the cell culture media to form a bilayer content in sterile 50 ml tubes (Corning, NY, USA). Mononuclear cells were isolated after density gradient centrifugation at 400 g for 25-30 minutes by keeping acceleration and deceleration at minimum (Beckmann Coulter Allegra X-22R, Indianapolis, IN, USA). Cloudy layer between histo-paque and bone marrow contents was carefully aspirated and transferred into sterile 50 mL tubes again which were then centrifuges at 1200 g for 10 minutes. The supernatant from the tubes were removed and the tube with pellet was added with growth media for macrophages containing Dulbecco's Modified Essential Media with 10% FBS, 100

U/mL penicillin, 100 g/mL, 100 g/mL streptomycin, and 0.292 mg/mL L-glutamine along with 20 ng/mL macrophage colony stimulating factor (Kingfisher biotech, St Paul, MN, USA). Cells were incubated in humidified incubator with 5 % CO_2 for 3 days followed by media replacement for every 2 days until stable macrophage culture was present.

Macrophages isolated were confirmed using microscopy, immune cytochemistry using mouse anti-chicken macrophage-UNLB antibody (Southern Biotech, Birmingham, AL, USA) **(Figure 4.1.1 & 1.2)**. Furthermore, to confirm ability of macrophages differentiating into osteoclasts TRAP (Tartrate-Resistant Acid Phosphatase) staining was performed **(Figure 4.1.3)**. The osteoclast differentiation was achieved by adding 20 ng/mL recombinant mouse RANKL (Kingfisher biotech, St Paul, MN, USA) to the growth media used for macrophages.

Coculture of mesenchymal stem cells and macrophages

Mesenchymal stem cells isolated earlier, were transferred to 6 well plates (Corning, NY, USA) at a density of 25,000 cells/cm^2 followed by addition of macrophages at 10,000 cells/cm^2. The cells were added with osteogenic differentiation media made with DMEM with 5% FBS, 10mM beta glycerophosphate, 50 µg/mL of Vitamin C, dexamethasone at 10^{-7} M to wells. After 24h, cells were harvested for mRNA isolation. This study was assigned into 4 treatments (A1, A2, A3, and A4) and 6 replicates where **A1** was control group which had co-culture treated with basal growth media. **A2** was treated with osteogenic differentiation media, **A3** was treated with 3.125 µg of LPS, and **A4** was treated with 25 µg of LPS. The doses taken in the current study was based on our previous study (Choppa et al., 2023).

Staining of mesenchymal stem cells co-cultured with macrophages

Mesenchymal stem cells were differentiated into osteocytes using osteogenic differentiation. 7 days following differentiation, macrophages were added to MSCs with a preformed mineralized matrix at 15,000 cells per well. 3 days after adding macrophages cells were stained with Calcein, Silver nitrate (Von Kossa), and TRAP (Tartrate-resistant acid phosphatase) staining. Calcein staining was performed using primary stock with 5 mg of calcein dissolved in 1M sodium hydroxide (0.04 mL) followed by distilled water (0.16 mL). Working solution with 50 μg/well was prepared by diluting primary stock with distilled water. Media from plate was discarded and then washed with PBS followed by adding 1mL (50 μg) of working solution. Plate was incubated at 37^{o}C for 1 h and washed twice with PBS followed by imaging at 4X using fluorescent microscope (BZ-Z800, Keyence Inc., Itasca, IL).

TRAP staining was performed using the protocol from manufacturer's (Cosmobio USA, Carlsbad, CA, USA). Similarly, Von Kossa staining (Silver nitrate) was performed using the protocols used on our earlier studies (Choppa et al., 2023; Tompkins et al., 2023a).

Lipopolysaccharide Microinjection on day 3 (Early embryonic stage)

This procedure was adapted from published literature (Chen et al., 2021b; Tompkins et al., 2023c). For day 3 microinjection of LPS, a total of 90 fertile eggs from Cobb Hatchery (Cleveland, GA, USA) were obtained and 30 eggs were assigned for each treatment. The eggs were incubated in a bench top incubator (GQF 1502, Savannah, GA, USA) maintained at 99-100^{o}F with optimum humidity without egg turning. The eggs were marked and placed horizontally on the egg trays to ensure appropriate position of embryo to ease injection procedure on day 3. Three days after incubation, eggs were surface sterilized, small amount of albumen was withdrawn using a sterile

syringe and a window was drilled around the mark made earlier. The window was used to pass the micro syringe where calculated volume of LPS dissolved in sterile distilled water and phosphate buffered saline (control) was injected into dorsal vein of embryo using Pico spritzer (Parker Precision Fluidics, NH, USA). The above steps were performed under microscope to visualize the vein to ensure accurate delivery of treatments and to avoid drying of membranes sterile PBS was instilled on the eggs after opening. The eggs were carefully incubated in same position and glued glass slide was placed on the window made to visualize the viability of embryos. **B1** was control which was injected with PBS, **B2** was injected with 3.125 µg of LPS, **B3** was injected with 25 µg of LPS. After 24 h of incubation viable embryos were carefully transferred to a sterile 1.7 ml tube (Corning, NY, USA) which were further processed for gene expression.

LPS injection for day 13 embryos (Late embryonic stage)

On day 0, fertilized eggs were assigned to 4 treatments and incubated in a bench top incubator with optimum temperature (99-100^{o}F) and humidity besides automatic turning of eggs. The treatments include control which was injected only with sterile PBS **(C1)**, **C2** was injected with 1.5 µg of LPS, **C3** was injected with 3.125 µg of LPS, and **C4** was injected with 6.25 µg of LPS. On day 13, for injecting above treatments, embryo and yolk sac position was identified with egg candler, then a small hole was made using sterile 18 G needle. Through the hole made with 18G needle, a sterile syringe having assigned treatments with a 27 G needle was passed carefully and injected into yolk sac without damaging yolk sac membrane or rupture of major blood vessels. The eggs which shown signs of leakage or rupture of blood vessels (constant oozing of blood from hole made) were disposed. The opening made was sealed using UV sterilized medical tape (3M^{TM} Nexcare^{TM} clear first aid tape, St. Paul, Mn, USA) with parafilm under it to prevent sticking of membranes to the tape **(Figure 4.2)**. Similarly, Calcein was injected into yolk sac on day 16

followed by sampling on day 18. Spleen and whole embryo were collected where spleen was used for mRNA isolation. Whole embryo was used for micro-Computed Tomography (micro-CT) and tibia was collected for mineral apposition rate.

Mineral Apposition rate (MAR) for late embryonic stages

Mineral apposition rate was modified from previous studies where calcein was injected at two time points (Tompkins et al., 2022; Choppa et al., 2023). In contrast, current study used a single calcein injection on day 16 (Sigma Aldrich, St. Louis, MO, USA) where the width was measured from periphery to calcein labeled fluorescent band using fluorescence microscope on bones sampled on day 18 (BZ-Z800, Keyence Inc., Itasca, IL) and analyzed using ImageJ software (National Institute of Health, Bethesda, MD, USA). Bone collected was sliced as thin as possible with scalpel and blade and bone slice was placed on glass slide and mounting.

Micro-CT of day 18 embryos treated with LPS

Micro-CT was performed for whole embryos which were stored in 70% ethanol. The embryos were held in 50 mL tubes with embryos and wrapped in cheese cloth to prevent movement. Embryos were scanned using Skyscan software (Skyscan 1275, Bruker micro-CT, MA, USA) and with X-ray settings at 65 kV and 153 μA and a pixel size of 50.8 and 0.5-mm aluminum filter to reduce beam hardening. 180^{o} scanning with 0.4 ^{o} rotation angle was used to capture 4 images per rotation. Scanned bones were reconstructed to 3D model, using N-recon software (Bruker micro-CT). 3D model was straightened using data viewer software followed by using CTAn software for selecting region of interest. Phantom with known densities of 0.25 and 0.75 g/cm^3 were used to calibrate bone mineral density. The region of interest was then processed for obtaining 3D parameters like tissue and bone volume, porosity, trabecular separation, trabecular thickness, etc.,

Quantitative real-time PCR analyses (qRT-PCR)

Cocultured MSCs and macrophages were lysed with QIAzol (Qiagen, Valencia, CA). The manufacturer's instructions were followed in isolating RNA. Similar but slight modification was made for day 3 embryo and spleen from day 18 embryo were homogenized first, and above instructions were applied to isolate RNA. RNA was checked for concentration and quality using NanoDrop Eight Spectrophotometer (Thermo Fischer Scientific, MA, USA). Complementary DNA (cDNA) synthesis from RNA was achieved using cDNA synthesis kits (Applied biosystems, Foster City, CA, USA). Relative gene expression was analyzed using $2^{-\Delta\Delta Ct}$ method. All the samples were run in duplicates and primers used in this study were designed using NCBI database, primer3 plus, and validated using BLAST tool. Primers (Integrated DNA technologies Inc., IA, USA) used in the current study are listed in the **table 4.1** below.

Statistical Analyses

Data from effect of LPS on macrophage coculture study, early embryonic stage (day 4 embryo), and late embryonic stage (day 18 embryo) were analyzed using JMP Pro 18 (SAS Institute, Inc., Cary, NC, USA). One way ANOVA, Student's t-test were used with post hoc tests like Tukey's HSD. Data was checked for normality and homogeneity; non-normal data was log transformed for above analyses. The data was expressed in mean and standard error. *P*-value was set to less than 0.05.

RESULTS

Staining and Gene expression for LPS treated macrophages cocultured with mesenchymal stem cells

Relative fold changes in gene expression for CTSK (cathepsin K), LRP5 (low-density lipoprotein-related protein 5), NFKB (nuclear factor kappa-light-chain-enhancer of activated B cells), NRF2 (nuclear factor erythroid 2 related factor 2), SOST (sclerostin), and TNFA (tumor necrosis factor-alpha) in MSCs cocultured with macrophages are shown in **Figure 4.3**. For A2 and A3, CTSK was significantly decreased for A2 and A3 where the relative fold change was 0.686 and 0.245 respectively ($P < 0.05$). On the other hand, A4 showed a higher CTSK expression with a fold change of 2.363 compared to A1 (1.00) ($P < 0.05$) **(Figure 4.3)**. Furthermore, LRP5 expression increased for treatments with fold changes of 1, 4.58, 10.46, and 17.58 respectively for A1, A2, A3, and A4 ($P < 0.05$) **(Figure 4.3)**. A2-A4 revealed significantly higher expression than A1 which had growth media with MSCs and macrophages ($P < 0.05$). No significant differences were observed for NFKB and BMP2 (data not shown). Corresponding to above gene expression for CTK and LRP5, NRF2 revealed highest expression for A4 with a fold change of 3.1 ($P < 0.05$) where A2, and A3 had lower expression with fold change of 0.5 and 0.55 compared to A1 ($P < 0.05$) **(Figure 4.3)**. SOST gene expression was significantly higher for A3 and A4 compared to T1 with fold changes of 23.1, 65.02, and 1 respectively ($P < 0.05$) and T2 had a fold change of 2.7 **(Figure 4.3)**. TNFα also revealed a highest gene expression expressed as fold change for A4 ($P < 0.05$). In contrast, A2 and A3 was significantly lower than A1with fold changes of 0.53, 0.38, and 1 respectively ($P < 0.05$). Interestingly, LRP5 to CTSK ratio revealed a significantly higher fold change ratio for A3 (35) compared to all other treatments A1, A2, and A4 showing ratios of 1, 9, and 7 respectively **(Figure 4.3)**. Staining using Calcein and silver nitrate revealed dose dependent

decrease in mineralization. Furthermore, an increased TRAP activity with increased dose of LPS **(Figure 4.4)**.

Gene expression for LPS treated day 3 chicken embryos

Relative fold changes in gene expression for CTSK were 1, 1.94, and 0.51 for B1, B2, and B3 respectively. CTSK was downregulated for B3 and upregulated for B2 compared to B1 ($P < 0.05$) **(Figure 4.5)**. LRP5 was upregulated for B2 and B3 compared to B1 where the fold change was 1 (B1), 3.97 (B2), and 6.18 (B3) respectively ($P < 0.05$) **(Figure 4.5)**. NFKB shown an upregulated B2 (2.08) compared to B1 (1) besides B3 (1.39) which indicates no significant difference with neither B1 nor B2 ($P < 0.05$). Additionally, SOST expression shown as fold change of 1, 1.18, 0.58 for B1, B2, and B3 respectively where B3 was significantly lower than B1 ($P < 0.05$) **(Figure 4.5)**. In contrast, TNF-alpha gene expression for T3 was significantly higher than T1 with fold change of 1.45 and 1 respectively ($P < 0.05$) **(Figure 4.5)**. On the other hand, ratios of LRP5/SOST and LRP5/CTSK revealed that both shown B3 had greater ratios than B1 besides B2 was significantly higher than B1 ($P < 0.05$). LRP5/SOST ratios, mean values were 0.93 (B1), 4.34 (B2), and 14.05 (B3). Furthermore, mean ratios for LRP5/CTSK were 0.93, 2.51, and 13.88 for B1, B2, and B3 respectively **(Figure 4.5)**.

Mineral apposition rate (MAR) for day 18 chicken embryos

MAR using calcein labeling reveals a least width for C1 (51.8 μm) compared to all other treatments where widths of C2, C3, and C4 were 125.7, 188.7, and 192.2 respectively ($P < 0.05$) **(Figure 4.6)**. The values shown have a reciprocal relationship with growth of the bone representing the lowest growth rate for C2, C3 and C4 ($P < 0.05$) **(Figure 4.6)**.

Micro computed tomography parameters

Micro-CT parameters like bone volume (mm^3), bone volume/tissue volume ratio, bone surface to bone volume ratio, trabecular thickness (mm), closed (%), and open porosity (%) were measured. Bone volume (BV) varied significantly between treatments where C2 (14,565.8 mm^3) had highest BV followed by C1 (10,785.6 mm^3), and C3 (5860.5 mm^3) and C4 (6094.2 mm^3) both had lowest BV ($P < 0.05$) **(Figure 4.7)**. Similarly, bone volume to tissue volume ratio revealed similar findings with C2 (84.76 %) having significantly higher ratio compared to C1 (65.45 %), C3 and C4 had lowest mean values of 35.59 and 36.53 % respectively ($P < 0.05$). Similarly, Trabecular thickness was significantly higher for C2 (1.118 mm) than other treatments C1, C3, and C4 with mean values of 0.529, 0.380, and 0.369 mm respectively ($P < 0.05$) **(Figure 4.7)**. In contrast, bone surface to bone volume ratio was lowest for C2 (2.39) followed by C1 (6.79) which were significantly lower than C3 and C4 with mean values of 13.57 and 13.38 respectively ($P < 0.05$) **(Figure 4.7)**.

Closed Porosity percentage for C1 and C2 had highest mean percentages of 0.986 and 1.121 % respectively. Nevertheless, C3 and C4 were significantly lower with 0.123 and 0.108 % respectively ($P < 0.05$) **(Figure 4.8)**. Contrarily, highest open porosity percentage was seen for C3 (64.37 %) and C4 (63.43 %) compared to C1 (0.986 %) and C2 (1.121 %) ($P < 0.05$) **(Figure 4.8)**.

Late embryonic stage (day 18) gene expression

Gene expression expressed as relative fold change for BMP2 (Bone morphogenetic protein 2), NFKB, TNFA, TLR4 (toll like receptor 4), and DICER1 (endoribonuclease DICER). BMP2 shown a significantly higher gene expression for C2 and C4 compared to C3 with relative fold change of 1.83, 1.98, and 0.81 respectively ($P < 0.05$) **(Figure 4.9)**. For NFKB, fold change for treatments was highly expressed in C3 (11.19) compared to C1 (1) besides a slightly lower

expression for C2 (6.24) compared to C1 ($P < 0.05$). TNF alpha expression was highest for C4 (2.14) compared to C3 (0.436) which is has the lowest expression ($P < 0.05$). Additionally, TLR4 expression for C2 (2.97) was significantly higher than C1 (1) and C4 (0.875) **(Figure 4.9)**. Furthermore, DICER1 relative fold change for C4 (3.67) was significantly greater than C1 (1), C2 (0.625), and C3 (0.562) respectively ($P < 0.05$) **(Figure 4.9)**.

DISCUSSION

In this study, osteogenic and inflammatory genes pertaining to bone health were profiled to understand how LPS affects bone homeostasis to simulate BCO pathogenesis. Co-culture study on MSCs and Macrophages, LPS exposure exhibited explicit changes in gene expression relative to controls. High dose (A4: 25 μg) shown a prominent inflammatory response reflected as TNF alpha gene expression showing proinflammatory cytokine production. This suggests osteocyte driven inhibition of osteoblastogenesis and bone resorption corresponding to SOST and CTSK expression. Furthermore, LRP5, a Wnt receptor for canonical Wnt signaling pathway which plays essential role in osteogenic differentiation was elevated in LPS treated co-cultures. This could be negative feedback from heightened expression of SOST which inhibits the pro-osteogenic signal (inhibits Wnt signaling) (Choppa et al., 2023). In contrast, low LPS doses (A3: 3.125 μg) induce moderate LRP5 and SOST response which aligns with our dose-response on avian MSCs (Choppa et al., 2023). In current co-culture model, osteogenic differentiation medium alone (A2) revealed a maintenance of lower TNFA expression indicating absence of strong inflammatory stimulus favoring osteogenic nature which can be seen with relatively heightened response of LRP5 to CTSK ratio. In contrast, SOST to LRP5 ratio was higher showing a Wnt inhibitory mechanism suggesting reduction of osteogenic activity without bone resorptive functions. These findings all

together points towards favored osteoclastogenesis with a suppressed osteoblast formation for high dose of LPS (A4).

In Chicken embryo experiments at various stages (Early and Later phases), LPS showed detrimental effects on skeletal development. On day 3 egg incubation, LPS exposure induced a rapid inflammatory response where high dose (B3: 25 μg) revealed elevated NFKB and TNFA gene expression, reflecting an acute innate immune response activation even in early developmental stage. Although overt bone formation has not started on day 3, this early pro-inflammatory cytokine surge alters the cascade of events involved in cartilage formation and ossification. Current study shows that even with lower LPS doses (B2: 3.125 μg) on day 3 embryos led to a detectable expression of inflammatory markers. The early-life inflammatory changes may have consequences altering gene regulatory pathways that would manifest as poor bone quality (Li et al., 2023). Although present study did not track the changes in development of day 3 embryos to later growth phases, strong induction of inflammatory pathways especially with LRP5/CTSK ratios and LRP5/SOST ratios. Precisely, these ratios strongly suggest a stronger negative feedback mechanisms to revert the changes like inhibition of LRP5/Wnt signaling along with CTSK downregulation due to high LPS doses (Williams, 2017; Jiao et al., 2023; Littman et al., 2023). Furthermore, downregulation of SOST and CTSK expression suggests a pressure on osteocytes to suppress release of sclerostin and a response to regulate bone resorption (Troen, 2006; Moriishi et al., 2012).

For Day 13 LPS injected embryos which were sampled on day 18 revealed a significant reduction of bone mass and deranged microarchitecture in a dose-dependent manner. Bone volume measurements revealed osteopenia at moderate (C3: 3.125 μg) and high LPS (C4: 6.25 μg) doses with a reduction of 40-50 % lower bone volume than controls. Additionally, bone surface to

volume ratio which indicates trabecular thinning and fragmentation was elevated for C3 and C4 (approximately two-fold) compared to control indicating structural porosity. These microstructural changes are characteristic of inflammatory changes associated with bone resorption. This is further supported by upregulation of CTSK in LPS treated groups besides higher expression of SOST on day 18. This suggests, increased production of sclerostin with systemic exposure of LPS would affect osteoblastic activity in developing bone (You et al., 2020). Osteogenic markers like Runx2, Osterix, and Osteocalcin have been downregulated in LPS-treated chick embryo bones (You et al., 2020). Although those genes were not directly analyzed in the current study, but elevated sclerostin and diminished bone formation would strongly point toward inhibition of osteogenesis. Furthermore, persistent upregulation of LRP5 in LPS affected embryos reflects the findings seen in co-culture experiment (macrophages and MSCs). Precisely, compensatory response expressed as sustained LRP5 elevation to reactivate Wnt signaling pathway besides concurrent high SOST levels likely blocking the above pro-osteogenic (Wnt) pathway. In contrast, lowest LPS dose (C2: 1.5 μg) show a slight increase in bone volume and bone volume fraction compared to control group. This finding is consistent observation seen in anabolic or bone remodeling process when triggered with a mild inflammatory stimulus (Croes et al., 2015). Low-grade inflammation is considered a natural element involved in bone formation or healing which can be triggered by low dose of LPS but can be quickly regulated by their own cellular mechanisms (Croes et al., 2015). This can be observed in a study showing that LPS and TNFA do not reveal any osteogenic properties but in the presence of osteogenic differentiation media, these cytokines contribute to alkaline phosphatase activity (Rundle et al., 2006; Lories and Schett, 2012; Geusens et al., 2013). Slight gain in bone mass for C2 group in the current study can be attributed to phenomenon similar

to In vivo environment with a lenient towards developmental osteogenesis expressed in response to mild reversible inflammation (Liu and Kerns, 2014; Henning et al., 2024).

CONCLUSION

Integrative approach to understand endotoxin -induced inflammation affecting bone was unveiled from Co-culture and embryo studies together. Acute and high levels of LPS altered bone homeostasis by cytokine activation besides upregulating CTSK and inhibiting Wnt signaling pathway (Sclerostin and LRP5 receptor). These molecular events were reflected as lower bone volume and highly porous bone suggesting a structural compromise. In contrast, mild inflammatory stimulus was well tolerated slightly enhanced bone measurements. Current findings are highly relevant in the context of osteoimmunological perspective, emphasizing the time and magnitude of inflammation as critical determinants of bone homeostasis. The integration of gene expression pattern with histomorphometry outcomes seen from above studies emphasize role of NFKB, TNFA, LRP5, and SOST in maintaining the equilibrium in the presence of inflammatory stress. Further studies should build a precise signaling and crosstalk besides investigating whether mitigation strategies work on restoring bone homeostasis in inflammatory environment. This can be further extended to develop interventions for BCO since current literature contribute to divergent skeletal fates.

REFERENCES

Aggarwal, N. R., L. S. King, and F. R. D'Alessio. 2014. Diverse macrophage populations mediate acute lung inflammation and resolution. American Journal of Physiology-Lung Cellular and Molecular Physiology 306:L709–L725.

Anthney, A., A. D. T. Do, and A. A. K. Alrubaye. 2024. Bacterial chondronecrosis with osteomyelitis lameness in broiler chickens and its implications for welfare, meat safety, and quality: a review. Front Physiol 15:1452318.

Cahill, E. F., L. M. Tobin, F. Carty, B. P. Mahon, and K. English. 2015. Jagged-1 is required for the expansion of CD4+ CD25+ FoxP3+ regulatory T cells and tolerogenic dendritic cells by murine mesenchymal stromal cells. Stem Cell Res Ther 6:1–13.

Chen, C., D. L. White, B. Marshall, and W. K. Kim. 2021. Role of 25-hydroxyvitamin D3 and 1, 25-dihydroxyvitamin D3 in chicken embryo osteogenesis, adipogenesis, myogenesis, and vitamin D3 metabolism. Front Physiol 12:637629.

Chiesa, S., S. Morbelli, S. Morando, M. Massollo, C. Marini, A. Bertoni, F. Frassoni, S. T. Bartolomé, G. Sambuceti, and E. Traggiai. 2011. Mesenchymal stem cells impair in vivo T-cell priming by dendritic cells. Proceedings of the National Academy of Sciences 108:17384–17389.

Choppa, V. S. R., and W. K. Kim. 2023. A Review on Pathophysiology, and Molecular Mechanisms of Bacterial Chondronecrosis and Osteomyelitis in Commercial Broilers. Biomolecules 13:1032.

Choppa, V. S. R., G. Liu, Y. H. Tompkins, and W. K. Kim. 2023. Altered Osteogenic Differentiation in Mesenchymal Stem Cells Isolated from Compact Bone of Chicken Treated with Varying Doses of Lipopolysaccharides. Biomolecules 13:1626.

Croes, M., F. C. Oner, M. C. Kruyt, T. J. Blokhuis, O. Bastian, W. J. A. Dhert, and J. Alblas. 2015. Proinflammatory mediators enhance the osteogenesis of human mesenchymal stem cells after lineage commitment. PLoS One 10:e0132781.

Davies, J. Q., and S. Gordon. 2005. Isolation and culture of murine macrophages.Pages 91–103 in Basic cell culture protocols. Springer.

Geusens, P., P. J. Emans, J. J. A. de Jong, and J. van den Bergh. 2013. NSAIDs and fracture healing. Curr Opin Rheumatol 25:524–531.

Gordon, S. 2003. Alternative activation of macrophages. Nat Rev Immunol 3:23–35.

Henning, P., A. Kassem, A. Westerlund, P. Lundberg, C. Engdahl, V. Lionikaite, P. Wikström, J. Wu, L. Li, and C. Lindholm. 2024. Toll-like receptor-2 induced inflammation causes local bone formation and activates canonical Wnt signaling. Front Immunol 15:1383113.

Hou, G.-Q., C. Guo, G.-H. Song, N. Fang, W.-J. Fan, X.-D. Chen, L. Yuan, and Z.-Q. Wang. 2013. Lipopolysaccharide (LPS) promotes osteoclast differentiation and activation by enhancing the MAPK pathway and COX-2 expression in RAW264. 7 cells. Int J Mol Med 32:503–510.

Huang, R.-L., Y. Yuan, G.-M. Zou, G. Liu, J. Tu, and Q. Li. 2014. LPS-stimulated inflammatory environment inhibits BMP-2-induced osteoblastic differentiation through crosstalk between TLR4/MyD88/NF-κB and BMP/Smad signaling. Stem Cells Dev 23:277–289.

Jiang, T., R. K. Mandal, R. F. Wideman, A. Khatiwara, I. Pevzner, and Y. M. Kwon. 2015. Molecular survey of bacterial communities associated with bacterial chondronecrosis with osteomyelitis (BCO) in broilers. PLoS One 10.

Jiao, Z., H. Chai, S. Wang, C. Sun, Q. Huang, and W. Xu. 2023. SOST gene suppression stimulates osteocyte Wnt/β-catenin signaling to prevent bone resorption and attenuates particle-induced osteolysis. J Mol Med 101:607–620.

Lang, C. H., C. Silvis, N. Deshpande, G. Nystrom, and R. A. Frost. 2003. Endotoxin stimulates in vivo expression of inflammatory cytokines tumor necrosis factor alpha, interleukin-1β,-6, and high-mobility-group protein-1 in skeletal muscle. Shock 19:538–546.

Li, Y., J. Ling, and Q. Jiang. 2021. Inflammasomes in alveolar bone loss. Front Immunol 12:691013.

Li, H., L. Sun, and Y. Wang. 2023. Inhibition of LPS-induced NLRP3 inflammasome activation by stem cell-conditioned culture media in human gingival epithelial cells. Mol Med Rep 27:106.

Li, F. R., X. G. Wang, C. Y. Deng, H. Qi, L. L. Ren, and H. Zhou. 2010. Immune modulation of co-transplantation mesenchymal stem cells with islet on T and dendritic cells. Clin Exp Immunol 161:357–363.

Littman, J., W. Yang, J. Olansen, C. Phornphutkul, and R. K. Aaron. 2023. LRP5, bone mass polymorphisms and skeletal disorders. Genes (Basel) 14:1846.

Liu, J., and D. G. Kerns. 2014. Mechanisms of guided bone regeneration: a review. Open Dent J 8:56.

Lories, R. J. U., and G. Schett. 2012. Pathophysiology of new bone formation and ankylosis in spondyloarthritis. Rheumatic Disease Clinics of North America 38:555–567.

Mandal, R. K., T. Jiang, A. A. Al-Rubaye, D. D. Rhoads, R. F. Wideman, J. Zhao, I. Pevzner, and Y. M. Kwon. 2016. An investigation into blood microbiota and its potential association with Bacterial Chondronecrosis with Osteomyelitis (BCO) in Broilers. Sci Rep 6:25882 Available at http://europepmc.org/abstract/MED/27174843.

Mandal, R. K., T. Jiang, R. F. Wideman, T. Lohrmann, and Y. M. Kwon. 2020. Microbiota Analysis of Chickens Raised Under Stressed Conditions . Frontiers in Veterinary Science 7:696 Available at https://www.frontiersin.org/article/10.3389/fvets.2020.482637.

Meirelles, L. da S., P. C. Chagastelles, and N. B. Nardi. 2006. Mesenchymal stem cells reside in virtually all post-natal organs and tissues. J Cell Sci 119:2204–2213.

Moriishi, T., R. Fukuyama, M. Ito, T. Miyazaki, T. Maeno, Y. Kawai, H. Komori, and T. Komori. 2012. Osteocyte network; a negative regulatory system for bone mass augmented by the induction of Rankl in osteoblasts and Sost in osteocytes at unloading. PLoS One 7:e40143.

Muralidharan, S., and P. Mandrekar. 2013. Cellular stress response and innate immune signaling: integrating pathways in host defense and inflammation. J Leukoc Biol 94:1167–1184.

Page, M. J., D. B. Kell, and E. Pretorius. 2022. The role of lipopolysaccharide-induced cell signalling in chronic inflammation. Chronic Stress 6:24705470221076390.

Pittenger, M. F., A. M. Mackay, S. C. Beck, R. K. Jaiswal, R. Douglas, J. D. Mosca, M. A. Moorman, D. W. Simonetti, S. Craig, and D. R. Marshak. 1999. Multilineage potential of adult human mesenchymal stem cells. Science (1979) 284:143–147.

Redlich, K., and J. S. Smolen. 2012. Inflammatory bone loss: pathogenesis and therapeutic intervention. Nat Rev Drug Discov 11:234–250.

Rundle, C. H., H. Wang, H. Yu, R. B. Chadwick, E. I. Davis, J. E. Wergedal, K.-H. W. Lau, S. Mohan, J. T. Ryaby, and D. J. Baylink. 2006. Microarray analysis of gene expression during the inflammation and endochondral bone formation stages of rat femur fracture repair. Bone 38:521–529.

Tompkins, Y. H., G. Liu, and W. K. Kim. 2023a. Impact of exogenous hydrogen peroxide on osteogenic differentiation of broiler chicken compact bones derived mesenchymal stem cells. Front Physiol 14:118.

Tompkins, Y., G. Liu, B. Marshall, M. K. Sharma, and W. K. Kim. 2023b. Effect of Hydrogen Oxide-Induced Oxidative Stress on Bone Formation in the Early Embryonic Development Stage of Chicken. Biomolecules 13:154.

Tompkins, Y. H., P. Teng, R. Pazdro, and W. K. Kim. 2022. Long bone mineral loss, bone microstructural changes and oxidative stress after Eimeria challenge in broilers. Front Physiol 13.

Troen, B. R. 2006. The regulation of cathepsin K gene expression. Ann N Y Acad Sci 1068:165–172.

Wideman, R. F. 2016. Bacterial chondronecrosis with osteomyelitis and lameness in broilers: a review. Poult Sci 95:325–344 Available at https://www.sciencedirect.com/science/article/pii/S0032579119321534.

Williams, B. O. 2017. LRP5: from bedside to bench to bone. Bone 102:26–30.

You, L., L. Zhu, P. Li, G. Wang, H. Cai, J. Song, D. Long, Z. Berman, L. Lin, and X. Cheng. 2020. Dysbacteriosis-derived lipopolysaccharide causes embryonic osteopenia through retinoic-acid-regulated DLX5 expression. Int J Mol Sci 21:2518.

Zhou, M., and D. T. Graves. 2022. Impact of the host response and osteoblast lineage cells on periodontal disease. Front Immunol 13:998244.

Table 4.1 showing nucleotide sequences and accession number of primers used in current study.

Gene name[1]	Accession number	F primer sequence	R primer sequence
Beta actin	NM_205518.2	CAACACAGTGCTGTCTGGTGGTA	ATCGTACTCCTGCTTGCTGATCC
NFKB	NM_204128.2	GAAGGAATCGTACCGGGAACA	CTCAGAGGGCCTTGTGACAGTAA
TLR4	NM_001030693.2	ACTCTTGGGGTGCTGCTG	TGTCCTGTGCATCTGAAAG
TNF-alpha	XM_040694846.2	CGTGGTTCGAGTCGCTGTAT	CCGTGCAGGTCGAGGTAC
LRP5	NM_001012897.2	GGTGCCCCCTTATATGACAG	GATCAGTAGCTGGGGATGGA
SOST	XM_004948551	ATCCCACCTCCTGCCCAACTCCATC	GGTTCGGTTTGCTGCTCCTGGCTC
DICER1	NM_001040465.2	GACCTGACCAATCTCAACCAG	TTTGCCTTCCTCTTCTCAGC
CTSK	NM_204971.3	AGTCTGCCCTCCTTCCAGTT	CTTGATGATCCAGTGCTTGG
NRF2	NM_205117.2	ATGCAGCTCTTGGCAGAAG	CTGGGTGGCTGAGTTTGATT

BMP2	NM_001398170.1	CCCCTACATGTTGGACCTC	CCCACTTGTTTCTGGCAGT

[1]NFKB1: nuclear factor kappa B subunit 1; TLR4: toll like receptor 4; TNF-alpha: tumor necrosis factor alpha; LRP5: Lipoprotein like receptor 5; CTSK: Cathepsin K; NRF2: Nuclear factor erythroid 2-related factor 2; BMP2: Bone morphogenetic protein 2; SOST: sclerostin; DICER1: dicer 1, ribonuclease III

Figure 4.1 shows the method used in verifying successful isolation of chicken bone marrow macrophages. 1st image on the top left represents microscopic image of macrophages isolated, next image (2) was immunocytochemistry and image overlay using mouse anti-chicken macrophage-UNLB antibody. Last image (3) shows TRAP (Tartrate-Resistant Acid Phosphatase) staining.

1. Microscope image-Macrophages

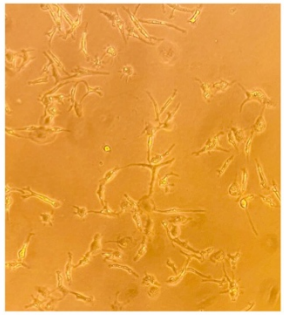

2. Immunocytochemistry of macrophages using UNLB (Unconjugated) (monocyte or macrophage specific)

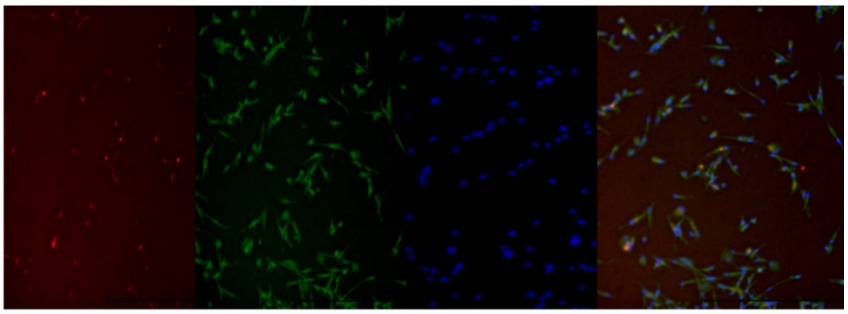

3. TRAP staining of Osteoclasts

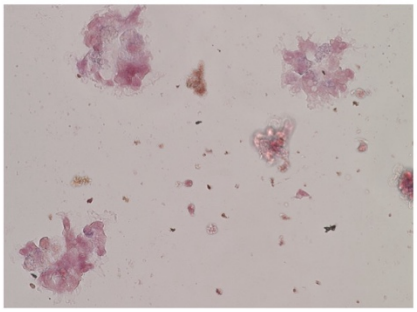

Figure 4.2 represents the procedure for LPS injection to day 13 embryo's yolk sac. 1. Indicates the candling of egg to visualize embryo's viability and locate yolk sac; 2. Small window was made to remove a small portion of eggshell followed by locating the yolk sac besides injection of LPS. Last image shows securing the opened window to prevent leakage of contents. Images shown were for better visualization only, but the window used in actual experiment was made as small as 18G needle diameter towards narrow end of egg.

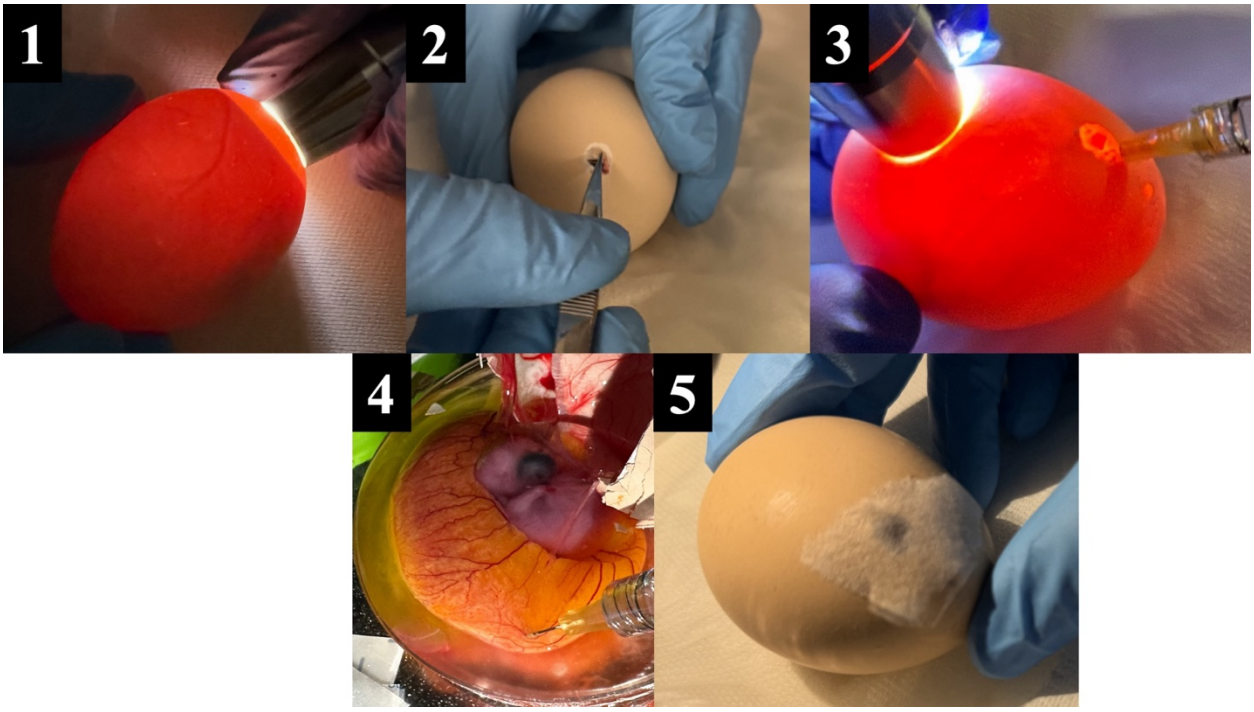

Figure 4.3 shows gene expression for coculture study (Macrophages and Mesenchymal Stem Cells) and key bone formation to resorption markers (1) and related ratios (2 & 3). LPS: Lipopolysaccharides; CTSK: Cathepsin K; LRP5: Lipoprotein receptor 5; NFKB: Nuclear factor kappa B); NRF2: Nuclear factor erythroid 2-related factor 2; SOST: Sclerostin; TNFA: Tumor necrosis factor alpha. A1: co-culture with basal growth media; A2: osteogenic differentiation media; A3: 3.125 µg of LPS; A4: 25 µg of LPS. The error bars represent standard error values. Letters which are not connected by the same letter differ significantly ($P < 0.05$, N =6).

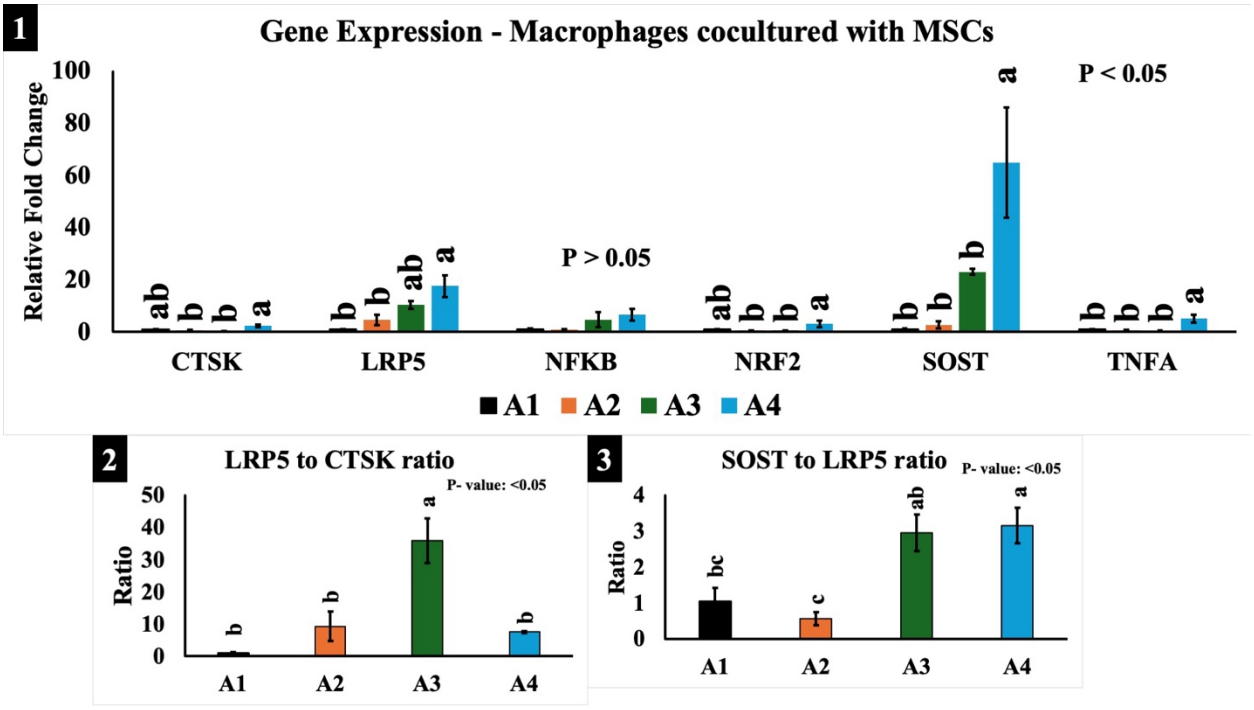

Figure 4.4 shows Von Kossa (silver nitrate) (1), TRAP (2), and Calcein staining for coculture study (Macrophages and Mesenchymal Stem Cells) (3). LPS: Lipopolysaccharides; MSCs: Mesenchymal stem cells; TRAP: Tartrate-resistant acid phosphatase. A: MSCs with differentiation media; B: MSCs and Macrophages with differentiation media; C: 3.125 µg of LPS; D: 6.25 µg of LPS; E: 12.5 µg of LPS; F: 25 µg of LPS.

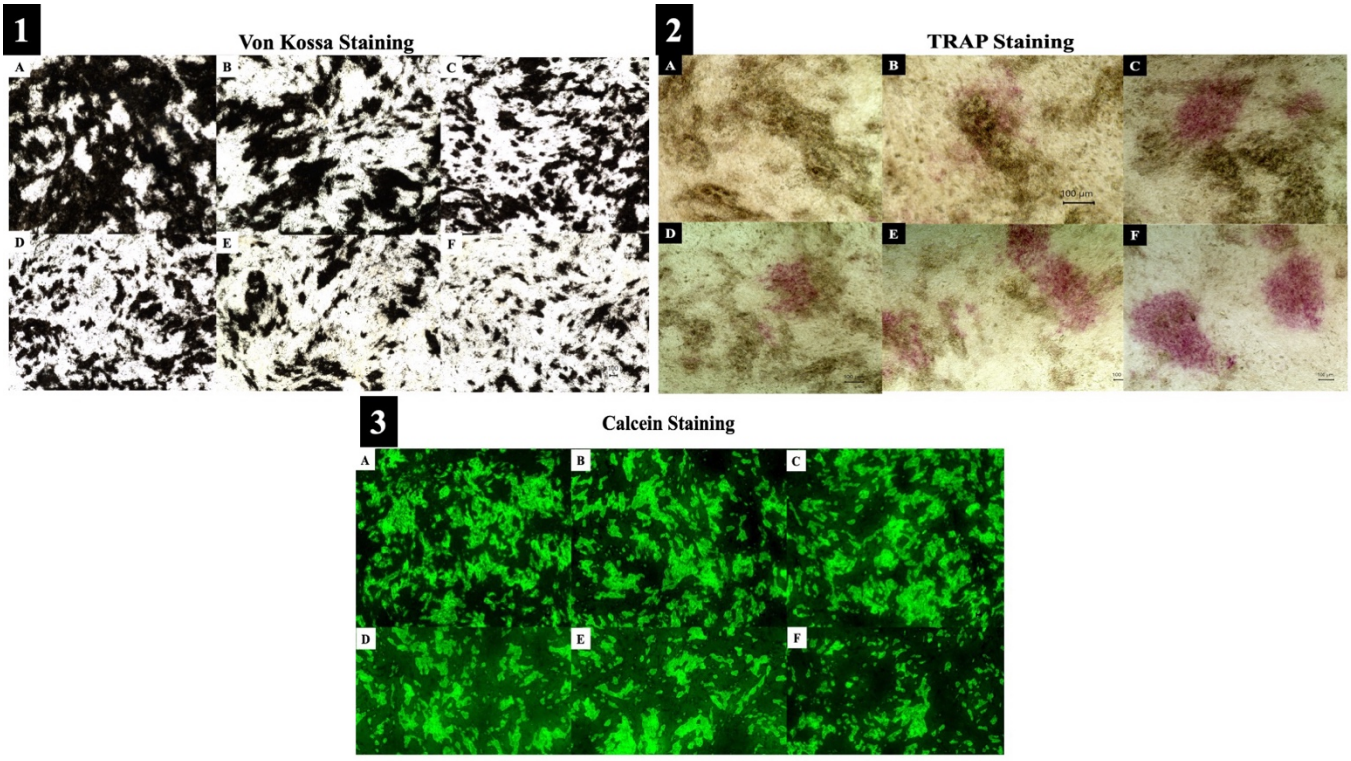

Figure 4.5 shows gene expression for key bone formation to resorption markers and related ratios for early embryonic stage (injected with LPS on day 3 of embryonic development and sampled after 24 h of challenge). LPS: Lipopolysaccharides; CTSK: Cathepsin K; LRP5: Lipoprotein receptor 5; NFKB: Nuclear factor kappa B); SOST: Sclerostin; TNFA: Tumor necrosis factor alpha. B1: Control (injected with PBS); B2: 3.125 µg of LPS; B3: 25 µg of LPS. The error bars represent standard error values. Letters which are not connected by the same letter differ significantly ($P < 0.05$, N =6).

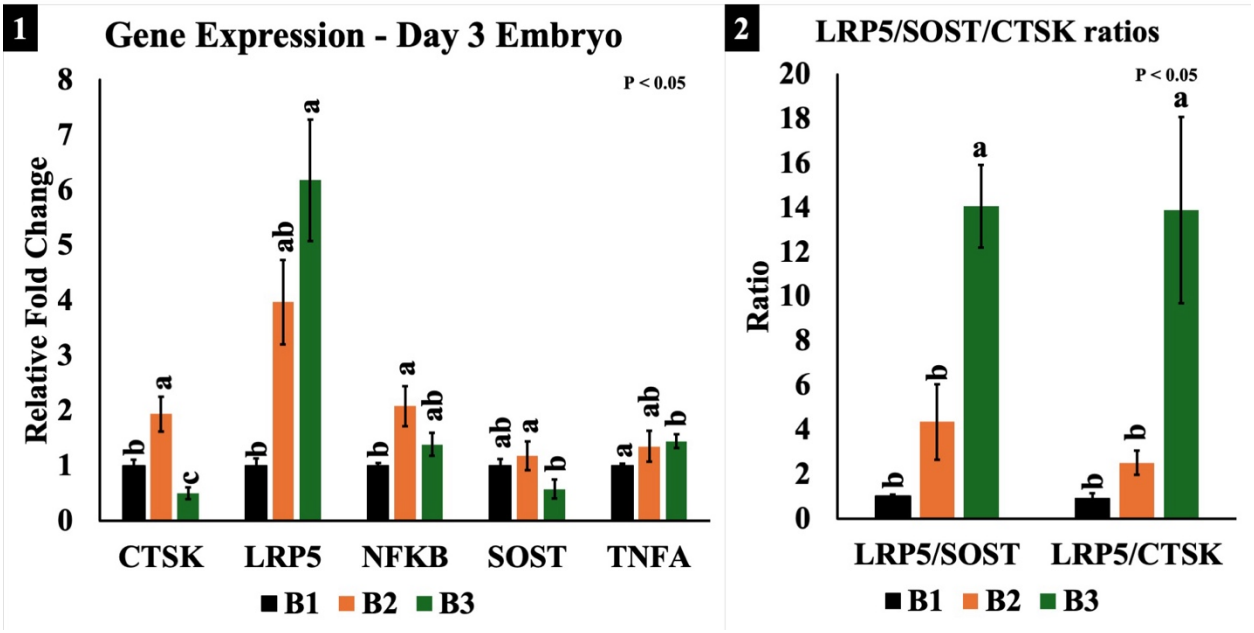

Figure 4.6 shows mineral apposition rate for day 18 chicken embryos injected with various doses of LPS (1 & 2). LPS: Lipopolysaccharides. C1: Control (injected with sterile PBS); C2: 1.5 µg of LPS; C3: 3.125 µg of LPS; C4: 6.25 µg of LPS. The error bars represent standard error values. Letters which are not connected by the same letter differ significantly ($P < 0.05$, N =8).

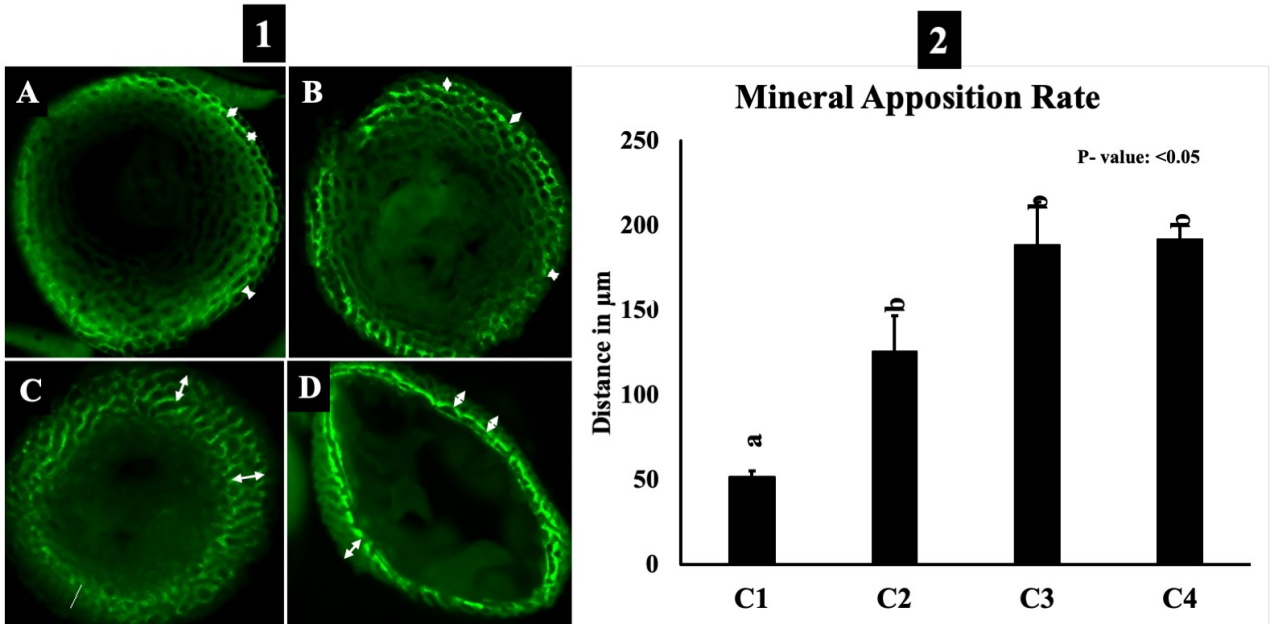

Figure 4.7 shows Micro-CT parameters like bone volume and their ratios (1, 2, & 3), trabecular thickness (4) on day 18 chicken embryos injected with various doses of LPS. Image 5 represents the differences in bone growth for respective treatments. LPS: Lipopolysaccharides. C1: Control (injected with sterile PBS); C2: 1.5 µg of LPS; C3: 3.125 µg of LPS; C4: 6.25 µg of LPS. The error bars represent standard error values. Letters which are not connected by the same letter differ significantly ($P < 0.05$, N =8).

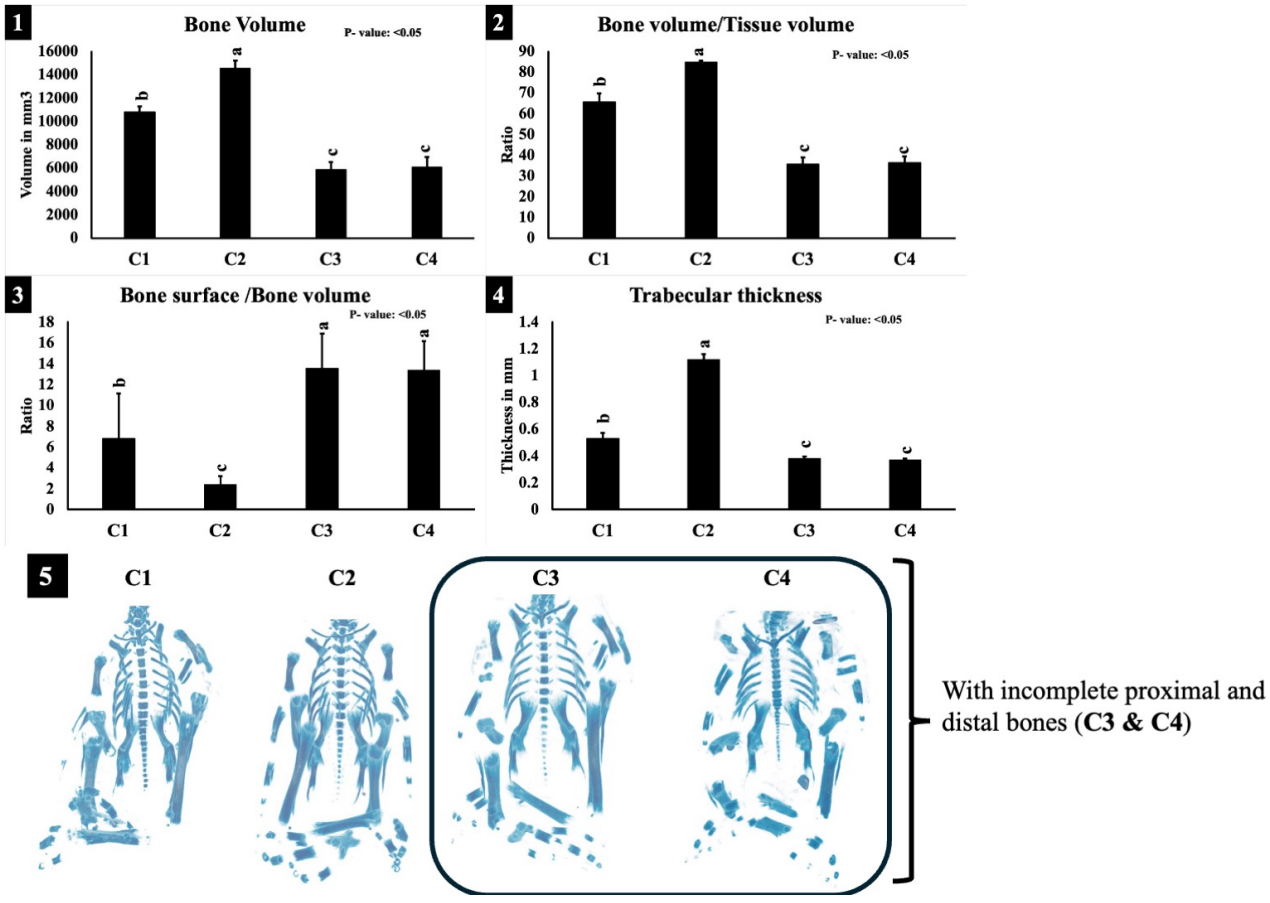

Figure 4.8 shows Micro-CT parameters like Closed (1) and Open (2) porosity on day 18 chicken embryos injected with various doses of LPS. LPS: Lipopolysaccharides. C1: Control (injected with sterile PBS); C2: 1.5 µg of LPS; C3: 3.125 µg of LPS; C4: 6.25 µg of LPS. The error bars represent standard error values. Letters which are not connected by the same letter differ significantly ($P < 0.05$, N =8).

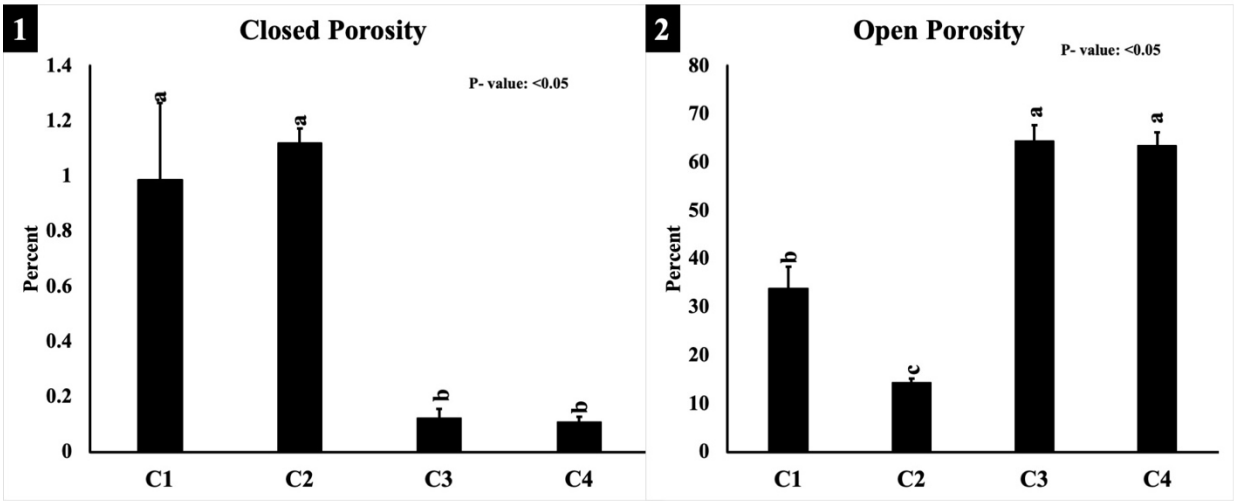

Figure 4.9 shows gene expression for key bone formation to resorption markers and related ratios on late embryonic stage (day 13 chicken embryo injected with LPS and sampled on day 18 of embryo development). LPS: Lipopolysaccharides; BMP2: Bone morphogenetic protein 2; NFKB: Nuclear factor kappa B); TNFA: Tumor necrosis factor alpha; TLR4: Toll like receptor 4; DICER1: Endoribonuclease 3. C1: Control (injected with sterile PBS); C2: 1.5 µg of LPS; C3: 3.125 µg of LPS; C4: 6.25 µg of LPS. The error bars represent standard error values. Letters which are not connected by the same letter differ significantly ($P < 0.05$, N =8).

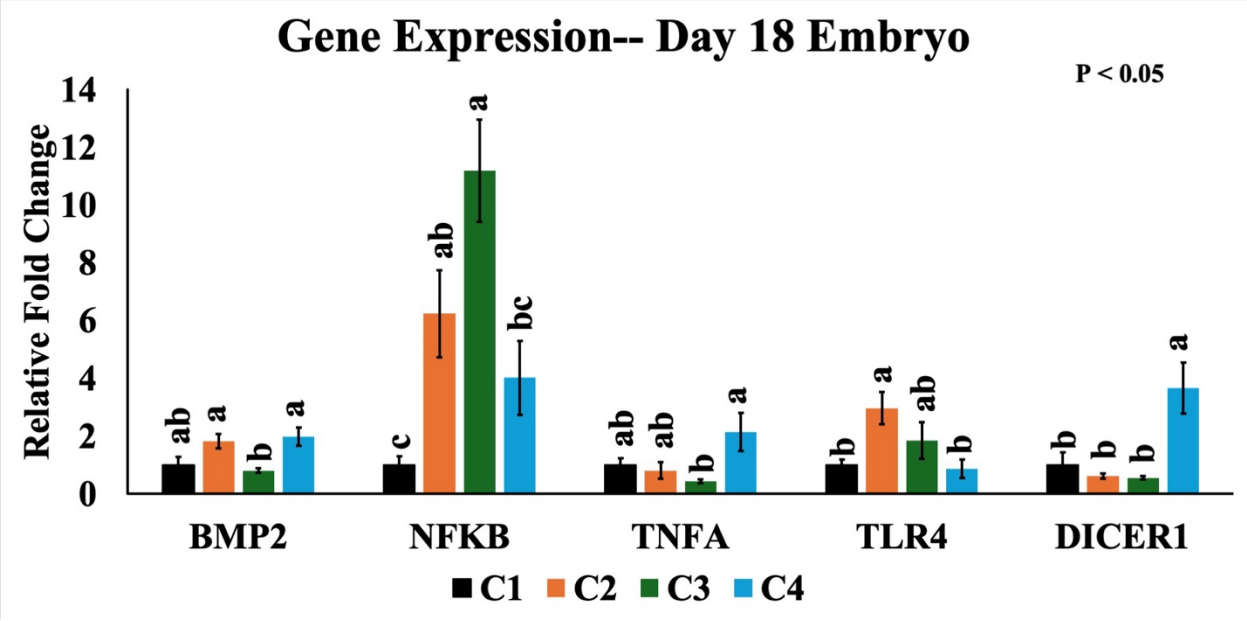

CHAPTER 5

SYNERGISTIC EFFECT OF LIPOPOLYSACCHARIDES AND *EIMERIA* SPP. ON INTESTINAL HEALTH OF BROILERS [1]

[1] Venkata Sesha Reddy Choppa, Guanchen Liu, Yuguo Hou Tompkins, Hanyi Shi, Woo Kyun Kim.

To be submitted to Poultry Science.

ABSTRACT

Lipopolysaccharides (**LPS**) and ***Eimeria* spp**., are associated with inflammation of intestine, where former is associated with triggering inflammatory response and latter is associated with damage to intestinal lining besides inflammatory response. Current study is aimed at evaluating the synergistic effects of *Eimeria* spp. and LPS on broiler performance, intestinal health, oxidative status, and immune responses. Six treatments were used in this study including non-challenged group (**NC/T1**), *Eimeria* only challenge (**T2**), *Eimeria* with LPS combinations with varying LPS doses (**T3-T6**). Growth performance parameters, gut permeability, intestinal morphology, antioxidant markers, IgG levels, and gene expression were analyzed. The study revealed significant differences between non challenged and remaining treatment groups but not among challenged treatments with respect to body weight, average daily gain, and feed intake. Gut permeability measured using FITC-D peaked in T6 representing a dose dependent effect of LPS. Furthermore, Intestinal morphology revealed atrophy of jejunal villi and decreased villus height to crypt depth ratios, with *Eimeria* challenge. Antioxidant parameters like total antioxidant capacity and superoxide dismutase (SOD) activity were low in LPS challenged groups. Similarly, this decrease is also seen with IgG levels in all challenged groups. Additionally, gene expression of Occludin, NF-κB and Mucin 2 were downregulated for challenged groups. Findings revealed a predominant effect of *Eimeria* on growth performance and intestinal damage but higher doses of LPS exacerbate intestinal permeability and oxidative stress. These results revealed a need for targeted mitigation strategies to alleviate concomitant stressors in poultry production.

Keywords: Broilers, Lipopolysaccharides, *Eimeria* spp., Intestinal permeability, Intestinal Morphology

INTRODUCTION

Lipopolysaccharides (LPS) are endotoxins which is a key component of gram-negative bacterial cell membrane and a potent stimulator of inflammatory reactions in host even at lower concentrations (Mireles et al., 2005). Additionally, it covers nearly 75 % of the bacterial surface, which is liberated during cell proliferation and death, but they enter circulation when there is a break in gut integrity. Furthermore, a study has shown that LPS found in sepsis is sourced from the intestine when the gut barrier is compromised since intestine harbors trillions of bacteria which could be gram positive and/or gram negative (Fine et al., 1959; Nikaido and Vaara, 1985; Reisinger et al., 2020). Although broilers are relatively resistant to LPS, they exhibit some clinical signs like lethargy, poor performance and this partially relates to unique property of toll-like receptor 4 (TLR4) lacking functional specific TRIF-related adaptor molecule – TIR domain- containing adaptor protein inducing interferon beta (TRAM-TRIF) signaling pathway (Keestra and van Putten, 2008; Reisinger et al., 2020). This systemic response is usually triggered by the acute phase response, and local inflammatory response associated with behavioral, hormonal, and metabolic changes (Koj, 1989; Klasing, 1998). In contrast, the studies on effect of LPS on broiler health are very limited which further limits our understanding with respect to its effect on gut health in the presence of other stressors (Irisa et al., 2001; Redlich and Smolen, 2012). Moreover, a study shown that with repeated oral administration when combined with mycotoxin as a stressor affected only mucosal gut barrier genes (Lucke et al., 2018). Additionally, the economic losses from protozoal disease, coccidiosis caused by Eimeria spp. is huge which is due to affected birds showing poor growth performance, high mortality and poor intestinal health (Teng et al., 2021a; Tompkins et al., 2022a). Besides, studies on broiler status in the presence of compromised gut integrity are seldom. This disruption could lead to bone growth imbalances too, which are closely linked to the immune

response and oxidative stress during Eimeria infection (Tompkins et al., 2023). This study aims at unmasking the effects of lipopolysaccharide (LPS) on gut health in the presence of coccidiosis besides focusing on the intestinal barrier integrity, immune system and antioxidant system.

MATERIALS AND METHODS

Experimental design

The current study was a completely randomized design with a total of 360 male broiler birds and approved by Institutional Animal Care and Use Committee at University of Georgia, Athens, GA (A2021 12-012). One-day-old Cobb male broiler chickens were randomly allotted to 6 treatments with 5 replicates, and 12 birds per cage. The treatments includes the control group (**T1/NC**) without any challenge, treatment 2 (**T2**) with *Eimeria spp.* cocktail, treatment 3 (**T3**) with *Eimeria spp.* cocktail and 1 mg/kg body weight (BW) of LPS (from *Salmonella enetrica* serotype typhimurium, Sigma-Aldrich, Cat.no:L6511, Saint Louis, MO, USA) at one time point, treatment 4 (**T4**) with *Eimeria spp.* cocktail and 2 mg/kg BW of LPS at one time point, treatment 5 (**T5**) with *Eimeria spp.* cocktail and 1 mg/kg BW of LPS at two time points, and treatment 6 (**T6**) with *Eimeria spp.* cocktail and 2 mg/kg BW of LPS at two time points. The timeline and sampling points are shown in **Figure 5.1**. The birds were gavaged with *Eimeria spp.* (62,500 oocysts of *E. acervulina*, 12,500 oocysts of *E. maxima* and *E. tenella*) and weighed before their placement into cages. *Ad libitum* feed and water were provided, and the temperature settings were followed based on Cobb management guidelines.

Growth Performance, Lesion scores and sample collection

The body weight (BW) per cage is recorded on zero-day postinfection (0 DPI), 6 DPI, and 12 DPI. Feed intake (FI) is recorded on daily basis from 0 DPI till end of the experiment. The body weight gain (BWG), average daily feed intake (ADFI), and feed conversion ratio (FCR) were calculated from day 14 to day 26. Moreover, mortalities were disposed and recorded to adjust calculated measures. On 6 DPI and 12 DPI birds were euthanized for sample collection. Furthermore, lesion scores were recorded using 4- point scale on 6 DPI (Johnson and Reid, 1970).

Gastrointestinal permeability

Gastrointestinal permeability was evaluated by administering fluorescein isothiocyanate dextran (FITC-d; MW 4000; Sigma-Aldrich, Canada). On 5 DPI, one bird per cage was given orally with 1 ml of FITC-d (2.2 mg/ml) followed by blood collection from euthanized birds after 2 h (Bortoluzzi et al., 2019; Teng et al., 2021a). Serum is separated from clotted blood stored in dark by centrifuging at 1000 xg. Standards were prepared by diluting FITC-d with a serum from extra unchallenged birds. The FITC-d levels in the treatments and standards were measured at an excitation wavelength of 485 nm and emission wavelength of 528 nm by using a microplate reader (Victor Nivo Multi-Mode Plate Reader, Avantor, PA, USA), respectively.

Intestinal Morphology and Morphometry

A 3 cm mid-sections of duodenum, jejunum, and ileum collected from each bird euthanized per pen were collected, rinsed with phosphate buffered saline, and fixed in 10 % formalin. Fixed tissues were sliced into small blocks followed by paraffin embedding which are made into 4 μm transverse sections. These sections were mounted on microscopic slides and stained with hematoxylin and eosin. Using compound microscope with camera (BZ-Z800, Keyence Inc., Itasca,

IL), and pictures were taken at 4X magnification. Villus height (VH) and crypt depth (CD) were measures as described by (Sharma et al., 2022)

Quantitative Real-Time PCR analysis (qPCR)

Jejunal mucosa, liver, and cecal tonsil were collected on 6 and 12 DPI and stored in -80°C which follows snap freezing in liquid nitrogen. For RNA extraction, tissues were homogenized with QiAzol lysis reagents (Qiagen, Valencia, CA) as described in manufacturer's instruction. The RNA concentration and quality were measured by NanoDrop 2000 spectrophotometer (Thermofischer Scientific, MA). Using cDNA synthesis kits (Applied Biosystems, Foster City, CA) RNA is reverse transcribed to cDNA. Using SYBR Green Master mix, Real-time PCR reaction was performed using Step One thermocycler (Applied Biosystems, Foster City, CA). Target genes' gene expression were interpreted using $2^{-\Delta\Delta Ct}$ method using cDNA samples ran in duplicate. Primers for housekeeping gene and target genes are listed in **table 5.1**.

Antioxidant status

Total glutathione (GSH), malondialdehyde (MDA), superoxide dismutase, and glutathione disulfide (GSSG) were measured in liver samples collected and frozen in liquid nitrogen followed by storage at -80°C from 6 and 12 DPI. Stored liver samples were homogenized (50-100 μg) and centrifuged according to the instructions given by manufacturer (Cayman chemical, GSH, GSSG, SOD assay kits, Ann Arbor, MI; MDA: Bioassay systems, Hayward, CA). The concentrations of GSH, SOD, MDA, and GSSG were corrected by dividing the obtained values by the BCA results (Castro et al., 2019). The level of lipid peroxidation in liver was determined using QuantiChro TBARS Assay Kit (Bioassay Systems, Hayward, CA, USA).

Statistical Analysis

The mean and standard error of the means were used to express all experimental data (SEM). The data were examined for studentized residual normality and homogeneity of variances. Using JMP Pro16 (SAS Institute, Inc., Cary, NC), the one-way ANOVA was used to statistically assess the differences between the treatment groups, and the Tukey's test was used to analyze the means. The threshold for statistical significance was chosen at $P<0.05$. For all the bone and growth factors, pairwise correlations (JMP Pro16) were assessed.

RESULTS

Body weight, feed intake, and average daily gain

On 6 days post challenge with *Eimeria* spp. (DPI), Non challenged group had an average body weight of 769 g but remaining treatments had significantly lower body weights. Surprisingly, there were no significant body weight differences between the challenged treatments, but slightly lower body weight was observed in treatments (T4 and T6) injected with higher LPS dose used in this study. Precisely, Birds challenged with only Eimeria (T2) had an average body weight of 557.9 g but the treatments injected with LPS at various doses (T3, T4, T5, and T6) had 527 g, 519.9 g, 540.2, and 514.1 g respectively (**Figure 5.2A**).

On DPI 12, Non challenged treatment had an average body weight of 1319.3 g. On the other hand, only *Eimeria spp* challenged treatment (T2) had a body weight of 857.9 g and other treatments (T3, T4, T5, and T6) had 899.5, 835.1, and 960.7, and 920.7 respectively (**Figure 5.2A**).

From DPI 0 to 12, Average daily feed intake for non-challenged treatment shown a steady increase but the treatments (T2, T3, T4, T5, and T6) challenged with *Eimeria spp* had a significant decrease in feed intake on DPI 5, 6, 7, and 8 but increased steadily (**Figure 5.2C**).

Furthermore, Average Daily Gain from DPI 0 to 12 shown a significant 40 g (approximate) decrease with *Eimeria* challenge compared to non-challenged treatments (**Figure 5.2B**). ADG from DPI 0 to 6 in non-challenged treatment was 68.6 g, on the other hand, the challenged treatments (T2, T3, T4, T5, and T6) had 33.5 g, 28.2 g, 27.6 g, 30.2 g, and 25.9 g. Additionally, ADG from DPI 7 to 12 was 1191.2 g, 764.9 g, 811.6 g, 748.4 g, 870.7, and 835 g respectively for the treatments (**Figure 5.2B**).

Lesion scores

Eimeria acervulina, *E. maxima*, and *E. tenella* were scored in their respective regions on DPI 6. There were no significant differences among the challenged treatments even among the treatments with different LPS doses. *E. acervulina* lesion scores among the challenged treatments ranged from 0 to 2 with an average of 0.93 to 1.47 (**Figure 5.3A**). Furthermore, *E. maxima* scores were similar to *E. acervulina* and the averages of challenged treatments were between 0.73 and 1.2 (**Figure 5.3B**). Similarly, *E. tenella* scores among the challenged treatments had scores between 0.73 to 0.93 (**Figure 5.3C**).

Gastrointestinal Permeability

Gut permeability which represents the gut leakage was significantly higher in treatment 6 compared to Non challenged treatment ($p < 0.05$). In terms of mean values, treatment 6 had 355.42 ng/ml of FITC- D in the serum. On the other hand, treatment 3 had 188.37 ng/ml FITC-D leaked into the serum in the birds challenged with 1 mg/kg of LPS injected once. Surprisingly, this was numerically lower than the treatment 2 for which the value was 257.35 ng/ml (p value = 0.339). Furthermore, treatment 3 and 5 which were injected once with 1 and 2 mg/kg of LPS, had similar gut leakage (p value = 0.906) (**Figure 5.4**).

Intestinal Morphology and Morphometry

For the current study, intestinal morphology and morphometry were analyzed which includes villus height of Duodenum, Jejunum, and Ileum (**Table 5.2**). Firstly, Jejunal villus height of all challenged treatments were significantly lower than the control. Jejunal villus height of non-challenged was 1.16 and remaining treatments were similar ranging from 1.07 to 0.82 mm. Interestingly, the T3 had lowest villus height among the treatments with villus height of 0.82 mm (**Table 5.2**). Similarly, Duodenum villus height was similar to the findings observed in Jejunum with treatment 3 measuring 1.68 mm and the NC/T1, T2, T4, T5 and T6 were 2.36, 2.04, 1.90, 1.94, and 2.17 mm respectively (**Table 5.2**). Furthermore, Ileum had similar measurements with lowest being T3 with 0.88 mm (Villus Height) and NC/T1, T2, T4, T5, T6 were 1.2, 1.01, 0.88, 1.05, 1.0, and 1.13 mm respectively (**Table 5.2**).

Jejunal villus height to crypt depth ratio was significantly lower for T2, T3, and T5 compared to other treatments. Non challenged treatment had a ratio of 5.15 but T2 had a ratio of 3.49 (**Figure 5.5**). Furthermore, Ileal villus height to crypt depth ratio was significantly lower for all challenged treatments compared to non-challenged group and T6. The ratio of non-challenged and T6 was 6.21 and 5.31 respectively but T2 had the lowest ratio with 3.29 (**Figure 5.5**). Interestingly, all the challenged treatments injected with LPS had numerically higher ratio compared to T2 (challenged treatment without LPS).

Antioxidant Status and IgG levels

On DPI 6, Total antioxidant capacity (TAC) was measured in serum samples and found to be significantly lower in T4, T6 compared to other treatments which was 489.1 and 550.5 mM respectively. In contrast, T5 was significantly lower than T2, T3 (656.5 and 666.8 mM respectively) (**Figure 5.6A**). On DPI 12, TAC was significantly higher for T3 (645.3 mM)

compared to Non challenged group (**Figure 5.6A**). Glutathione, which is key endogenous antioxidant compound was statistically insignificant (data not shown). Additionally, Superoxide dismutase (SOD) was significantly lower for T5 and T6 on DPI 6 with 0.695 and 0.834 U/mL respectively compared to other treatment groups (**Figure 5.6B**).

IgG/ IgY antibody levels were significantly lower for all the treatments except nonchallenged treatment group. Precisely, all the treatments had less than 5 µg/ml but nonchallenged treatment had 11.424 µg/ml. Moreover, T4 and T6 had significantly lower IgG levels (**Figure 5.7**).

Gene Expression

Transmembrane protein, Occludin gene expression was significantly low (approximately half fold) for all the treatments except non-challenged (**Figure 5.8A**). Furthermore, Mucin 2 (MUC2) gene expression was significantly downregulated for T3 and T6 compared to non-challenged group and T5 by 0.304 and 0.358 respectively (**Figure 5.8B**). Moreover, NFκB (Nuclear factor kappa B) was significantly downregulated for all the treatment groups except non-challenged group (**Figure 5.8C**).

DISCUSSION

Poultry production is affected by several factors where intestinal inflammation is considered a primary contributor to poor broiler performance (Bryant et al., 2010). Factors which affect gut barrier can be due to coccidiosis or LPS released from altered gut microbiota. Moreover, coccidiosis which is often termed as a costly disease is caused by *Eimeria* spp. (Li et al., 2015a; Jiang et al., 2021). Moreover, LPS is an endotoxin which impairs gut integrity, immune functions. Furthermore, these factors lead to gut leakage and aggravated immune response causing

suppressed broilers growth performance (Choi and Kim, 2022; Tompkins et al., 2022b). Although studies focused on Eimeria infections are available in broilers, none of the studies are available on gut challenged with *Eimeria* spp., and LPS injected broilers. This study emphasizes on the above lacuna in the broiler industry which would help in understanding the role of circulating lipopolysaccharide besides coccidiosis.

Studies on mixed *Eimeria* spp., revealed a decreased growth performance, average daily feed intake, gut leakage, and average body weight gain in broilers. For the dose used in current study revealed decrease in all broiler performance parameters which is similar to findings in previous studies (Teng et al., 2020, 2021b; Choi et al., 2023; Liu et al., 2024a; Tompkins et al., 2024). Interestingly, LPS injection did not reveal any significant changes among the challenged treatments. Studies on lipopolysaccharide alone revealed intestinal damage and their subsequent effects on broilers growth (Bryant et al., 2010; Li et al., 2015a; Wang et al., 2015; Chen et al., 2018; Jiang et al., 2021; Zhang et al., 2022). LPS given at 0.5 mg/kg in a study revealed no significant differences among final body weight, ADFI, Average body weight gain which reveals similar findings even with 1 and 2 mg/kg LPS used in current study (Hu et al., 2011). In contrast, at 5 mg/kg LPS dose in another study revealed a decrease in body weight and organ weights of broilers (Xie et al., 2000). Lesion scores for upper intestine (*E. acervulina*), Mid intestine (*E. maxima*), and lower intestine (*E. tenella*) were not affected by LPS injection but *E. acervulina* and *E. maxima* lesion scores were slightly decreased among challenged treatments. Interestingly, gastrointestinal permeability using FITC-D revealed a significant increase in gut leakage for *Eimeria* spp., challenged and LPS (2mg/kg on DPI 0 and DPI 4) injected broilers. This could indicate the effect of LPS at certain dose will affect gut permeability. A study has shown effect of LPS on normal microflora which alter permeability of gut barrier (Wu et al., 2013). Some studies

revealed similar findings with coccidia and heat stress model where gut permeability was greater, but the mRNA expression of occludin was not correlated (G. Schneiders, 2020). However, studies revealed, LPS (*E.coli* serotype O 55) alone did not affect the intestinal permeability in chickens but increased when measured by D -lactate and diamine oxidase levels (Wu et al., 2013; Gilani et al., 2017). This could be because of the alterations in sampling times where increased permeability was observed when sampled after 24 h of final injection where latter was done 2h after final injection. In the current study, 2mg/kg given twice on DPI 0 and DPI 5 revealed an increased permeability on 48 h (DPI 6) from the final injection. This suggests induction of aberrations in intestinal permeability depends on the dose besides repeated doses.

Current study revealed a significant decrease in jejunal villus height among challenged treatments compared to non-challenged treatment but not between challenged treatments. This suggests there is no effect of LPS on jejunal villus height but there are significant differences between challenged and non-challenged treatments. Similarly, jejunal VH:CD ratio was significantly lower for challenged treatments. Ileal villus height was significantly lower besides VH:CD ratio which was lower for challenged treatments compared to non-challenged treatments. These findings are similar to findings in *Eimeria* spp., challenged studies (Teng et al., 2020; Belote et al., 2023; Liu et al., 2024b; Tompkins et al., 2024). LPS challenged treatments indicates a mild LPS trigger (1mg/kg at single time point) causes significant decrease in duodenal, jejunal, and ileal villus height. In contrast, highest LPS dose given twice revealed villus height and VH:CD ratio of intestine was similar to non-challenged treatment which is interesting and similar to other studies (Li et al., 2015b; Dias et al., 2024). Differences in crypt depth, villus height, and their respective ratios would attribute to findings in TAC, SOD and IgG/Y levels where these levels are significantly lower for T5/T6 and T4/T6 respectively. These findings were similar to previous

studies where birds were injected with 1mg/kg LPS but current study shown similar findings with 2mg/kg LPS (Liu et al., 2024b). SOD (Oxidative stress marker) activity is often significantly higher in response to *Eimeria* and LPS injection. From the current study findings where these levels are low reveals either loss of antioxidant activity with higher LPS doses (T5 and T6) or inhibition/activation of neutrophil-mediated inflammation which occurs in response to infection (Younus, 2018; van der Meer et al., 2019; Choppa et al., 2023; Rentería-Solís et al., 2024). Furthermore, similar finding is seen with total antioxidant capacity which further support the above statement. Moreover, IgG levels were significantly lower for all challenged groups but far lower for T4 and T6. LPS injection in a mice has been reported to cause an increase IgG levels but the current study in the presence of *Eimeria* spp., challenge revealed a different finding (Parmentier et al., 2010; Kyvelidou et al., 2018). In a study, supplementing IgY/3-1E powder conferred passive immunization thereby protecting chickens against coccidiosis (Lillehoj et al., 2004). Current results suggest a weakened immune system for the infection in the presence of *Eimeria* spp., challenge and LPS.

Occludin gene expression in the current did not reveal significant differences between the challenged treatments. This pattern is similar for NF-κB which signify activated immune response (Tompkins et al., 2024). This tight junction protein which maintains intestinal integrity is altered by *Eimeria* spp., compromising intestinal barrier (Lillehoj et al., 2004). Findings in current study and other studies indicates coccidiosis disrupt gut barrier but can be enhanced using curcumin, probiotics, and organic acids supplementation (Kaingu et al., 2017; Wang et al., 2017; Mustafa et al., 2021; Zhou et al., 2023; Chen et al., 2024). Similarly, LPS has also revealed similar findings, but current study did not show any aggravated responses with *Eimeria* spp., challenge and LPS (Tan et al., 2023).

CONCLUSION

Study investigated on the concomitant effects of *Eimeria* spp., and lipopolysaccharide (LPS) on broiler's growth performance, gut integrity, antioxidant and immune status. Although *Eimeria* spp., lead to significant decrease in body weight, feed intake, and average daily gain. LPS injections cause slightly higher but statistically insignificant weight loss at doses injected in the current study. Severity of *Eimeria* lesions didn't correlate with LPS. Interestingly, *Eimeria* challenge significantly increased gut permeability with LPS injection (2mg/kg x 2 doses) revealing additive effects. Intestinal morphology showed aberrations in all challenged groups, but LPS did not exacerbate these changes which suggests *Eimeria* predominantly contributing to intestinal morphological changes. Similarly, total antioxidant capacity and superoxide dismutase activity were significantly decreased in LPS injected groups indicating oxidative stress and a failed antioxidant system. Furthermore, IgG levels suggest immune exhaustion or synergistic immunosuppression. Finally, findings in current study indicates, use of probiotics, phytochemicals or essential oils could mitigate dysbiosis and gut leakage besides antioxidants and IgY/G supplementation.

REFERENCES

Belote, B. L., I. Soares, A. W. D. Sanches, C. de Souza, R. Scott-Delaunay, L. Lahaye, M. H. Kogut, and E. Santin. 2023. Applying different morphometric intestinal mucosa methods and the correlation with broilers performance under Eimeria challenge. Poult Sci 102:102849.

Bortoluzzi, C., B. Lumpkins, G. F. Mathis, M. França, W. D. King, D. E. Graugnard, K. A. Dawson, and T. J. Applegate. 2019. Zinc source modulates intestinal inflammation and intestinal integrity of broiler chickens challenged with coccidia and Clostridium perfringens. Poult Sci 98:2211–2219.

Bryant, C. E., D. R. Spring, M. Gangloff, and N. J. Gay. 2010. The molecular basis of the host response to lipopolysaccharide. Nat Rev Microbiol 8:8–14.

Castro, F. L. S., H. Y. Kim, Y. G. Hong, and W. K. Kim. 2019. The effect of total sulfur amino acid levels on growth performance, egg quality, and bone metabolism in laying hens subjected to high environmental temperature. Poult Sci 98:4982–4993.

Chen, Y., L. Liu, L. Yu, S. Li, N. Zhu, and J. You. 2024. Curcumin Supplementation Improves Growth Performance and Anticoccidial Index by Improving the Antioxidant Capacity, Inhibiting Inflammatory Responses, and Maintaining Intestinal Barrier Function in Eimeria tenella-Infected Broilers. Animals 14:1223.

Chen, Y., H. Zhang, Y. Cheng, Y. Li, C. Wen, and Y. Zhou. 2018. Dietary l-threonine supplementation attenuates lipopolysaccharide-induced inflammatory responses and intestinal barrier damage of broiler chickens at an early age. British Journal of Nutrition 119:1254–1262.

Choi, J., D. Goo, M. K. Sharma, H. Ko, G. Liu, D. Paneru, V. S. R. Choppa, J. Lee, and W. K. Kim. 2023. Effects of different Eimeria inoculation doses on growth performance, daily feed intake, gut health, gut microbiota, foot pad dermatitis, and Eimeria gene expression in broilers raised in floor pens for 35 days. Animals 13:2237.

Choi, J., and W. Kim. 2022. Interactions of microbiota and mucosal immunity in the ceca of broiler chickens infected with Eimeria tenella. Vaccines (Basel) 10:1941.

Choppa, V. S. R., G. Liu, Y. H. Tompkins, and W. K. Kim. 2023. Altered Osteogenic Differentiation in Mesenchymal Stem Cells Isolated from Compact Bone of Chicken Treated with Varying Doses of Lipopolysaccharides. Biomolecules 13:1626.

Dias, K. M. M., C. H. Oliveira, A. A. Calderano, H. S. Rostagno, K. M. Gomes, K. E. O'Connor, R. Davis, M. Walsh, J. Britton, and E. A. Altieri. 2024. Dietary Hydroxytyrosol Supplementation on Growth Performance, Gut Morphometry, and Oxidative and Inflammatory Status in LPS-Challenged Broilers. Animals 14:871.

Fine, J., S. Rutenburg, and F. B. Schweinburg. 1959. The role of the reticulo-endothelial system in hemorrhagic shock. J Exp Med 110:547–569.

G. Schneiders, J. F. A. R. M. M. A. F. R. R. et al. 2020. Assessing intestinal permeability: FITC-d versus mRNA expression of tight junction genes.in Int Poultry Scientific Forum.

Gilani, S., G. S. Howarth, S. M. Kitessa, C. D. Tran, R. E. A. Forder, and R. J. Hughes. 2017. Intestinal permeability induced by lipopolysaccharide and measured by lactulose, rhamnose and mannitol sugars in chickens. Animal 11:1174–1179.

Hu, X., Y. Guo, J. Li, G. Yan, S. Bun, and B. Huang. 2011. Effects of an early lipopolysaccharide challenge on growth and small intestinal structure and function of broiler chickens. Can J Anim Sci 91:379–384.

Irisa, T., T. Yamamoto, K. Miyanishi, A. Yamashita, Y. Iwamoto, Y. Sugioka, and K. Sueishi. 2001. Osteonecrosis induced by a single administration of low-dose lipopolysaccharide in rabbits. Bone 28:641–649.

Jiang, J., L. Qi, Q. Wei, and F. Shi. 2021. Maternal stevioside supplementation ameliorates intestinal mucosal damage and modulates gut microbiota in chicken offspring challenged with lipopolysaccharide. Food Funct 12:6014–6028.

Johnson, J., and W. M. Reid. 1970. Anticoccidial drugs: lesion scoring techniques in battery and floor-pen experiments with chickens. Exp Parasitol 28:30–36.

Kaingu, F., D. Liu, L. Wang, J. Tao, R. Waihenya, and H. Kutima. 2017. Anticoccidial effects of Aloe secundiflora leaf extract against Eimeria tenella in broiler chicken. Trop Anim Health Prod 49:823–828.

Keestra, A. M., and J. P. M. van Putten. 2008. Unique properties of the chicken TLR4/MD-2 complex: selective lipopolysaccharide activation of the MyD88-dependent pathway. The Journal of Immunology 181:4354–4362.

Klasing, K. C. 1998. Avian macrophages: regulators of local and systemic immune responses. Poult Sci 77:983–989.

Koj, A. 1989. The Role of Interleukin-6 as the Hepatocyte Stimulating Factor in the Network of Inflammatory Cytokines a. Ann N Y Acad Sci 557:1–8.

Kyvelidou, C., D. Sotiriou, I. Zerva, and I. Athanassakis. 2018. Protection against lipopolysaccharide-induced immunosuppression by IgG and IgM. Shock 49:474–482.

Li, Y., H. Zhang, Y. P. Chen, M. X. Yang, L. L. Zhang, Z. X. Lu, Y. M. Zhou, and T. Wang. 2015a. Bacillus amyloliquefaciens supplementation alleviates immunological stress and intestinal damage in lipopolysaccharide-challenged broilers. Anim Feed Sci Technol 208:119–131.

Li, Y., H. Zhang, Y. P. Chen, M. X. Yang, L. L. Zhang, Z. X. Lu, Y. M. Zhou, and T. Wang. 2015b. Bacillus amyloliquefaciens supplementation alleviates immunological stress and intestinal damage in lipopolysaccharide-challenged broilers. Anim Feed Sci Technol 208:119–131.

Lillehoj, H., S. Ngyyen, J. Donahue, A. Yokohama, and Y. Kodama. 2004. Passive Protection Against Two Eimeria Species in Chickens by Orally Administered Antibodies Specific for a Single Eimeria Protein. Am Assoc Veterinary Parasitologists Proc:21.

Liu, G., V. S. R. Choppa, M. K. Sharma, H. Ko, J. Choi, and W. K. Kim. 2024a. Effects of Methionine Supplementation Levels in Normal or Reduced Protein Diets on the Body Composition and Femur Bone Characteristics of Broilers Challenged with Coccidia. Animals 14:917.

Liu, H., H. Meng, M. Du, H. Lv, Y. Wang, and K. Zhang. 2024b. Chlorogenic acid ameliorates intestinal inflammation by inhibiting NF-κB and endoplasmic reticulum stress in lipopolysaccharide-challenged broilers. Poult Sci 103:103586.

Lucke, A., J. Böhm, Q. Zebeli, and B. U. Metzler-Zebeli. 2018. Dietary deoxynivalenol contamination and oral lipopolysaccharide challenge alters the cecal microbiota of broiler chickens. Front Microbiol 9:804.

van der Meer, A. J., C. Ding, A. J. Hoogendijk, A. F. de Vos, L. Boon, S. S. Zeerleder, and T. van der Poll. 2019. Neutrophils mitigate the systemic host response during endotoxemia in mice. Immunology 156:277–281.

Mustafa, A., S. Bai, Q. Zeng, X. Ding, J. Wang, Y. Xuan, Z. Su, and K. Zhang. 2021. Effect of organic acids on growth performance, intestinal morphology, and immunity of broiler chickens with and without coccidial challenge. AMB Express 11:1–18.

Nikaido, H., and M. Vaara. 1985. Molecular basis of bacterial outer membrane permeability. Microbiol Rev 49:1–32.

Parmentier, H. K., G. de Vries Reilingh, P. Freke, R. E. Koopmanschap, and A. Lammers. 2010. Immunological and physiological differences between layer-and broiler chickens after concurrent intratracheal administration of lipopolysaccharide and human serum albumin. Int J Poult Sci 9:574–583.

Redlich, K., and J. S. Smolen. 2012. Inflammatory bone loss: pathogenesis and therapeutic intervention. Nat Rev Drug Discov 11:234–250.

Reisinger, N., C. Emsenhuber, B. Doupovec, E. Mayer, G. Schatzmayr, V. Nagl, and B. Grenier. 2020. Endotoxin translocation and gut inflammation are increased in broiler chickens receiving an oral lipopolysaccharide (LPS) bolus during heat stress. Toxins (Basel) 12:622.

Rentería-Solís, Z., L. M. R. Silva, T. Grochow, R. Zhang, T. Nguyen-Ho-Bao, A. Daugschies, A. Taubert, I. Conejeros, and C. Hermosilla. 2024. Interaction of chicken heterophils and Eimeria tenella results in different phenotypes of heterophil extracellular traps (HETs). Poultry 3:318–329.

Sharma, M. K., G. Liu, D. L. White, Y. H. Tompkins, and W. K. Kim. 2022. Effects of mixed Eimeria challenge on performance, body composition, intestinal health, and expression of nutrient transporter genes of Hy-Line W-36 pullets (0-6 wks of age). Poult Sci 101:102083.

Tan, H., W. Zhen, D. Bai, K. Liu, X. He, K. Ito, Y. Liu, Y. Li, Y. Zhang, and B. Zhang. 2023. Effects of dietary chlorogenic acid on intestinal barrier function and the inflammatory response in broilers during lipopolysaccharide-induced immune stress. Poult Sci 102:102623.

Teng, P.-Y., J. Choi, Y. Tompkins, H. Lillehoj, and W. Kim. 2021a. Impacts of increasing challenge with Eimeria maxima on the growth performance and gene expression of biomarkers associated with intestinal integrity and nutrient transporters. Vet Res 52:1–12.

Teng, P.-Y., J. Choi, Y. Tompkins, H. Lillehoj, and W. Kim. 2021b. Impacts of increasing challenge with Eimeria maxima on the growth performance and gene expression of biomarkers associated with intestinal integrity and nutrient transporters. Vet Res 52:1–12.

Teng, P.-Y., S. Yadav, F. L. de Souza Castro, Y. H. Tompkins, A. L. Fuller, and W. K. Kim. 2020. Graded Eimeria challenge linearly regulated growth performance, dynamic change of gastrointestinal permeability, apparent ileal digestibility, intestinal morphology, and tight junctions of broiler chickens. Poult Sci 99:4203–4216.

Tompkins, Y. H., V. S. R. Choppa, and W. K. Kim. 2024. n-3 enriched Fish oil diet enhanced intestinal barrier integrity in broilers after Eimeria infection. Poult Sci 103:103660.

Tompkins, Y., G. Liu, B. Marshall, M. K. Sharma, and W. K. Kim. 2023. Effect of Hydrogen Oxide-Induced Oxidative Stress on Bone Formation in the Early Embryonic Development Stage of Chicken. Biomolecules 13:154.

Tompkins, Y. H., P. Teng, R. Pazdro, and W. K. Kim. 2022a. Long bone mineral loss, bone microstructural changes and oxidative stress after Eimeria challenge in broilers. Front Physiol 13.

Tompkins, Y. H., P. Teng, R. Pazdro, and W. K. Kim. 2022b. Long bone mineral loss, bone microstructural changes and oxidative stress after Eimeria challenge in broilers. Front Physiol 13.

Wang, J., S. S. Ghosh, and S. Ghosh. 2017. Curcumin improves intestinal barrier function: modulation of intracellular signaling, and organization of tight junctions. American Journal of Physiology-Cell Physiology 312:C438–C445.

Wang, X., Y. Li, J. Shen, S. Wang, J. Yao, and X. Yang. 2015. Effect of Astragalus polysaccharide and its sulfated derivative on growth performance and immune condition of lipopolysaccharide-treated broilers. Int J Biol Macromol 76:188–194.

Wu, Q. J., Y. M. Zhou, Y. N. Wu, L. L. Zhang, and T. Wang. 2013. The effects of natural and modified clinoptilolite on intestinal barrier function and immune response to LPS in broiler chickens. Vet Immunol Immunopathol 153:70–76.

Xie, H., N. C. Rath, G. R. Huff, W. E. Huff, and J. M. Balog. 2000. Effects of Salmonella typhimurium lipopolysaccharide on broiler chickens. Poult Sci 79:33–40.

Younus, H. 2018. Therapeutic potentials of superoxide dismutase. Int J Health Sci (Qassim) 12:88.

Zhang, B., Q. Zhong, N. Liu, P. Song, P. Zhu, C. Zhang, and Z. Sun. 2022. Dietary glutamine supplementation alleviated inflammation responses and improved intestinal mucosa barrier of LPS-challenged broilers. Animals 12:1729.

Zhou, X., L. Wang, Z. Wang, P. Zhu, Y. Chen, C. Yu, S. Chen, and Y. Xie. 2023. Impacts of Eimeria coinfection on growth performance, intestinal health and immune responses of broiler chickens. Vet Parasitol 322:110019.

Table 5.1 represents primer sequences used for real-time PCR.

Gene name[1]	Accession number	F primer sequence	R primer sequence
Beta actin	NM_205518.2	CAACACAGTGCTGTCTGGTGGTA	ATCGTACTCCTGCTTGCTGATCC
NFKB1	NM_204128.2	GAAGGAATCGTACCGGGAACA	CTCAGAGGGCCTTGTGACAGTAA
OCLN	NM_205128.1	ACGGCAGCACCTACCTCAA	GGCGAAGAAGCAGATGAG
MUC2	XM_040673077.2	ATGCGATGTTAACACAGGACTC	GTGGAGCACAGCAGACTTTG
ZO2	NM_001396728.1	GGCAAATCATTGAGCAGGA	ATTGATGGTGGCTGTAAAGAG

[1] NFKB1: nuclear factor kappa B subunit 1; OCLN: occludin; MUC2: mucin 2; ZO2: Zonula occludens 2.

Table 5.2 illustrates effect of Eimeria challenge and Lipopolysaccharides on Intestinal morphology. DPI: Days Post inoculation. NC/T1: Non-challenged, T2: *Eimeria* challenge, T3: *Eimeria* challenge + LPS 1 mg/kg (0 DPI), T4: *Eimeria* challenge + LPS 2 mg/kg (0 DPI), T5: *Eimeria* challenge + LPS 1 mg/kg (0 and 4 DPI), T6: *Eimeria* challenge + LPS 2 mg/kg (0 and 4 DPI). *P*-value <0.05.

DPI 6

	Jejunum			Duodenum			Ileum		
	Villus Height (in mm)	Crypt Depth (in mm)	Villus Width (in mm)	Villus Height (in mm)	Crypt Depth (in mm)	Villus Width (in mm)	Villus Height (in mm)	Crypt Depth (in mm)	Villus Width (in mm)
NC/ T1	1.16± 0.05^{a}	0.24±0. 02^{c}	0.26±0. 02^{a}	2.36±0. 07^{a}	0.37±0. 03	0.36±0. 01^{a}	1.2±0.0 4^{a}	0.2±0.0 1^{d}	0.29±0. 03^{a}
T2	1.04± 0.06^{b}	0.31±0. 02^{a}	0.26±0. 02^{a}	2.04±0. 07^{b}	0.38±0. 02	0.17±0. 01^{c}	1.01±0. 02^{bc}	0.32±0. 02^{a}	0.24±0. 02^{ab}
T3	0.82± 0.03^{b}	0.24±0. 02^{c}	0.16±0. 01^{b}	1.68±0. 13^{c}	0.3±0.0 1	0.22±0. 01^{bc}	0.88±0. 05^{c}	0.22±0. 01^{cd}	0.28±0. 02 ^{a}
T4	1.07± 0.04^{b}	0.25±0. 02^{bc}	0.19±0. 0^{ab}	1.9±0.0 7^{bc}	0.36±0. 02	0.23±0. 02^{b}	1.05±0. 05^{b}	0.26±0. 02^{b}	0.23±0. 03^{ab}
T5	0.97± 0.04^{b}	0.3±0.0 1^{ab}	0.26±0. 03^{a}	1.94±0. 05^{bc}	0.31±0. 02	0.32±0. 01^{a}	1±0.04^{b} ^{c}	0.24±0. 01^{bc}	0.3±0.0 2^{a}

T6	1.07± 0.04^{b}	0.24±0. 01^{c}	0.2±0.0 1^{ab}	2.17±0. 04^{ab}	0.35±0. 01	0.24±0. 02^{b}	1.13±0. 03^{ab}	0.22±0. 01^{cd}	0.2±0.0 2^{b}

Figure 5.1 represents the timeline of events including days of challenge of *Eimeria* and Lipopolysaccharides injection.

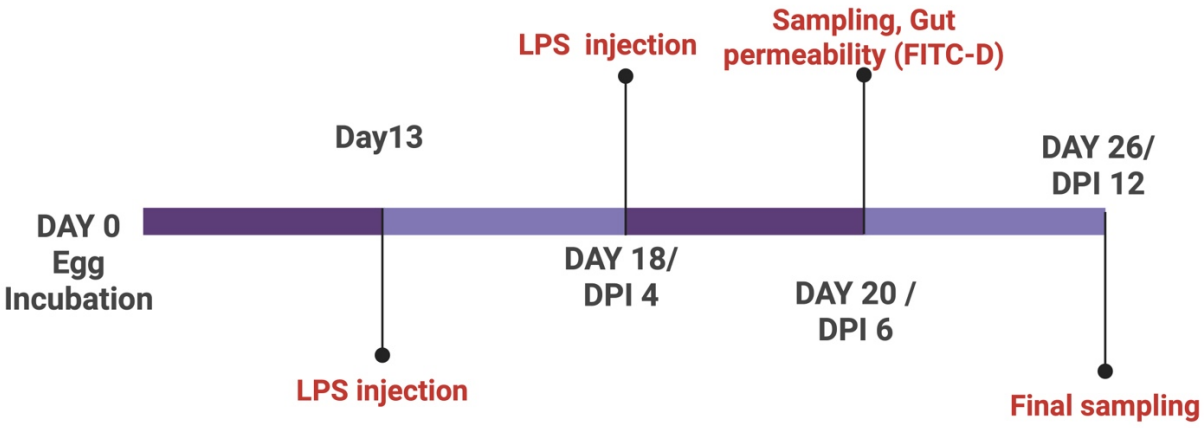

Figure 5.2 illustrates effect of *Eimeria* challenge and Lipopolysaccharides on average body weight, average daily gain (0-12 DPI), Average daily feed intake of the broilers. The error bars represent treatment's standard error. Letters which are not connected by same letters are significantly different. *P*-value < 0.05. DPI: Days Post inoculation. NC/T1: Non-challenged, T2: *Eimeria* challenge, T3: *Eimeria* challenge + LPS 1 mg/kg (0 DPI), T4: *Eimeria* challenge + LPS 2 mg/kg (0 DPI), T5: *Eimeria* challenge + LPS 1 mg/kg (0 and 4 DPI), T6: *Eimeria* challenge + LPS 2 mg/kg (0 and 4 DPI).

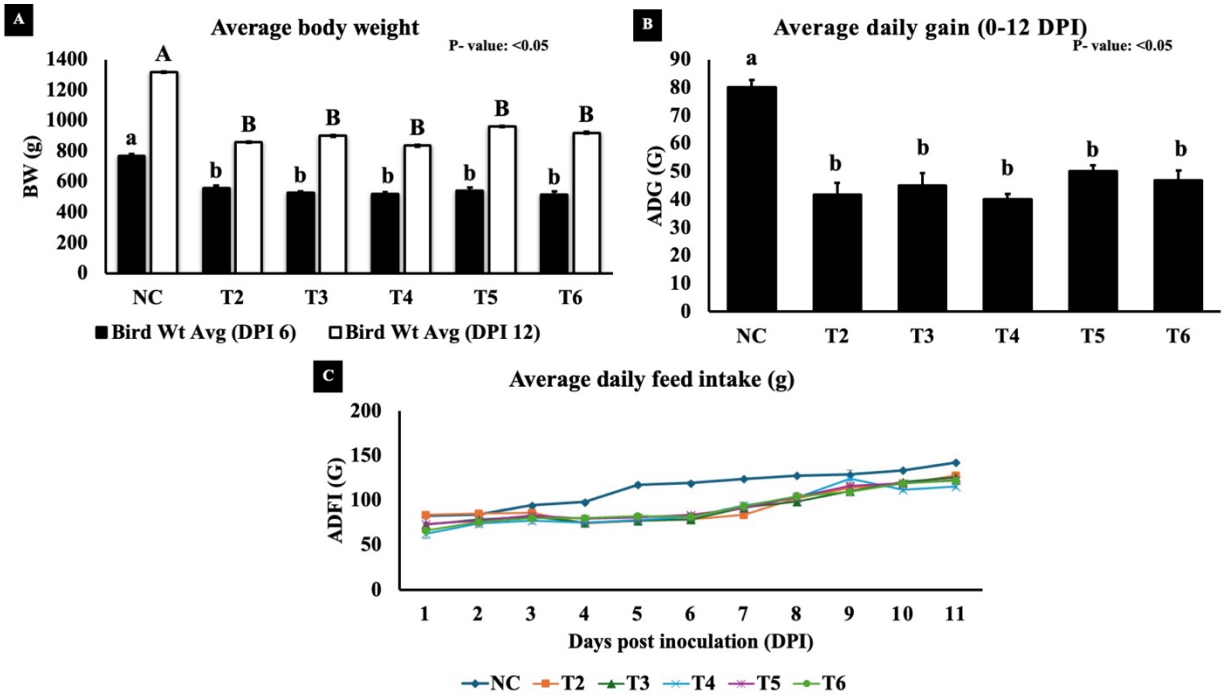

Figure 5.3 illustrates effect of *Eimeria* challenge and Lipopolysaccharides on lesion scores of *Eimeria acervulina* (Upper Intestine), *Eimeria maxima* (Mid intestine), *Eimeria tenella* (Lower intestine). The error bars represent treatment's standard error. DPI: Days Post inoculation. T2: *Eimeria* challenge, T3: *Eimeria* challenge + LPS 1 mg/kg (0 DPI), T4: *Eimeria* challenge + LPS 2 mg/kg (0 DPI), T5: *Eimeria* challenge + LPS 1 mg/kg (0 and 4 DPI), T6: *Eimeria* challenge + LPS 2 mg/kg (0 and 4 DPI).

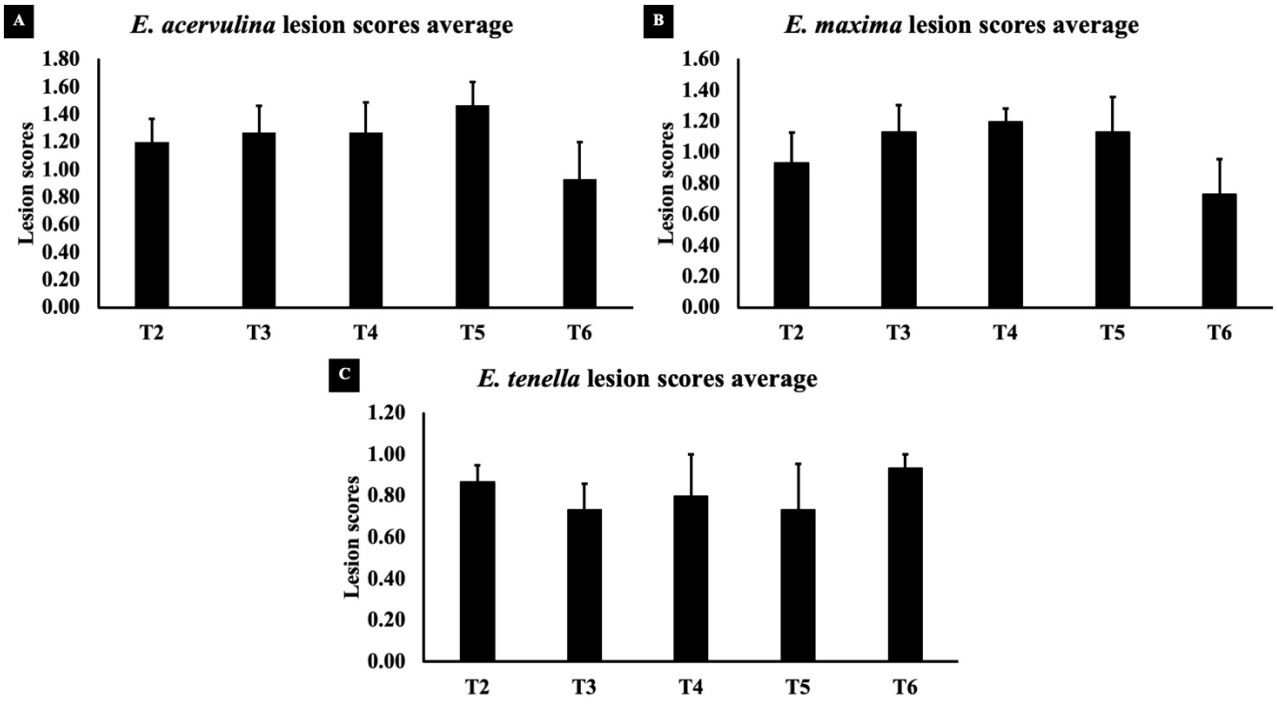

Figure 5.4 illustrates effect of *Eimeria* challenge and Lipopolysaccharides on Intestinal Permeability (FITC-D). The error bars represent treatment's standard error. Letters which are not connected by same letters are significantly different. DPI: Days Post inoculation, FITC-D: Fluorescein Isothiocyanate-Dextran. NC/T1: Non-challenged, T2: *Eimeria* challenge, T3: *Eimeria* challenge + LPS 1 mg/kg (0 DPI), T4: *Eimeria* challenge + LPS 2 mg/kg (0 DPI), T5: *Eimeria* challenge + LPS 1 mg/kg (0 and 4 DPI), T6: *Eimeria* challenge + LPS 2 mg/kg (0 and 4 DPI).

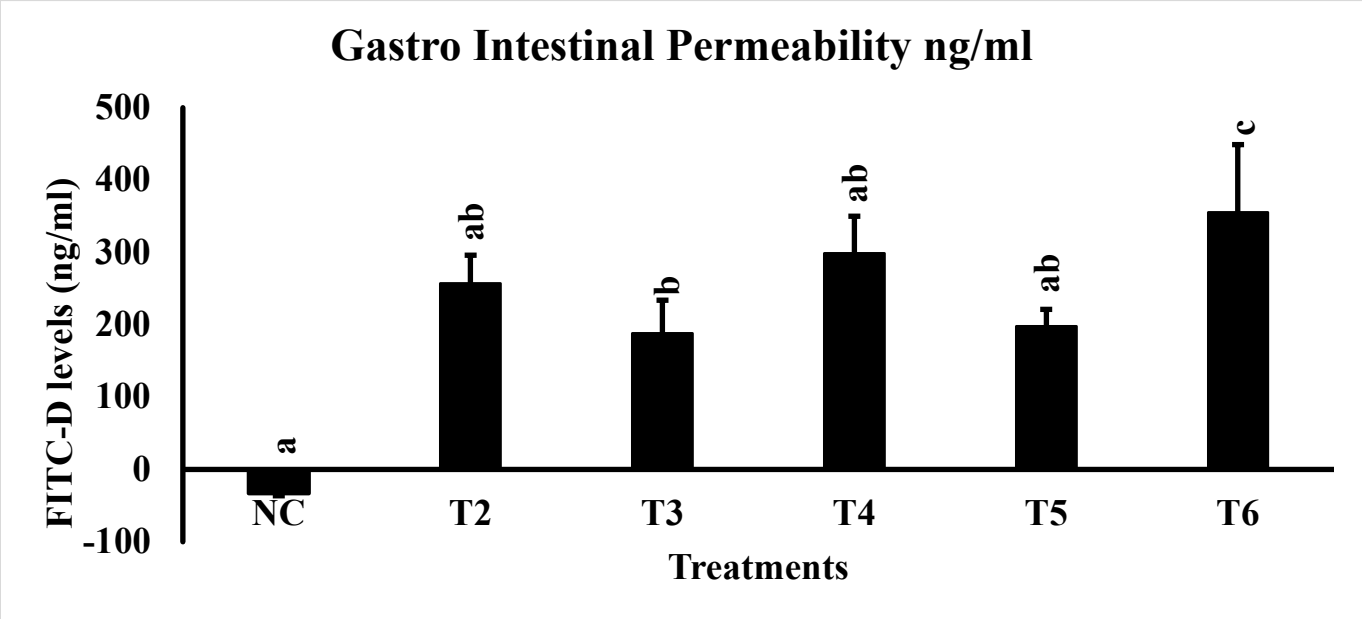

Figure 5.5 illustrates effect of *Eimeria* challenge and Lipopolysaccharides on villus height to crypt depth ratio. The error bars represent treatment's standard error. Letters which are not connected by same letters are significantly different. DPI: Days Post inoculation. NC/T1: Non-challenged, T2: *Eimeria* challenge, T3: *Eimeria* challenge + LPS 1 mg/kg (0 DPI), T4: *Eimeria* challenge + LPS 2 mg/kg (0 DPI), T5: *Eimeria* challenge + LPS 1 mg/kg (0 and 4 DPI), T6: *Eimeria* challenge + LPS 2 mg/kg (0 and 4 DPI).

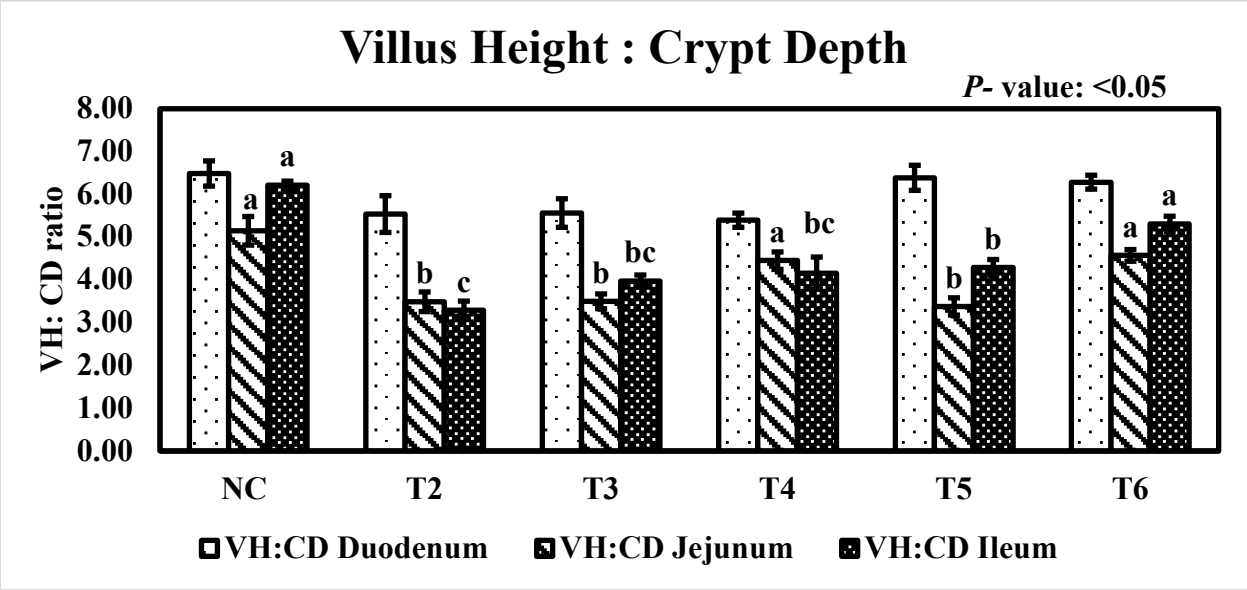

Figure 5.6 illustrates effect of *Eimeria* challenge and Lipopolysaccharides on Total antioxidant Capacity (TAC) and Superoxide Dismutase (SOD). The error bars represent treatment's standard error. Letters which are not connected by same letters are significantly different. DPI: Days Post inoculation. NC/T1: Non-challenged, T2: *Eimeria* challenge, T3: *Eimeria* challenge + LPS 1 mg/kg (0 DPI), T4: *Eimeria* challenge + LPS 2 mg/kg (0 DPI), T5: *Eimeria* challenge + LPS 1 mg/kg (0 and 4 DPI), T6: *Eimeria* challenge + LPS 2 mg/kg (0 and 4 DPI). *P*-Value < 0.05.

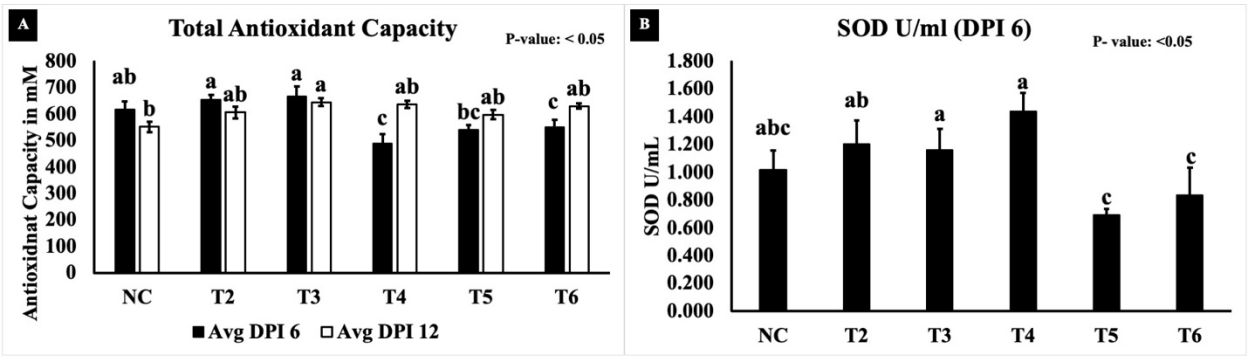

Figure 5.7 illustrates effect of *Eimeria* challenge and Lipopolysaccharides on Immunoglobulin G/Y levels. The error bars represent treatment's standard error. Letters which are not connected by same letters are significantly different. DPI: Days Post inoculation. NC/T1: Non-challenged, T2: *Eimeria* challenge, T3: *Eimeria* challenge + LPS 1 mg/kg (0 DPI), T4: *Eimeria* challenge + LPS 2 mg/kg (0 DPI), T5: *Eimeria* challenge + LPS 1 mg/kg (0 and 4 DPI), T6: *Eimeria* challenge + LPS 2 mg/kg (0 and 4 DPI). *P*-Value < 0.05

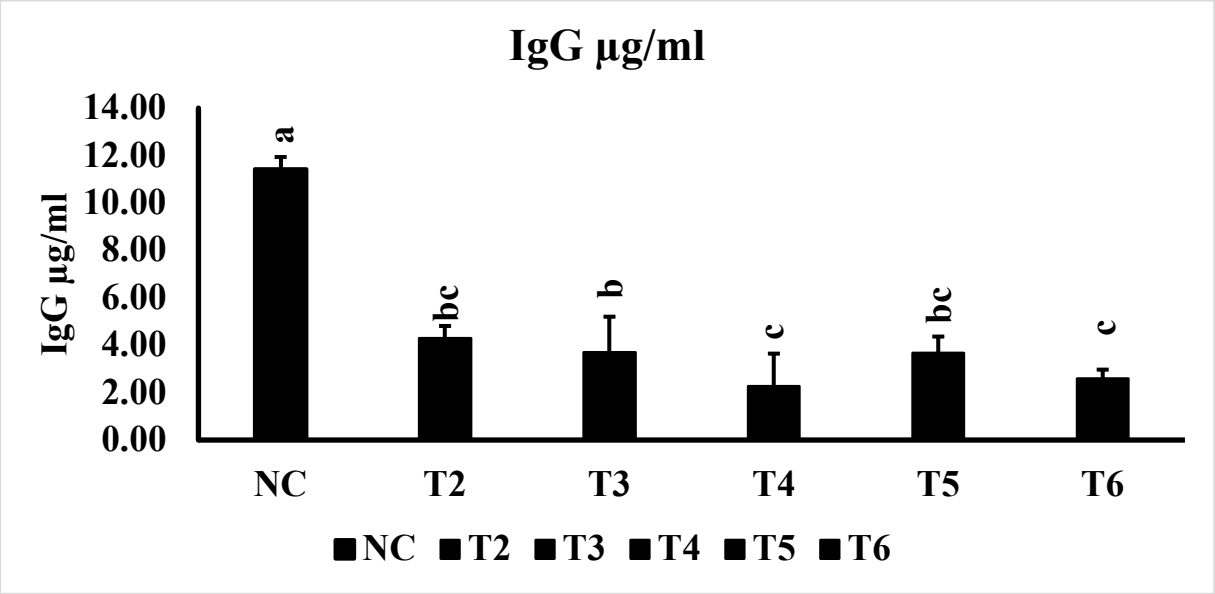

Figure 5.8 illustrates effect of *Eimeria* challenge and Lipopolysaccharides on gene expression of Occludin (OCLN), Mucin 2 (MUC2), and Nuclear Factor- Kappa B (NF-κB1). The error bars represent treatment's standard error. Letters which are not connected by same letters are significantly different. DPI: Days Post inoculation. NC/T1: Non-challenged, T2: *Eimeria* challenge, T3: *Eimeria* challenge + LPS 1 mg/kg (0 DPI), T4: *Eimeria* challenge + LPS 2 mg/kg (0 DPI), T5: *Eimeria* challenge + LPS 1 mg/kg (0 and 4 DPI), T6: *Eimeria* challenge + LPS 2 mg/kg (0 and 4 DPI). *P*-Value < 0.05.

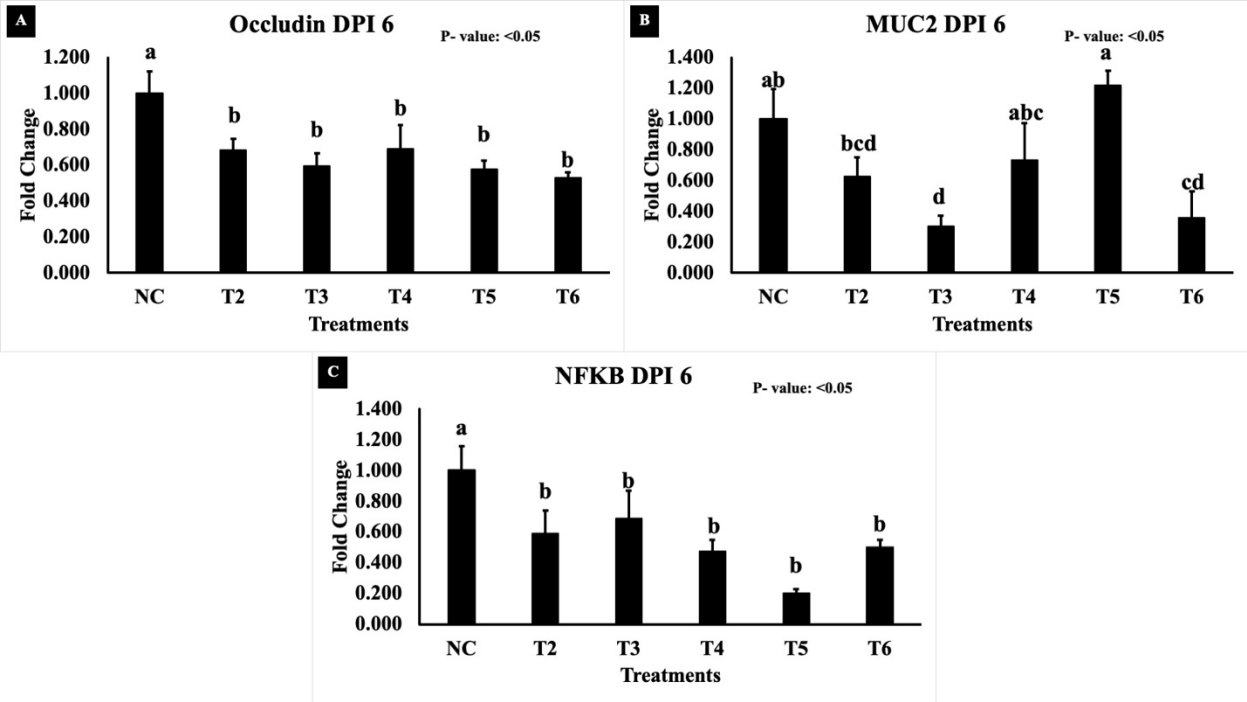

CHAPTER 6

EFFECT OF LIPOPOLYSACCHARIDES AND MIXED *EIMERIA* SPP. CHALLENGE ON PERFORMANCE AND BONE DEVELOPMENT IN BROILERS [1]

[1]Choppa, V. S. R., Liu, G., Shi, H., Sharma, M. K., Goo, D., & Kim, W. K. (2025). *Poultry Science*, 105501.

ABSTRACT

Modern-day broilers are prone to disproportionate bone development besides beneficial broiler performance parameters. Cardinally, global concerns on production and welfare parameters are associated with altered intestinal health and bone homeostatic disturbances pertaining to oxidative stress and inflammation caused by coccidiosis. Nonetheless, lipopolysaccharides (**LPS**) released into systemic circulation during gut barrier integrity disruption also inhibits bone formation. The current study focused on bone health following the co-challenge of LPS and coccidia in broilers. Cobb500 male broilers were randomly assigned to 6 treatments (**T1-T6**) and 5 replicates with 12 birds in each pen. Mixed *Eimeria* spp., 12,500 *E. maxima*, 12,500 *E. tenella*, and 62,500 *E. acervuline*, were inoculated orally on day 14 for all treatments except for the non-challenged control (**NC** or **T1**) group. On the same day, LPS was injected intraperitoneally to T3 and T4 at 1 and 2 mg/kg, respectively. T5 and T6 had intraperitoneal injections of LPS at 1 and 2 mg/kg, respectively, on both days 14 and 18. Data obtained from Dual Energy X-ray Absorptiometry (**DEXA**) showed a significantly lower bone mineral content for the challenged treatments (T2-T6) compared to the non-challenged treatment. Furthermore, bone mineral density (**BMD**) for 6 days post *Eimeria* spp. inoculation (**DPI**) was significantly lower in T4, T5, and T6. Interestingly, micro-CT data revealed that tibial cortical bone porosity parameters such as closed pores number, volume of open pores, and total volume of pores at DPI 12 were significantly lower for T4 and T6. Moreover, sclerostin (**SOST**) levels in serum were significantly higher in T6, showing an evidence on aberrations in bone homeostasis following coccidiosis and LPS challenge. Reinforcing the above statement, calcein labelling for dynamic bone histomorphometry also revealed similar findings. Finally, the current study shows that higher doses of LPS and concomitant coccidiosis

adversely affect bone development in broilers which improves our understanding on gut-bone axis besides deciphering novel findings on concomitant effects of both challenge candidates.

Keywords: Broilers, Lipopolysaccharide (LPS), *Eimeria*, Sclerostin, Bone homeostasis

INTRODUCTION

Despite advancements in genetics and production systems, skeletal anomalies have remained prevalent. These abnormalities are primarily associated with economically significant gastrointestinal diseases such as coccidiosis (Chapman, 2014; Chapman and Rathinam, 2022; Tompkins et al., 2022b; Liu et al., 2024). Coccidiosis in broilers is primarily associated with break in intestinal integrity by damaging intestine leading to decreased nutrient absorption which manifests as poor broilers performance. Above factors along with pro-inflammatory factors and oxidative stress is reported to contribute for compromising bone homeostasis (Kakhki et al., 2019; Tompkins et al., 2022a, 2023; Chen et al., 2025). Furthermore, compromised intestinal integrity from coccidiosis and/or other pathogens would cause aberrations in microbiome leading to release bacterial components like lipopolysaccharides (LPS) (gram-negative bacteria) into the systemic circulation (endotoxemia), in turn stimulating inflammatory reactions in the host (Nikaido and Vaara, 1985; Martin et al., 2011; Reisinger et al., 2020; Choi and Kim, 2022; Choi et al., 2023). Reduction in feed intake and associated disruption in nutrient absorption besides inflammation affects bone development by disrupting calcium (Ca) and phosphorus (P) metabolism, ultimately reducing bone formation (Fountos et al., 1998; Tompkins et al., 2022b). Emphasizing on inflammation, pro-inflammatory cytokines such as IL-1β, IL-6, and TNF-α, inhibit bone growth synergistic interactions and antagonizing the function of growth hormones (Iotsova et al., 1997; Fountos et al., 1998). Moreover, Wnt (Wingless integrated-1) signaling pathway which plays key role in cell fate determination, cell migration and polarity would potentially be blocked by sclerostin in the presence of bacterial component like LPS (Holdsworth et al., 2012; Gao et al., 2013; Houschyar et al., 2019). Substantiating the above mechanisms, our previous study on mesenchymal stem cells treated with LPS revealed decreased osteogenic differentiation (Choppa

et al., 2023). Although inflammation and its associated bone diseases have been studied, their effects in chickens remain poorly understood. Nutritional deficiency and physical stress have long been believed to be primary contributors to bone disorders during *Eimeria* infection (Santos et al., 2020; Tompkins et al., 2023a). However, immune response and oxidative stress play a significant role in bone modeling and remodeling by modulating differentiation and activity of bone cells (osteoblasts, osteoclasts, and osteocytes) (AlQranei et al., 2021; Cooney et al., 2021; Rath and Durairaj, 2022; Tompkins et al., 2023). Although effects of bacterial component like LPS on intestinal inflammation have been studied (Irisa et al., 2001; Redlich and Smolen, 2012), its impact on bone is largely unexplored, particularly in the presence of intestinal damage caused by *Eimeria* spp. Thus, this study aimed to investigate the effects of lipopolysaccharide (LPS) on bone development in broilers with coccidiosis, specifically examining its role in bone growth and inflammation.

MATERIALS AND METHODS

Experimental design

The current study was approved by the Institutional Animal Care and Use Committee and conducted at the Poultry Research Center, University of Georgia (A2021 12-012). A total of 360, one-day-old Cobb male broiler chickens were randomly allocated to six treatments (**T1-T6**) with five replicates and 12 birds per cage and fed feed and water *ad libitum*. Cobb management guidelines were followed for temperature setting. Descriptions of six treatments in the current study are provided in **Table 6.1**. The timeline and sampling points are shown in **Figure 6.1**. Birds were inoculated with *Eimeria spp.* (62,500 oocysts of *E. acervulina*, 12,500 oocysts of *E. maxima* and *E. tenella* per mL of inoculum per bird). Briefly, mixed *Eimeria* spp., were inoculated orally on day 14 for all treatments (**T2-T6**) except for the non-challenged control (**NC** or **T1**) group. T1

was given with equal volume (1mL) of PBS orally. On the same day, LPS (from *Salmonella enetrica* serotype typhimurium, Sigma-Aldrich, Cat.no:L6511, Saint Louis, MO, USA) was injected intraperitoneally to T3 and T4 at 1 and 2 mg/kg, respectively. T5 and T6 had intraperitoneal injections of LPS at 1 and 2 mg/kg, respectively, on both days 14 and 18. Sampling were performed on DPI (days post inoculation of *Eimeria*) 6 and 12 which refers to day 20 and 26 respectively.

Dual-energy X-ray absorptiometry

Body composition parameters of birds include total tissue weight, lean weight, body fat percentage, bone mineral density (**BMD**), and bone mineral content (**BMC**). These parameters were assessed using dual-energy X-ray absorptiometry (**DEXA**, GE Healthcare, Chicago, IL, USA). At 6 and 12 DPI, birds were euthanized and positioned chest-up in the DEXA scanner, and whole-body scans were performed (Chen et al., 2020). Scans were performed at a speed of 2.5 mm/s with a voxel resolution of 0.07 x 0.07 x 0.50 mm (Paneru et al., 2025). Before performing the scans, DEXA system was calibrated using a phantom with a known BMD. Data were analyzed using Lunar Prodigy software (GE healthcare, encore software version 12.20.023).

Micro - Computed Tomography (Micro-CT)

Tibial bones were sampled on DPI (days post inoculation) 6 and 12 followed by removal of soft tissues and wrapping in a wet cheesecloth. The samples were stored at -20°C and thawed before analysis. Bones were held in low-density 50 mL tubes using cheesecloth to avoid random movement. Bones were scanned using a Skyscan Micro-CT scanner (Skyscan 1275, Bruker microCT, Billerica, MA). X-ray settings used for scan were 77 kV and 129 μA with pixel size of 25 μm and a 0.5 mm aluminum filter to reduce beam hardening. The 180° scanning was used with

a 0.4° rotation angle which captured 4 images per rotation. N-recon (Bruker microCT) software was used to reconstruct 2D image to a 3D model. This 3D model was straightened using data viewer software (Bruker microCT), followed by region of interest selection using the CTAn program (Bruker microCT). The phantoms at 0.25 and 0.75 g/cm^3 density were used for calibration of bone mineral density. The selected region was then processed for cortical and trabecular separation using procedures described in previous studies (Chen and Kim, 2020; Sharma et al., 2023; Shi et al., 2023).

Quantitative Real-Time PCR analysis (qRT-PCR)

Bone marrow, liver, and cecal tonsils were collected on 6 and 12 DPI, frozen, and stored in -80°C. For RNA extraction, tissues were homogenized with QIAzol lysis reagents (Qiagen, Valencia, CA) following product instructions. RNA concentration and quality were assessed using NanoDrop 2000 spectrophotometer (Thermo Fischer Scientific, MA). Complementary DNA (cDNA) was synthesized from RNA using cDNA synthesis kits (Applied Biosystems, Foster City, CA. Real-time PCR was performed using SYBR Green Master mix and a Step One thermocycler (Applied Biosystem). Gene expression levels were analyzed using $2^{-\Delta\Delta Ct}$ method, with cDNA samples were run in duplicate. Primers (Integrated DNA Technologies Inc., IA, USA) used for housekeeping and target genes are listed in **Table 6.2**.

Mineral apposition rate using calcein labeling

Calcein can chelate to calcium and be visualized as relatively broad fluorescent band. Dynamic histomorphometry for bone formation (mineral apposition rate: **MAR**) was measured using calcein labeling (Sigma Aldrich, St. Louis, MO). First, calcein was dissolved in 1 M sodium hydroxide solution and 2 % working solution was prepared by mixing the above solution with

sterile distilled water. Birds were injected intraperitoneally with 20 mg/kg body weight calcein solution at different time points (**Figure 6.1**). Tibial bones were collected at 12 DPI and preserved in 70% ethanol. A bone slice was taken from mid-diaphysis using a saw (Ryobi, Anderson, SC, USA) and mounted on a glass slide. A fluorescence microscope (BZ-Z800, Keyence Inc., Itasca, IL) was used to measure the distance (ImageJ software, National Institute of Health, Bethesda, MD, USA) between two calcein labels indicating the bone growth(Tompkins et al., 2023).

Sclerostin levels

Serum sclerostin levels were measured using SOST ELISA kits (MyBioSource, Inc. San Diego, CA, USA). The samples were stored at -80°C before analysis. Samples were prepared and analyzed, and data analysis was done based on the manufacturer's instruction manual.

Statistical Analyses

Data from the current study were analyzed using JMP Pro16 (SAS Institute, Inc., Cary, NC, USA). One-way ANOVA were used to statistically assess the differences between the treatment groups, and post-hoc tests such as Tukey's HSD, Dunn's and Student's t-test were used to analyze the means. Log transformations were applied to non-normal data and checked for normality and homogeneity before employing statistical analyses like ANOVA and student's t test. The mean and standard error of the mean were used to express all experimental data (SEM). Statistical significance was set at $P < 0.05$.

RESULTS

Dual-energy X-ray absorptiometry

DEXA data revealed significant differences in BMC (g/kg body weight) of DPI 6 and DPI 12 birds. Specifically, these BMC differences were observed between non-challenged and

challenged treatments; the NC group had 6.756 g/kg, whereas the challenged treatments (T2-T6) had significantly lower BMC ranging between 5 to 6.21 g/kg (**Figure 6.2A**). Among these, T5 had 6.21 grams of BMC, and T6 had the lowest BMC of 5.310 g/kg (**Figure 6.2A**). Interestingly, DPI 12 data revealed significant differences between non-challenged treatments and *Eimeria* challenged ones (T2-T6) (**Figure 6.2C**) with non-challenged BMC of 22 g/kg and T2, T3, T4, T5, and T6 were having 15.2, 11.8, 11.2, 12.4, and 11.6 g/kg respectively.

BMD for DPI 6 and 12 was significantly lower for T4, T5, and T6 with 0.118, 0.117, and 0.114 g/cm^2 respectively compared to non-challenged, T2, and T3 with 0.130, 0.121, and 0.123 g/cm^2 respectively (Figure 6.2B and D). Furthermore, DPI 12 data showed Non challenged (0.16 g/cm^2) is significantly higher than other treatments (Figure 6.2B and D).

Mineral apposition rates using calcein labeling

MAR using calcein labeling technique, which enabled us to obtain dynamic bone histomorphometry, uncovered interesting findings including lower bone growth rate for the T4, T5, and T6 having MAR of 56.5, 113.2, and 50.3 mm, respectively, compared to the NC, T2, and T3 with 501.2, 222.8, 223.3 mm, respectively (**Figure 6.3**). Statistically, T1 or non-challenged was significantly higher than other treatments followed by T2, T3 were significantly higher compared to T5. T5 was significantly greater than T4 and T6. In addition, the T2 and T3 had significantly lower MAR compared to the NC ($P < 0.05$). Linear effect with T2, T3, T4 were observed. Furthermore, Linear effect for T2, T5, and T6 were also observed.

Sclerostin levels

Sclerostin levels on DPI 6 were significantly higher in T6 with 625 pg/ml compared to other treatments. Among the significantly lower treatment groups, NC and T2 were lowest with

134 and 104.3 pg/ml respectively. Furthermore, T3, T4, and T5 had insignificantly higher levels of 251, 403, 342.7 pg/ml respectively (**Figure 6.4**). T2, T3, T4 shown linear effect and the same effect was observed for T2, T5, and T6.

Micro Computed Tomography

On DPI 12, cortical bone 3D analyses revealed that tissue and bone volume were significantly lower for all challenged treatments with an approximate tissue volume difference greater than 98 mm^3 and bone volume difference of more than 67 mm^3 (**Figure 6.5A**). Similarly, tissue and bone surface was significantly lower for the challenged treatments approximately less than 144 and 834 mm^2 respectively compared to the non-challenged group (**Figure 6.5B and C**). Interestingly, interaction surface was significantly lower in the T5 and T6 compared to one in the NC which are 281.2, 237.18, and 237.46 mm^2 respectively (**Figure 6.5D**).

Closed pores number was significantly lower for the T4 (638.75) and T6 (721) compared to the NC (2215) (**Figure 6.6A**). Similarly, the volume of open pores and total volume of pores were notably lower for the T4 and T6 compared to the NC. Specifically, the volumes of open pores for the NC, T4, and T6 were 63.9, 22.65, and 22.15 mm^3, respectively (**Figure 6.6B**). On the other hand, total volumes of pores were 65.7, 23.08, and 22.8 mm^3 for NC, T4 and T6 respectively (**Figure 6.6C**).

Gene Expression

Toll Like Receptor (**TLR**) 4 gene expression in the liver on DPI 6 was upregulated for T2, T4, and T6 with a fold change of 5.7, 4.9, and 5.3, respectively (**Figure 6.7A**). Furthermore, Nuclear Factor Kappa B (**NFKB**) in the cecal tonsil was downregulated for the challenged treatments (T2, T3, T4, T5, and T6) compared to the NC (**Figure 6.7B**). Similarly, Tumor Necrosis

Factor Alpha (TNFA) in the cecal tonsil on DPI 6 was downregulated for the challenged treatments (T2, T3, T4, T5, and T6) with a fold change of 0.321, 0.482, 0.575, 0.525 and 0.454, respectively, compared to the NC (**Figure 6.7C**).

DISCUSSION

Coccidiosis is a global poultry disease associated with significant economic losses to the poultry industry (Chapman, 2014). Besides intestinal disturbances leading to growth performance aberrations, *Eimeria* spp. are associated with decreased bone growth which would lead to gait abnormalities (Applegate and Lilburn, 2002; Tompkins et al., 2023). Studies related to these skeletal disorders were attributed to physical, nutritional, and physiological factors (Rath and Durairaj, 2022). Furthermore, immune system and its cross talk with bone cells in the presence of various infectious and non-infectious factors also contribute to alterations in bone homeostasis (D'Amelio and Sassi, 2016). Moreover, this would extend to lipopolysaccharides, which are released with shift in gut microbiome, serving as a driving factor to disturb bone homeostasis through several pathways including conserved pro-bone pathways like Wnt signaling pathway (Gao et al., 2013; Wassenaar and Zimmermann, 2018; Page et al., 2022; Choppa and Kim, 2023a; Choppa et al., 2023). However, lacunae exist in understanding effects of bacterial cell wall component like LPS and *Eimeria* spp. in bone health of broilers which is addressed in the current study.

Dual energy X-ray absorptiometry (DEXA) is commonly used in determining bone mineral content and density in identifying osteoporosis (Cummings et al., 2002a; Ramos et al., 2012; Schallier et al., 2019a). Measurements from DEXA are differentiated into soft and hard tissues using attenuation of two different energy X-ray beams with different energy levels. Furthermore, the data from DEXA have high correlations with bone ash which makes this a reliable parameter

in understanding bone health in broilers (Cummings et al., 2002b; Kim et al., 2012; Schallier et al., 2019a; b)**.** DEXA findings from the current study revealed significant changes in bone mineral content of birds on DPI 6 and 12. On DPI 6 and 12, significant differences were observed between *Eimeria* challenged and non-challenged groups. Furthermore, these results are in agreement with previous studies on *Eimeria* challenge (Tompkins et al., 2023, 2024; Liu et al., 2024). This could be due to altered inflammatory and related pathways due to *Eimeria* spp. which can be justified from sclerostin levels and mineral apposition rate representing decreased bone formation and increased resorption (Holdsworth et al., 2012; Shim, 2016). Among these two, BMC represents overall bone mineral closely related to the size of bone, and BMD represents amount of mineral for a given area (grams per square centimeter) (Lampe and Rock, 2001).

Based on the above findings, Micro-CT was employed to understand the microstructural changes in tibial bones among the treatments. Findings were not significant on DPI 6, but interesting findings with respect to interaction surface were observed on DPI 12 where the groups challenged with 1 and 2 mg/kg injected at two time points (T5 and T6) had significantly lower interaction surface compared to the other challenged treatments. Moreover, the higher dosage (2 mg/kg) of LPS injection groups (T4 and T6) revealed significant differences in closed pores number, volume of open pores, and total volume of pores representing the decreased space for migration and proliferation of osteoblasts (Siris et al., 2004; Hannink and Arts, 2011)(Siris et al., 2004). Although differences in micro-CT parameters in only *Eimeria* challenge were similar to previous studies (Tompkins et al., 2022b, 2023), porosity differences are novel findings observed with *Eimeria* challenge and LPS injection at 1 and 2mg/kg at two time points. These porosity differences indicate altered bone strength and vascular porosity (Zebaze and Seeman, 2015). Additionally, pores represent actively developing, contracting, infilling, and expanding closed or

open pores where open pores represent pores on endosteal and periosteal surfaces (Surowiec et al., 2022a). Moreover, the relationship between porosity and bone stiffness is reported to have altered ability to counter the external stressors. Specifically, increase in porosity is associated with a poor bone elastic modulus or stiffness (Surowiec et al., 2022b; Jiao et al., 2023). In contrast, increased porosity often represents greater surface area and increased vascularity which are essential for dynamic characteristics of cortical bone like bone remodeling and growth to attain strong bone (Bortel et al., 2015; Jiao et al., 2023). The above micro-CT findings can be related to mineral apposition rates, sclerostin levels, and gene expression.

Firstly, MAR by calcein labeling reflects dynamic changes in bone. This method is based on the principle of calcium chelating ability in calcein (fluorochrome) by forming fluorescent complexes with calcium in mineralizing bone (Turner, 1994; Shim, 2016). Injecting the calcein at two different time points allows calcein to chelate with two different layers of calcium which are measurable as width using microscope (Turner, 1994). A significantly lower mineral apposition rate for the T4, T5, and T6 which evidently represents decreased bone development. This suggests detrimental effects of LPS in the presence of *Eimeria* challenge on bone development. This likely shows the combined impact of LPS and *Eimeria* challenge, corroborating findings from both DEXA and micro-CT analyses. Furthermore, Linear decrease in MAR shows a reduction in bone growth with increase in dose of LPS (T2, T3, T4). Similarly, Linear decrease in MAR was observed when LPS (1 and 2 mg/kg) were given two time points (T2, T5, and T6). This shows dose-effect relationship between LPS and bone development which was supportively observed in our previous invitro study. This indicates that the LPS when considered as a bacterial representative which is released into circulation will hinder bone growth. Similar findings from sclerostin uncovers the possible involvement of Wnt signaling pathway inhibition in reducing the bone development.

Sclerostin, a glycoprotein secreted by osteocytes to negatively regulate bone anabolism (Xiaohui et al., 2024). This acts as a key molecule inhibiting osteoblastogenesis which is achieved by inhibiting Wingless-related integration site interaction (Wnt) with low-density lipoprotein protein 4/5/6 (Wnt co-receptors) (Atkins et al., 2011; Leupin et al., 2011; Holdsworth et al., 2012). Wnt Signaling activation leads to mineralization of bone by allowing differentiation of mesenchymal stem cells to osteoblasts which embed into bone matrix followed by differentiation into osteocytes (Atkins et al., 2011; Ke et al., 2012). These osteocytes release sclerostin that maintains bone lining cells and inhibits canonical Wnt signaling pathway, suppressing late osteoblasts differentiation into osteocytes (Leupin et al., 2011; Hong et al., 2022). Furthermore, Sclerostin inhibits bone morphogenetic protein (BMP) signaling especially in osteocytes and promoting apoptosis of osteoblasts by activation of caspases (Sutherland et al., 2004). Sclerostin levels which are significantly higher in the T6 and numerically greater in the T3, T4, and T5 showing a possible inhibition of Wnt signaling pathway and above stated pathways which leads to negative impact on osteogenesis (Zhong et al., 2012; Gao et al., 2013; Choppa and Kim, 2023b). Moreover, linear effect was observed with T2, T3, T4 and T2, T5, T6 which shows dose dependent release of sclerostin which manifests as disturbance in bone homeostasis. Low dose of LPS (3.125 μg) treated on mesenchymal stem cells isolated from chicken compact bones in our earlier study shows, sclerostin was upregulated inhibiting Wnt signaling pathway which can be reflected from gene expression from beta catenin and LRP5 receptor upregulation (Choppa and Kim, 2023a; Choppa et al., 2023). Additionally, at high doses of LPS (50 and 25 μg) on mesenchymal stem cells revealed DICER1 dysregulation and interleukin 1-beta upregulation which suggests decreased osteoclast activity which can be related to the findings in the current study (Choppa et al., 2023).

In the current study, the gene expression of Toll-like receptor 4 (TLR4) was upregulated in the *Eimer*ia challenge alone or both *Eimeria* and higher LPS challenged groups (T2, T4, and T6), suggesting an enhanced inflammatory response, whereas other treatments had a downregulation of those genes, indicating a negative feedback mechanism following acute inflammatory response (Ciesielska et al., 2021). Moreover, LPS follows noncanonical inflammasome activation which might not involve TLR4 (Ciesielska et al., 2021). Generally, TLR4 triggers inflammation after recognizing LPS which activates pro-inflammatory cytokines and ROS production (Niu et al., 2021a; b; Xiao et al., 2024). Contrasting results for other treatments in the current study could be related to negative feedback mechanism which follows initial triggered inflammatory response (de Zoete et al., 2010; Gruffaz et al., 2017; Rehman et al., 2021). Although, the current study did not find significant differences among innate immune response related genes like NOD-like receptor Pyrin 3 (NLRP3), Lipoprotein receptor-related protein 5 (LRP5), Endoribonuclease 1 (DICER1) gene expression, but these findings could possibly be imputed to negative feedback mechanisms possibly due to heightened effects of acute inflammatory responses during the initial 24 h period (Delgado-Calle et al., 2017; Hoss et al., 2019; Choppa et al., 2023; Kim et al., 2024). The above statement can be extended to nuclear factor kappa B and tumor necrosis factor alpha gene expression in the current study which were surprisingly downregulated in all *Eimeria* spp. challenged treatments (T2-T6). Targets like sclerostin, NLRP inflammasomes, proinflammatory cytokines which disharmonize the bone health in broilers would help in alleviating concerns related to bone health which are not limited to bacterial chondronecrosis and osteomyelitis (often termed as femoral head necrosis) (Wideman Jr et al., 2015; Wideman, 2016; Choppa and Kim, 2023a; Choppa et al., 2023). Based on available literature, maintaining appropriate gut-brain axis with use of probiotics, phytobiotics, and other feed supplements (curcumin, beta hydroxybutyrate)

which possess anti-inflammatory properties would be helpful(Lucas et al., 2018; Jiang et al., 2021; Johnson et al., 2024; Lu et al., 2025). Although monoclonal antibodies specifically targeting sclerostin are available in human research, cost effective targets are yet to develop for poultry industry (Fabre et al., 2020).

CONCLUSION

The current study reveals the *Eimeria* spp. challenge and LPS injections affect bone health in broilers. This was concluded from findings like bone mineral content, bone mineral density, and bone volume differences between the challenged and non-challenged treatments. Furthermore, dynamic histomorphometry of bone and sclerostin levels indicated impaired bone development under the dual stressors (*Eimeria* and LPS). Increased sclerostin levels by the dual stressors, especially in the T6, reveals potential inhibition of a key regulator of osteogenesis, contributing to compromised bone integrity. Gene expression analysis revealed upregulation of TLR4 indicating heightened inflammatory responses. In contrast, NF-κB and TNF-α represent immune modulation in response to negative feedback mechanisms. The findings suggest synergistic effects of *Eimeria* spp. and LPS on bone health, while emphasizing the need for mitigation strategies to enhance poultry production and welfare.

REFERENCES

AlQranei, M. S., L. T. Senbanjo, H. Aljohani, T. Hamza, and M. A. Chellaiah. 2021. Lipopolysaccharide- TLR-4 Axis regulates Osteoclastogenesis independent of RANKL/RANK signaling. BMC Immunol 22:23 Available at https://doi.org/10.1186/s12865-021-00409-9.

Applegate, T. J., and M. S. Lilburn. 2002. Growth of the femur and tibia of a commercial broiler line. Poult Sci 81:1289–1294.

Atkins, G. J., P. S. Rowe, H. P. Lim, K. J. Welldon, R. Ormsby, A. R. Wijenayaka, L. Zelenchuk, A. Evdokiou, and D. M. Findlay. 2011. Sclerostin is a locally acting regulator of late-osteoblast/preosteocyte differentiation and regulates mineralization through a MEPE-ASARM-dependent mechanism. Journal of Bone and Mineral Research 26:1425–1436.

Bortel, E. L., G. N. Duda, S. Mundlos, B. M. Willie, P. Fratzl, and P. Zaslansky. 2015. Long bone maturation is driven by pore closing: A quantitative tomography investigation of structural formation in young C57BL/6 mice. Acta Biomater 22:92–102.

Chapman, H. D. 2014. Milestones in avian coccidiosis research: a review. Poult Sci 93:501–511.

Chapman, H. D., and T. Rathinam. 2022. Focused review: The role of drug combinations for the control of coccidiosis in commercially reared chickens. Int J Parasitol Drugs Drug Resist 18:32–42 Available at https://www.sciencedirect.com/science/article/pii/S221132072200001X.

Chen, C., and W. K. Kim. 2020. The application of micro-CT in egg-laying hen bone analysis: introducing an automated bone separation algorithm. Poult Sci 99:5175–5183.

Chen, P., M. U. Rehman, Y. He, A. Li, F. Jian, L. Zhang, and S. Huang. 2025. Exploring the interplay between Eimeria spp. infection and the host: understanding the dynamics of gut barrier function. Veterinary Quarterly 45:1–22.

Chen, C., B. Turner, T. J. Applegate, G. Litta, and W. K. Kim. 2020. Role of long-term supplementation of 25-hydroxyvitamin D3 on laying hen bone 3-dimensional structural development. Poult Sci 99:5771–5782.

Choi, J., D. Goo, M. K. Sharma, H. Ko, G. Liu, D. Paneru, V. S. R. Choppa, J. Lee, and W. K. Kim. 2023. Effects of different Eimeria inoculation doses on growth performance, daily feed

intake, gut health, gut microbiota, foot pad dermatitis, and Eimeria gene expression in broilers raised in floor pens for 35 days. Animals 13:2237.

Choi, J., and W. Kim. 2022. Interactions of microbiota and mucosal immunity in the ceca of broiler chickens infected with Eimeria tenella. Vaccines (Basel) 10:1941.

Choppa, V. S. R., and W. K. Kim. 2023a. A Review on Pathophysiology, and Molecular Mechanisms of Bacterial Chondronecrosis and Osteomyelitis in Commercial Broilers. Biomolecules 13:1032.

Choppa, V. S. R., and W. K. Kim. 2023b. A Review on Pathophysiology, and Molecular Mechanisms of Bacterial Chondronecrosis and Osteomyelitis in Commercial Broilers. Biomolecules 13:1032.

Choppa, V. S. R., G. Liu, Y. H. Tompkins, and W. K. Kim. 2023. Altered Osteogenic Differentiation in Mesenchymal Stem Cells Isolated from Compact Bone of Chicken Treated with Varying Doses of Lipopolysaccharides. Biomolecules 13:1626.

Ciesielska, A., M. Matyjek, and K. Kwiatkowska. 2021. TLR4 and CD14 trafficking and its influence on LPS-induced pro-inflammatory signaling. Cellular and molecular life sciences 78:1233–1261.

Cooney, O. D., P. R. Nagareddy, A. J. Murphy, and M. K. S. Lee. 2021. Healthy gut, healthy bones: targeting the gut microbiome to promote bone health. Front Endocrinol (Lausanne) 11:620466.

Cummings, S. R., D. Bates, and D. M. Black. 2002a. Clinical use of bone densitometry: scientific review. JAMA 288:1889–1897.

Cummings, S. R., D. Bates, and D. M. Black. 2002b. Clinical use of bone densitometry: scientific review. JAMA 288:1889–1897.

D'Amelio, P., and F. Sassi. 2016. Osteoimmunology: from mice to humans. Bonekey Rep 5:802 Available at https://pubmed.ncbi.nlm.nih.gov/27195109.

Delgado-Calle, J., A. Y. Sato, and T. Bellido. 2017. Role and mechanism of action of sclerostin in bone. Bone 96:29–37.

Fabre, S., T. Funck-Brentano, and M. Cohen-Solal. 2020. Anti-sclerostin antibodies in osteoporosis and other bone diseases. J Clin Med 9:3439.

Fountos, G., E. Kounadi, M. Tzaphlidou, S. Yasumura, and D. Glaros. 1998. The effects of inflammation-mediated osteoporosis (IMO) on the skeletal Ca/P ratio and on the structure of rabbit bone and skin collegen. Applied radiation and isotopes 49:657–659.

Gao, Y., E. Huang, H. Zhang, J. Wang, N. Wu, X. Chen, N. Wang, S. Wen, G. Nan, and F. Deng. 2013. Crosstalk between Wnt/β-catenin and estrogen receptor signaling synergistically promotes osteogenic differentiation of mesenchymal progenitor cells. PLoS One 8:e82436.

Gruffaz, M., K. Vasan, B. Tan, S. Ramos da Silva, and S.-J. Gao. 2017. TLR4-mediated inflammation promotes KSHV-induced cellular transformation and tumorigenesis by activating the STAT3 pathway. Cancer Res 77:7094–7108.

Hannink, G., and J. J. C. Arts. 2011. Bioresorbability, porosity and mechanical strength of bone substitutes: what is optimal for bone regeneration? Injury 42:S22–S25.

Holdsworth, G., P. Slocombe, C. Doyle, B. Sweeney, V. Veverka, K. Le Riche, R. J. Franklin, J. Compson, D. Brookings, and J. Turner. 2012. Characterization of the interaction of sclerostin with

the low density lipoprotein receptor-related protein (LRP) family of Wnt co-receptors. Journal of Biological Chemistry 287:26464–26477.

Hong, A. R., J.-Y. Yang, J. Y. Lee, J. Suh, Y.-S. Lee, J.-E. Kim, and S. W. Kim. 2022. Reactivation of bone lining cells are attenuated over repeated anti-sclerostin antibody administration. Calcif Tissue Int 111:495–505.

Hoss, F., J. L. Mueller, F. Rojas Ringeling, J. F. Rodriguez-Alcazar, R. Brinkschulte, G. Seifert, R. Stahl, L. Broderick, C. D. Putnam, and R. D. Kolodner. 2019. Alternative splicing regulates stochastic NLRP3 activity. Nat Commun 10:3238.

Houschyar, K. S., C. Tapking, M. R. Borrelli, D. Popp, D. Duscher, Z. N. Maan, M. P. Chelliah, J. Li, K. Harati, and C. Wallner. 2019. Wnt pathway in bone repair and regeneration–what do we know so far. Front Cell Dev Biol 6:170.

Iotsova, V., J. Caamaño, J. Loy, Y. Yang, A. Lewin, and R. Bravo. 1997. Osteopetrosis in mice lacking NF-κB1 and NF-κB2. Nat Med 3:1285–1289.

Irisa, T., T. Yamamoto, K. Miyanishi, A. Yamashita, Y. Iwamoto, Y. Sugioka, and K. Sueishi. 2001. Osteonecrosis induced by a single administration of low-dose lipopolysaccharide in rabbits. Bone 28:641–649.

Jiang, S., F.-F. Yan, J.-Y. Hu, A. Mohammed, and H.-W. Cheng. 2021. Bacillus subtilis-based probiotic improves skeletal health and immunity in broiler chickens exposed to heat stress. Animals 11:1494.

Jiao, J., Q. Hong, D. Zhang, M. Wang, H. Tang, J. Yang, X. Qu, and B. Yue. 2023. Influence of porosity on osteogenesis, bone growth and osteointegration in trabecular tantalum scaffolds fabricated by additive manufacturing. Front Bioeng Biotechnol 11:1117954.

Johnson, A. M., A. Clark, M. G. Anderson, E. Corbin, M. Arguelles-Ramos, and A. B. A. Ali. 2024. The influence of dietary synbiotic on agonistic behavior, stress, and brain monoamines via modulation of the microbiota–Gut–Brain axis in laying hens. Poultry 3:129–146.

Kakhki, R. A. M., Z. Lu, A. Thanabalan, H. Leung, M. Mohammadigheisar, and E. Kiarie. 2019. Eimeria challenge adversely affected long bone attributes linked to increased resorption in 14-day-old broiler chickens. Poult Sci 98:1615–1621.

Ke, H. Z., W. G. Richards, X. Li, and M. S. Ominsky. 2012. Sclerostin and Dickkopf-1 as therapeutic targets in bone diseases. Endocr Rev 33:747–783.

Kim, W. K., S. A. Bloomfield, T. Sugiyama, and S. C. Ricke. 2012. Concepts and methods for understanding bone metabolism in laying hens. Worlds Poult Sci J 68:71–82.

Kim, Y., S. Lee, and Y. H. Park. 2024. NLRP3 Negative Regulation Mechanisms in the Resting State and Its Implications for Therapeutic Development. Int J Mol Sci 25:9018.

Lampe, J. W., and C. L. Rock. 2001. Biomarkers and biological indicators of change.

Leupin, O., E. Piters, C. Halleux, S. Hu, I. Kramer, F. Morvan, T. Bouwmeester, M. Schirle, M. Bueno-Lozano, and F. J. R. Fuentes. 2011. Bone overgrowth-associated mutations in the LRP4 gene impair sclerostin facilitator function. Journal of Biological Chemistry 286:19489–19500.

Liu, G., V. S. R. Choppa, M. K. Sharma, H. Ko, J. Choi, and W. K. Kim. 2024. Effects of Methionine Supplementation Levels in Normal or Reduced Protein Diets on the Body

Composition and Femur Bone Characteristics of Broilers Challenged with Coccidia. Animals 14:917.

Lu, Y.-N., T.-J. Yue, W.-L. Ding, B.-W. Xu, A.-Y. Li, and S.-C. Huang. 2025. Gut–X Axis and Its Role in Poultry Bone Health: A Review. Microorganisms 13:757.

Lucas, S., Y. Omata, J. Hofmann, M. Böttcher, A. Iljazovic, K. Sarter, O. Albrecht, O. Schulz, B. Krishnacoumar, and G. Krönke. 2018. Short-chain fatty acids regulate systemic bone mass and protect from pathological bone loss. Nat Commun 9:55.

Martin, L. T., M. P. Martin, and H. J. Barnes. 2011. Experimental reproduction of enterococcal spondylitis in male broiler breeder chickens. Avian Dis 55:273–278.

Nikaido, H., and M. Vaara. 1985. Molecular basis of bacterial outer membrane permeability. Microbiol Rev 49:1–32.

Niu, H., H. Song, Y. Guan, X. Zong, R. Niu, S. Zhao, C. Liu, W. Yan, W. Guan, and X. Wang. 2021a. Chicken bone marrow mesenchymal stem cells improve lung and distal organ injury. Sci Rep 11:17937.

Niu, H., H. Song, Y. Guan, X. Zong, R. Niu, S. Zhao, C. Liu, W. Yan, W. Guan, and X. Wang. 2021b. Chicken bone marrow mesenchymal stem cells improve lung and distal organ injury. Sci Rep 11:17937.

Page, M. J., D. B. Kell, and E. Pretorius. 2022. The role of lipopolysaccharide-induced cell signalling in chronic inflammation. Chronic Stress 6:24705470221076390.

Paneru, D., M. K. Sharma, H. Shi, D. Goo, V. S. R. Choppa, I. Gyawali, R. Shanmugasundaram, and W. K. Kim. 2025. Effects of deoxynivalenol contaminated corn distiller’s dried grains with

solubles on growth performance, body composition, immunological response, and gastrointestinal health in young pullets. Poult Sci 104:104611 Available at https://www.sciencedirect.com/science/article/pii/S0032579124011891.

Ramos, R. M. L., J. A. Armán, N. A. Galeano, A. M. Hernández, J. M. G. Gómez, and J. G. Molinero. 2012. Dual energy X-ray absorptimetry: fundamentals, methodology, and clinical applications. Radiología (English Edition) 54:410–423.

Rath, N. C., and V. Durairaj. 2022. Chapter 22 - Avian bone physiology and poultry bone disorders.Pages 549–563 in Sturkie's Avian Physiology (Seventh Edition). Scanes, C.G., Dridi, S., eds. Academic Press, San Diego.

Redlich, K., and J. S. Smolen. 2012. Inflammatory bone loss: pathogenesis and therapeutic intervention. Nat Rev Drug Discov 11:234–250.

Rehman, M. S., S. U. Rehman, W. Yousaf, F. Hassan, W. Ahmad, Q. Liu, and H. Pan. 2021. The potential of toll-like receptors to modulate avian immune system: exploring the effects of genetic variants and phytonutrients. Front Genet 12:671235.

Reisinger, N., C. Emsenhuber, B. Doupovec, E. Mayer, G. Schatzmayr, V. Nagl, and B. Grenier. 2020. Endotoxin translocation and gut inflammation are increased in broiler chickens receiving an oral lipopolysaccharide (LPS) bolus during heat stress. Toxins (Basel) 12:622.

Schallier, S., C. Li, J. Lesuisse, G. P. J. Janssens, N. Everaert, and J. Buyse. 2019a. Dual-energy X-ray absorptiometry is a reliable non-invasive technique for determining whole body composition of chickens. Poult Sci 98:2652–2661.

Schallier, S., C. Li, J. Lesuisse, G. P. J. Janssens, N. Everaert, and J. Buyse. 2019b. Dual-energy X-ray absorptiometry is a reliable non-invasive technique for determining whole body composition of chickens. Poult Sci 98:2652–2661.

Sharma, M. K., G. Liu, D. L. White, Y. H. Tompkins, and W. K. Kim. 2023. Graded levels of Eimeria challenge altered the microstructural architecture and reduced the cortical bone growth of femur of Hy-Line W-36 pullets at early stage of growth (0–6 wk of age). Poult Sci 102:102888.

Shi, H., J. Wang, D. White, O. J. T. Martinez, and W. K. Kim. 2023. Impacts of phytase and coccidial vaccine on growth performance, nutrient digestibility, bone development, and intestinal gene expression of broilers fed a nutrient reduced diet. Poult Sci 102:103062.

Shim, M.-J. 2016. Bone changes in femoral bone of mice using calcein labeling. Korean Journal of Clinical Laboratory Science 48:114–117.

Siris, E. S., Y.-T. Chen, T. A. Abbott, E. Barrett-Connor, P. D. Miller, L. E. Wehren, and M. L. Berger. 2004. Bone mineral density thresholds for pharmacological intervention to prevent fractures. Arch Intern Med 164:1108–1112.

Surowiec, R. K., E. A. Swallow, S. J. Warden, and M. R. Allen. 2022a. Tracking changes of individual cortical pores over 1 year via HR-pQCT in a small cohort of 60-year-old females. Bone Rep 17:101633.

Surowiec, R. K., E. A. Swallow, S. J. Warden, and M. R. Allen. 2022b. Tracking changes of individual cortical pores over 1 year via HR-pQCT in a small cohort of 60-year-old females. Bone Rep 17:101633.

Sutherland, M. K., J. C. Geoghegan, C. Yu, E. Turcott, J. E. Skonier, D. G. Winkler, and J. A. Latham. 2004. Sclerostin promotes the apoptosis of human osteoblastic cells: a novel regulation of bone formation. Bone 35:828–835.

Tompkins, Y. H., C. Chen, K. M. Sweeney, M. Kim, B. H. Voy, J. L. Wilson, and W. K. Kim. 2022a. The effects of maternal fish oil supplementation rich in n-3 PUFA on offspring-broiler growth performance, body composition and bone microstructure. PLoS One 17:e0273025.

Tompkins, Y. H., J. Choi, P.-Y. Teng, M. Yamada, T. Sugiyama, and W. K. Kim. 2023. Reduced bone formation and increased bone resorption drive bone loss in Eimeria infected broilers. Sci Rep 13:616.

Tompkins, Y. H., V. S. R. Choppa, and W. K. Kim. 2024. n-3 enriched Fish oil diet enhanced intestinal barrier integrity in broilers after Eimeria infection. Poult Sci 103:103660.

Tompkins, Y. H., P. Teng, R. Pazdro, and W. K. Kim. 2022b. Long bone mineral loss, bone microstructural changes and oxidative stress after Eimeria challenge in broilers. Front Physiol 13.

Turner, R. T. 1994. Cancellous bone turnover in growing rats: Time-dependent changes in association between calcein label and osteoblasts. Journal of bone and mineral research 9:1419–1424.

Wassenaar, T. M., and K. Zimmermann. 2018. Lipopolysaccharides in food, food supplements, and probiotics: should we be worried? Eur J Microbiol Immunol (Bp) 8:63–69.

Wideman, R. F. 2016. Bacterial chondronecrosis with osteomyelitis and lameness in broilers: a review. Poult Sci 95:325–344 Available at https://www.sciencedirect.com/science/article/pii/S0032579119321534.

Wideman Jr, R. F., J. Blankenship, I. Y. Pevzner, and B. J. Turner. 2015. Efficacy of 25-OH vitamin D3 prophylactic administration for reducing lameness in broilers grown on wire flooring. Poult Sci 94:1821–1827.

Xiao, C., L. Comer, X. Pan, N. Everaert, M. Schroyen, and Z. Song. 2024. Zinc glycinate alleviates LPS-induced inflammation and intestinal barrier disruption in chicken embryos by regulating zinc homeostasis and TLR4/NF-κB pathway. Ecotoxicol Environ Saf 272:116111.

Xiaohui, T., L. Wang, X. Yang, H. Jiang, N. Zhang, H. Zhang, D. Li, X. Li, Y. Zhang, and S. Wang. 2024. Sclerostin inhibition in rare bone diseases: molecular understanding and therapeutic perspectives. J Orthop Translat 47:39–49.

Zebaze, R., and E. Seeman. 2015. Cortical bone: a challenging geography. Journal of Bone and Mineral Research 30:24–29.

Zhong, Z., C. R. Zylstra-Diegel, C. A. Schumacher, J. J. Baker, A. C. Carpenter, S. Rao, W. Yao, M. Guan, J. A. Helms, and N. E. Lane. 2012. Wntless functions in mature osteoblasts to regulate bone mass. Proceedings of the National Academy of Sciences 109:E2197–E2204.

de Zoete, M. R., A. M. Keestra, P. Roszczenko, and J. P. M. van Putten. 2010. Activation of human and chicken toll-like receptors by Campylobacter spp. Infect Immun 78:1229–1238.

Table 6.1. Treatments in the current study.

Treatments	Lipopolysaccharide dosage	*Eimeria* spp. Challenge
Treatment 1 (T1; NC)	Not given	Not given
Treatment 2 (T2)	Not given	Orally inoculated[2]
Treatment 3 (T3)	1 mg/kg IP[1] on day 14	Orally inoculated
Treatment 4 (T4)	2 mg/kg IP on day 14	Orally inoculated
Treatment 5 (T5)	1 mg/kg IP on day 14 and day 18	Orally inoculated
Treatment 6 (T6)	2 mg/kg IP on day 14 and day 18	Orally inoculated

[1] IP: Intraperitoneal injection

[2] Oral inoculation with 62,500 oocysts of *E. acervulina*, 12,500 oocysts of *E. maxima* and *E. tenella*

Table 6.2. Nucleotide sequences and accession number of primers used in real-time PCR.

Gene name[1]	Accession number	F primer sequence	R primer sequence
Beta actin	NM_205518.2	CAACACAGTGCTGTC TGGTGGTA	ATCGTACTCCTGCT TGCTGATCC
NFKB1	NM_204128.2	GAAGGAATCGTACCG GGAACA	CTCAGAGGGCCTTG TGACAGTAA
TLR4	NM_001030693.2	ACTCTTGGGGTGCTG CTG	TGTCCTGTGCATCT GAAAG
TNF-alpha	XM_040694846.2	CGTGGTTCGAGTCGC TGTAT	CCGTGCAGGTCGA GGTAC
IL-1B	XM_015297469.2	TGCCTGCAGAAGAAG CCTCG	GACGGGCTCAAAA ACCTCCT
SOST	XM_004948551	ATCCCACCTCCTGCCC AACTCCATC	GGTTCGGTTTGCTG CTCCTGGCTC
DICER1	NM_001040465.2	GACCTGACCAATCTC AACCAG	TTTGCCTTCCTCTT CTCAGC

[1]NFKB1: nuclear factor kappa B subunit 1; TLR4: toll like receptor 4; TNF-alpha: tumor necrosis factor alpha; IL-1B: interleukin 1 beta; SOST: sclerostin; DICER1: dicer 1, ribonuclease III

Figure 6.1. The timeline of events in the current study. T1, non-challenged treatment; T2, *Eimeria* spp. challenge group; T3, mixed *Eimeria spp.* and 1 mg/kg body weight (BW) of LPS at one time point (day 14); T4, mixed *Eimeria spp.* and 2 mg/kg body weight (BW) of LPS at one time point (day 14); T5, mixed *Eimeria spp.* and 1 mg/kg body weight (BW) of LPS at two time points (day 14 and 18); T6, mixed *Eimeria spp.* and 2 mg/kg body weight (BW) of LPS at two time points (day 14 and 18).

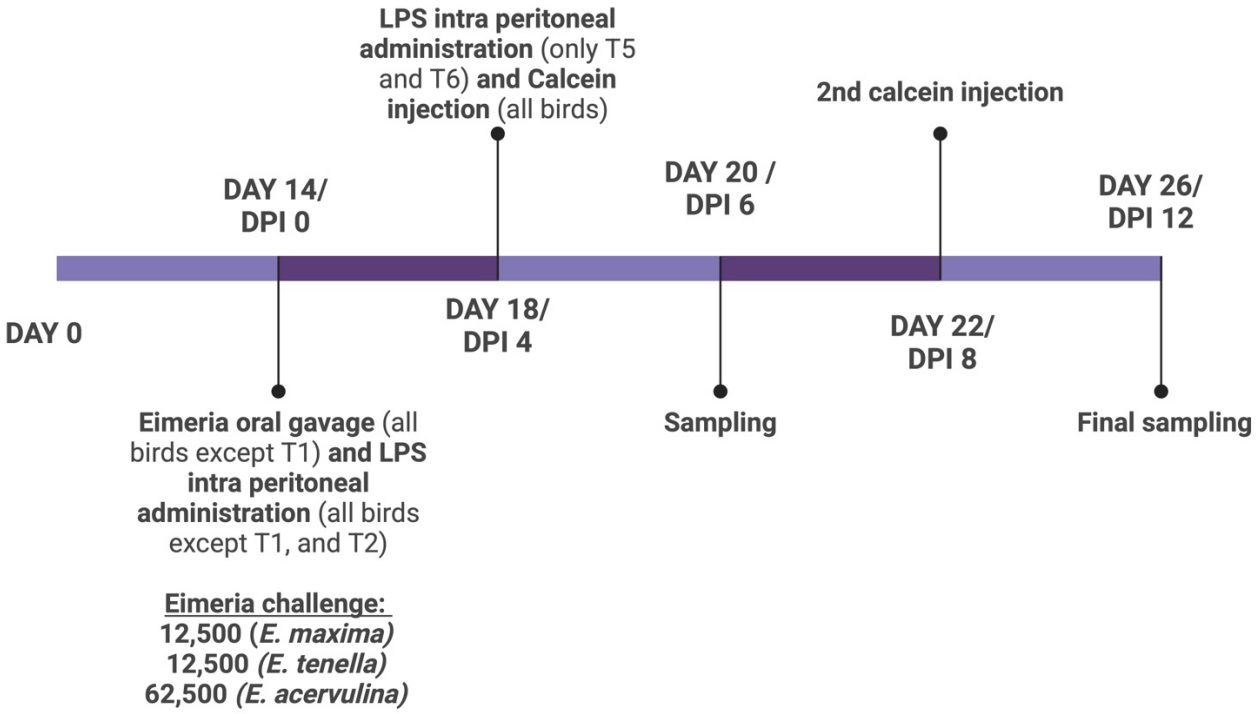

Figure 6.2. The effect of treatments on broilers' dual energy x-ray absorptiometry bone parameters on DPI 6 and 12. DPI: days post inoculation; BMC: Bone Mineral Content in grams per kilogram bodyweight; BMD: bone Mineral Density in grams per square centimeter; T1, non-challenged treatment (NC); T2, *Eimeria* spp. challenge group; T3, mixed *Eimeria spp.* and 1 mg/kg body weight (BW) of LPS at one time point (day 14); T4, mixed *Eimeria spp.* and 2 mg/kg body weight (BW) of LPS at one time point (day 14); T5, mixed *Eimeria spp.* and 1 mg/kg body weight (BW) of LPS at two time points (day 14 and 18); T6, mixed *Eimeria spp.* and 2 mg/kg body weight (BW) of LPS at two time points (day 14 and 18). The error bars represent standard error values. Letters which are not connected by the same letters differ significantly ($P < 0.05$, N =5).

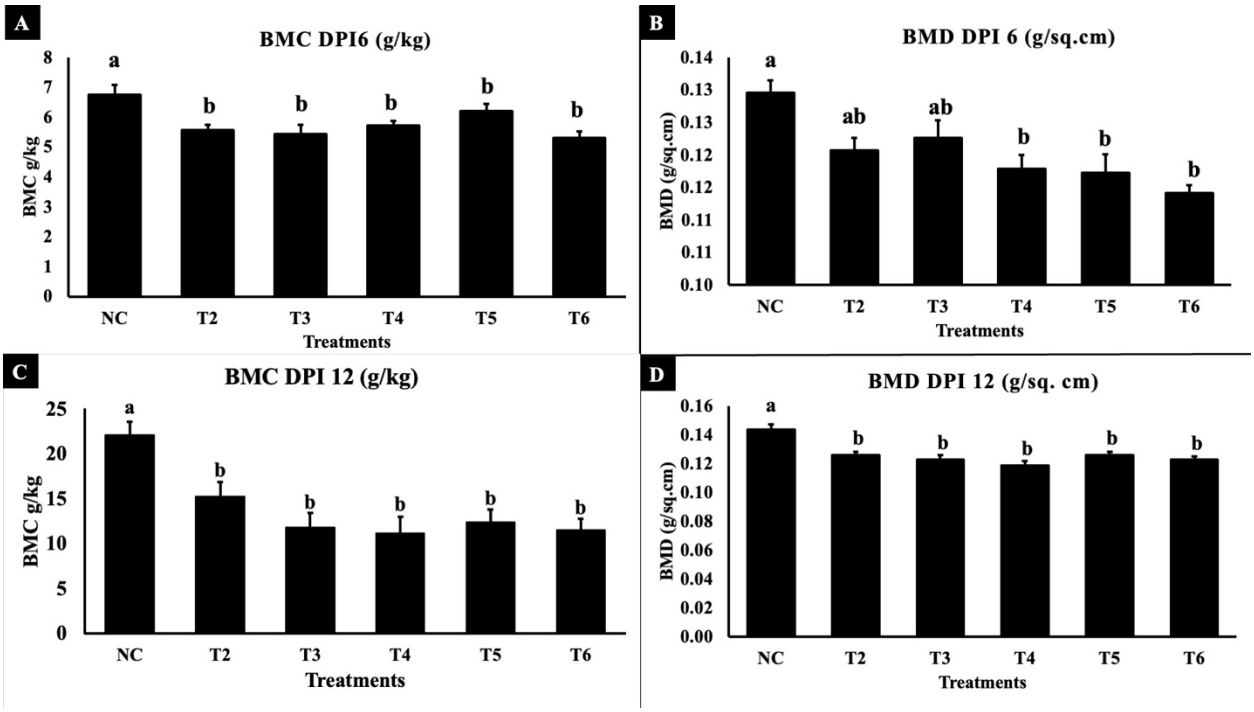

Figure 6.3. The effect of treatments on broilers' bone dynamic histomorphometry (Calcein labeling). T1, non-challenged treatment (NC); T2, *Eimeria* spp. challenge group; T3, mixed *Eimeria spp.* and 1 mg/kg body weight (BW) of LPS at one time point (day 14); T4, mixed *Eimeria spp.* and 2 mg/kg body weight (BW) of LPS at one time point (day 14); T5, mixed *Eimeria spp.* and 1 mg/kg body weight (BW) of LPS at two time points (day 14 and 18); T6, mixed *Eimeria spp.* and 2 mg/kg body weight (BW) of LPS at two time points (day 14 and 18). The error bars represent standard error values. Letters which are not connected by the same letter differ significantly ($P < 0.05$, N =5).

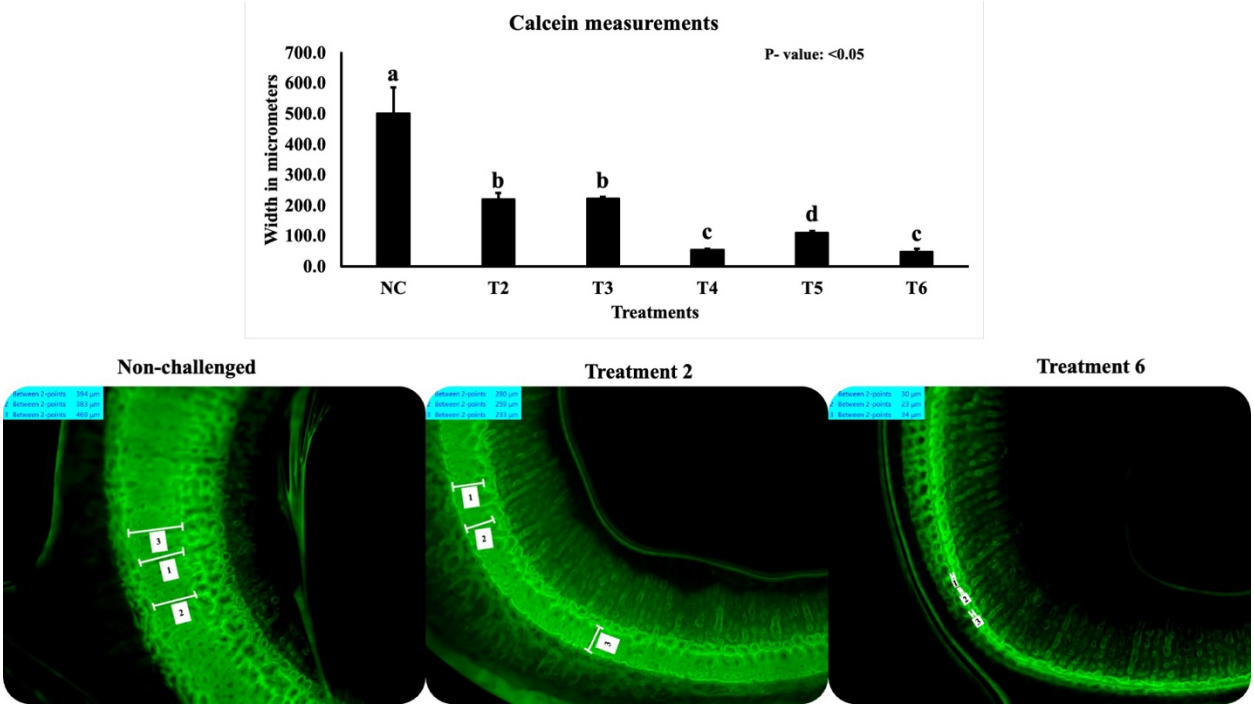

Figure 6.4. The effect of treatments on broilers sclerostin levels in serum on DPI 6. DPI: days post inoculation; T1, non-challenged treatment (NC); T2, *Eimeria* spp. challenge group; T3, mixed *Eimeria spp.* and 1 mg/kg body weight (BW) of LPS at one time point (day 14); T4, mixed *Eimeria spp.* and 2 mg/kg body weight (BW) of LPS at one time point (day 14); T5, mixed *Eimeria spp.* and 1 mg/kg body weight (BW) of LPS at two time points (day 14 and 18); T6, mixed *Eimeria spp.* and 2 mg/kg body weight (BW) of LPS at two time points (day 14 and 18). The error bars represent standard error values. Letters which are not connected by the same letter differ significantly ($P < 0.05$, N =5).

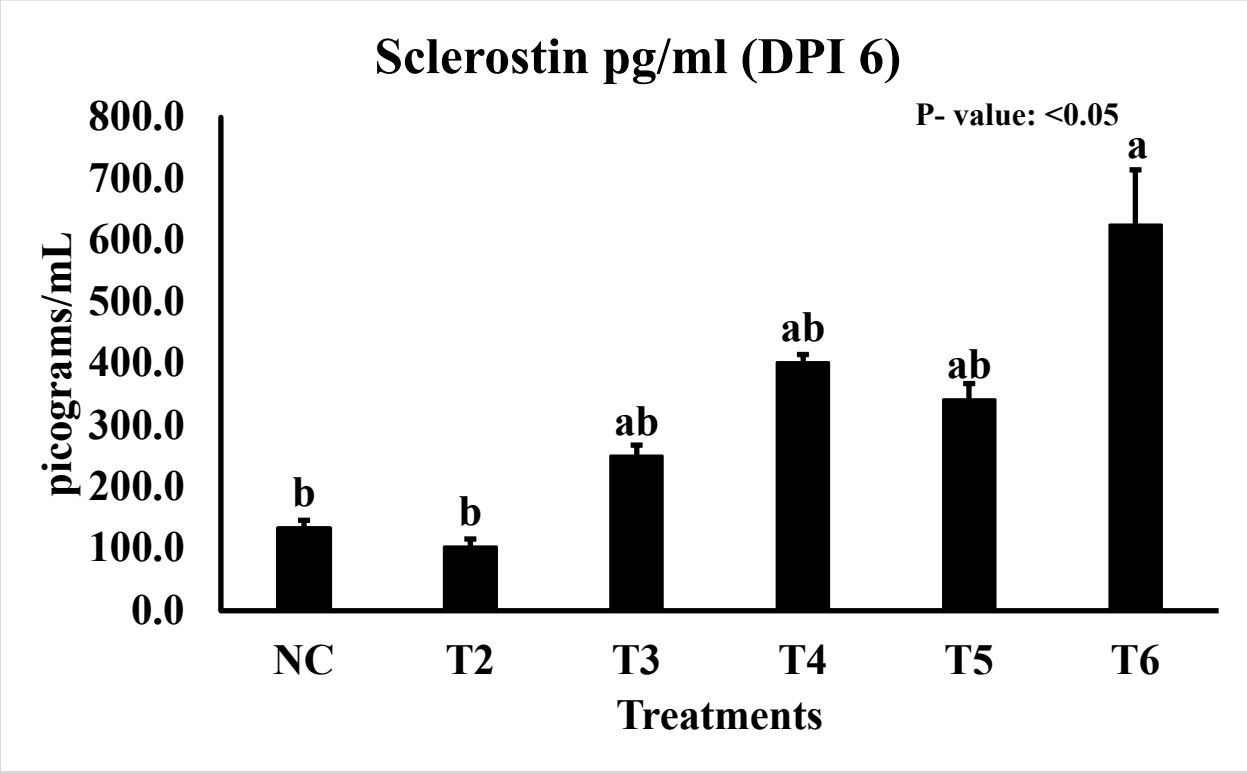

Figure 6.5. The effect of treatments on broilers micro computed tomography on tibial cortical bone parameters on DPI 12. DPI: days post inoculation; T1, non-challenged treatment; T2, *Eimeria* spp. challenge group; T3, mixed *Eimeria spp.* and 1 mg/kg body weight (BW) of LPS at one time point (day 14); T4, mixed *Eimeria spp.* and 2 mg/kg body weight (BW) of LPS at one time point (day 14); T5, mixed *Eimeria spp.* and 1 mg/kg body weight (BW) of LPS at two time points (day 14 and 18); T6, mixed *Eimeria spp.* and 2 mg/kg body weight (BW) of LPS at two time points (day 14 and 18). The error bars represent standard error values. Letters which are not connected by the same letter differ significantly ($P < 0.05$, N =5).

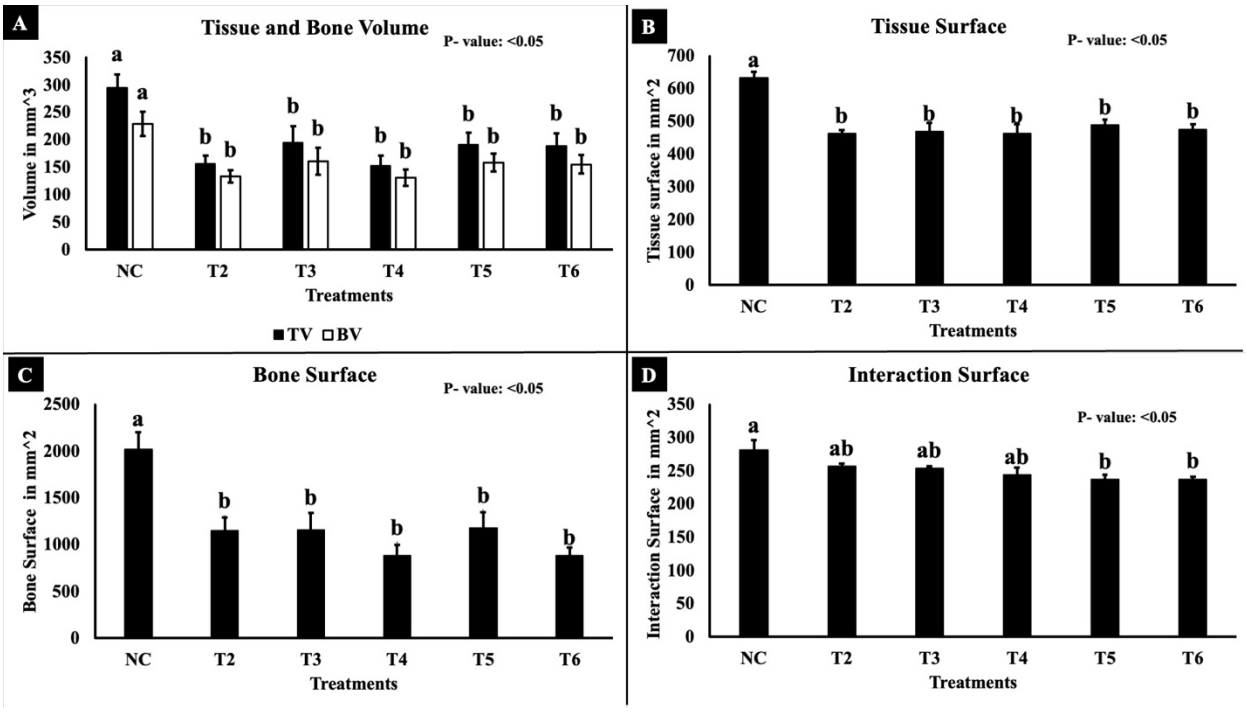

Figure 6.6. The effect of treatments on broilers micro computed tomography on tibial cortical bone parameters on DPI 12. DPI: days post inoculation; T1, non-challenged treatment (NC); T2, *Eimeria* spp. challenge group; T3, mixed *Eimeria spp.* and 1 mg/kg body weight (BW) of LPS at one time point (day 14); T4, mixed *Eimeria spp.* and 2 mg/kg body weight (BW) of LPS at one time point (day 14); T5, mixed *Eimeria spp.* and 1 mg/kg body weight (BW) of LPS at two time points (day 14 and 18); T6, mixed *Eimeria spp.* and 2 mg/kg body weight (BW) of LPS at two time points (day 14 and 18). The error bars represent standard error values. Letters which are not connected by the same letter differ significantly ($P < 0.05$, N =5).

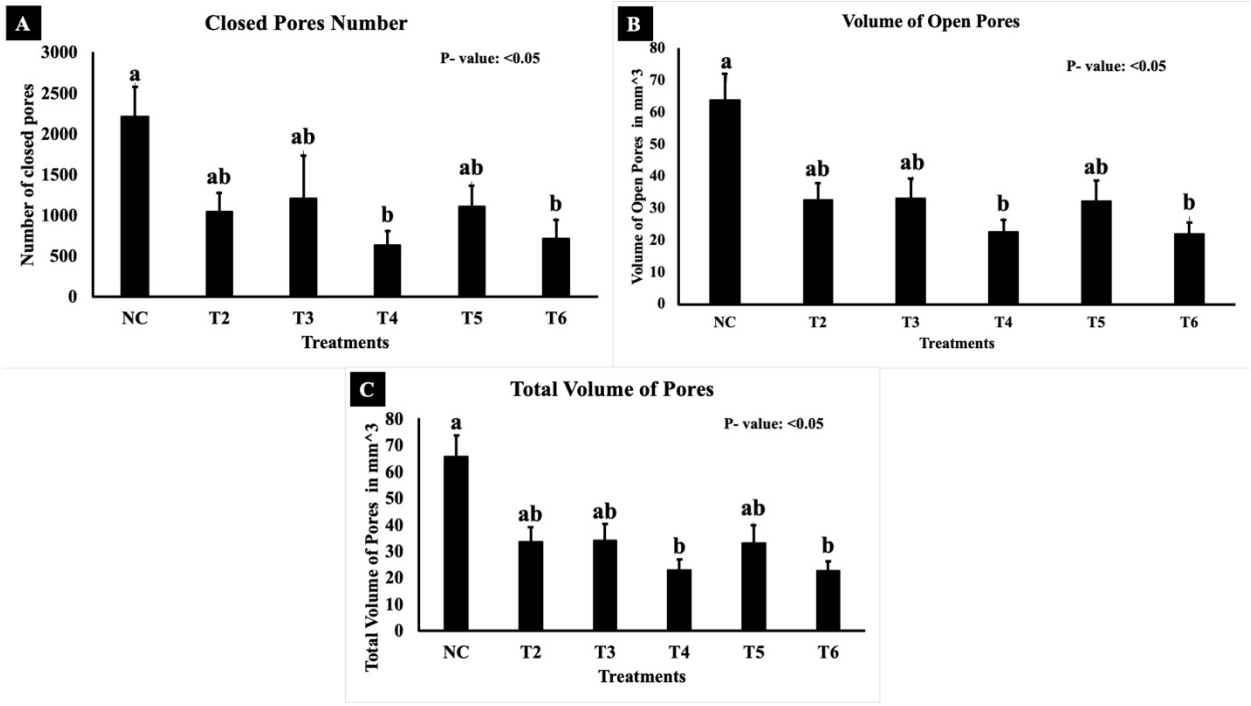

Figure 6.7. The effect of treatments on broilers gene expression from cecal tonsils. DPI: days post inoculation; TLR4: toll like receptor 4; TNFA: tumor necrosis factor alpha; NFKB1: nuclear factor kappa B subunit 1; T1, non-challenged treatment (NC); T2, *Eimeria* spp. challenge group; T3, mixed *Eimeria spp.* and 1 mg/kg body weight (BW) of LPS at one time point (day 14); T4, mixed *Eimeria spp.* and 2 mg/kg body weight (BW) of LPS at one time point (day 14); T5, mixed *Eimeria spp.* and 1 mg/kg body weight (BW) of LPS at two time points (day 14 and 18); T6, mixed *Eimeria spp.* and 2 mg/kg body weight (BW) of LPS at two time points (day 14 and 18). The error bars represent standard error values. Letters which are not connected by the same letter differ significantly ($P < 0.05$, N =5).

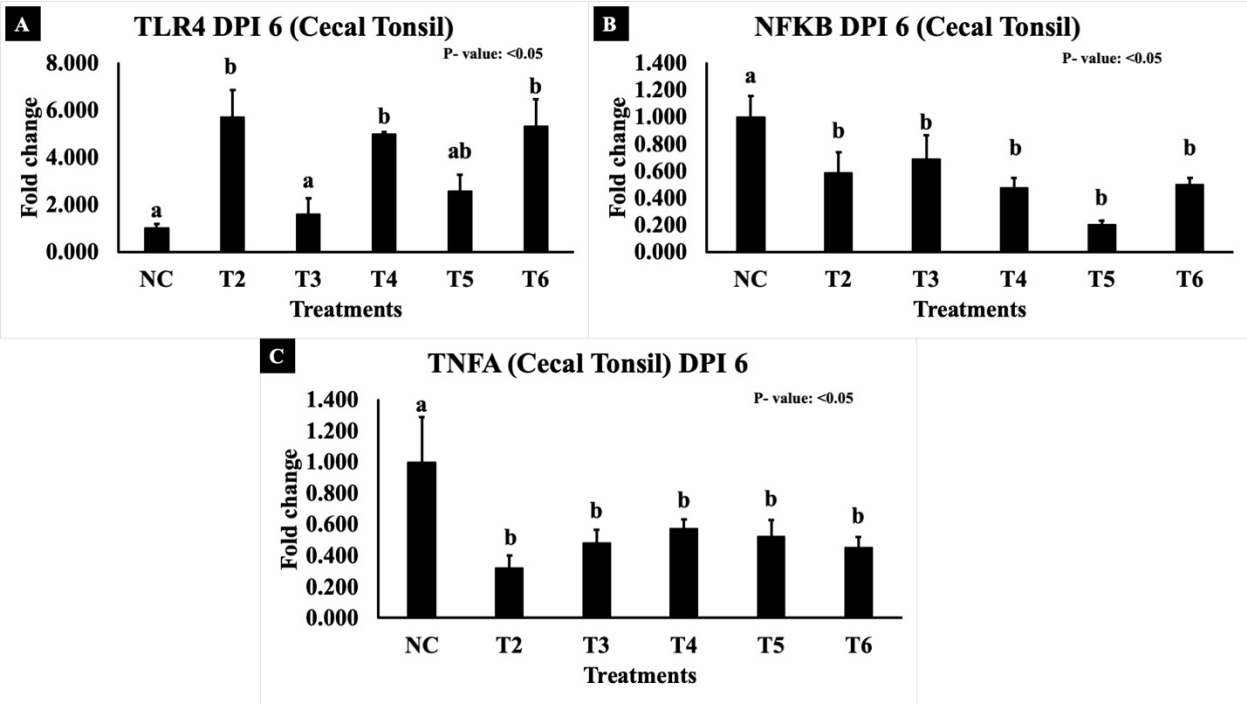

CHAPTER 7

EFFECT OF *EIMERIA* SPP. AND *STAPHYLOCOCCUS AUREUS* CHALLENGE ON INTESTINAL AND BONE HEALTH OF MODERN-DAY BROILERS [1]

[1]Venkata Sesha Reddy Choppa, Doyun Goo, Hanseo Ko, Hamid Reza Rafieian Naeini, Hemanth Reddy Katha, and Woo Kyun Kim

To be submitted to Poultry Science.

ABSTRACT

Bacterial chondronecrosis and osteomyelitis (BCO) is a leading cause of lameness. Among several pathogens, *Staphylococcus aureus* is commonly associated with BCO. This study emphasized the effects of *Eimeria* spp. co-challenge with *S. aureus* on intestinal and bone health. Six hundred broilers were assigned to eight treatments (5 replicates x 15 birds). non-challenged control (T1), *Eimeria* spp. challenged control (T2). Other treatments were challenged with *Eimeria* spp. and *S. aureus* (2 x 10^5 CFU) on day 0 (T3); 2 x 10^5 CFU on day 18 (T4); 2 x 10^8 CFU on day 0 (T5); 2 x 10^8 CFU on day 18 (T6); 2 x 10^5 CFU on day 0 and 18 (T7); and 2 x 10^8 CFU on day 0 and 18 (T8). Intestinal permeability, lesion scores for *Eimeria* spp. and bone quality was analyzed using dual-energy X-ray absorptiometry, micro-computed tomography (micro-CT), and tibial breaking strength. Plasma lipopolysaccharide (LPS) and sclerostin (SOST) concentrations were measured using ELISA. Co-challenged birds revealed significant reduction of body weights and lowest in T8 by day 26 compared to non-challenged control ($P < 0.05$). Fluorescein isothiocyanate-dextran (FITC-d) concentrations were elevated in *Eimeria* challenged control (T2) and T8, whereas T7 remained lower ($P < 0.05$) indicating disrupted intestinal barrier integrity. Moreover, LPS levels were highest in birds challenged with both pathogens and receiving repeated *S. aureus* exposure (T7 and T8) and lowest for T6 and T2, suggesting a possible endotoxemia. Similarly, micro-CT showed reduced cortical bone volume and surface (T6-T8 vs T1). Trabecular thickness was increased besides a decrease in trabecular number for T2 compared to T1 or T4. Plasma SOST were elevated with co-challenge (T4, T5, T7, and T8) and lowest in T6, T1, and T2, reflecting systemic inflammation induced bone growth disruption. These findings showed the effect of co-challenge in compromising intestinal integrity and bone health through systemic inflammation and

activation of gut-bone axis emphasizing the need for integrated strategies to mitigate above concerns.

Key Words: *Eimeria* spp., *Staphylococcus aureus*, bone health, broiler, gut-bone axis

INTRODUCTION

Poor bone health leading to lameness has become one of the key issues due to compromised welfare and consequent economic losses (McNamee and Smyth, 2000; Wideman, 2016). Bacterial Chondronecrosis and Osteomyelitis (BCO) is considered most common form of lameness and contribute to 17.3% of the lame birds and constitute 28% of culling and mortality (Szafraniec et al., 2020). This had been associated with multiple infectious etiologies where *Staphylococcus* spp. was considered principal cause and species are not limited to *S.aureus* (Wijesurendra et al., 2017; Rath and Durairaj, 2022). Additionally, other bacteria like *Enterococcus* spp. and *Escherichia coli* were also isolated from vertebral or femoral lesions (Rath et al., 2000; Wijesurendra et al., 2017). An estimate of 12.5 billion broilers was affected by skeletal problems globally and nearly 30 % of broilers reared in intensive system exhibit lameness in one or other form (Nicol, 2013; SANTE, 2016). Furthermore, *Staphylococcus* spp. is present in poultry litter and hatchery environment along with other pathogens like *Enterococcus* spp. and coliforms which are among cultivable aerobic bacteria (Lu et al., 2003; Szafraniec et al., 2020). Although accurate identification of microbiome using culturing techniques is very limited some studies used 16S rDNA libraries for estimating litter microflora composition which revealed highest abundance of gram-positive bacteria (Szafraniec et al., 2020). Furthermore, above mentioned bacteria are opportunistic which has been considered etiologies of BCO during stress from rapid growth in broilers, environmental stress, and intestinal disturbances like coccidiosis (Mandal et al., 2020; Ramser et al., 2021). Additionally, induction of BCO is associated with increased expression of proinflammatory cytokines like interleukin-1 beta (IL-1β), tumor necrosis factorα (TNFα) and inflammasomes (Ramser et al., 2021). This indicates there is undergoing systemic inflammation which would be possibly associated with changes in microbiome (dysbiosis) and release of lipopolysaccharides

(LPS) into circulation triggering above inflammatory cascade. Current study was hypothesized from concept of hematogenous spread of pathogens in the presence of stressors (Wideman and Prisby, 2013; Wideman, 2016; Choppa and Kim, 2023). In the presence of coccidiosis, intestinal epithelium is damaged leading to compromised barrier integrity which allows luminal opportunistic pathogens and endotoxins into blood stream (Tomal et al., 2023). The objective of this study was to determine the effects of co-challenge with *Eimeria* spp. and *Staphylococcus aureus* on intestinal permeability, lesion severity, systemic inflammatory responses, and bone health of broiler chickens.

MATERIALS AND METHODS

Experimental design

This study was conducted at Poultry Research Center, the University of Georgia (A2021 12-012) following the approval from Institutional Animal Care and Use Committee. A total of 600 broiler birds were randomly allocated to eight treatments with five replicates (15 birds per replicate) each treatment. Birds had ad libitum access to basal diet and nipple drinkers throughout the experiment. On day 14, *Eimeria* oral challenge (1 mL per bird) consisted of *E. maxima* (12,500 oocysts), *E. tenella* (12,500 oocysts), and *E. acervulina* (62,500 oocysts) administered orally to all birds except the non-challenged control (T1). Eight treatments were assigned as follows: T1 was non-challenged control; T2 was *Eimeria* challenged control; T3 was challenged with *Staphylococcus aureus* (2×10^5 CFU) on day 0; T4 was challenged with *Staphylococcus aureus* (2×10^5 CFU) on day 18; T5 was challenged with *Staphylococcus aureus* (2×10^8 CFU) on day 0; T6 was challenged with *Staphylococcus aureus* (2×10^8 CFU) on day 18; T7 was challenged with *Staphylococcus aureus* (2×10^5 CFU) on day 0 and 18; and T8 was challenged with *Staphylococcus*

aureus (2 x 10^8 CFU) on day 0 and 18. Birds were orally inoculated with 0.5 mL of bacterial suspension on day 0 and 1 mL on day 18 which were adjusted for desired bacterial concentration.

Staphylococcus aureus preparation and oral inoculation

Method of preparation was followed according to the details provided in our earlier study (Choppa et al., 2025b). as Baird-Parker agar (BD, DIFCO, NJ, USA) was supplemented with 3.5 % tellurite and 30 % egg yolk suspension (Sigma, St. Louis, MO, USA). Isolation and enumeration of *S. aureus* was followed according to manufacturer's guidelines. Initial isolate of *S. aureus* was obtained from femoral heads of eight clinically lame broilers from Poultry Research Center at the University of Georgia, Athens, GA, USA. A single colony with black and halo appearance was inoculated to brain heart infusion broth and incubated for 36 h, followed by centrifugation to obtain a bacterial pellet. Pellet was resuspended in 4 mL of 0.1 % peptone water, and the optical density was measured at 600 nm using UV-visible spectrophotometer (Genesys 10S UV-Vis, Thermofischer Scientific, NJ, USA). Serial dilution and plating was done following a standard curve generation followed by determining colony forming units (CFU). The desired bacterial concentrations were prepared freshly on day of inoculation and administered on day 0 and/or 18 to the treatments stated earlier.

Broiler performance, sample collection, and lesion scoring

Initial body weight and feed weights were recorded on days 14, 20, and 26. Two birds were sampled for femur bones (day 26), plasma (day 20), tibial bones (day 26), lesion scoring (day 20) for *Eimeria* spp. Two birds were euthanized by cervical dislocation which were used for lesion scoring on duodenum (upper intestine), jejunum (mid-intestine), and ceca (lower intestine) using 4- score scale (Johnson and Reid, 1970).

Intestinal permeability assay

Fluoroscein isothiocyanate-dextran (FITC-d; Sigma-Aldrich, Saint Louis, MO, USA) was used to assess intestinal permeability following slightly modified methods from earlier studies (Bortoluzzi et al., 2019; Tompkins et al., 2022; Choi et al., 2023; Graham et al., 2023). On the day of sampling (d 20), one bird per replicate was orally inoculated with 1 mL of FITC-d solution (2.2 mg/mL). Birds were euthanized two hours post-inoculation and blood samples were collected. Samples were kept at room temperature for 2 h in the dark followed by centrifugation at 1000 g-force for 10 mins to obtain serum. A standard curve was established by serial dilution of FITC-d in pooled serum from non-challenged birds. Serum FITC-d concentrations were determined using microplate reader (Victor Nivo™ plate readers, Avantor, Radnor, PA) at an excitation and emission wavelengths of 485 nm and 528 nm respectively.

Dual-energy X-ray absorptiometry

Body composition parameters including total tissue weight, lean mass, body fat percentage, bone mineral density (BMD), and bone mineral content (BMC) were determined using dual-energy-X-ray absorptiometry scanner (DEXA, GE healthcare, Chicago, IL, USA). Using Lunar prodigy software (Encore version 12.20.023), euthanized birds were positioned in dorsal recumbency for whole-body scanning. Consistent with established protocols, scans were performed at the speeds of 2.5 mm/s with a voxel resolution of 0.07 x 0.07 x 0.5 mm (Tompkins et al., 2022; Choppa et al., 2025a).

Micro-computed tomography (Micro-CT)

Femur bones collected on day 26 were stored at -20°C for further analysis. Bones were placed in 50 mL tubes after thawing, using cheese cloth, and scanned using Skyscan 1275 software

(Bruker micro-CT, Billerica, MA, USA). Scanning parameters like 72 KV voltage, 131 μA current, pixel size of 25 μm, and 0.5 mm aluminum filter. Scans were taken over 180° with 0.4° rotation which captures four images per rotation. Image reconstruction software (NRecon software, Bruker micro-CT) was used to create 2D projections to 3D models. Furthermore, Data viewer software was used to straighten image followed by CTAn software for regions of interest (ROI). BMD calibration was performed using 0.25 and 0.75 g/cm^3 hydroxyapatite phantoms with same X-ray settings. Cortical and trabecular bone segmentation were performed using established methodologies (Liu et al., 2024; Choppa et al., 2025a).

Bone breaking strength

Muscle tissue around the tibial bones were removed before using them for bone breaking strength analyses. Analyses were conducted using Instron universal testing systems (model 3365 (5 kilonewtons capacity), Instron corp., Canton, MA). Tibial height and width were measured using vernier calipers. To be consistent, all left tibial bones were oriented in same position with a span of 5 cm. A 5 kN load cell at 20 mm/s speed was applied at the mid diaphyseal region. Maximum force required to break the bone was measured in kilogram force which was analyzed using Instron Bluehill software (version 2.5.391).

Lipopolysaccharides and Sclerostin ELISA

Plasma samples collected on day 20 were stored in -80°C which were thawed for conducting lipopolysaccharides and sclerostin ELISA. Respective kits were used for obtaining results after following manufacturer's instructions (MyBiosource, Inc. San Diego, CA, USA). Standard curves were obtained from the protocol, and analyses were made using the OD values which were corrected against blank.

Statistical Analysis

Data was expressed in mean and standard errors. For statistical analysis like ANOVA, data was verified for normality and homogeneity of variances. One way ANOVA was used for identifying statistical significance and post hoc test like Tukey's HSD was used for multiple comparisons. Nonparametric data like lesion scores were analyzed using Kruskal Wallis test and multiple comparisons using Dunn all pairs for joint rank. *P*-value was set to less than 0.05 for the entire data.

RESULTS

Average body weight and average feed intake

On day 14, body weights did not differ significantly between treatments (data not shown) ($P > 0.05$). On day 20, T1 had the highest body weight average of 611.7 grams but other treatments which were challenged with *Eimeria* spp. were significantly lower with average body weight of 511.5 g (T2), 465.4 g (T3), 513.2 g (T4), 478.1 g (T5), 481.4 g (T6), 498.7 g (T7), and 466.8 g (T8). Furthermore, on day 26, T1 (1309.5 g) had significantly higher body weight compared to other treatments and T2 (1023.8 g) average body weights were significantly greater than T8 (772 g) ($P < 0.05$).

Average daily feed intake on day 19 for T1 (119.8 g) was significantly greater than T3 (118.7 g), T5 (111.8 g), T6 (113.5 g), T7 (113.3 g), and T8 (94.2 g). Similarly, on day 22, T1 had the highest average of 163.5 grams which is greater than T3 (94.5 g), T5, T6 (93.8 g), and T8 (97.9 g) ($P < 0.05$). Interestingly, average feed intake did not vary significantly between the treatment groups for other days during the study period ($P > 0.05$).

Lesion scores and intestinal permeability

Intestinal permeability was measured on day 20 and findings showed a significantly higher permeability for T2 (1338.6 ng/mL) and T8 (1023.8 ng/mL) compared to T1 (295.1 ng/mL) and T7 (279.2 ng/mL) ($P < 0.05$). Additionally, intestinal permeability for T7 was significantly lower compared to T2 and T5 (910.3 ng/mL) ($P < 0.05$).

Lesion scores for *Eimeria acervulina*, *E. maxima*, and *E. tenella* were assessed in respective regions (upper, mid and lower intestine regions). *Eimeria acervulina* (upper intestine) lesions were identified in duodenum and scores were significantly higher for all *Eimeria* challenged treatments (T2-T8) ($P < 0.05$). Interestingly, no significant differences were observed between *Eimeria* challenged treatments. No significant differences were observed for *E. maxima* between treatments ($P > 0.05$). Furthermore, *E. tenella* scores for T4 (2.3) was significantly higher than T1 (0.1) with interesting intermediate scores for other treatments (1.8-2.2) ($P < 0.05$).

Bone breaking strength, Dual-energy X-ray absorptiometry, and micro-computed tomography

Bone breaking strength was measured as maximum flexure load in kilogram-force (KGF). Although numerical decrease was observed between treatments (lower KGF for *Eimeria* challenged treatments), these findings were not significant ($P > 0.05$) (data not shown). Furthermore, Dual-energy X-ray absorptiometry parameters like bone mineral content (BMC), bone mineral density (BMD), fat %, and lean tissue (g) were measured on day 20 and 26. Numerical differences between treatments were observed but these findings were not significant ($P > 0.05$) (data not shown).

On day 26, three dimensional cortical parameters were measured which revealed a significantly lower bone volume for T8 (144.25 mm^3) compared to T1 (220.93 mm^3) and T2

(243.76 mm^3). Furthermore, T1 and T2 is significantly had higher bone volume compared to T6 (172.96 mm^3) and T7 (172.70 mm^3) along with T8 which was mentioned earlier ($P < 0.05$). Additionally, bone surface for T6 (1019.14 mm^2), T7 (971.79 mm^2), and T8 (919.79 mm^2) were significantly lower compared to T1 (1825.41 mm^2) ($P < 0.05$). Interestingly, bone surface to volume ratio was significantly lower for T2 (4.8) compared to T1 (8.13) and T4 (8.0) ($P < 0.05$). In contrast, trabecular thickness of T2 (0.75 mm) was significantly greater than T1 (0.43 mm) and T4 (0.44 mm) ($P < 0.05$). Additionally, trabecular number for T1 (1.89 per mm) and T4 (1.81 per mm) were significantly higher than T2 (1.2 per mm) ($P < 0.05$).

Lipopolysaccharides and Sclerostin ELISA

Lipopolysaccharides concentration detected from plasma samples were significantly lower for T6 (31.69 ng/ml) compared to T3 (92.30 ng/ml), T4 (137.22 ng/ml), T7 (163.97 ng/ml), and T8 (191.62 ng/ml) ($P < 0.05$). Interestingly, compared to T7 and T8 LPS concentrations, T2 (50.68 ng/ml) and T6 LPS levels were significantly lower ($P < 0.05$). Furthermore, compared to LPS concentration in T8, all other treatments except T4 (137.23 ng/ml) and T7 ($P < 0.05$).

Sclerostin levels for T6 were significantly lower for T6 (132.49 pg/ml) compared to T4 (490.62 pg/ml), T5 (379.37 pg/ml), T7 (400.62 pg/ml), and T8 (403.62 pg/ml). T1 (180.94 pg/ml) and T2 (217.37 pg/ml) sclerostin levels were significantly lower than all the treatments except T6 ($P < 0.05$). Furthermore, sclerostin levels in T3 (293.96 pg/ml) were similar to other treatments ($P > 0.05$).

DISCUSSION

This study clearly demonstrates that *Eimeria* spp. and *Staphylococcus aureus* challenged to broilers impaired their growth performance. Furthermore, *Eimeria* co-challenge with high dose

of *S.aureus* on day 0 and 18 (T8) revealed significant decrease in body weight and feed intake compared to non-challenged and only *Eimeria* challenged control which reflects the well-known impact of coccidiosis on growth. In this study, *Eimeria* spp. challenge produced classic signs of subclinical coccidiosis targeting reduction in body weights with moderate lesion development suggesting a commercial production like growth depression (Graham et al., 2023). Interestingly, these effects were pronounced with concurrent challenge with *S. aureus*, representing role of compounding effects of pathogenic stressors on body performance. *Eimeria* lesion score severity suggests mucosal injury through the invasion of enterocytes and disrupt gut integrity leading to inflammation and malabsorption (Blake et al., 2020; Gautier et al., 2020). Moreover, this study shows a possible tight junction breakdown and mucosal damage which was observed from heightened intestinal permeability similar to previous studies with *Eimeria* challenge (Teng et al., 2020). A compromised intestinal integrity facilitates translocation of luminal microbes and lipopolysaccharides to enter circulation (Wideman, 2016; Anthney et al., 2024). Furthermore, increase in systemic lipopolysaccharide levels suggests endotoxin leakage from gram-negative microflora which is a possible sequalae from compromised intestinal barrier (Choppa et al., 2025b). *Staphylococcus aureus* challenge and *Eimeria* induced barrier leakage would create systemic inflammation and tissue infection along with shift in microbiome (Anthney et al., 2024; Choppa et al., 2025b).

Evidence of heightened systemic inflammation in this study reflects gut-systemic axis by engaging toll-like receptors and proinflammatory cytokine release. To elaborate, known TLR4 (toll like receptor) signaling leads to upregulation of acute phase response with release of Interleukin-6 (IL-6), Interleukin-1 beta (IL-1β), and tumor necrosis factor-alpha (TNFα) (Einhorn et al., 1995; Nakashima et al., 2000; Jiang et al., 2023; Choppa et al., 2025b). Although, this study did not

measure cytokine expression, the above findings and elevated endotoxemia strongly suggests a surge in inflammatory mediators. Moreover, excess cytokine release can drive anorexia and muscle catabolism besides growth depression and showing effects on the bone homeostasis (Sanjaya et al., 2024). IL-1β was reported to have effect on release of sclerostin from osteocytes which is a potent Wnt signaling antagonist which suppress osteoblastogenesis (Delgado-Calle et al., 2017; Jiang et al., 2023). Thus, systemic inflammatory milieu impaired overall metabolism along with compromised bone development in co-challenged broilers.

This co-challenge study also revealed significant findings with respect to bone quality and strength. DEXA findings revealed a lower BMD and BMC in birds challenged with *Eimeria* spp. which are partially similar. Term, partial similarity was used because of numerically lower, but not statistically significant findings. Coccidiosis can significantly reduce bone mineralization which was observed in previous studies as decreased tibial ash content and breaking strength in broilers (Tompkins et al., 2022). Furthermore, *E. acervulina* or *E. maxima* infections led to decreased BMD and BMC. In this study, micro-CT analysis further showed microstructural aberrations like bone volume and surface parameters along with their trabecular structure. Similarly, previous work showed that high dose of *Eimeria* spp. preferentially affected trabecular bone in metaphysis while sparing cortical bone (Tompkins et al., 2022). These findings reflect, weakened and less denser bones further showing the tendency of bone to microfractures which are attributed to inducing BCO lameness (Ekesi et al., 2021; Choppa and Kim, 2023; Anthney et al., 2024). Our findings cannot be attributed to decreased feed intake since inflammation itself plays essential role in bone deficits. Furthermore, a study shown greater bone loss and turnover than pair-fed uninfected birds with similar feed intake compared to *Eimeria* infected birds (Tompkins et al., 2022).

Coccidiosis is known to impair uptake of key minerals like Ca, P, Zn, etc. and fat-soluble vitamins which are essential for bone mineralization (Oikeh et al., 2019; Sakkas et al., 2019). Severe damage to upper intestine (duodenum) can lead to malabsorption of above nutrients (calcium and vitamin D) leading to rickets-like osteopenia (Sakkas et al., 2019). Moreover, bone mineral loss during coccidiosis has been linked to decreased Ca and P absorption along with decreased fat digestion (reducing vitamin D and K availability) enhancing osteoclastogenesis (Kakhki et al., 2019). Additionally, inflammatory immune response and oxidative stress have deleterious effects on bone cells during systemic infection (Tompkins et al., 2023). Meanwhile, pro-inflammatory cytokines elevate osteoclast differentiation and activity, accelerating bone resorption (Jiang et al., 2023). Increased sclerostin in our findings in challenged groups (T7 and T8) reveal a inhibition on Wnt-mediated osteogenesis by blocking LRP5 receptor, thereby suppressing osteoblastogenesis (Choppa and Kim, 2023; Choppa et al., 2023, 2025a). Furthermore, findings are further supported by our findings in a published literature on the same treatments and cecal microbiome changes (Choppa et al., 2025b). Findings in the above stated study strongly suggests gut-bone axis involvement which was influenced through metabolites (short chain fatty acids, vitamins) and immune modulation (Choppa et al., 2025b; Lu et al., 2025).

CONCLUSION

Co-challenge of broilers with coccidia and *Staphylococcus aureus* created a cascade of pathogenic events connecting gut and bone. Intestinal *Eimeria* infection led to intestinal integrity concerns, pathogen translocation along with systemic endotoxemia (increased LPS concentrations) leading to a robust inflammatory milieu. The result was suppressed growth performance, heightened systemic inflammation, break in intestinal barrier, and increased sclerostin levels collectively compromised skeletal integrity characterized by lower bone parameters. These

findings provide clear evidence that enteric challenge and systemic inflammation synergistically affects gut-bone axis in broilers besides allowing translocation of opportunistic pathogens to extra-intestinal organs (bone) reflected as BCO lameness. This suggests role of mitigating intestinal damage and inflammation using dietary supplements, probiotics or coccidia control (all are yet to be studied). These measures would serve as lameness alleviating strategies by preserving bone development in commercial flocks. Overall, results highlight the need for collective gut-skeletal management approaches in modern broiler production systems, acknowledge maintaining intestinal integrity is essential not only for productivity but also long-term bone health and flock welfare.

Figure 7.1 illustrates the average body weight on d 20 and 26 of broilers challenged with *Eimeria* spp. and *Staphylococcus aureus*. T1, non-challenged treatment; T2, *Eimeria* spp. challenged group; T3, *Eimeria spp.* challenge and 2 x 10^5 CFU *S. aureus* day old challenge; T4, *Eimeria spp.* challenge and 2 x 10^5 CFU *S. aureus* day 18 challenge; T5, *Eimeria spp.* challenge and 2 x 10^8 CFU *S. aureus* day old challenge; T6, *Eimeria spp.* challenge and 2 x 10^8 CFU *S. aureus* day 18 challenge; T7, *Eimeria spp.* challenge and 2 x 10^5 CFU *S. aureus* day old and day 18 challenge; T8, *Eimeria spp.* challenge and 2 x 10^8 CFU *S. aureus* day old and day 18 challenge. Letters not connected by same letter is significantly different ($P < 0.05$, N =5).

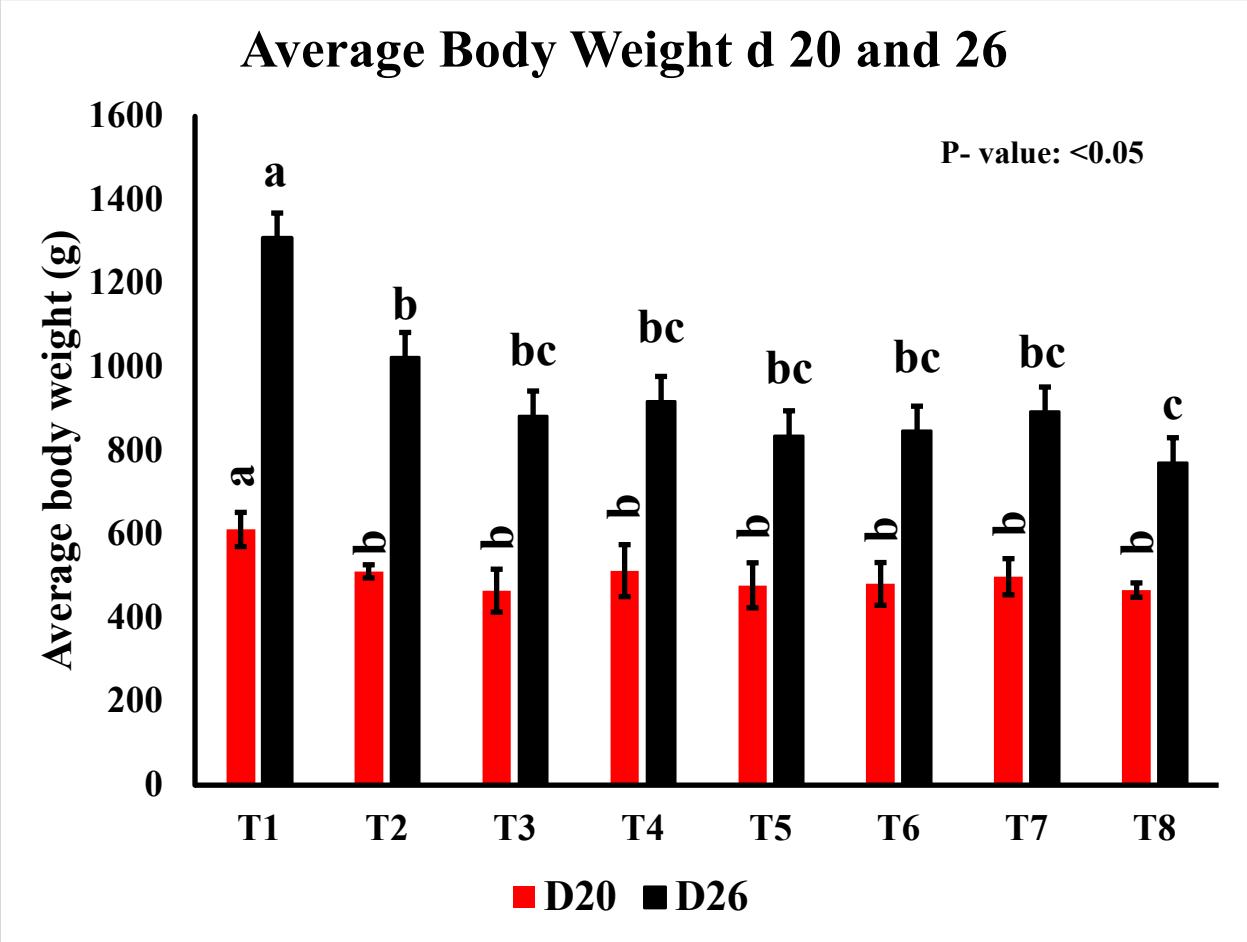

Figure 7.2 illustrates the average daily feed intake throughout the study period (d 0 to d 26) of broilers challenged with *Eimeria* spp. and *Staphylococcus aureus*. T1, non-challenged treatment; T2, *Eimeria* spp. challenged group; T3, *Eimeria spp.* challenge and 2 x 10^5 CFU *S. aureus* day old challenge; T4, *Eimeria spp.* challenge and 2 x 10^5 CFU *S. aureus* day 18 challenge; T5, *Eimeria spp.* challenge and 2 x 10^8 CFU *S. aureus* day old challenge; T6, *Eimeria spp.* challenge and 2 x 10^8 CFU *S. aureus* day 18 challenge; T7, *Eimeria spp.* challenge and 2 x 10^5 CFU *S. aureus* day old and day 18 challenge; T8, *Eimeria spp.* challenge and 2 x 10^8 CFU *S. aureus* day old and day 18 challenge. Letters not connected by same letter is significantly different ($P < 0.05$, N =5).

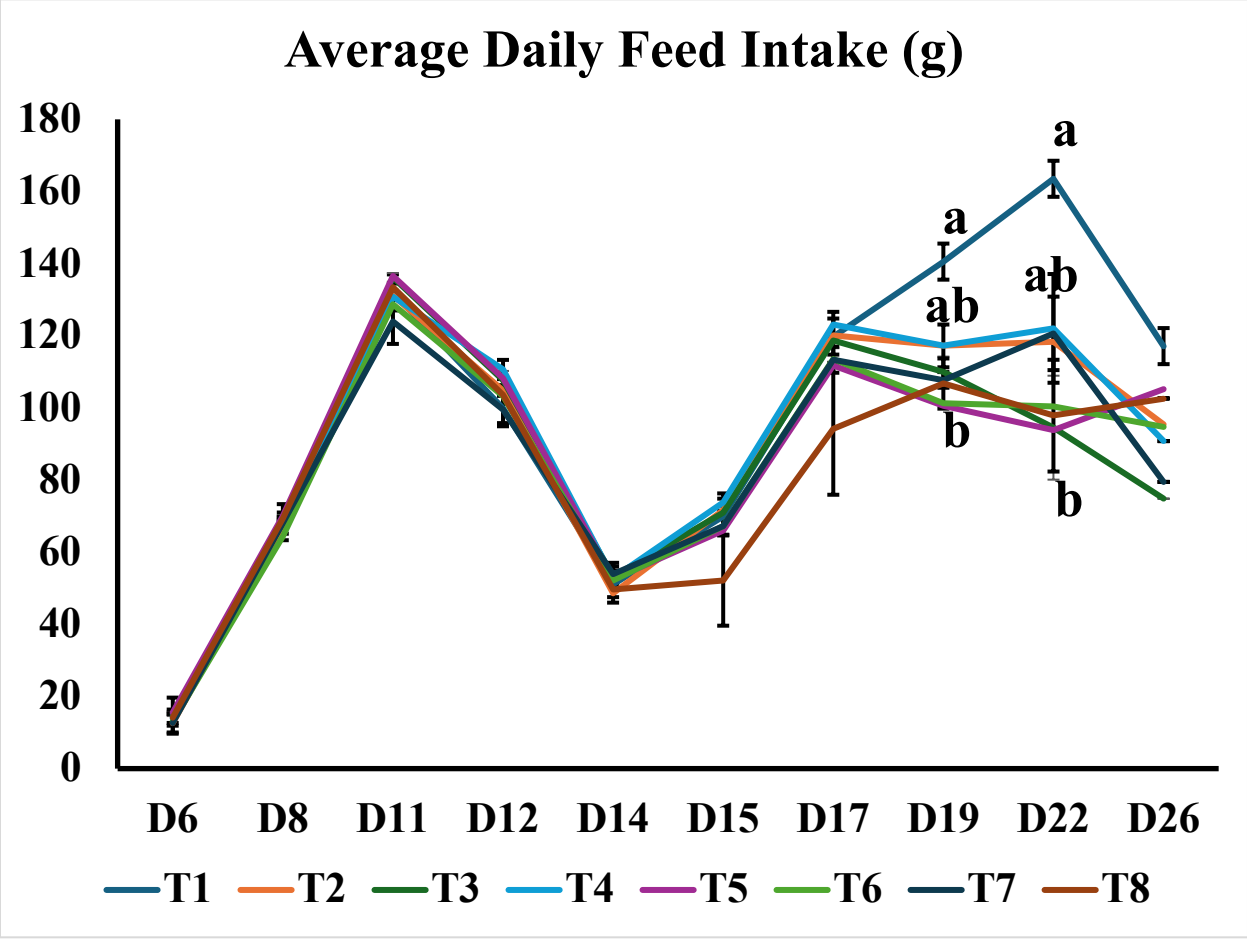

Figure 7.3 illustrates the lesion scores (average) of *Eimeria acervulina* (upper intestine), *Eimeria maxima* (mid intestine), *Eimeria tenella* (lower intestine) in broilers challenged with *Eimeria* spp. and *Staphylococcus aureus*. T1, non-challenged treatment; T2, *Eimeria* spp. challenged group; T3, *Eimeria spp.* challenge and 2 x 10^5 CFU *S. aureus* day old challenge; T4, *Eimeria spp.* challenge and 2 x 10^5 CFU *S. aureus* day 18 challenge; T5, *Eimeria spp.* challenge and 2 x 10^8 CFU *S. aureus* day old challenge; T6, *Eimeria spp.* challenge and 2 x 10^8 CFU *S. aureus* day 18 challenge; T7, *Eimeria spp.* challenge and 2 x 10^5 CFU *S. aureus* day old and day 18 challenge; T8, *Eimeria spp.* challenge and 2 x 10^8 CFU *S. aureus* day old and day 18 challenge. Letters not connected by same letter is significantly different ($P < 0.05$, N =5).

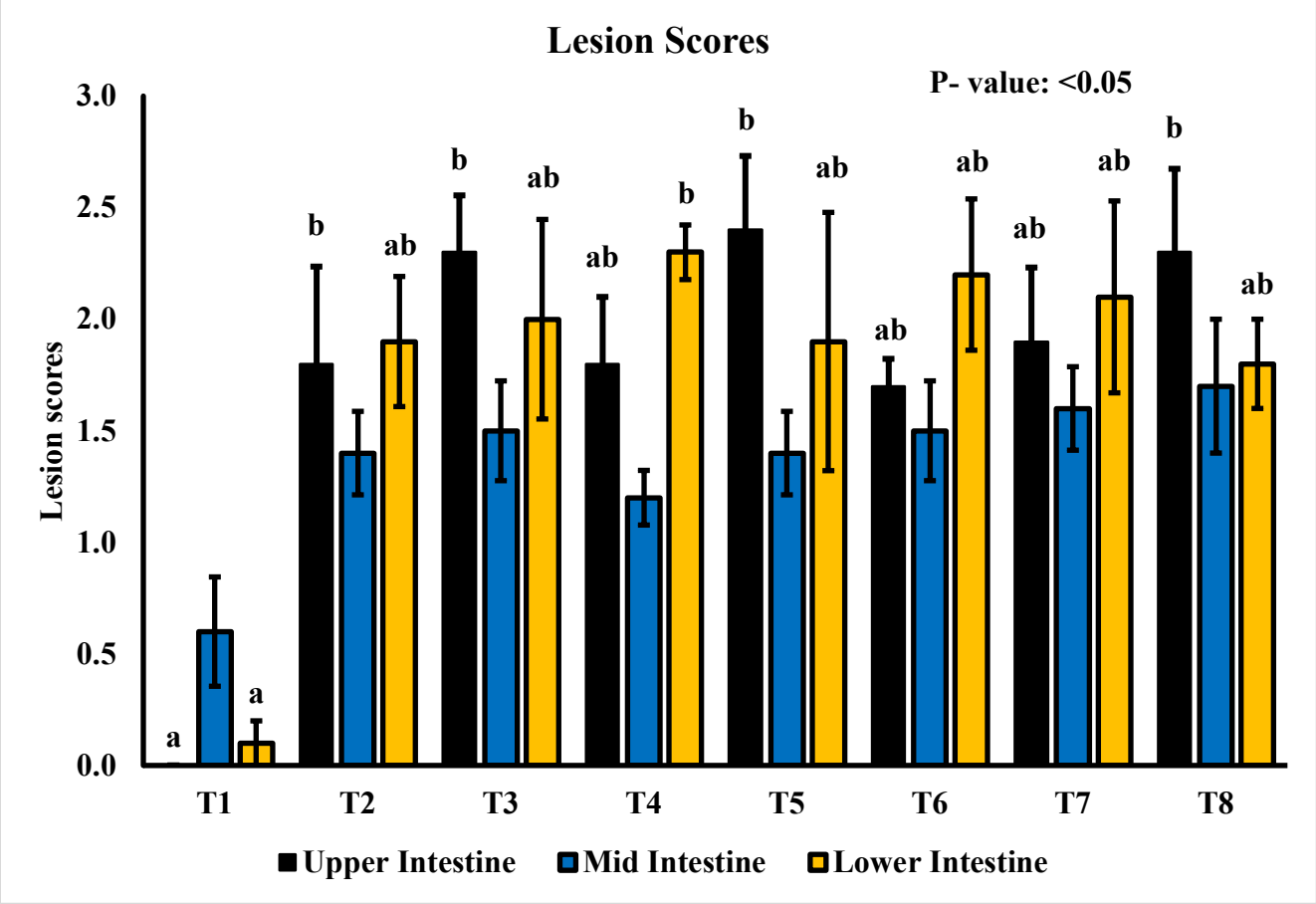

32

Figure 7.4 illustrates the intestinal permeability (using fluorescein isothiocyanate- dextran) of broilers challenged with *Eimeria* spp. and *Staphylococcus aureus*. T1, non-challenged treatment; T2, *Eimeria* spp. challenged group; T3, *Eimeria spp.* challenge and 2 x 10^5 CFU *S. aureus* day old challenge; T4, *Eimeria spp.* challenge and 2 x 10^5 CFU *S. aureus* day 18 challenge; T5, *Eimeria spp.* challenge and 2 x 10^8 CFU *S. aureus* day old challenge; T6, *Eimeria spp.* challenge and 2 x 10^8 CFU *S. aureus* day 18 challenge; T7, *Eimeria spp.* challenge and 2 x 10^5 CFU *S. aureus* day old and day 18 challenge; T8, *Eimeria spp.* challenge and 2 x 10^8 CFU *S. aureus* day old and day 18 challenge. Letters not connected by same letter is significantly different ($P < 0.05$, N =5).

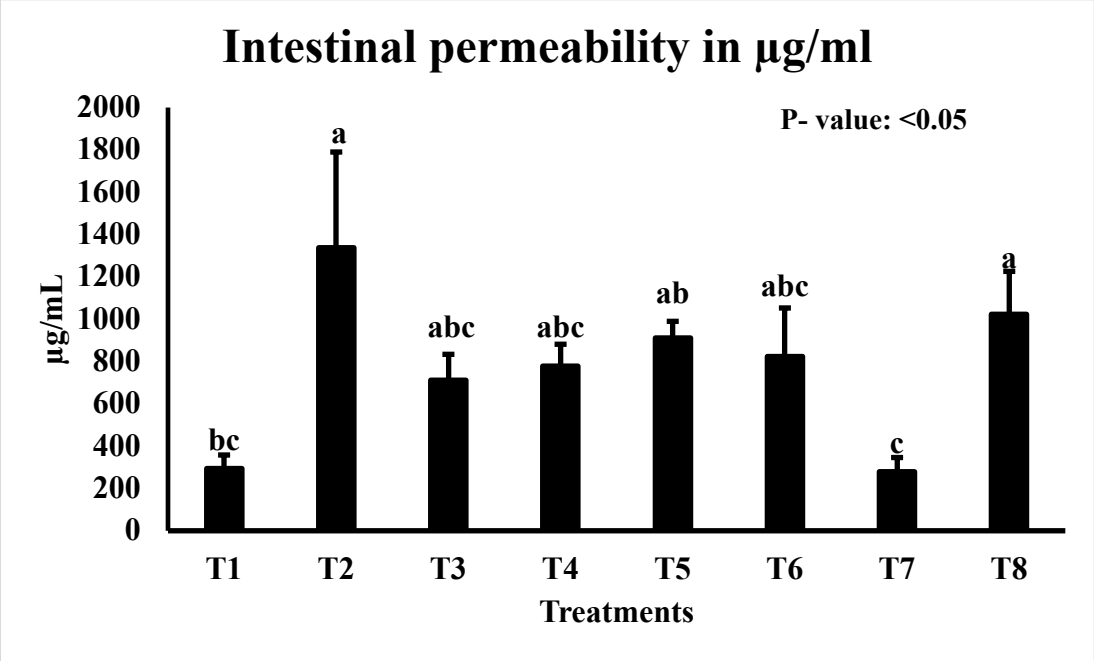

Figure 7.5 illustrates the plasma sclerostin (SOST) levels of broilers challenged with *Eimeria* spp. and *Staphylococcus aureus*. T1, non-challenged treatment; T2, *Eimeria* spp. challenged group; T3, *Eimeria spp.* challenge and 2 x 10^5 CFU *S. aureus* day old challenge; T4, *Eimeria spp.* challenge and 2 x 10^5 CFU *S. aureus* day 18 challenge; T5, *Eimeria spp.* challenge and 2 x 10^8 CFU *S. aureus* day old challenge; T6, *Eimeria spp.* challenge and 2 x 10^8 CFU *S. aureus* day 18 challenge; T7, *Eimeria spp.* challenge and 2 x 10^5 CFU *S. aureus* day old and day 18 challenge; T8, *Eimeria spp.* challenge and 2 x 10^8 CFU *S. aureus* day old and day 18 challenge. Letters not connected by same letter is significantly different ($P < 0.05$, N =5).

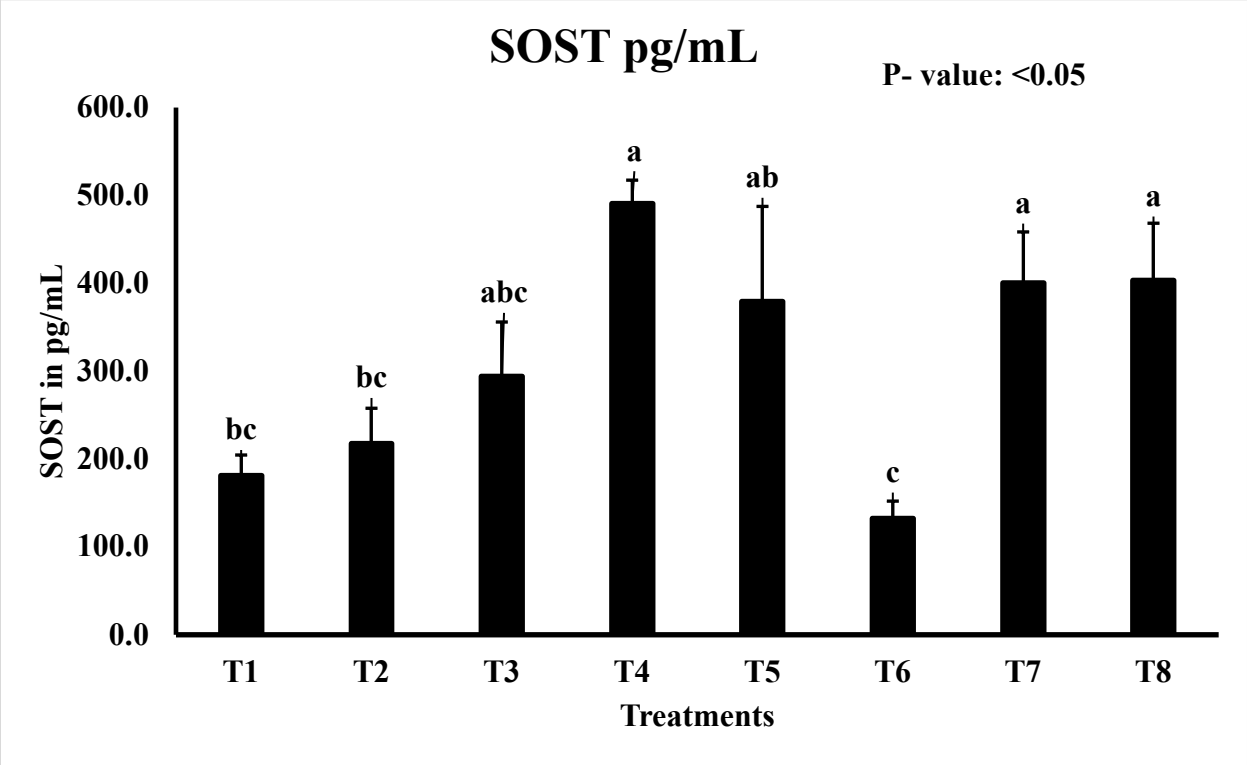

Figure 7.6 illustrates the plasma lipopolysaccharides (LPS) levels of broilers challenged with *Eimeria* spp. and *Staphylococcus aureus*. T1, non-challenged treatment; T2, *Eimeria* spp. challenged group; T3, *Eimeria spp.* challenge and 2 x 10^5 CFU *S. aureus* day old challenge; T4, *Eimeria spp.* challenge and 2 x 10^5 CFU *S. aureus* day 18 challenge; T5, *Eimeria spp.* challenge and 2 x 10^8 CFU *S. aureus* day old challenge; T6, *Eimeria spp.* challenge and 2 x 10^8 CFU *S. aureus* day 18 challenge; T7, *Eimeria spp.* challenge and 2 x 10^5 CFU *S. aureus* day old and day 18 challenge; T8, *Eimeria spp.* challenge and 2 x 10^8 CFU *S. aureus* day old and day 18 challenge. Letters not connected by same letter is significantly different ($P < 0.05$, N =5).

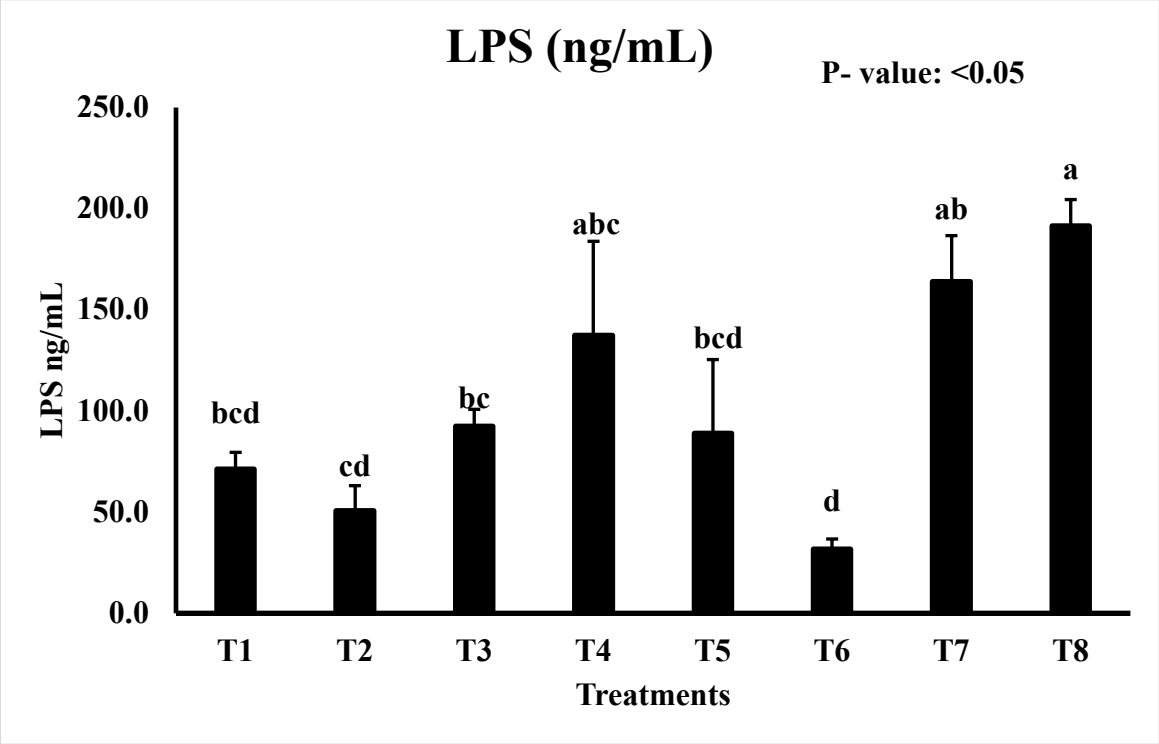

Figure 7.7 illustrates the tibial bone breaking strength of broilers challenged with *Eimeria* spp. and *Staphylococcus aureus*. T1, non-challenged treatment; T2, *Eimeria* spp. challenged group; T3, *Eimeria spp.* challenge and 2 x 10^5 CFU *S. aureus* day old challenge; T4, *Eimeria spp.* challenge and 2 x 10^5 CFU *S. aureus* day 18 challenge; T5, *Eimeria spp.* challenge and 2 x 10^8 CFU *S. aureus* day old challenge; T6, *Eimeria spp.* challenge and 2 x 10^8 CFU *S. aureus* day 18 challenge; T7, *Eimeria spp.* challenge and 2 x 10^5 CFU *S. aureus* day old and day 18 challenge; T8, *Eimeria spp.* challenge and 2 x 10^8 CFU *S. aureus* day old and day 18 challenge.

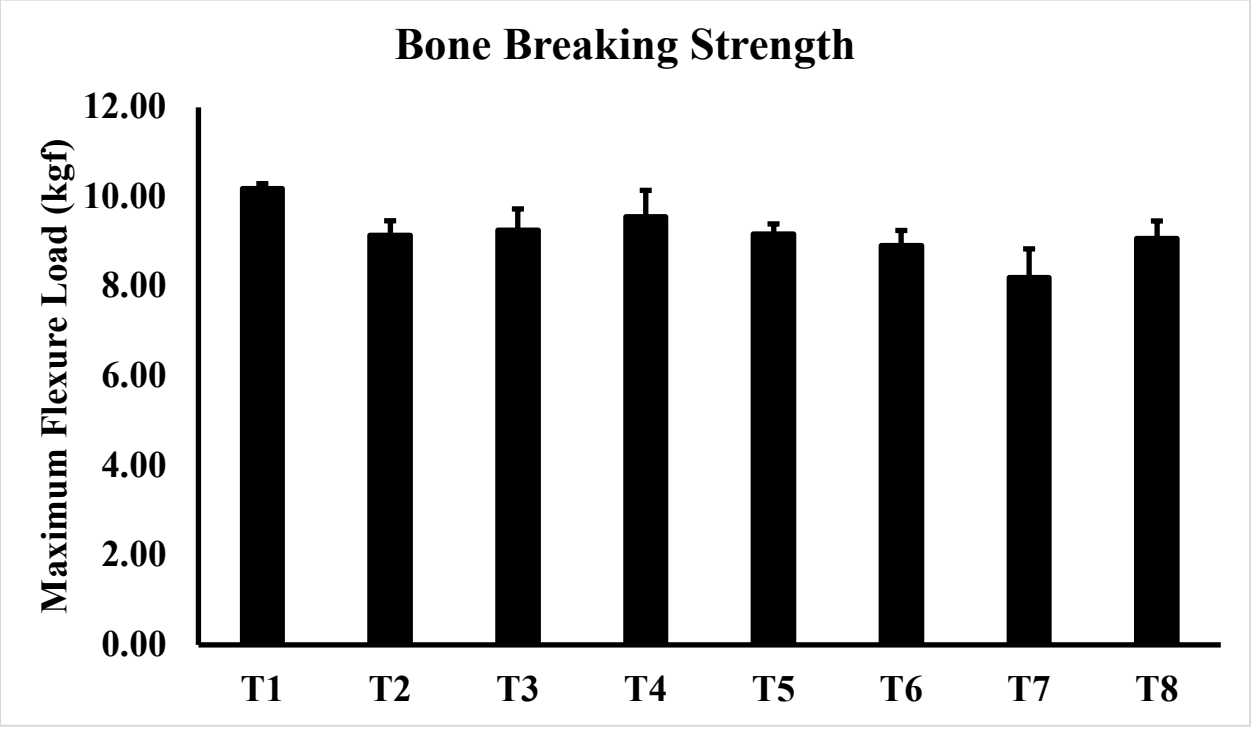

Figure 7.7 illustrates micro-computed tomography parameters (cortical and trabecular) of femur bones in broilers challenged with *Eimeria* spp. and *Staphylococcus aureus*. A: Cortical bone volume, B: Cortical bone surface, C: Cortical bone volume to tissue volume, D: Trabecular thickness, E: Trabecular number. T1, non-challenged treatment; T2, *Eimeria* spp. challenged group; T3, *Eimeria spp.* challenge and 2 x 10^5 CFU *S. aureus* day old challenge; T4, *Eimeria spp.* challenge and 2 x 10^5 CFU *S. aureus* day 18 challenge; T5, *Eimeria spp.* challenge and 2 x 10^8 CFU *S. aureus* day old challenge; T6, *Eimeria spp.* challenge and 2 x 10^8 CFU *S. aureus* day 18 challenge; T7, *Eimeria spp.* challenge and 2 x 10^5 CFU *S. aureus* day old and day 18 challenge; T8, *Eimeria spp.* challenge and 2 x 10^8 CFU *S. aureus* day old and day 18 challenge. Letters not connected by same letter is significantly different ($P < 0.05$, N =5).

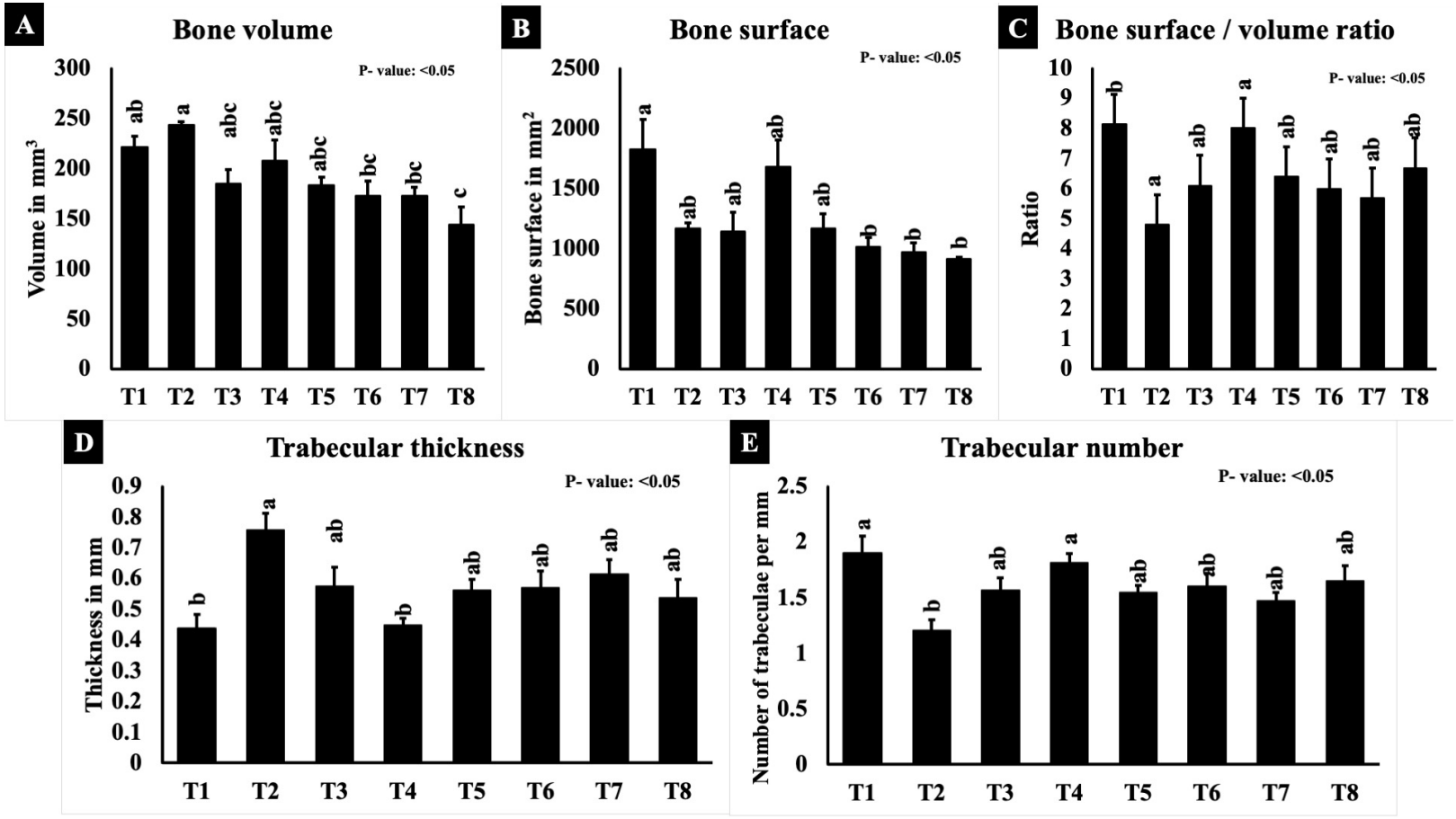
A
Bone volume
P- value: <0.05
Volume in mm3
300
250
200
150
100
50
0
ab
a
abc
abc
abc
bc
bc
c
T1 T2 T3 T4 T5 T6 T7 T8
B
Bone surface
P- value: <0.05
Bone surface in mm2
2500
2000
1500
1000
500
0
a
ab
ab
ab
ab
b
b
b
T1 T2 T3 T4 T5 T6 T7 T8
C
Bone surface / volume ratio
P- value: <0.05
Ratio
10
9
8
7
6
5
4
3
2
1
0
b
a
ab
a
ab
ab
ab
ab
T1 T2 T3 T4 T5 T6 T7 T8
D
Trabecular thickness
P- value: <0.05
Thickness in mm
0.9
0.8
0.7
0.6
0.5
0.4
0.3
0.2
0.1
0
b
a
ab
b
ab
ab
ab
ab
T1 T2 T3 T4 T5 T6 T7 T8
E
Trabecular number
P- value: <0.05
Number of trabeculae per mm
2.5
2
1.5
1
0.5
0
a
b
ab
a
ab
ab
ab
ab
T1 T2 T3 T4 T5 T6 T7 T8

80

CHAPTER 8

EFFECT OF *EIMERIA* SPP. AND *STAPHYLOCOCCUS AUREUS* CHALLENGE ON CECAL MICROBIOME IN BROILERS [1]

[1] Choppa, V.S.R., Naeini, H.R.R., Lee, D.J., Katha, H.R., Ko, H., Paneru, D., Kim, Y. and Kim, W.K., 2025. *Poultry Science*, p.105814.

ABSTRACT

Staphylococcus aureus, associated with Bacterial Chondronecrosis and Osteomyelitis (**BCO**), is a leading cause of lameness in modern-day broilers, often seen with concomitant gut health aberrations such as coccidiosis. This study aims to uncover changes in cecal microbiome which hasn't been characterized well in broilers challenged with *S. aureus* and *Eimeria* spp. Day-old male Cobb broilers were randomly allocated to eight treatments with five replicates each receiving various doses ($2x10^5$ or $2x10^8$ CFU/mL) and timings (Day 0 and/or 18) of *S. aureus*. A mixed challenge of *E. acervulina* (62,500 Oocysts)*, E. maxima* (12,500 Oocysts)*, and E. tenella* (12,500 Oocysts) were administered orally on day 14 to all treatments except non challenged control (T1). Cecal contents were collected on days 20 and 26 from each bird per replicate for microbial analysis and 16s rRNA gene sequencing. On days 20 and 26, significant changes among the treatments were found in alpha diversity (Shannon Index and Faith's phylogenetic diversity) and beta diversity (unweighted and weighted UniFrac). Higher and /or repeated exposure of *S. aureus* induced greater microbial shifts which can be seen from taxonomic composition at the phylum and family levels where *Actinobacteria*, *Microbacteraceae*, and elevated *Leuconostocaceae*. On day 26, high dose treatments revealed higher *Bacteroidetes* with decreased firmicutes besides shift in their ratios. Furthermore, functional pathway analysis unveils alterations in lipid metabolism, osteoclast differentiation, MAPK signaling, Fc gamma R mediated phagocytosis which are directly or indirectly linked with bone health. The above changes were spotlighted among the co-challenged high dose *S.aureus* treatments indicating the link for BCO pathogenesis. This study demonstrates that co-challenge with *Eimeria* and *S.aureus* alters cecal microbiome in a dose and time dependent way, leading to possible predisposition of BCO in broilers. This marks the need of

exploring microbiome targeted mitigation strategies alleviating the prevailing skeletal problems in poultry.

Keywords: Broilers, *Staphylococcus aureus, Eimeria* spp., BCO, Microbial Functional Profiles

INTRODUCTION

Gut microbiota play a crucial role in maintaining health and well-being of the host. They adhere to the intestinal epithelium, forming a protective barrier against pathogenic bacteria colonization (Yegani and Korver, 2008). Furthermore, these bacteria produce short-chain fatty acids, vitamins, organic acids, and bacteriocins, which enhance host nutrition and immunity and stimulate non-pathogenic immune responses (Jeurissen et al., 2002; Apajalahti, 2005; Yegani and Korver, 2008; Mancabelli et al., 2016; Kumar et al., 2018). Conversely, microbiome alterations can promote colonization of pathogenic bacteria or vice versa which manifest as dysbiosis (Kumar et al., 2018). This could result from infectious and non-infectious stressors among which renowned contributors like environmental changes, dietary imbalances, mycotoxins, poor management, viral or bacterial infections, and coccidiosis plays key role (Yegani and Korver, 2008). This can progress to colonization of sterile bone matrix by pathogenic microbes, resulting in osteomyelitis and other osseus diseases. Although complex networks of events are essential in changing the state of bone metabolism, this could start from gastrointestinal (GI) tract of chickens where the established microbiota maintains gut homeostasis under stress-free and favorable environment conditions (Chen et al., 2022). Among the different regions, cecum has the most diverse and sTable 8.microbial population, including anaerobes (Oakley et al., 2014). Earlier studies on broilers did not emphasize the significance of *Staphylococcus aureus* in altering microbiomes. This is deemed to be important because of the involvement of this pathogen in causing osteomyelitis of femur or femoral head necrosis since this disease incidence was discovered in 1972 (Nairn and Watson, 1972; Ramser et al., 2021; Asnayanti et al., 2024). *S. aureus* can infiltrate all types of osseus tissues and persist in a quiescent state as quasi-dormant small colony variants (SCVs) (Yang et al., 2018; Chen et al., 2021). Studies have shown that SCV phenotypes can rapidly become virulent, leading

to osteomyelitis (Tuchscherr et al., 2011). A major lacuna in understanding *S. aureus* induced osteomyelitis lies in the lack of data on associated microbiome alterations. This is particularly concerning given the gut's role as a major organ involved in host metabolism and immune regulation. The objective of the current study is to evaluate changes in cecal microbiome of broilers challenged with *Eimeria* spp. and *Staphylococcus aureus* at different time points. Understanding these changes uncover the potential link between gut microbiota and BCO.

MATERIALS AND METHODS

Birds, Diet, and Challenge

This study was reviewed and approved by the Institutional Animal Care and Use Committee at University of Georgia (A2021 12-012). A total of 600 birds were allocated to 8 treatments and 5 replicates per treatment in battery cages. Each pen had 15 birds, and all the birds were provided with *ad libitum* basal diet and water. Furthermore, challenge of *Staphylococcus aureus* was given orally on day 0 and day 18 to all birds except Treatment 1 and 2. 12,500 of *E. maxima*, 12,500 of *E. tenella*, and 62,500 of *E. acervulina* were inoculated orally to all birds except Control (Treatment 1). One mL of inoculum given to birds was checked prior to inoculation to ensure desired oocyst counts. **Treatment 1 (T1)** is non-challenged control and **Treatment 2 (T2)** is *Eimeria* challenge control. **Treatment 3 (T3)** was challenged with *S. aureus* at 2 x 10^5 CFU only on day 0 and **Treatment 4 (T4)** was challenged with the same dose but only day 18 respectively. Similarly, **Treatment 5 (T5)** received 2 x 10^8 CFU of *S. aureus* only day 0 and **Treatment 6 (T6)** received same dose on day 18, respectively. **Treatment 7 (T7)** and **Treatment 8 (T8)** were challenged with 2 x 10^5 CFU and 2 x 10^8 CFU of *S. aureus* respectively on both days (day 0 and 18). Birds were orally inoculated with 0.5 mL and 1 mL for day 0 and 18, respectively, which were

adjusted to desired CFU. Detailed description of challenge and respective treatments were provided in Table below (**Table 8.1**).

Staphylococcus aureus preparation

Baird Parker agar (BD DIFCO, NJ, USA) with 3.5 % tellurite in 30% egg yolk suspension (Sigma, St louis, MO, USA) was used for isolation and enumeration of *Staphylococcus aureus.* Agar was prepared according to manufacturer's guidelines. Primary stock of *S. aureus* was isolated from the 8 lame birds' femoral heads from Poultry Research Center, University of Georgia, Athens, GA. Clinically lame birds were selected based on gait scoring, and the femur from these birds were collected in sterile packs *(Whirl Pak®, Nasco Sampling LLC, Chicago, IL, USA)* and transferred to buffered peptone water (Himedia LLC, PA, USA) and homogenized. Following this, homogenized mixture was transferred to Baird parker agar plate. S. aureus was presumptively identified using colony characteristics like black colonies with halo appearance further confirmation was done using coagulase test (Ollis et al., 1995; Capita et al., 2001; Horwitz and Latimer, 2007). Following the above steps, single colony was transferred to BHI broth and incubated for 36 hours and then centrifuged to get a pellet which was diluted with 4 mL of 0.1 % peptone water. Optical density of this solution was measured at 600 nm using a UV-Vis spectrometer (Genesys 10S UV-Vis, Thermofisher Scientific, NJ, USA). With known OD standard curve was created followed by serial dilution and plating to check CFU in respective dilutions. Desired concentration needed for inoculation was prepared on the day of inoculation and given to respective treatments on day 0 and 18.

Sample preparation for microbial analysis

Two birds were euthanized by cervical dislocation and sprayed with 70 % ethanol on the surface to reduce surface contaminants followed by collection of required tissues. Ceca and

jejunum tissues from 2 birds were collected and transferred to a sterile filter bag (Whirl Pak®, Nasco Sampling LLC, Chicago, IL, USA). Following this, sample bags were individually weighed and added with 10 mL of buffered peptone water. Tissues were homogenized (Neutec, Seward Ltd, West Sussex, UK) with subsequent serial dilutions which were plated on BPA plates and enumerated following 24-36 hours of incubation at 37°C.

Microbiome Analysis and preparation

Cecal contents were collected and transferred to liquid nitrogen and stored in -80°C for further analysis. DNA was extracted using QIAamp Fast DNA stool mini kit (Qiagen GmbH, Hilden, Germany) and following manufacturer's protocol. Initially, 40-50 mg of cecal content was transferred to nuclease free microcentrifuge tubes (Avantor, Radnor, PA) which were added with 0.2 silicon beads to facilitate disruption of contents. This was followed by implementation of manufacturer's protocol. DNA quality and concentration was measured using Nanodrop 200 spectrophotometer (Thermo Fisher Scientific, Waltham, MA, USA) and shipped to LC Sciences (Houston, TX, USA) for 16s rRNA gene sequencing. V3-V4 regions were amplified with primers 5′-CCTACGGGNGGCWGCAG-3′ (forward) and 5′-GACTACHVGGGTATCTAATCC-3′ (reverse). Qiime2 was used to analyze gene sequences including alpha diversity, beta diversity, phylum and family level composition (Version 2024.10) (Bolyen et al., 2019; Choi et al., 2023). Amplicon specific variants (ASVs) were processed using DADA2 algorithm implemented in QIIME2. Furthermore, taxonomic classification used in the current study was based on Naïve Bayes classifier trained on the SILVA reference database (release 138) restricted to 16S rRNA gene V4 region amplified with primers 515F/806R.

Microbial community functions were predicted using PICRUSt2 based on the ASV Table 8.and representative sequences generated from QIIME2 (Bolyen et al., 2019; Choi et al., 2023).

KEGG pathway-level functional profiles were then analyzed using STAMP (Statistical Analysis of Metagenomic Profiles) to compare differences between the two groups. Statistical significance was assessed using Welch's t-test, and features with $P < 0.05$ were considered significant.

Statistical Analyses

Statistical analyses were performed on JMP pro 17 (SAS Institute Inc, Cary, NC, USA). ANOVA for all the parameters after checking normality, independent, and homogeneity of variance and data deviating from the above criteria were analyzed using Kruskal Wallis test. Post-hoc analyses like Tukey's Honest Significant Difference for ANOVA, and Wilcoxon Pair wise comparisons for Kruskal Wallis test were performed to identify significantly different parameters. Data is represented as means and standard error in the results below. *P-value* is set to less than 0.05.

S.aureus counts which were converted Log CFU/g which were analyzed using ANOVA and Tukey's HSD. Similarly, alpha diversity parameters like Shannon, Evenness, and Faith's PD were analyzed using ANOVA and Tukey HSD (Post-hoc). For Beta diversity, significant differences in distance from respective treatments can be identified using upper and lower decision limits from Dunnet's least square means. The values above or below these limits are considered significant ($P < 0.05$). Unweighted and weighted UniFrac distance were computed from rarefied feature tables. Furthermore, principal coordinates analysis was applied to each matrix. To express each sample's distance to control, Euclidean distance from that sample's PCoA scored to the control group centroid. Current study analyzed this measure with a linear model and reported as least square means and standard error. Dunnet contrasts were used to compared distances between treatments. Furthermore, relative abundances were analyzed using Kruskal-Wallis and post-hoc

tests like Steel-Dwass were used. Functional analyses were statistically analyzed using Welch's t-test, and features with $P < 0.05$ were considered significant.

RESULTS

Microbial Enumeration

Jejunal tissues were collected for microbial analysis, but *S.aureus* counts were undetecTable 8.among some of the replicates and were statistically insignificant (data not shown) ($P > 0.05$). On day 3 sampling of cecal tissues, T1 which is control group had 1 log CFU/g and T2 challenged with *Eimeria* only had *S.aureus* counts. Among treatments, T5 and T8, challenged with high *S. aureus* counts ($2x10^8$ CFU) had higher bacterial counts with 3.6 and 3.63 log CFU/g respectively ($P < 0.05$) **(Figure 8.1A)**. On day 20, *S. aureus* counts were higher in T5 and T8 with 4.9 and 4.7 log CFU/g respectively ($P < 0.05$) (**Figure 8.1B**). On day 26, T1 bacterial counts were negligible. T2 *S. aureus* counts were lower compared to T8 only and with 2.55 and 4.96 log CFU/g respectively. Furthermore, T3, T4, T5, and T6 counts were similar with bacterial counts of 3.69, 3.16, 3.55, and 3.96 log CFU/g respectively (**Figure 8.1C**).

Cecal Microbiome - Alpha Diversity

On day 20, the evenness among the treatments was not different, but Faith's PD which is another indicator for evenness was significant besides significant observed features and Shannon entropy. To elaborate, the evenness of treatment was more than 0.6 for T1, T2, T3, T4, and T8 with 0.704 for T8 (**Table 8.2**). Faith PD was higher for T1, T2, T3, and T4 with diversity scores of 25.06 20.86, 20.63, and 20.66 respectively ($P < 0.05$). Observed features were similar for treatments T1, T2, and T8 with means of 231.4, 206, and 216.8 respectively. On the other hand, T5, T6, and T7 were lower than the above treatments with 141, 158.8, and 164.8 respectively ($P < 0.05$). Precisely,

Shannon index was higher for T1, T2, and T8 with 5.134, 5.299, and 5.46 respectively compared to T5, T6, and T7 with 3.99, 3.83, and 3.89 respectively. Additionally, T3 and T4 Shannon entropy values were 4.683 and 4.613 respectively.

On day 26, Evenness, observed features, and Shannon index were different ($P < 0.05$) (**Table 8.3**) but not for Faith PD. Evenness was lower for T2, T3, and T7 with 0.63, 0.59, and 0.65 compared to T1 and T8 which were 0.77 and 0.76, respectively. Shannon index was also lower for T3 (4.39) compared to T1, T5, and T8 with 6.09, 5.58, and 6.17, respectively ($P < 0.05$). Furthermore, observed features were higher for T8 (282.6) compared to T2, T3, T4, T6, and T7 with 185.6, 168.4, 215.6, 216, and 213, respectively. Moreover, T1 and T5 had 239.8 and 245.4 observed features, respectively (**Table 8.3**).

Cecal Microbiome - Beta Diversity

On day 20, unweighted UniFrac data revealed that the distances from T1 were higher in T5, T6, T7, and T8 with LS mean of 0.308 for control (**Figure 8.2**) ($P < 0.05$). Similarly, the distances from T2, T3 and T4 (LS mean of 0.403, 0.379, and 0.434 respectively) to treatments T5, T6, T7, and T8 were higher (**Figure 8.2**) ($P < 0.05$). Moreover, the distance from T7 and T8 (LS mean of 0.463 and 0.441 respectively) were greater to T1, T2, T3, T4, and T5 (**Figure 8.2**) ($P < 0.05$).

Unweighted UniFrac on day 26 reveals, distance from T1 (LS mean of 0.478) was higher for all the treatments challenged with *S. aureus* (T3, T4, T5, T6, T7, and T8) (**Figure 8.3**) ($P < 0.05$). Furthermore, the distances from T2 (LS mean of 0.411) to other treatments were higher (Except T4). Distances from T3 (LS mean of 0.379) to T5, T6, T7, and T8 were higher. Distances from T4 (LS mean of 0.454) was greater for T1 and T6. Distance from T5 (LS mean of 0.408) to

all treatments (except T6 and T7) were higher. Similarly, distance from T7 (LS mean of 0.478) to T1 was higher (**Figure 8.3**) ($P < 0.05$).

Weighted Unifrac measurement which also includes abundance besides diversity deciphers the distance between treatments. On day 20, the distances from T2 (LS mean of 0.106) to T5, T6, and T7 were higher. Additionally, the distance from T3 (LS mean of 0.135) to T5, T6, and T7 were greater. The distance from T8 (LS mean of 0.117) to T5, T6, and T7 were higher which reveals the greater differences in diversity between the respective treatments (**Figure 8.4**). On the other hand, on day 26, the distances for T1 (LS mean of 0.308) to T5, T6, T7, and T8 were greater. Similarly, the distances from T2 (LS mean of 0.403) to T5, T6, T7, and T8; T3 (LS mean of 0.379) to T5, T6, T7, and T8; T4 (LS mean of 0.434) to T5, T6, T7, and T8 treatments were higher. Furthermore, the distances from T8 (LS mean of 0.441) to all treatments except T6, and T7 were also higher (**Figure 8.5**).

Microbial composition

On day 20, phyla differences between treatments did not vary except actinobacteria which was lower for T5 (0.14 %), T6 (0.16%), T7 (0.18 %), and T8 (0.21 %) ($P < 0.05$) (**Figure 8.5**). The family *Leuconostocaceae* was higher in T7 and T8 with 0.144 and 0.166 %, respectively; but other treatments were less than 0.07 % (**Figure 8.6**). Furthermore, *Microbacteraceae* was lower for T6, T7, and T8 with 0.040, 0.013, and 0.012 % respectively (**Figure 8.6**).

On day 26, the phyla *Bacteroidetes* and *Firmicutes* were different among the treatments with highest *Bacteroidetes* percentage among T6 and T7 with 19.99 and 29.5 %, respectively ($P < 0.05$) (**Figure 8.7**). Furthermore, *Firmicutes* percentage was higher in T1 and T8 with 69.98 and 66.30 %, respectively, which had significant differences with T2 (44.89 %), T3 (47.02 %), and T6

(48.73 %) (**Figure 8.7**). Furthermore, *Firmicutes* to *Bacteroidetes* ratio revealed lower ratios for T2, T3, T6, and T7 with ratios 2.26, 2.29, 2.44, and 1.62 respectively compared to treatments T1, T4, T5, and T8 (12.2, 7.43, 3.44, and 8.21, respectively) ($P < 0.05$). Surprisingly, although there were numerical differences among the treatments for day 26 families, there were no significant differences (**Figure 8.8**).

Microbial community functional Analyses

Microbial community functional analyses for all treatments were compared to control group (T1) which was neither challenged with *S. aureus* nor *Eimeria.* Furthermore, comparisons between other treatments to T2 (only *Eimeria* challenged) was expected to reveal differences when challenged with *S. aureus*.

On day 20, treatment 1 (non-challenged control) vs other treatments revealed different functional gene differences which are provided in detail below. T1 vs T5 showed affected some important pathways associated with bone turnover and cell differentiation like N-glycan biosynthesis, Fc gamma R-mediated phagocytosis, and Fatty acid elongation. Furthermore, T1 vs T6 similarly have affected Fc gamma R-mediated phagocytosis, MAPK signaling pathway, and Fatty acid elongation **(Figure 8.10)**. Moreover, T1 vs T7 and T1 vs T8 shown affected MAPK signaling, Fc gamma R-mediated phagocytosis, Osteoclast differentiation, Insulin signaling pathway, p53 signaling pathway, and key metabolic pathways directly and indirectly related to bone health which are shown in **Figure 8.11.**

Functional analysis differences between only *Eimeria* challenged (T2) and other treatment groups on day 20 revealed affected Steroid biosynthesis, important metabolic pathways, fatty acid elongation, primary immunodeficiency (higher in T5), and Osteoclast differentiation (higher in

T5) **(Figure 8.12)**. T2 vs T6 shown a significant reduction of MAPK signaling pathway, mRNA surveillance pathway, Fc gamma R-mediated phagocytosis, and fatty acid elongation **(Figure 8.12)**. Similarly, for T2 vs T7, in addition to the above pathways, osteoclast differentiation, steroid hormone biosynthesis, p53 signaling, insulin signaling pathway, and other metabolic pathways **(Figure 8.13)**. Finally, T2 vs T8 revealed altered Fc gamma R-mediated phagocytosis and other metabolic pathways **(Figure 8.13)**.

On day 26, the comparisons between T1 vs T5-T8 **(Figure 8.14 and 15)** shown significant differences ($P < 0.05$) higher metabolic pathways for T5, higher lysosome activity with increased apoptotic activity in T6, higher glycosaminoglycan degradation and increased steroid hormone biosynthesis in T6, increased lipopolysaccharide biosynthesis for T7, increased valine, leucine and isoleucine degradation (for T7), besides decreased peptidoglycan degradation (for T7), decreased homologous recombination (for T7) **(Figure 8.15)**. Furthermore, for T8 revealed glycosaminoglycan degradation along with decreased lysosome activity, increased folate biosynthesis **(Figure 8.15)**.

DISCUSSION

All the treatments except T1 were challenged with *Eimeria* spp. Other treatments inoculated with *S. aureus* (T3-T8) revealed increased bacterial counts on day 20, particularly in groups challenged with higher bacterial challenge (T5 (Day 0 *S.aureus* challenge) and T8 (Day 0 and 18 *S.aureus* challenge). Although present study does not include treatment groups challenged with *S.aureus* only, this dramatic increase of *S.aureus* counts in the *Eimeria* spp. co-challenge allowed cecal colonization of *S.aureus* like other pathogens such as *Clostridium perfringens* and *Salmonella* (Pham et al., 2021).

Studies on *Eimeria* spp. revealed disrupted cecal microbiota indicating decline in beneficial bacteria allowing pathogens to dominate or alter the microbiome (Martynova-Van Kley et al., 2012; Macdonald et al., 2017; Madlala et al., 2021; Campos et al., 2022; Choi and Kim, 2022; Yu et al., 2023). To elaborate, these changes weaken the colonization resistance of gut thereby allowing domination of *Enterobacteriaceae* and *Bacteroides* (Martynova-Van Kley et al., 2012; Jebessa et al., 2022). This shift is not limited to above taxa, where increase in *Proteobacteria* besides a decrease in *firmicutes* were observed which strongly suggest opportunistic pathogens replacing beneficial fermentative bacteria (Pham et al., 2021; Choi and Kim, 2022). In the current study which was challenged with *S.aureus* and *Eimeria* (T3-T8) revealed disruptions in bacterial compositions. This would trigger pathological changes, including inflammation in multiple organs such as bone due to microbial translocation. Furthermore, a possible release of lipopolysaccharide (LPS) into the bloodstream would alter cytokine signaling and Wnt pathways (Ahlawat et al., 2021; Choppa and Kim, 2023; Choppa et al., 2023). Compliantly, decrease in Firmicutes to Bacteroidetes ratio for some treatments (T2, T3, T6, T7) suggests possible lipopolysaccharides release into circulation (Aruwa et al., 2021; El-Ghany, 2021).

Our study has shown a significantly higher phylogenetic diversity with low challenge treatment groups (T1, T2, T3, and T4) which is measured by sum of branch lengths of phylogenetic tree connecting all species in the assemblage (Faith, 2018). Interestingly, a study on blood microbiome revealed BCO affected broilers' microbial community structure with abundant genera like *Staphylococcus*, *Granulicatella*, and *Microbacterium* which was found to be partially relevant to the current results (Mandal et al., 2016). The findings suggest a potential temporal change in cecal microbiome adapting to the challenged environment which is influenced by early microbial exposure in developing latter microbial communities (Ramírez et al., 2020; De Jong et al., 2022;

Kayal et al., 2022). The above statement can be further reinforced by the findings in beta diversity parameters which reveal significant differences with high doses of *S. aureus* challenge birds and low dose of this pathogen given on day 0 and 18 (T5-T8).

Although *Staphylococcus* spp. is of least concern in terms of dysbiosis potential, current study revealed altered *Firmicutes* to *Bacteroidetes* ratio which was discussed earlier. This in relation to the above challenge would raise the concerns on the aberrations to microbiome associated with bone physiology (Mandal et al., 2016, 2020). These concerns would heighten, when *Eimeria* spp. challenge is prevailing in the host environment which alter the microbial diversity besides allowing the pathogenic bacteria to thrive by decreasing some beneficial bacterial families *Lachnospiraceae* and *Faecalibacterium* (Chen et al., 2020; Campos et al., 2022). Interestingly, present study shows decrease in abundance of *Actinobacteria* for treatments challenged with *Eimeria* and *S. aureus* at higher doses like 2 x 10^8 CFU on day 0 and/or day 18 along with low dose (2 x 10^5 CFU) on day 0 and 18 (T5, T6, T7, and T8) compared to non-challenged, only *Eimeria* challenged, *Eimeria* and *S. aureus* challenge on day 0 and day 18 groups (T1, T2, T3, and T4). This decrease in *Actinobacteria* has been reported to be associated with aberrations in bone homeostasis which are discussed below.(Cholewińska et al., 2021; Singh et al., 2023; Agabalaev and Pak, 2024; Wu et al., 2024) For instance, a study showed altering feed composition (fermented rapeseed meal addition) and housing conditions improved shift of cutaneous microbiota (increasing *Firmicutes* and *Actinobacteria*) (Cholewińska et al., 2021). Similarly, shift in fermentative microbes in litter are important in enhancing production of SCFAs (especially butyrate) which are associated with improved mineral absorption besides exerting anti-inflammatory, immunomodulatory properties to promote bone formation and decrease bone resorption (Huang et al., 2023; Agabalaev and Pak, 2024). Although above findings reveal

importance of *Actinobacteria* to relate with present study, it also hints importance of optimized feed and litter to maintain bone homeostasis even under challenged conditions (*Eimeria* and *S. aureus*).

Moreover, predicted functional pathways showed noTable 8.shifts in gut microbiome metabolism compared to non-challenged control (T1). Importantly, this analysis revealed shift in lipid metabolism through fatty acid elongation pathways, a pathway known to be upregulated during microbiome shift observed in the current findings (Zhao et al., 2018). Furthermore, enriched NOD-like receptor (NLR) pathway along with MAPK signaling represents maturation of IL-1beta and tumor necrosis factor alpha which accelerate bone resorption besides decreased osteoblast formation (Weng et al., 2024). In addition, day 20 family composition revealed an increase in *Leuconostocaceae* among T6, T7, and T8 compared to other treatments. Contrarily, *Microbacteraceae* percentage was lower for T5, T6, T7, and T8 treatments. Although these families are not well understood in chickens, *leuconostoc* are heterofermentative bacteria with symbiotic relationships to *Lactococcus* spp (Nieminen et al., 2014). Studies related to humans revealed, increase in *Leuconostocaceae* is positive sign since this enhances fermentation of carbohydrates which is associated with production of lactic acid and SCFA production (Forbes et al., 2016; Hati et al., 2019). In contrast, *Microbacteraceae* which is less understood have a positive correlation with complex feed degradation besides indirect association with SCFA production (Park et al., 1993). Furthermore, being a part of beneficial bacterial community, *Microbacteriaceae* resist pathogen colonization which is clearly lacking in the current study for the treatments challenged with *Eimeria* and *Staphylococcus* spp at higher or lower doses given on day 0 and or 18 (T5, T6, T7, and T8) (Abdel-Kafy et al., 2022). These differences in commensals (highly abundant *Leuconostocaceae* and less abundant *Microbacteraceae*) for the above treatments (T5-

T8) could possibly represent the need for diverse microbiota. This opens the way for a need in understanding whether to promote or stabilize *Leuconostocaceae* and *Microbacteraceae* when mitigating BCO.

CONCLUSION

Dysbiosis induced by *Eimeria* spp. and *S. aureus* co-challenge disrupts microbial community structure in a time and dose dependent manner. Birds which were exposed to high *S. aureus* dose ($2x10^8$ CFU) on days 0 and 18 exhibited the most pronounced reduction in alpha diversity metrics besides significant beta diversity aberrations which were further narrowed down to marked increase in pathobionts (*Leuconostocaceae*) and decreased beneficial taxa (*Actinobacteria*). These shifts correlated with decreased *Firmicutes* to *Bacteriodetes* ratio representing changes of cecal microbiota potentially linked with LPS-driven inflammation. These findings suggest that *S. aureus* and *Eimeria*-induced dysbiosis would possibly facilitate bacterial chondronecrosis and osteomyelitis (BCO). Prospective studies should validate causal relationship of microbiome alterations in BCO pathogenesis besides exploring therapeutic strategies to restore microbial resilience.

REFERENCES

Abdel-Kafy, E.-S. M., S. F. Youssef, M. Magdy, S. S. Ghoneim, H. A. Abdelatif, R. A. Deif-Allah, Y. Z. Abdel-Ghafar, H. M. A. Shabaan, H. Liu, and A. Elokil. 2022. Gut microbiota, intestinal morphometric characteristics, and gene expression in relation to the growth performance of chickens. Animals 12:3474.

Agabalaev, D. N. O., and I. V. Pak. 2024. Diversity of the taxonomic structure present in the litter of broiler chickens under industrial conditions. Acta Agriculturae Serbica 28.

315 Ahlawat, S., Asha, and K. K. Sharma. 2021. Gut–organ axis: a microbial outreach and networking.
316 Lett Appl Microbiol 72:636–668.

317 Apajalahti, J. 2005. Comparative gut microflora, metabolic challenges, and potential opportunities.
318 Journal of Applied Poultry Research 14:444–453.

319 Aruwa, C. E., C. Pillay, M. M. Nyaga, and S. Sabiu. 2021. Poultry gut health–microbiome
320 functions, environmental impacts, microbiome engineering and advancements in characterization
321 technologies. J Anim Sci Biotechnol 12:1–15.

322 Asnayanti, A., A. D. T. Do, and A. Alrubaye. 2024. Microbiology, induction, and management
323 practices to mitigate lameness caused by bacterial chondronecrosis with osteomyelitis in broiler
324 chickens. Ger. J. Vet. Res 4:14–30.

325 Bolyen, E., J. R. Rideout, M. R. Dillon, N. A. Bokulich, C. C. Abnet, G. A. Al-Ghalith, H.
326 Alexander, E. J. Alm, M. Arumugam, and F. Asnicar. 2019. Reproducible, interactive, scalable and
327 extensible microbiome data science using QIIME 2. Nat Biotechnol 37:852–857.

328 Campos, P. M., K. B. Miska, S. Kahl, M. C. Jenkins, J. Shao, and M. Proszkowiec-Weglarz. 2022.
329 Effects of Eimeria tenella on cecal luminal and mucosal microbiota in broiler chickens. Avian Dis
330 66:39–52.

331 Capita, R., C.-A. Calleja, and B. Moreno. 2001. Assessment of Baried-Parker Agar as Screening
332 Test for Determination of Staphylococcus aureus in Poultry Meat. Journal of Microbiology
333 39:321–325.

334 Chen, J., A. Xiong, Y. Ma, C. Qin, and C. L. Ho. 2021. Impact of the host-microbiome on
335 osteomyelitis pathogenesis. Front Mol Biosci 8:702484.

Chen, P., T. Xu, C. Zhang, X. Tong, A. Shaukat, Y. He, K. Liu, and S. Huang. 2022. Effects of probiotics and gut microbiota on bone metabolism in chickens: a review. Metabolites 12:1000.

Chen, H.-L., X.-Y. Zhao, G.-X. Zhao, H.-B. Huang, H.-R. Li, C.-W. Shi, W.-T. Yang, Y.-L. Jiang, J.-Z. Wang, and L.-P. Ye. 2020. Dissection of the cecal microbial community in chickens after Eimeria tenella infection. Parasit Vectors 13:1–15.

Choi, J., D. Goo, M. K. Sharma, H. Ko, G. Liu, D. Paneru, V. S. R. Choppa, J. Lee, and W. K. Kim. 2023. Effects of different Eimeria inoculation doses on growth performance, daily feed intake, gut health, gut microbiota, foot pad dermatitis, and Eimeria gene expression in broilers raised in floor pens for 35 days. Animals 13:2237.

Choi, J., and W. Kim. 2022. Interactions of microbiota and mucosal immunity in the ceca of broiler chickens infected with Eimeria tenella. Vaccines (Basel) 10:1941.

Cholewińska, P., M. Michalak, K. Wojnarowski, S. Skowera, J. Smoliński, and K. Czyż. 2021. Levels of firmicutes, actinobacteria phyla and lactobacillaceae family on the skin surface of broiler chickens (Ross 308) depending on the nutritional supplement and the housing conditions. Agriculture 11:287.

Choppa, V. S. R., and W. K. Kim. 2023. A Review on Pathophysiology, and Molecular Mechanisms of Bacterial Chondronecrosis and Osteomyelitis in Commercial Broilers. Biomolecules 13:1032.

Choppa, V. S. R., G. Liu, Y. H. Tompkins, and W. K. Kim. 2023. Altered Osteogenic Differentiation in Mesenchymal Stem Cells Isolated from Compact Bone of Chicken Treated with Varying Doses of Lipopolysaccharides. Biomolecules 13:1626.

El-Ghany, W. A. A. 2021. Staphylococcus aureus in poultry, with special emphasis on methicillin-resistant strain infection: a comprehensive review from one health perspective.

Faith, D. P. 2018. Phylogenetic diversity and conservation evaluation: perspectives on multiple values, indices, and scales of application. Phylogenetic diversity: Applications and challenges in biodiversity science:1–26.

Forbes, J. D., G. Van Domselaar, and C. N. Bernstein. 2016. The gut microbiota in immune-mediated inflammatory diseases. Front Microbiol 7:1081.

Hati, S., M. Patel, B. K. Mishra, and S. Das. 2019. Short-chain fatty acid and vitamin production potentials of Lactobacillus isolated from fermented foods of Khasi Tribes, Meghalaya, India. Ann Microbiol 69:1191–1199.

Horwitz, W., and G. W. Latimer. 2007. Official methods of analysis of AOAC International, 2000. Gaithersburg, Maryland.

Huang, S.-C., Y.-F. He, P. Chen, K.-L. Liu, and A. Shaukat. 2023. Gut microbiota as a target in the bone health of livestock and poultry: roles of short-chain fatty acids. Animal Diseases 3:23.

Jebessa, E., L. Guo, X. Chen, S. F. Bello, B. Cai, M. Girma, O. Hanotte, and Q. Nie. 2022. Influence of Eimeria maxima coccidia infection on gut microbiome diversity and composition of the jejunum and cecum of indigenous chicken. Front Immunol 13:994224.

Jeurissen, S. H., F. Lewis, J. D. van der Klis, Z. Mroz, J. M. Rebel, and A. A. Ter Huurne. 2002. Parameters and techniques to determine intestinal health of poultry as constituted by immunity, integrity, and functionality. Curr Issues Intest Microbiol 3:1–14.

De Jong, I. C., D. Schokker, H. Gunnink, M. Van Wijhe, and J. M. J. Rebel. 2022. Early life environment affects behavior, welfare, gut microbiome composition, and diversity in broiler chickens. Front Vet Sci 9:977359.

Kayal, A., D. Stanley, A. Radovanovic, D. Horyanto, T. T. H. Van, and Y. S. Bajagai. 2022. Controlled intestinal microbiota colonisation in broilers under the industrial production system. Animals 12:3296.

Kumar, S., C. Chen, N. Indugu, G. O. Werlang, M. Singh, W. K. Kim, and H. Thippareddi. 2018. Effect of antibiotic withdrawal in feed on chicken gut microbial dynamics, immunity, growth performance and prevalence of foodborne pathogens. PLoS One 13:e0192450.

Macdonald, S. E., M. J. Nolan, K. Harman, K. Boulton, D. A. Hume, F. M. Tomley, R. A. Stabler, and D. P. Blake. 2017. Effects of Eimeria tenella infection on chicken caecal microbiome diversity, exploring variation associated with severity of pathology. PLoS One 12:e0184890.

Madlala, T., M. Okpeku, and M. A. Adeleke. 2021. Understanding the interactions between Eimeria infection and gut microbiota, towards the control of chicken coccidiosis: a review. Parasite 28.

Mancabelli, L., C. Ferrario, C. Milani, M. Mangifesta, F. Turroni, S. Duranti, G. A. Lugli, A. Viappiani, M. C. Ossiprandi, and D. van Sinderen. 2016. Insights into the biodiversity of the gut microbiota of broiler chickens. Environ Microbiol 18:4727–4738.

Mandal, R. K., T. Jiang, A. A. Al-Rubaye, D. D. Rhoads, R. F. Wideman, J. Zhao, I. Pevzner, and Y. M. Kwon. 2016. An investigation into blood microbiota and its potential association with Bacterial Chondronecrosis with Osteomyelitis (BCO) in Broilers. Sci Rep 6:25882 Available at http://europepmc.org/abstract/MED/27174843.

Mandal, R. K., T. Jiang, R. F. Wideman, T. Lohrmann, and Y. M. Kwon. 2020. Microbiota Analysis of Chickens Raised Under Stressed Conditions . Frontiers in Veterinary Science 7:696 Available at https://www.frontiersin.org/article/10.3389/fvets.2020.482637.

Martynova-Van Kley, M. A., E. O. Oviedo-Rondón, S. E. Dowd, M. Hume, and A. Nalian. 2012. Effect of Eimeria infection on cecal microbiome of broilers fed essential oils.

Nairn, M. E., and A. R. A. Watson. 1972. Leg weakness of poultry-a clinical and pathological characterisation.

Nieminen, T. T., E. Säde, A. Endo, P. Johansson, and J. Björkroth. 2014. The family leuconostocaceae.Pages 215–240 in The prokaryotes: Firmicutes and tenericutes. Springer-Verlag.

Oakley, B. B., H. S. Lillehoj, M. H. Kogut, W. K. Kim, J. J. Maurer, A. Pedroso, M. D. Lee, S. R. Collett, T. J. Johnson, and N. A. Cox. 2014. The chicken gastrointestinal microbiome. FEMS Microbiol Lett 360:100–112.

Ollis, G. W., S. A. Rawluk, M. Schoonderwoerd, and C. Schipper. 1995. Detection of Staphylococcus aureus in bulk tank milk using modified Baird-Parker culture media. The Canadian Veterinary Journal 36:619.

Park, Y.-H., K.-I. Suzuki, D.-G. Yim, K.-C. Lee, E. Kim, J. Yoon, S. Kim, Y.-H. Kho, M. Goodfellow, and K. Komagata. 1993. Suprageneric classification of peptidoglycan group B actinomycetes by nucleotide sequencing of 5S ribosomal RNA. Antonie Van Leeuwenhoek 64:307–313.

Pham, H. H. S., M. Matsubayashi, N. Tsuji, and T. Hatabu. 2021. Relationship between Eimeria tenella associated-early clinical signs and molecular changes in the intestinal barrier function. Vet Immunol Immunopathol 240:110321.

Ramírez, G. A., E. Richardson, J. Clark, J. Keshri, Y. Drechsler, M. E. Berrang, R. J. Meinersmann, N. A. Cox, and B. B. Oakley. 2020. Broiler chickens and early life programming: Microbiome transplant-induced cecal community dynamics and phenotypic effects. PLoS One 15:e0242108.

Ramser, A., E. Greene, R. Wideman, and S. Dridi. 2021. Local and systemic cytokine, chemokine, and FGF profile in bacterial chondronecrosis with osteomyelitis (BCO)-Affected broilers. Cells 10:3174.

Tuchscherr, L., E. Medina, M. Hussain, W. Völker, V. Heitmann, S. Niemann, D. Holzinger, J. Roth, R. A. Proctor, and K. Becker. 2011. Staphylococcus aureus phenotype switching: an effective bacterial strategy to escape host immune response and establish a chronic infection. EMBO Mol Med 3:129–141.

Weng, S., E. Tian, M. Gao, S. Zhang, G. Yang, and B. Zhou. 2024. Eimeria: Navigating complex intestinal ecosystems. PLoS Pathog 20:e1012689.

Yang, D., A. R. Wijenayaka, L. B. Solomon, S. M. Pederson, D. M. Findlay, S. P. Kidd, and G. J. Atkins. 2018. Novel insights into Staphylococcus aureus deep bone infections: the involvement of osteocytes. mBio 9:10–1128.

Yegani, M., and D. R. Korver. 2008. Factors affecting intestinal health in poultry. Poult Sci 87:2052–2063.

Yu, H., Q. Wang, J. Tang, L. Dong, G. Dai, T. Zhang, G. Zhang, K. Xie, H. Wang, and Z. Zhao. 2023. Comprehensive analysis of gut microbiome and host transcriptome in chickens after Eimeria tenella infection. Front Cell Infect Microbiol 13:1191939.

Zhao, L., Y. Huang, L. Lu, W. Yang, T. Huang, Z. Lin, C. Lin, H. Kwan, H. L. X. Wong, and Y. Chen. 2018. Saturated long-chain fatty acid-producing bacteria contribute to enhanced colonic motility in rats. Microbiome 6:107.

Table 8.1 represents the treatment names and respective challenge of *Eimeria* and *Staphylococcus aureus.*

	Bacterial Challenge	*Eimeria* Challenge on day 14 12,500 *E. maxima*; 12,500 *E. tenella*; 62,500 *E. acervulina*
Treatment 1 (T1)	No	No
Treatment 2 (T2)	No	Yes
Treatment 3 (T3)	2 x 10^5 CFU day old challenge	Yes
Treatment 4 (T4)	2 x 10^5 CFU day 18	Yes
Treatment 5 (T5)	2 x 10^8 CFU day old challenge	Yes
Treatment 6 (T6)	2 x 10^8 CFU day 18	Yes
Treatment 7 (T7)	2 x 10^5 CFU day old and day 18/DPI 4 challenge	Yes
Treatment 8 (T8)	2 x 10^8 CFU day old and day 18/DPI 4 challenge	Yes

Table 8.2 represents alpha diversity parameters for the treatments on day 20 along with *p* values.

[1]T1, non-challenged treatment; T2, *Eimeria* spp. challenged group; T3, *Eimeria* spp. challenge and 2 x 10^5 CFU *S. aureus* day old challenge; T4, *Eimeria* spp. challenge and 2 x 10^5 CFU *S. aureus* day 18 challenge; T5, *Eimeria* spp. challenge and 2 x 10^8 CFU *S. aureus* day old challenge; T6, *Eimeria* spp. challenge and 2 x 10^8 CFU *S. aureus* day 18 challenge; T7, *Eimeria* spp. challenge and 2 x 10^5 CFU *S. aureus* day old and day 18 challenge; T8, *Eimeria* spp. challenge and 2 x 10^8 CFU *S. aureus* day old and day 18 challenge. Letters not connected by same letter is significantly different ($P < 0.05$, N =5).

DAY 20				
TREATMENTS[1]	Evenness	Faith PD	Observed Features	Shannon Entropy
T1	0.654 ± 0.041	25.06 ± 1.58^{a}	231.4 ± 24.87^{a}	5.13 ± 0.42
T2	0.693 ± 0.031	20.86 ± 1.56^{ab}	206 ± 14.76^{abc}	5.30 ± 0.17^{a}
T3	0.626 ± 0.029	20.63 ± 2.12^{ab}	180.2 ± 19.74^{bcd}	4.68 ± 0.3^{abc}
T4	0.604 ± 0.051	20.66 ± 2.26^{ab}	198.6 ± 16.68^{abc}	4.61 ± 0.45^{abc}
T5	0.558 ± 0.054	12.55 ± 1.73^{c}	141 ± 10.19^{d}	3.99 ± 0.44^{bc}
T6	0.522 ± 0.064	14.91 ± 1.58^{c}	158.8 ± 20.41^{cd}	3.83 ± 0.56^{c}
T7	0.526 ± 0.077	15.89 ± 1.97^{bc}	164.8 ± 15.5^{cd}	3.89 ± 0.61^{c}
T8	0.704 ± 0.023	16.17 ± 1.62^{bc}	216.8 ± 2.8^{ab}	5.46 ± 0.19^{a}
***P*-VALUE**	0.0568	0.0006	0.0076	0.0397

Table 8.3 represents alpha diversity parameters for the treatments on day 26 along with *p* values.

[1] T1, non-challenged treatment; T2, *Eimeria* spp. challenged group; T3, *Eimeria* spp. challenge and 2 x 10^5 CFU *S. aureus* day old challenge; T4, *Eimeria* spp. challenge and 2 x 10^5 CFU *S. aureus* day 18 challenge; T5, *Eimeria* spp. challenge and 2 x 10^8 CFU *S. aureus* day old challenge; T6, *Eimeria* spp. challenge and 2 x 10^8 CFU *S. aureus* day 18 challenge; T7, *Eimeria* spp. challenge and 2 x 10^5 CFU *S. aureus* day old and day 18 challenge; T8, *Eimeria* spp. challenge and 2 x 10^8 CFU *S. aureus* day old and day 18 challenge. Letters not connected by same letter is significantly different ($P < 0.05$, N =5).

DAY 26				
TREATMENTS[1]	Evenness	Faith PD	Observed Features	Shannon index d26
T1	0.77 ± 0.033^{a}	19.76 ± 1.825	239.8 ± 16.95^{ab}	6.09 ± 0.31^{a}
T2	0.63 ± 0.02^{bc}	15.03 ± 0.862	185.6 ± 18.36^{bc}	4.70 ± 0.22^{bc}
T3	0.59 ± 0.069^{c}	13.48 ± 1.563	168.4 ± 26.82^{c}	4.39 ± 0.62^{c}
T4	0.72 ± 0.04^{ab}	14.22 ± 1.431	215.6 ± 15.73^{bc}	5.58 ± 0.34^{ab}
T5	0.72 ± 0.022^{ab}	20.18 ± 1.523	245.4 ± 15.98^{ab}	5.68 ± 0.19^{ab}
T6	0.67 ± 0.054^{abc}	20.35 ± 2.481	216 ± 27.84^{bc}	5.25 ± 0.53^{abc}
T7	0.65 ± 0.036^{bc}	15.66 ± 2.385	213 ± 32.83^{bc}	4.96 ± 0.40^{bc}
T8	0.76 ± 0.01^{a}	16.38 ± 2.292	282.6 ± 21.44^{a}	6.17 ± 0.11^{a}
***P*-VALUE**	0.0185	0.0651	0.0401	0.0185

Figure 8.1 illustrates the *Staphylococcus aureus* counts with treatments from 1 to 8 on day 3 (A), 20 (B), 26 (C).

[1] T1, non-challenged treatment; T2, *Eimeria* spp. challenged group; T3, *Eimeria* spp. challenge and 2 x 10^5 CFU *S. aureus* day old challenge; T4, *Eimeria* spp. challenge and 2 x 10^5 CFU *S. aureus* day 18 challenge; T5, *Eimeria* spp. challenge and 2 x 10^8 CFU *S. aureus* day old challenge; T6, *Eimeria* spp. challenge and 2 x 10^8 CFU *S. aureus* day 18 challenge; T7, *Eimeria* spp. challenge and 2 x 10^5 CFU *S. aureus* day old and day 18 challenge; T8, *Eimeria* spp. challenge and 2 x 10^8 CFU *S. aureus* day old and day 18 challenge. Letters not connected by same letter is significantly different ($P < 0.05$, N =5).

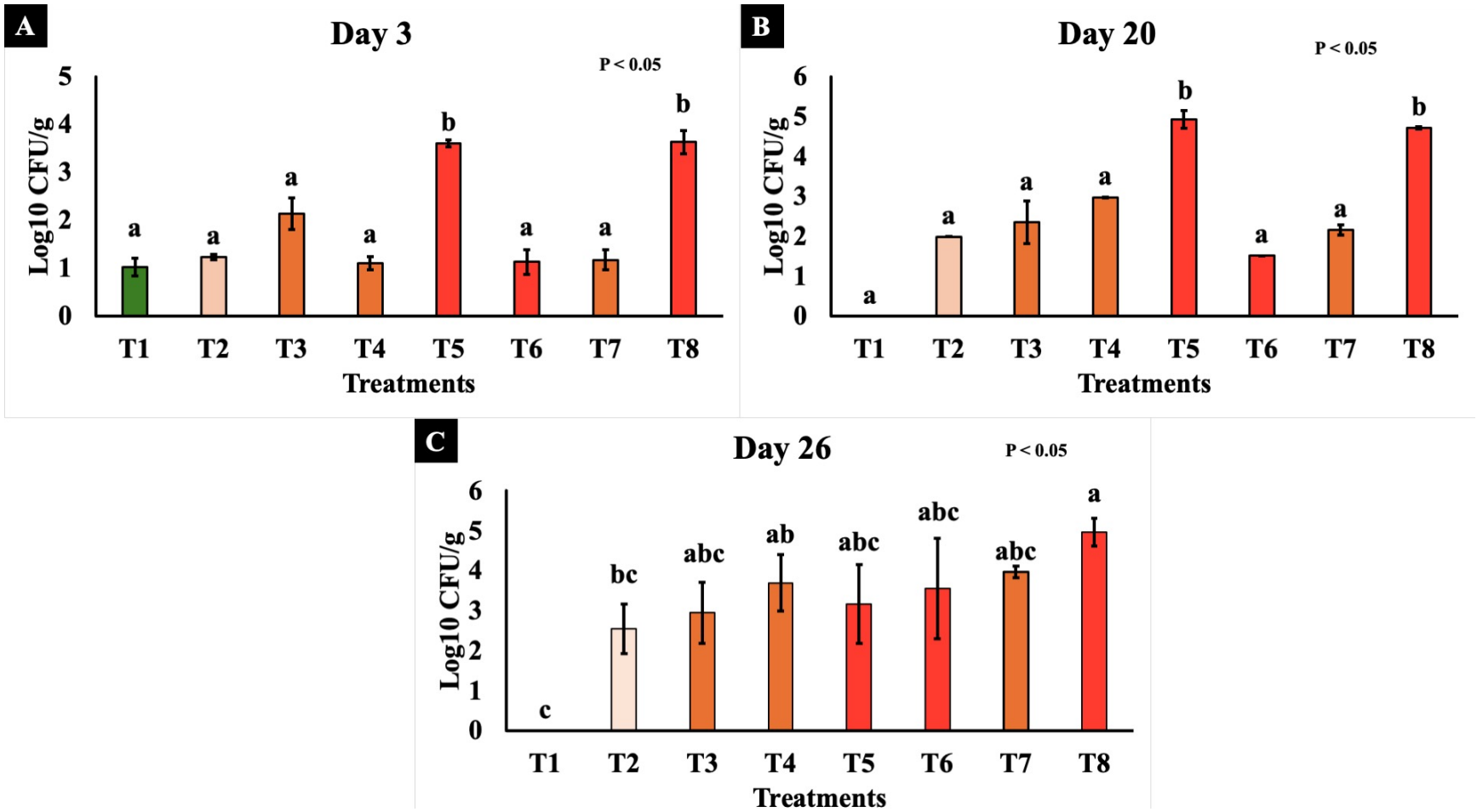
A
Day 3
P < 0.05
Log10 CFU/g
0
1
2
3
4
5
a
a
a
a
b
a
a
b
T1
T2
T3
T4
T5
T6
T7
T8
Treatments
B
Day 20
P < 0.05
Log10 CFU/g
0
1
2
3
4
5
6
a
a
a
a
b
a
a
b
T1
T2
T3
T4
T5
T6
T7
T8
Treatments
C
Day 26
P < 0.05
Log10 CFU/g
0
1
2
3
4
5
6
c
bc
abc
ab
abc
abc
abc
a
T1
T2
T3
T4
T5
T6
T7
T8
Treatments

473

Figure 8.2 unweighted UniFrac (quantitative beta diversity) showing the distance from one treatment to other treatments on day 20. Graphs having green needle head represents in significant distances. Red needle head represents significantly distance between the respective treatments ($P < 0.05$). UDL=Upper detection limit; LDL=Lower detection limit. T1, non-challenged treatment; T2, *Eimeria* spp. challenged group; T3, *Eimeria* spp. challenge and 2 x 10^5 CFU *S. aureus* day old challenge; T4, *Eimeria* spp. challenge and 2 x 10^5 CFU *S. aureus* day 18 challenge; T5, *Eimeria* spp. challenge and 2 x 10^8 CFU *S. aureus* day old challenge; T6, *Eimeria* spp. challenge and 2 x 10^8 CFU *S. aureus* day 18 challenge; T7, *Eimeria* spp. challenge and 2 x 10^5 CFU *S. aureus* day old and day 18 challenge; T8, *Eimeria* spp. challenge and 2 x 10^8 CFU *S. aureus* day old and day 18 challenge. Letters not connected by same letter is significantly different ($P < 0.05$, N =5).

Unweighted Unifrac Measurement (Quantitative Beta Diversity)– Day 20

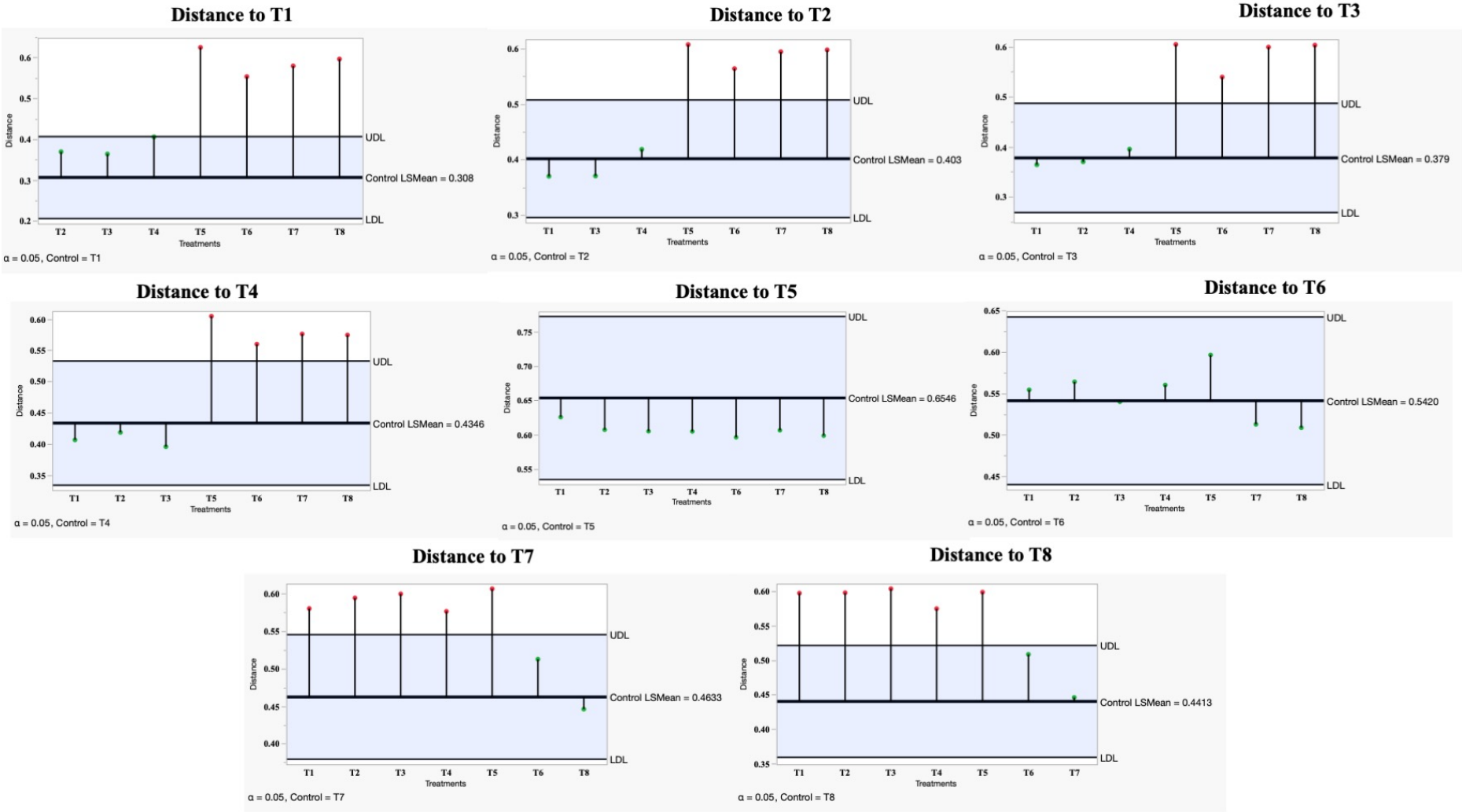

482

Figure 8.3 unweighted UniFrac (quantitative beta diversity) showing the distance from one treatment to other treatments on day 26. Graphs having green needle head represents in significant distances. Red needle head represents significantly distance between the respective treatments ($P < 0.05$). UDL=Upper detection limit; LDL=Lower detection limit. T1, non-challenged treatment; T2, *Eimeria* spp. challenged group; T3, *Eimeria* spp. challenge and 2 x 10^5 CFU *S. aureus* day old challenge; T4, *Eimeria* spp. challenge and 2 x 10^5 CFU *S. aureus* day 18 challenge; T5, *Eimeria* spp. challenge and 2 x 10^8 CFU *S. aureus* day old challenge; T6, *Eimeria* spp. challenge and 2 x 10^8 CFU *S. aureus* day 18 challenge; T7, *Eimeria* spp. challenge and 2 x 10^5 CFU *S. aureus* day old and day 18 challenge; T8, *Eimeria* spp. challenge and 2 x 10^8 CFU *S. aureus* day old and day 18 challenge.

Unweighted Unifrac Measurement (Quantitative Beta Diversity)– Day 26

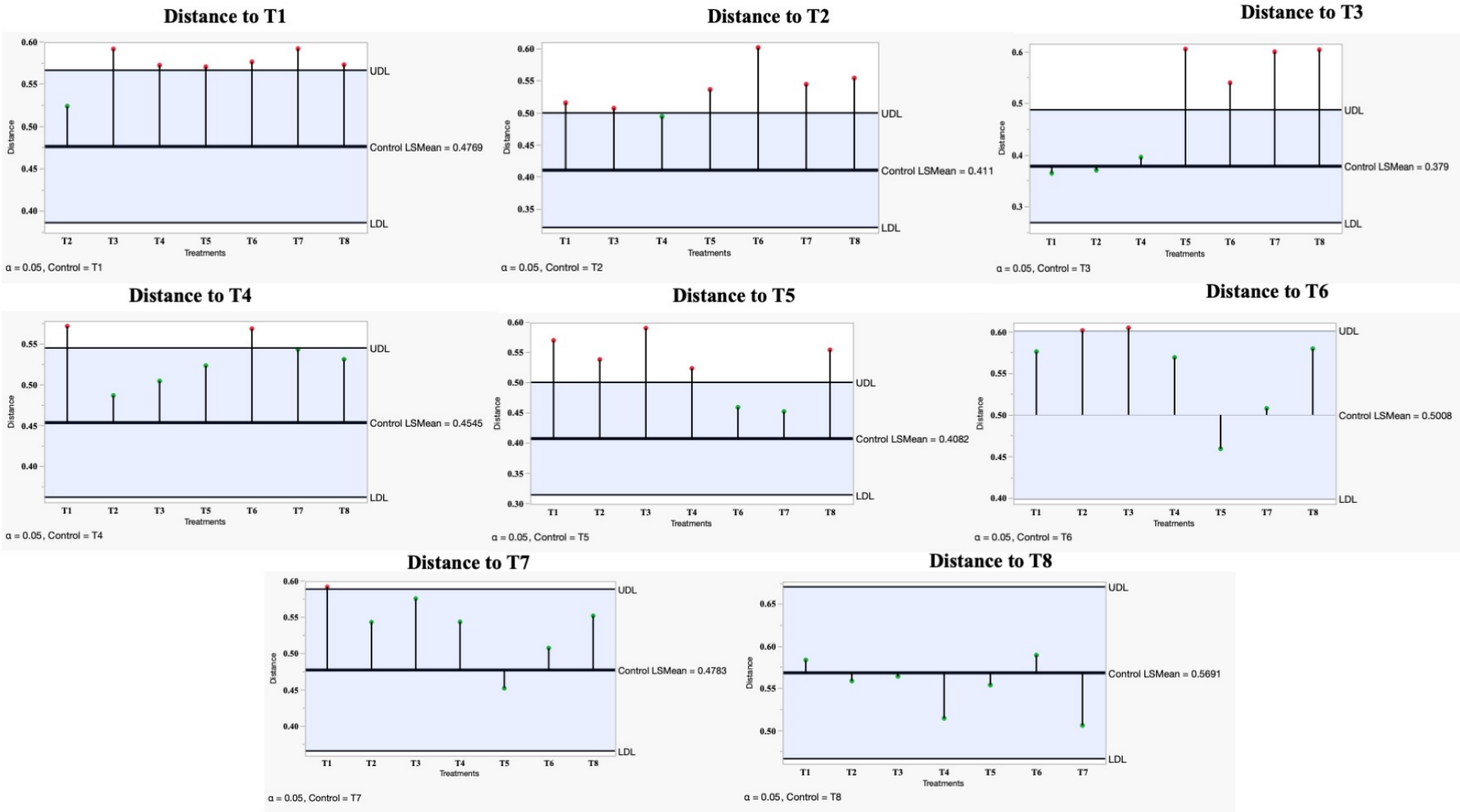

490

Figure 8.4 weighted UniFrac (quantitative beta diversity) showing the distance from one treatment to other treatments on day 20. Graphs having green needle head represents in significant distances. Red needle head represents significantly distance between the respective treatments ($P < 0.05$). UDL=Upper detection limit; LDL=Lower detection limit. T1, non-challenged treatment; T2, *Eimeria* spp. challenged group; T3, *Eimeria* spp. challenge and 2 x 10^5 CFU *S. aureus* day old challenge; T4, *Eimeria* spp. challenge and 2 x 10^5 CFU *S. aureus* day 18 challenge; T5, *Eimeria* spp. challenge and 2 x 10^8 CFU *S. aureus* day old challenge; T6, *Eimeria* spp. challenge and 2 x 10^8 CFU *S. aureus* day 18 challenge; T7, *Eimeria* spp. challenge and 2 x 10^5 CFU *S. aureus* day old and day 18 challenge; T8, *Eimeria* spp. challenge and 2 x 10^8 CFU *S. aureus* day old and day 18 challenge.

Weighted Unifrac Measurement (Quantitative Beta Diversity)– Day 20

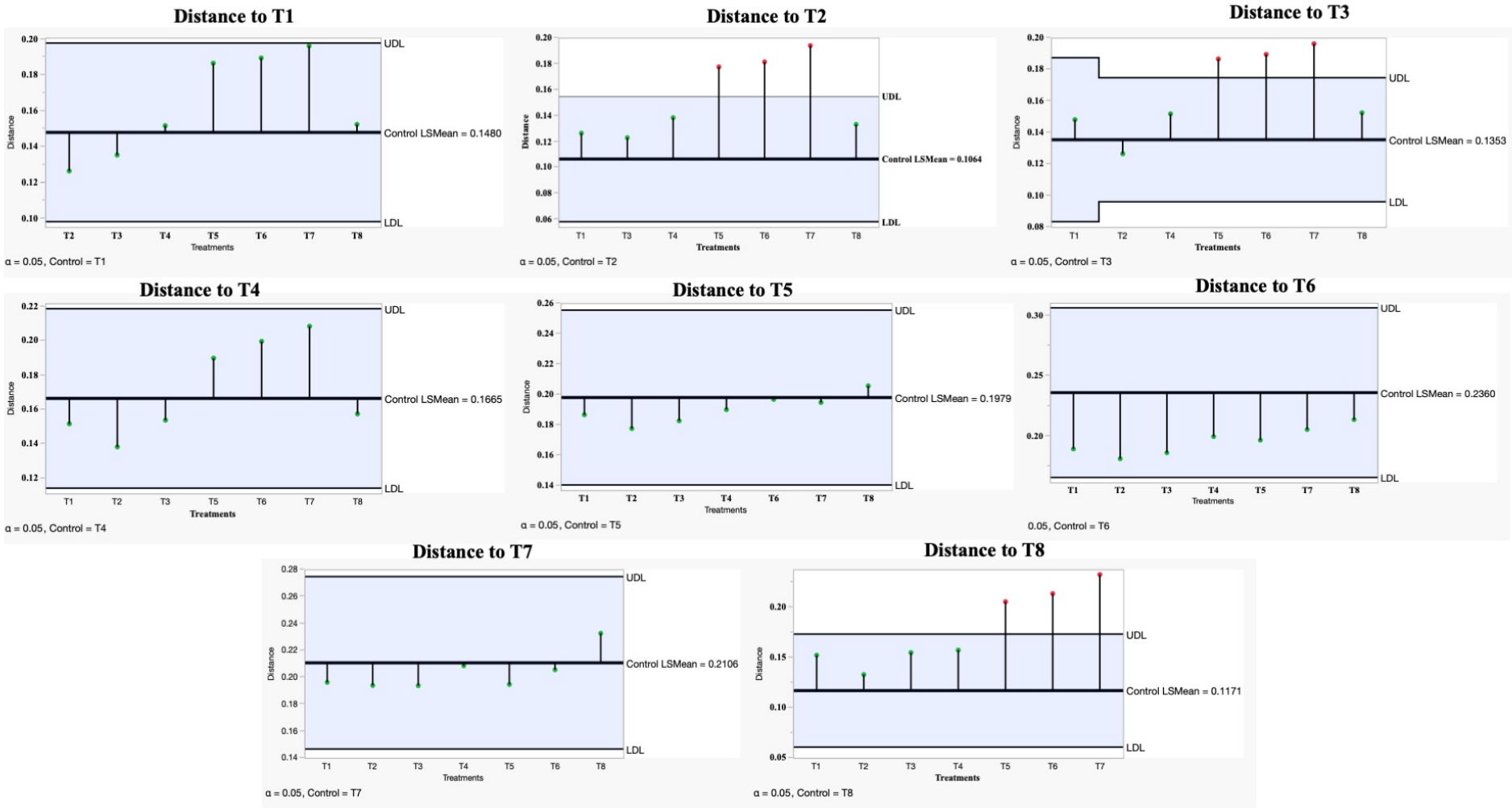

498

Figure 8.5 weighted Unifrac (quantitative beta diversity) showing the distance from one treatment to other treatments on day 26. Graphs having green needle head represents in significant distances. Red needle head represents significantly distance between the respective treatments ($P < 0.05$). UDL=Upper detection limit; LDL=Lower detection limit. T1, non-challenged treatment; T2, *Eimeria* spp. challenged group; T3, *Eimeria* spp. challenge and 2 x 10^5 CFU *S. aureus* day old challenge; T4, *Eimeria* spp. challenge and 2 x 10^5 CFU *S. aureus* day 18 challenge; T5, *Eimeria* spp. challenge and 2 x 10^8 CFU *S. aureus* day old challenge; T6, *Eimeria* spp. challenge and 2 x 10^8 CFU *S. aureus* day 18 challenge; T7, *Eimeria* spp. challenge and 2 x 10^5 CFU *S. aureus* day old and day 18 challenge; T8, *Eimeria* spp. challenge and 2 x 10^8 CFU *S. aureus* day old and day 18 challenge.

Weighted Unifrac Measurement (Quantitative Beta Diversity)– Day 26

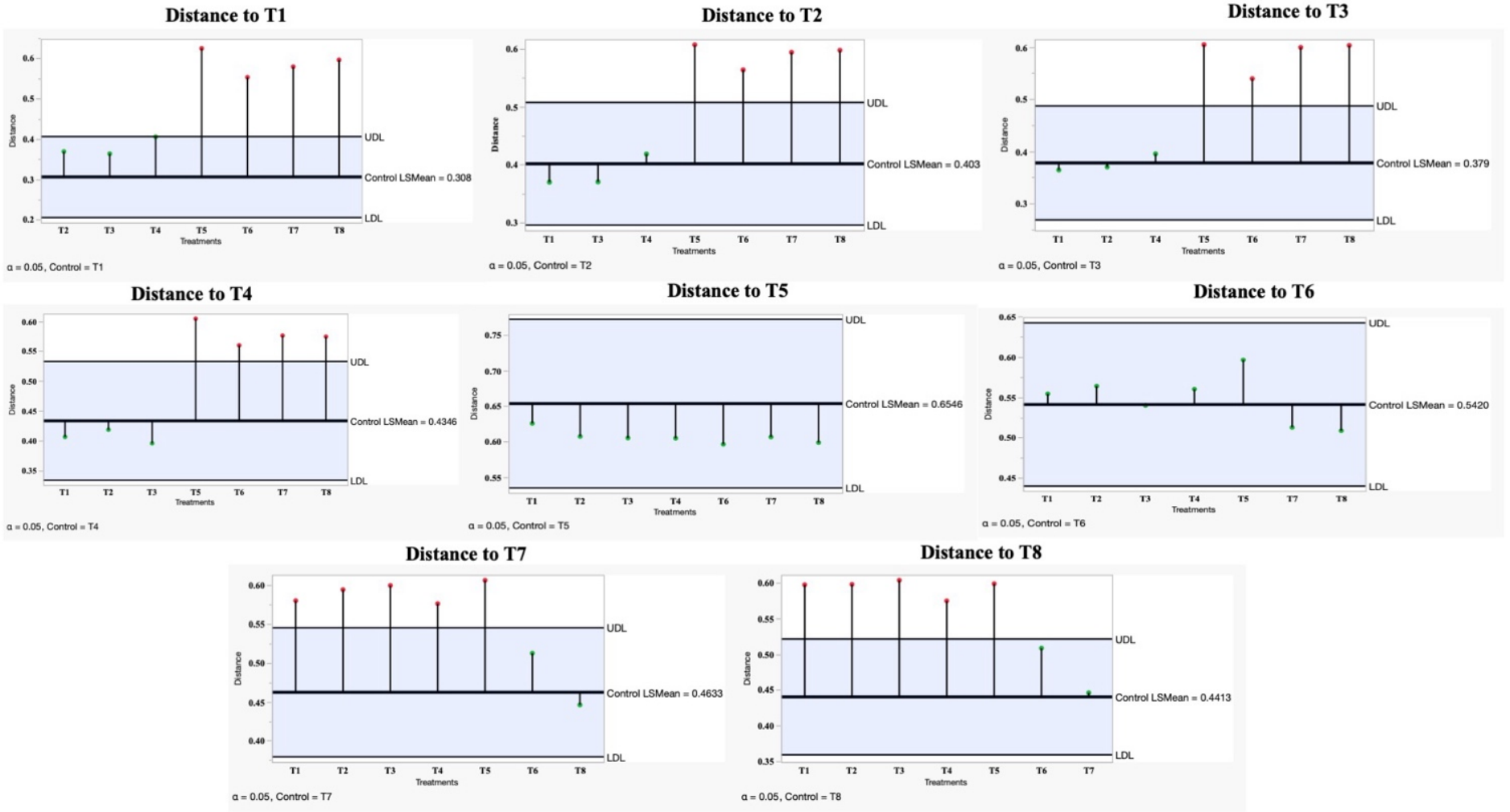

506

Figure 8.6 heat map representing the dominant phyla among the treatments on day 20 (A). Graph with Actinobacteria having significant differences are shown below ($P < 0.05$) (B). T1, non-challenged treatment; T2, *Eimeria* spp. challenged group; T3, *Eimeria* spp. challenge and 2 x 10^5 CFU *S. aureus* day old challenge; T4, *Eimeria* spp. challenge and 2 x 10^5 CFU *S. aureus* day 18 challenge; T5, *Eimeria* spp. challenge and 2 x 10^8 CFU *S. aureus* day old challenge; T6, *Eimeria* spp. challenge and 2 x 10^8 CFU *S. aureus* day 18 challenge; T7, *Eimeria* spp. challenge and 2 x 10^5 CFU *S. aureus* day old and day 18 challenge; T8, *Eimeria* spp. challenge and 2 x 10^8 CFU *S. aureus* day old and day 18 challenge. Letters not connected by same letter is significantly different ($P < 0.05$, N =5).

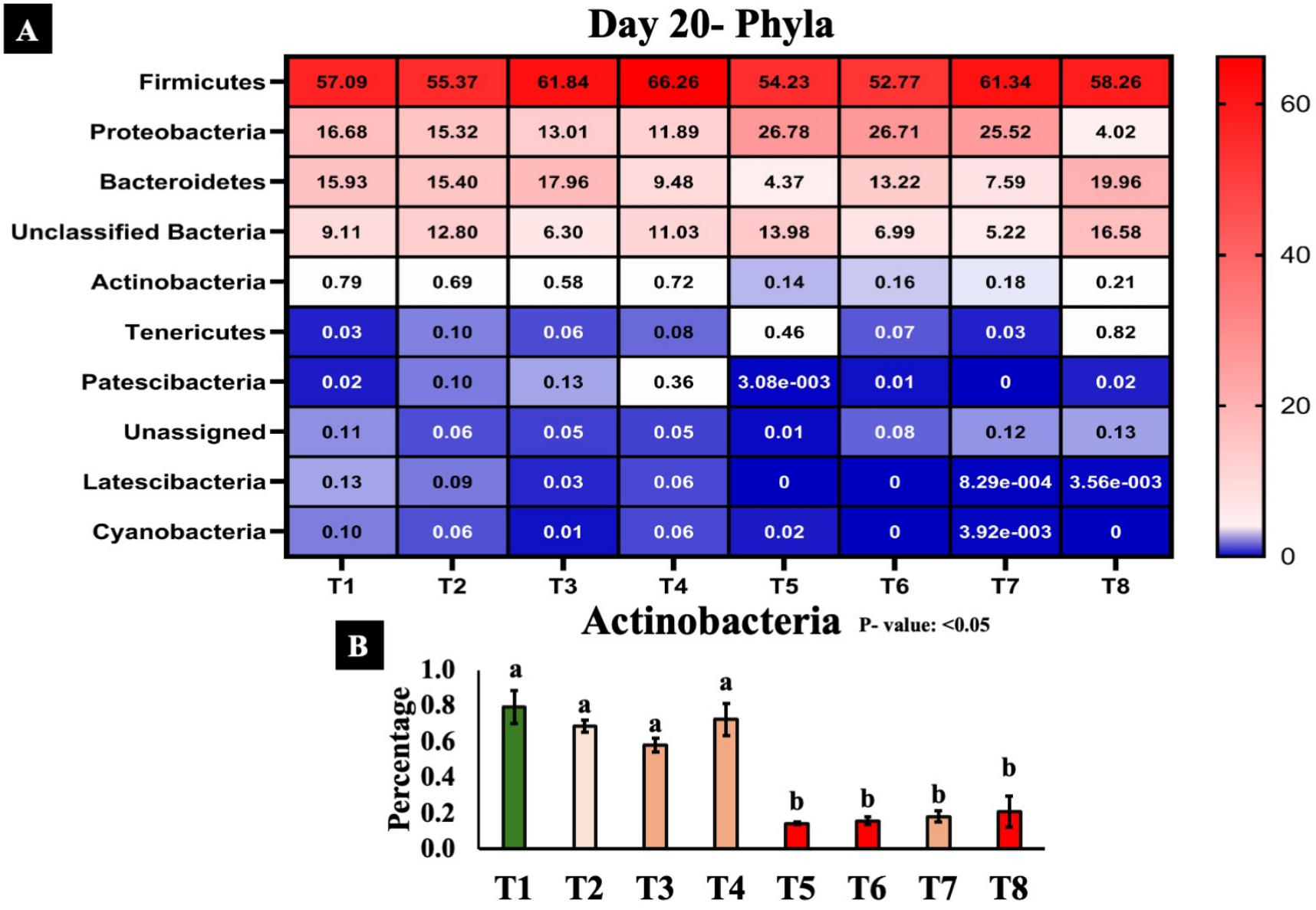
A
Day 20- Phyla
Firmicutes 57.09 55.37 61.84 66.26 54.23 52.77 61.34 58.26
Proteobacteria 16.68 15.32 13.01 11.89 26.78 26.71 25.52 4.02
Bacteroidetes 15.93 15.40 17.96 9.48 4.37 13.22 7.59 19.96
Unclassified Bacteria 9.11 12.80 6.30 11.03 13.98 6.99 5.22 16.58
Actinobacteria 0.79 0.69 0.58 0.72 0.14 0.16 0.18 0.21
Tenericutes 0.03 0.10 0.06 0.08 0.46 0.07 0.03 0.82
Patescibacteria 0.02 0.10 0.13 0.36 3.08e-003 0.01 0 0.02
Unassigned 0.11 0.06 0.05 0.05 0.01 0.08 0.12 0.13
Latescibacteria 0.13 0.09 0.03 0.06 0 0 8.29e-004 3.56e-003
Cyanobacteria 0.10 0.06 0.01 0.06 0.02 0 3.92e-003 0
T1 T2 T3 T4 T5 T6 T7 T8
60
40
20
0
B
Actinobacteria P- value: <0.05
Percentage
1.0
0.8
0.6
0.4
0.2
0.0
a a a a b b b b
T1 T2 T3 T4 T5 T6 T7 T8

514

Figure 8.7 heat map representing the dominant families among the treatments on day 20 (A). Graph with *Leuconostocaceae*, *Microbacteraceae* having significant differences are shown below ($P < 0.05$) (B and C). T1, non-challenged treatment; T2, *Eimeria* spp. challenged group; T3, *Eimeria* spp. challenge and 2 x 10^5 CFU *S. aureus* day old challenge; T4, *Eimeria* spp. challenge and 2 x 10^5 CFU *S. aureus* day 18 challenge; T5, *Eimeria* spp. challenge and 2 x 10^8 CFU *S. aureus* day old challenge; T6, *Eimeria* spp. challenge and 2 x 10^8 CFU *S. aureus* day 18 challenge; T7, *Eimeria* spp. challenge and 2 x 10^5 CFU *S. aureus* day old and day 18 challenge; T8, *Eimeria* spp. challenge and 2 x 10^8 CFU *S. aureus* day old and day 18 challenge. Letters not connected by same letter is significantly different ($P < 0.05$, N =5).

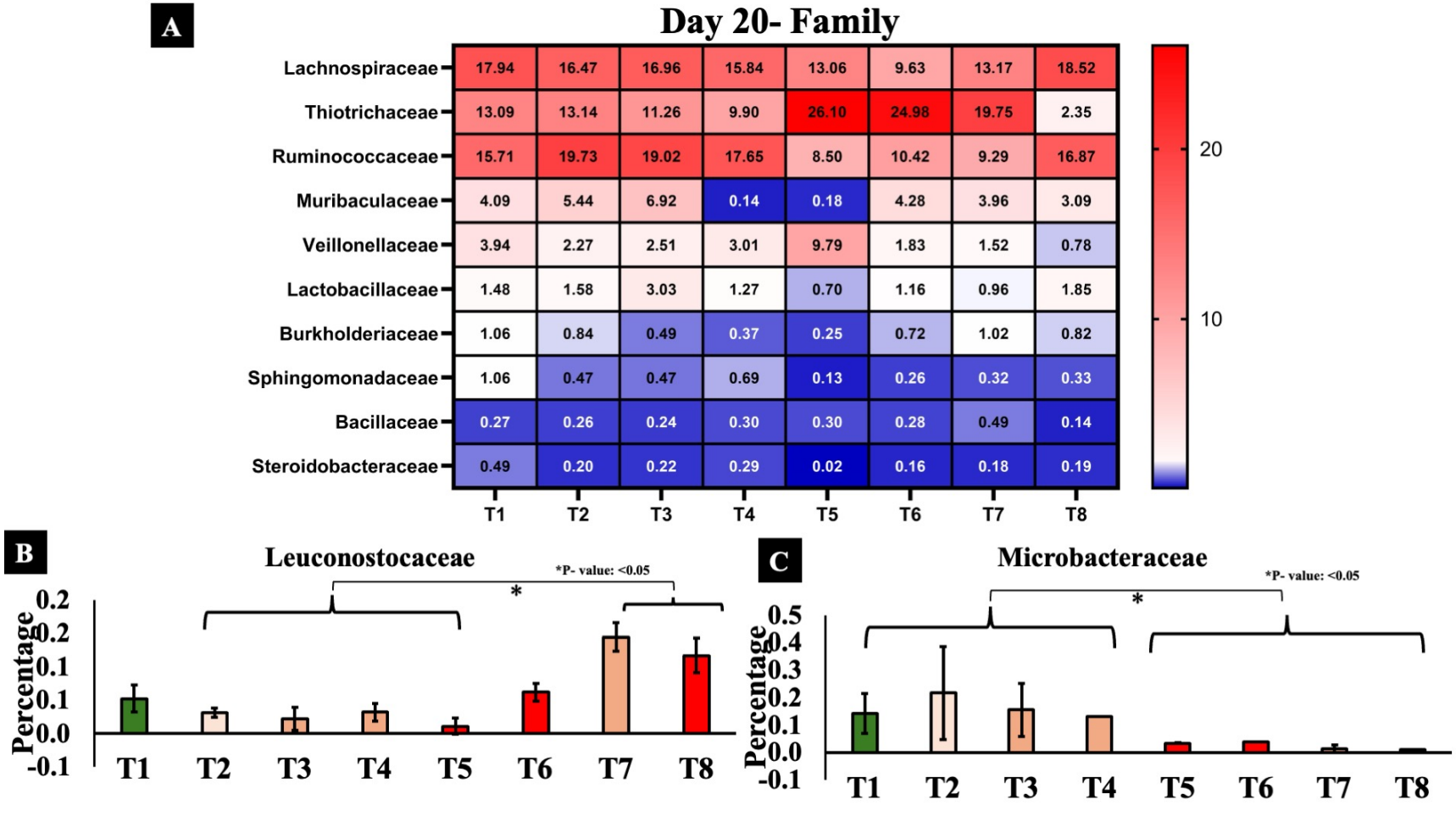
A
Day 20- Family
Lachnospiraceae 17.94 16.47 16.96 15.84 13.06 9.63 13.17 18.52
Thiotrichaceae 13.09 13.14 11.26 9.90 26.10 24.98 19.75 2.35
Ruminococcaceae 15.71 19.73 19.02 17.65 8.50 10.42 9.29 16.87
Muribaculaceae 4.09 5.44 6.92 0.14 0.18 4.28 3.96 3.09
Veillonellaceae 3.94 2.27 2.51 3.01 9.79 1.83 1.52 0.78
Lactobacillaceae 1.48 1.58 3.03 1.27 0.70 1.16 0.96 1.85
Burkholderiaceae 1.06 0.84 0.49 0.37 0.25 0.72 1.02 0.82
Sphingomonadaceae 1.06 0.47 0.47 0.69 0.13 0.26 0.32 0.33
Bacillaceae 0.27 0.26 0.24 0.30 0.30 0.28 0.49 0.14
Steroidobacteraceae 0.49 0.20 0.22 0.29 0.02 0.16 0.18 0.19
T1 T2 T3 T4 T5 T6 T7 T8
20
10
B
Leuconostocaceae
*P- value: <0.05
*
Percentage
0.2 0.2 0.1 0.1 0.0 -0.1
T1 T2 T3 T4 T5 T6 T7 T8
C
Microbacteraceae
*P- value: <0.05
*
Percentage
0.5 0.4 0.3 0.2 0.1 0.0 -0.1
T1 T2 T3 T4 T5 T6 T7 T8

522

Figure 8.8 heat map representing the dominant families among the treatments on day 26 (A). Graph with Bacteroidetes (B), Firmicutes (C), and Firmicutes to Bacteroidetes ratio (D) having significant differences are shown below ($P < 0.05$). T1, non-challenged treatment; T2, *Eimeria* spp. challenged group; T3, *Eimeria* spp. challenge and 2 x 10^5 CFU *S. aureus* day old challenge; T4, *Eimeria* spp. challenge and 2 x 10^5 CFU *S. aureus* day 18 challenge; T5, *Eimeria* spp. challenge and 2 x 10^8 CFU *S. aureus* day old challenge; T6, *Eimeria* spp. challenge and 2 x 10^8 CFU *S. aureus* day 18 challenge; T7, *Eimeria* spp. challenge and 2 x 10^5 CFU *S. aureus* day old and day 18 challenge; T8, *Eimeria* spp. challenge and 2 x 10^8 CFU *S. aureus* day old and day 18 challenge. Letters not connected by same letter is significantly different ($P < 0.05$, N =5).

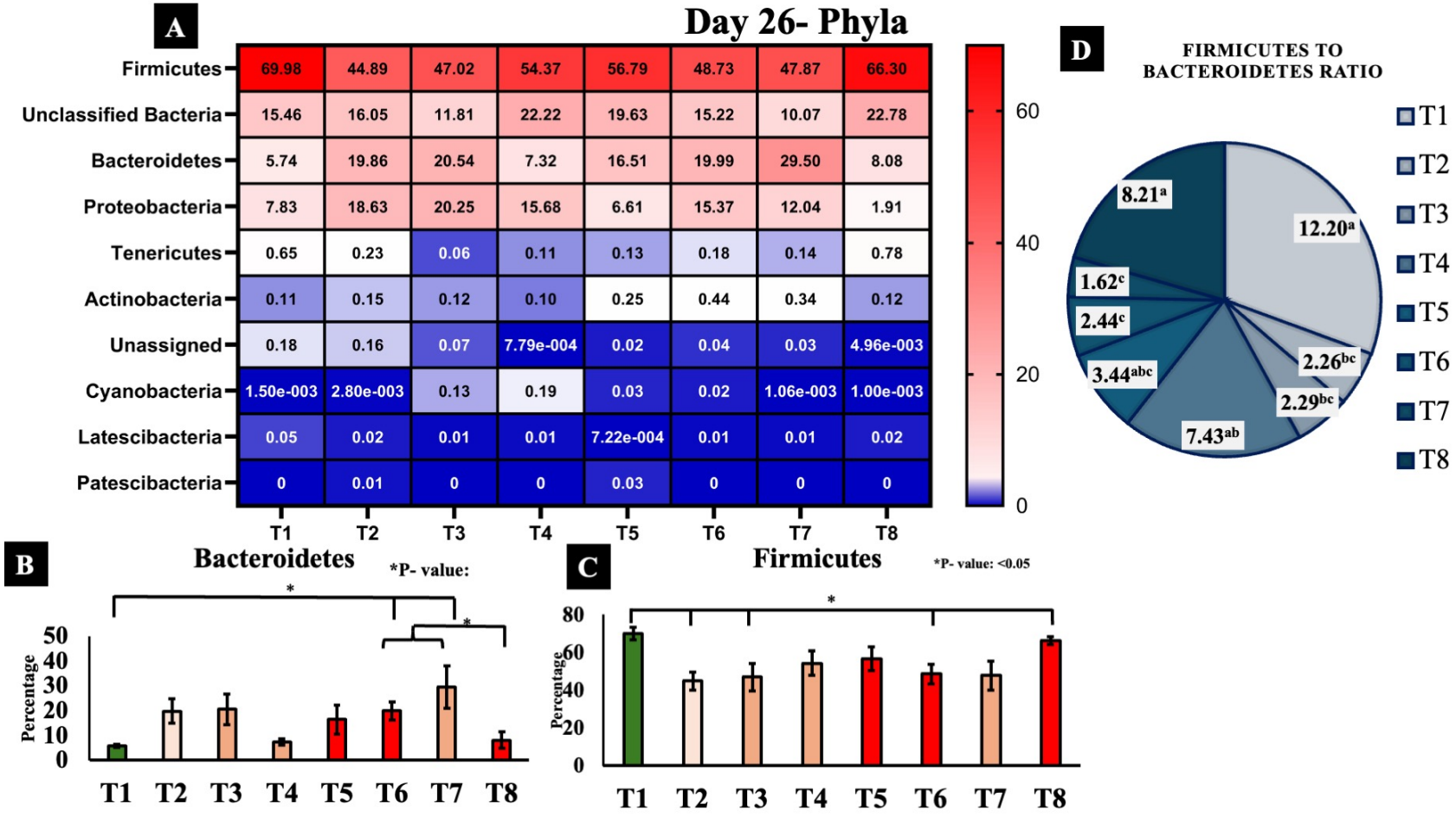
A
Day 26- Phyla
Firmicutes 69.98 44.89 47.02 54.37 56.79 48.73 47.87 66.30
Unclassified Bacteria 15.46 16.05 11.81 22.22 19.63 15.22 10.07 22.78
Bacteroidetes 5.74 19.86 20.54 7.32 16.51 19.99 29.50 8.08
Proteobacteria 7.83 18.63 20.25 15.68 6.61 15.37 12.04 1.91
Tenericutes 0.65 0.23 0.06 0.11 0.13 0.18 0.14 0.78
Actinobacteria 0.11 0.15 0.12 0.10 0.25 0.44 0.34 0.12
Unassigned 0.18 0.16 0.07 7.79e-004 0.02 0.04 0.03 4.96e-003
Cyanobacteria 1.50e-003 2.80e-003 0.13 0.19 0.03 0.02 1.06e-003 1.00e-003
Latescibacteria 0.05 0.02 0.01 0.01 7.22e-004 0.01 0.01 0.02
Patescibacteria 0 0.01 0 0 0.03 0 0 0
T1 T2 T3 T4 T5 T6 T7 T8
60
40
20
0
D
FIRMICUTES TO BACTEROIDETES RATIO
8.21a
12.20a
1.62c
2.44c
2.26bc
3.44abc
2.29bc
7.43ab
T1
T2
T3
T4
T5
T6
T7
T8
B
Bacteroidetes
*P- value:
Percentage
50
40
30
20
10
0
T1 T2 T3 T4 T5 T6 T7 T8
C
Firmicutes
*P- value: <0.05
Percentage
80
60
40
20
0
T1 T2 T3 T4 T5 T6 T7 T8

531

Figure 8.9 heat map representing the dominant family in the microbiome among the treatments on day 26. T1, non-challenged treatment; T2, *Eimeria* spp. challenged group; T3, *Eimeria* spp. challenge and 2 x 10^5 CFU *S. aureus* day old challenge; T4, *Eimeria* spp. challenge and 2 x 10^5 CFU *S. aureus* day 18 challenge; T5, *Eimeria* spp. challenge and 2 x 10^8 CFU *S. aureus* day old challenge; T6, *Eimeria* spp. challenge and 2 x 10^8 CFU *S. aureus* day 18 challenge; T7, *Eimeria* spp. challenge and 2 x 10^5 CFU *S. aureus* day old and day 18 challenge; T8, *Eimeria* spp. challenge and 2 x 10^8 CFU *S. aureus* day old and day 18 challenge. Letters not connected by same letter is significantly different ($P < 0.05$, N =5).

Day 26- Family

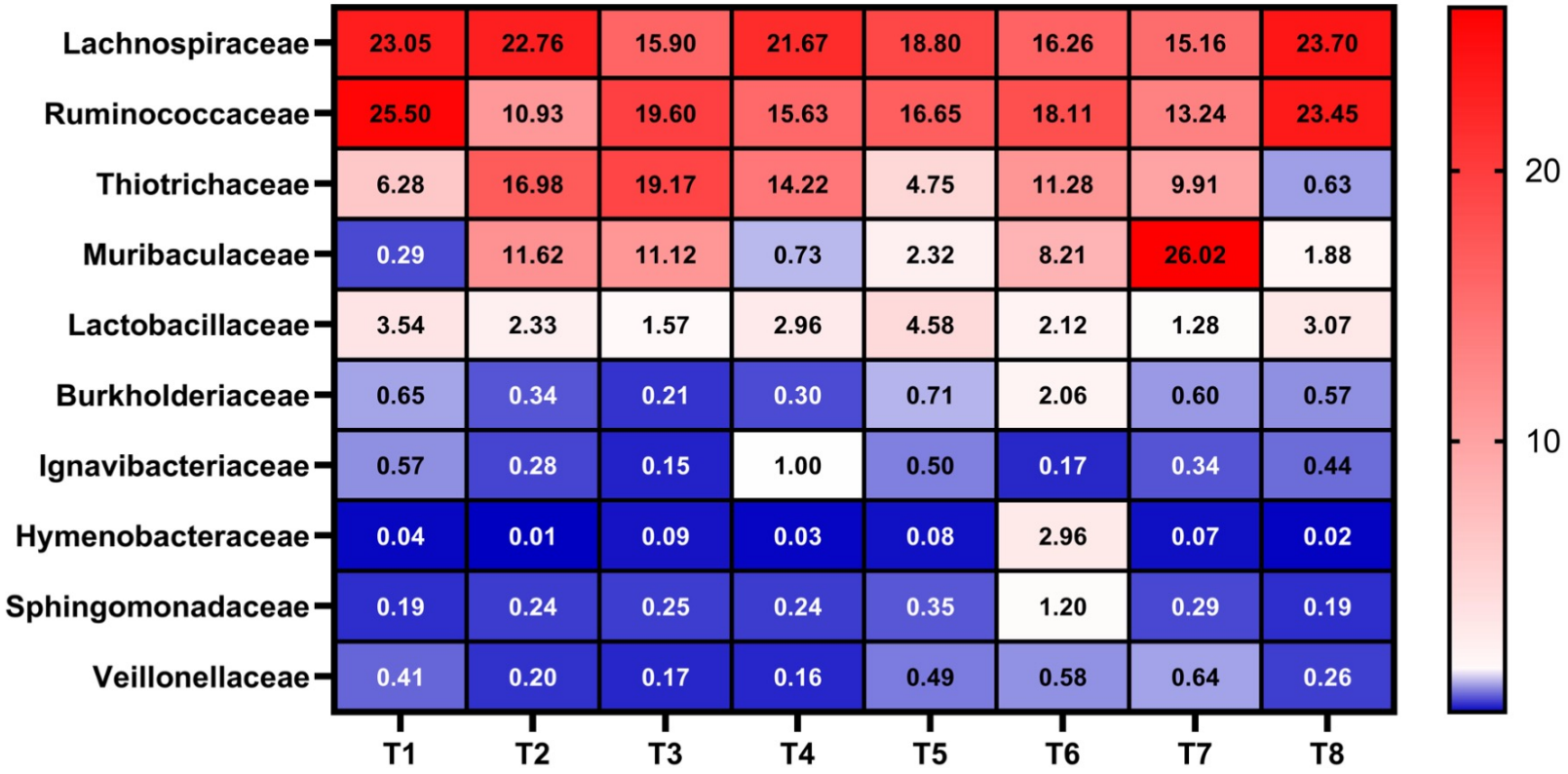

538

Figure 8.10 KEGG pathway- level functional profiles obtained from representative sequences generated from QIIME2 for T1 vs T5 and T6 on day 20. T1, non-challenged treatment; T5, *Eimeria* spp. challenge and 2 x 10^8 CFU *S. aureus* day old challenge; T6, *Eimeria* spp. challenge and 2 x 10^8 CFU *S. aureus* day 18 challenge.

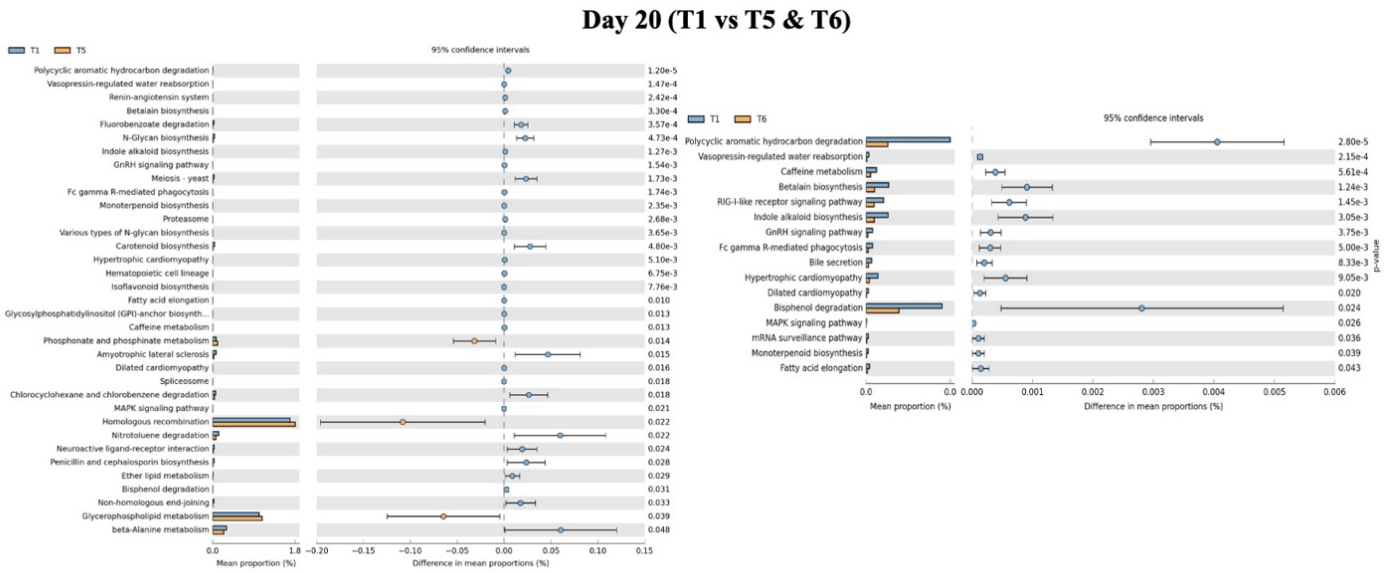

Figure 8.11 KEGG pathway- level functional profiles obtained from representative sequences generated from QIIME2 for T1 vs T7 and T8 on day 20. T1, non-challenged treatment; T7, *Eimeria* spp. challenge and 2 x 10^5 CFU *S. aureus* day old and day 18 challenge; T8, *Eimeria* spp. challenge and 2 x 10^8 CFU *S. aureus* day old and day 18 challenge.

Day 20 (T1 vs T7 & T8)

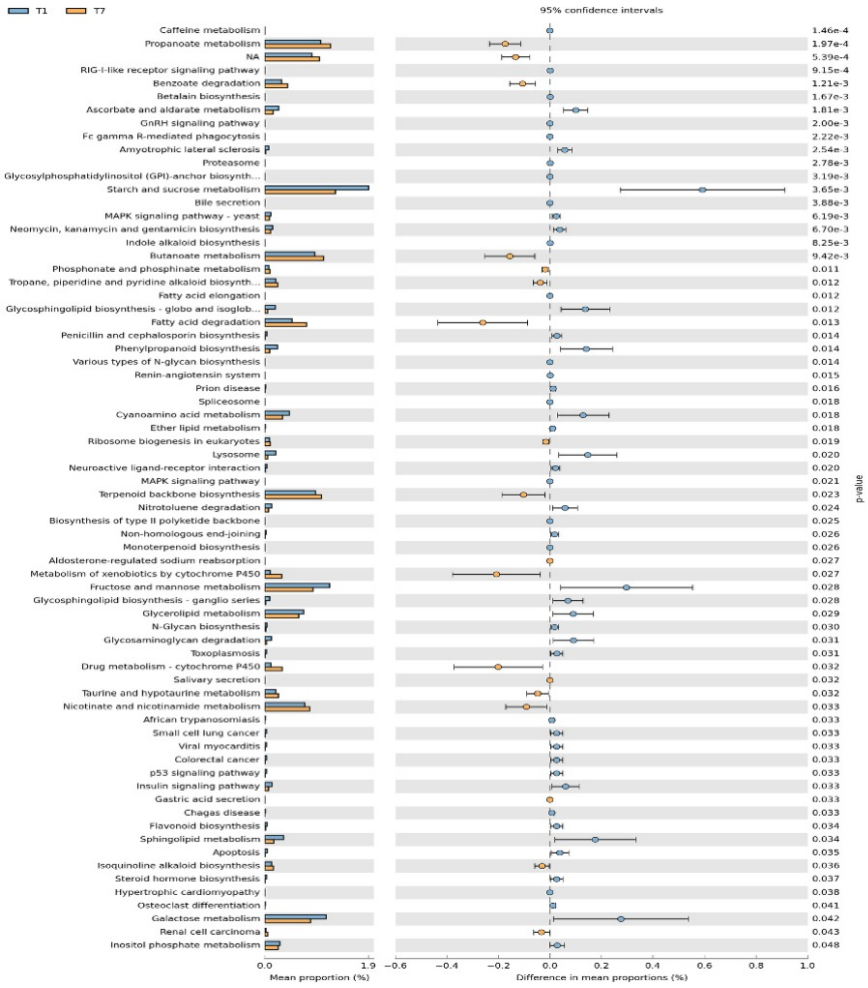

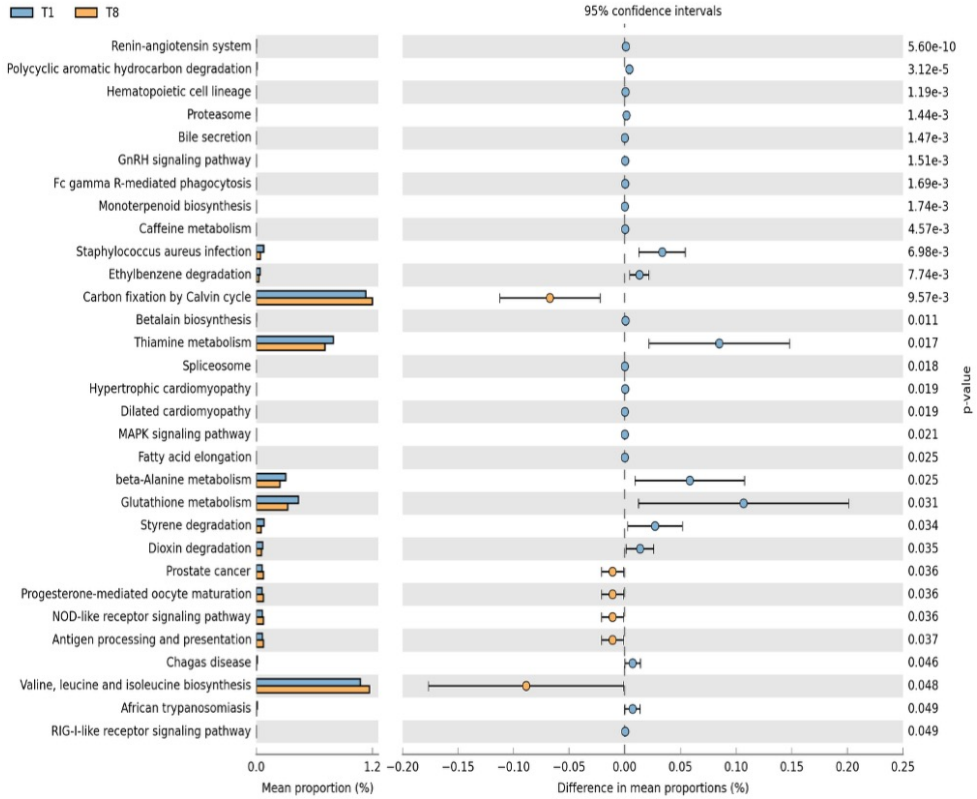

Figure 8.12 KEGG pathway- level functional profiles obtained from representative sequences generated from QIIME2 for T2 vs T5 and T6 on day 20. T2, *Eimeria* spp. challenged group; T5, *Eimeria* spp. challenge and 2 x 10^8 CFU *S. aureus* day old challenge; T6, *Eimeria* spp. challenge and 2 x 10^8 CFU *S. aureus* day 18 challenge.

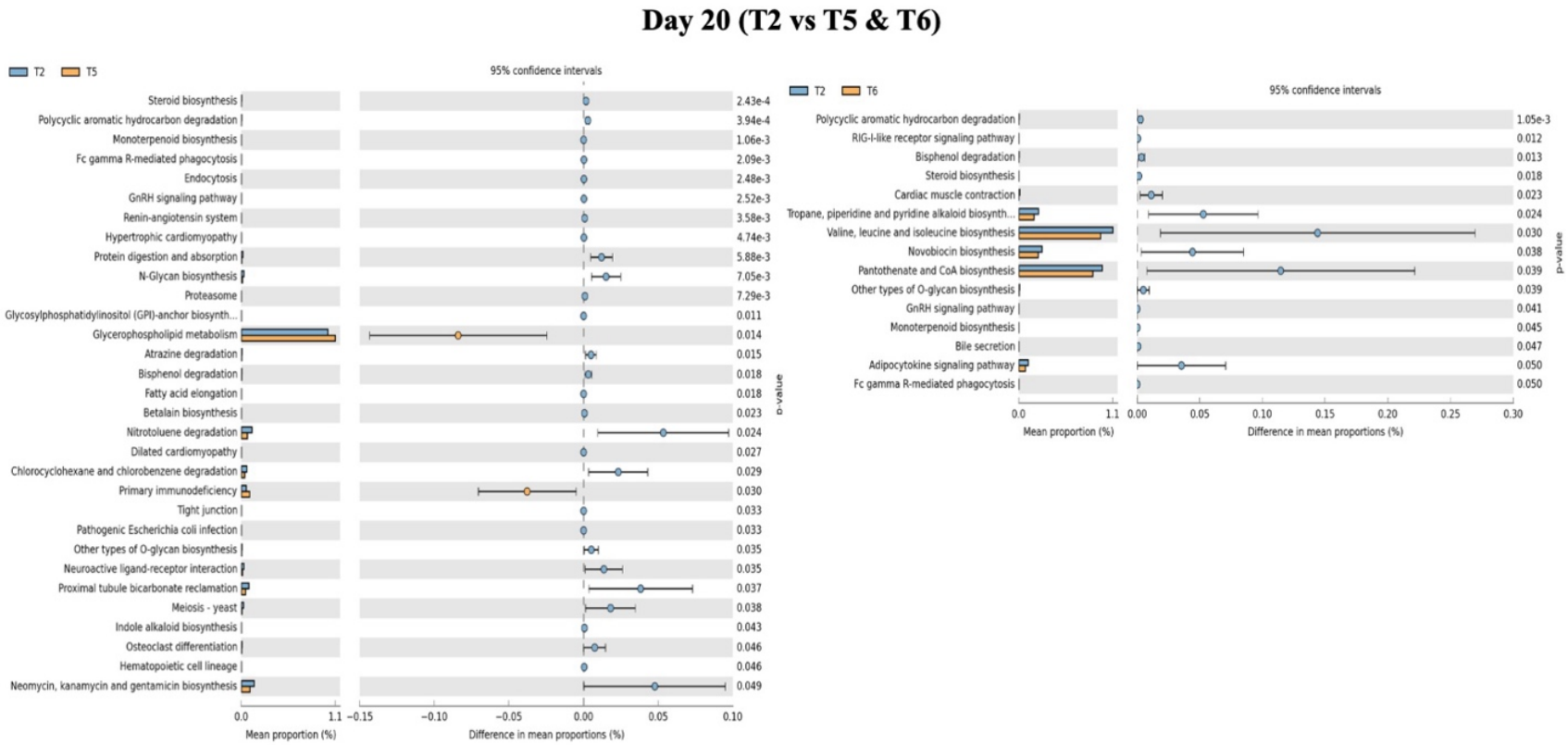

Figure 8.13 KEGG pathway- level functional profiles obtained from representative sequences generated from QIIME2 for T2 vs T7 and T8 on day 20. T2, *Eimeria* spp. challenged group; T7, *Eimeria* spp. challenge and 2 x 10^5 CFU *S. aureus* day old and day 18 challenge; T8, *Eimeria* spp. challenge and 2 x 10^8 CFU *S. aureus* day old and day 18 challenge.

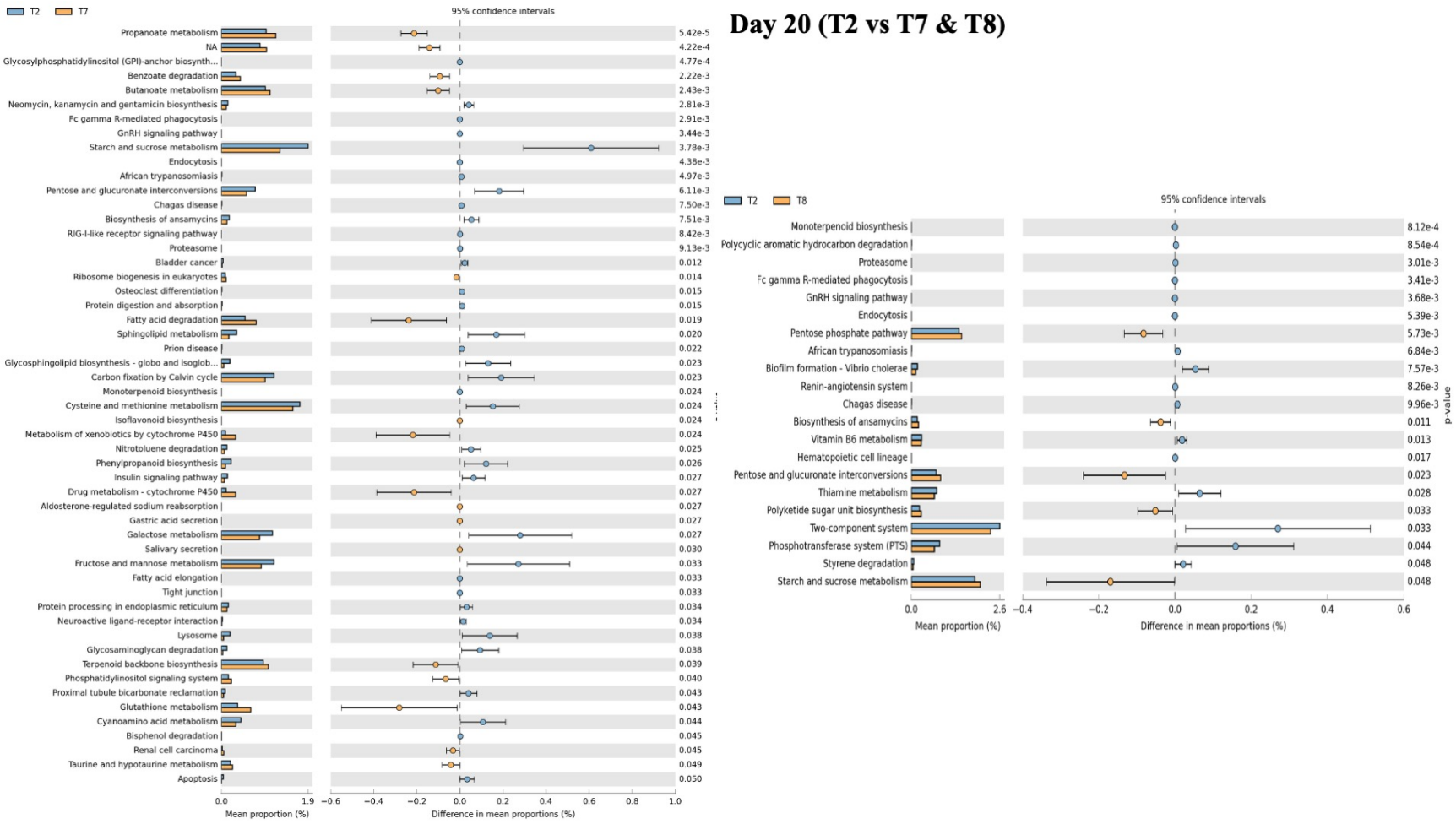

Figure 8.14 KEGG pathway- level functional profiles obtained from representative sequences generated from QIIME2 for T1 vs T5 and T6 on day 26. T1, non-challenged treatment; T5, *Eimeria* spp. challenge and 2 x 10^8 CFU *S. aureus* day old challenge; T6, *Eimeria* spp. challenge and 2 x 10^8 CFU *S. aureus* day 18 challenge.

Day 26 (T1 vs T5 & T6)

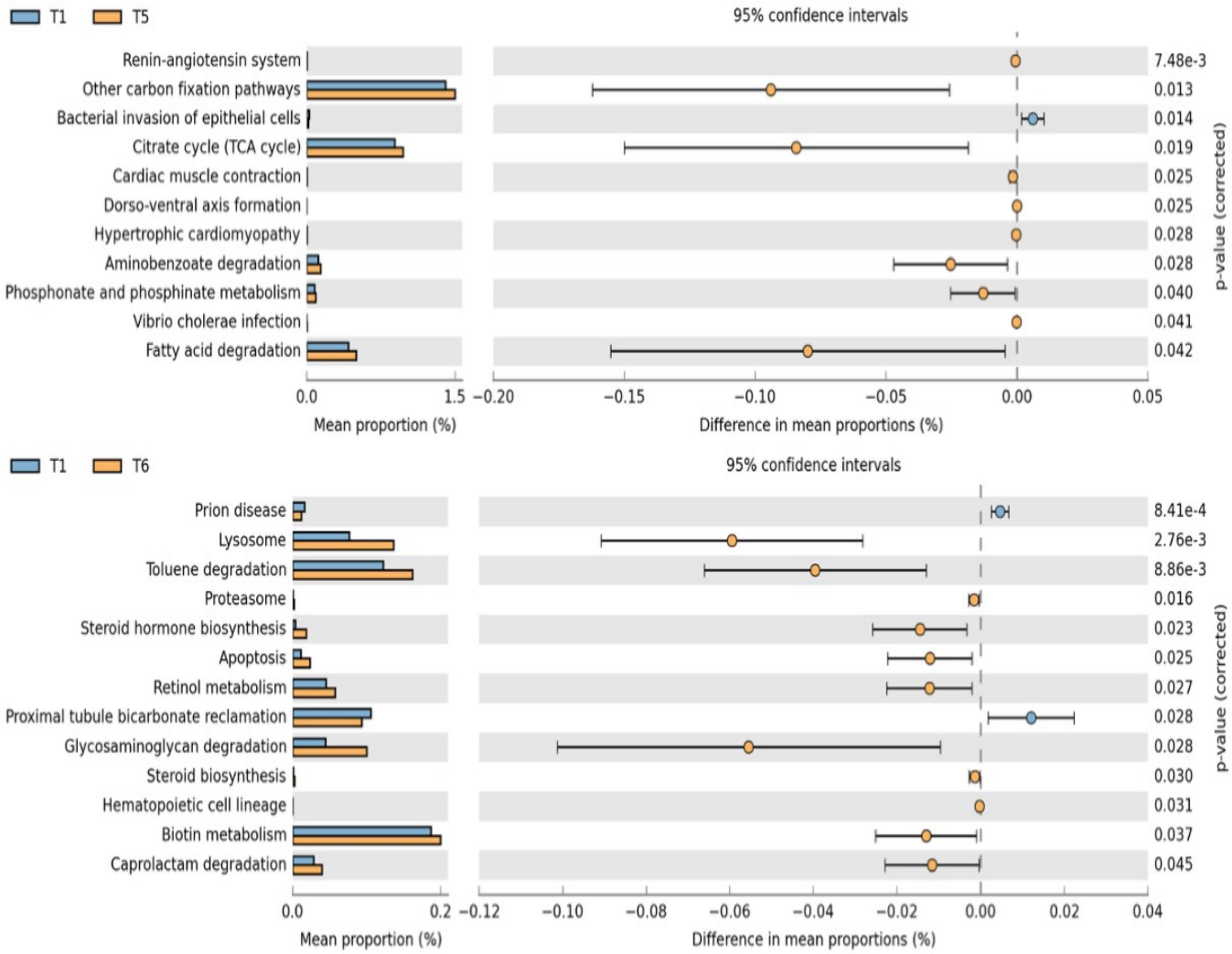

559

Figure 8.15 KEGG pathway- level functional profiles obtained from representative sequences generated from QIIME2 for T1 vs T7 and T8 on day 26. T1, non-challenged treatment; T7, *Eimeria* spp. challenge and 2 x 10^5 CFU *S. aureus* day old and day 18 challenge; T8, *Eimeria* spp. challenge and 2 x 10^8 CFU *S. aureus* day old and day 18 challenge.

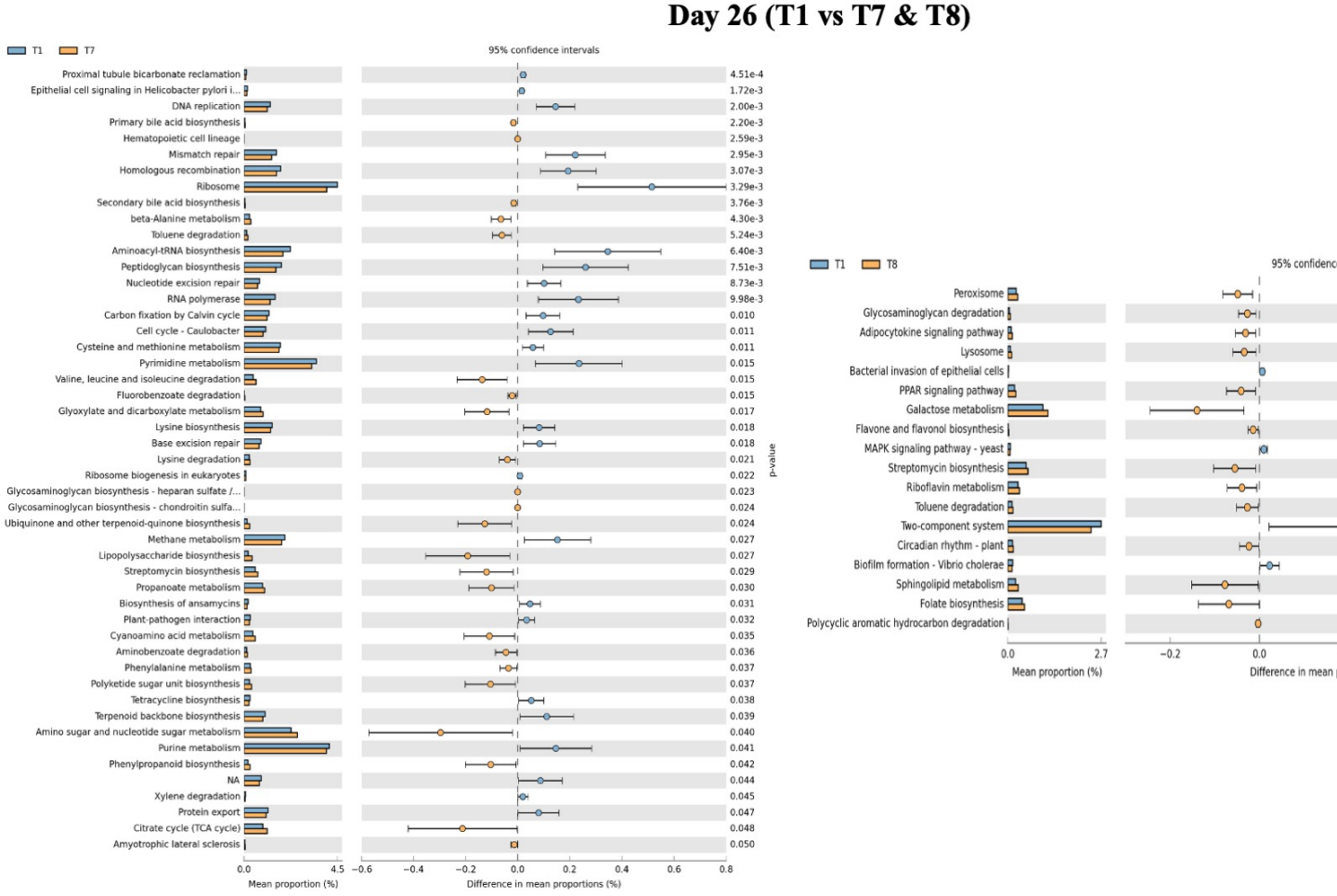

CHAPTER 9

EFFECT OF ORAL AND INTRAPERITONEAL *STAPHYLOCOCCUS AUREUS* ON INDUCING BACTERIAL CHONDRONECROSIS AND OSTEOMYELITIS, BROILERS' PERFORMANCE, BONE HEALTH AND MICROBIOME OF MODERN-D BROILER CHICKENS [1]

[1] Venkata Sesha Reddy Choppa, Jihwan Lee, Daniel Junpyo Lee, Hamid Reza Rafieian Naeini, Hanseo Ko, Doyun Goo, Hemanth Reddy Katha, Venkata Prathap Reddy K, Younghoon Kim, Hector M. Cervantes, Charles Hofacre, Chongxiao Chen, and Woo Kyun Kim.

To be submitted to Poultry Science.

ABSTRACT

Bacterial Chondronecrosis and Osteomyelitis (BCO) in broiler chickens has become a leading cause of lameness besides incurring economic losses to the poultry industry. The lacunae exist in understanding its pathogenesis through route of infection and exposure load. This study aims to understand the effects of various routes (oral or intraperitoneal) and exposure (single or consecutive) of *Staphylococcus aureus* on inducing BCO, bone health, and microbiome (gut and bone). Birds raised for 40 d were reallocated to five treatments in a different floor pen house. T1 was non-challenged/naturally infected, T2 was a single oral challenge (10^9 CFU on d 42), T3 was orally challenged for 3 d (d 42, 43, 44). Similarly to T2, T4 was intraperitoneally challenged with 10^7 CFU on d 42 and T5 for 3 days (d 42, 43, 44). Bone health was assessed using gait and BCO scoring, mineral apposition rate, micro-CT, DEXA. Additionally, serum lipopolysaccharides, sclerostin levels, and microbiome analyses (16s rRNA sequencing and predicted functional pathways) for bone and ceca to unveil changes with dosing frequency and route of infection. Findings revealed, T2 had a significantly higher body weight gain (938 g) compared to T4 and T5 (421.38 and 382.08 g). Interestingly, oral and intraperitoneal challenge (single and repeated) (T3-T5) exhibited severe scores with a pronounced average gait score of 4.38 in T5. Furthermore, high colonization of *S. aureus* in bone (3.98 log CFU/g), reduced bone parameters and increased porosity (DEXA and Micro-CT) in T4 and T5 suggestive of bone osteopathology. Moreover, T4 and T5 showed ceca and bone dysbiosis reflected as decreased microbial diversity with increased relative abundance of Pseudomonadota and Actinomycetota. Additionally, functional metagenome analysis revealed significantly higher MAPK signaling, oxidative phosphorylation, apoptotic pathways besides suppressed Wnt/Notch signaling which are suggestive of severe BCO pathogenesis. Finally, route and consecutive challenge of *S. aureus* modulate BCO induction and

bone homeostasis advocate intervention strategies basing on above findings emphasize stabilization of microbiome to alleviate opportunistic pathogen colonization during persistent challenge conditions.

Keywords: *Staphylococcus aureus,* lameness, microbiome, chondronecrosis, broilers

INTRODUCTION

Commercial poultry production has grown significantly with improvements in genetics, nutrition, and management resulting in faster growth rates with lower feed conversion. However, fast growing broilers have been associated with poor mineralization of chondrocytes often near the coxofemoral (typically) joint resulting in microfractures that aid opportunistic bacteria to colonize these microfractures in bone hematogenously (Choppa & Kim, 2023a; R. F. Wideman, 2016; R. Wideman & Prisby, 2013). Articular cartilage is primarily made of chondrocytes and extracellular matrix (ECM). Chondrocytes synthesize proteoglycans (heparan sulfate, keratan sulfate, chondroitin sulfate), hyaluronic acid, fibrous proteins, glycosaminoglycan, and type II Collagen which are integral part of the ECM. Integrin mediated signaling plays a significant role in chondrocytes' mineralization where integrins mediate cell adhesion to its surroundings(Yu et al., 2020). Furthermore, chondrogenesis depends on Wnt signaling pathway, nitric oxide signal. Type X collagen predominates before mineralization event and this is accompanied by decreased collagen II (Gao et al., 2014). This occurs because of interactions between annexin V and collagen (type II/X) which increases extracellular calcium ions influx into the growth plate through alkaline phosphatase activity. This represents degree of mineralization, which is the final event of endochondral bone formation replaces cartilage by bone (Gao et al., 2014).

Even though mineralization occurs through this pathway in both mammals and avian species, there are significant differences with respect to how the ossification of cartilage occurs. In mammals, longitudinally arranged chondrocytes mature from the zone of proliferation to hypertrophy with progressive calcification of longitudinal septa, blood vessels invades the spaces in the cartilage and osteoblasts deposit bone along the longitudinal septa (Roach & Shearer, 1989). In the chicken embryo, bone is formed within the space preoccupied by cartilage. Due to absence of vertical

columns, bone is deposited onto the cartilage matrix with viable chondrocytes which means that the inner perimeter of the cartilage lacunae was deposited with bone (Intrachondral bone) (Roach & Shearer, 1989).

Formation of microfractures is followed by bacterial colonization which will lead to suppurative inflammation at the site of microfractures which leads to necrosis of the femoral head which is often termed as bacterial chondronecrosis and osteomyelitis (BCO) of femoral head (Choppa & Kim, 2023a; R. F. Wideman, 2016). Entry of bacteria occurs in several routes like transmission from breeder birds, eggshell contamination, hatchery, and farm environment. These bacteria enter the bird through the integumentary, respiratory or gastrointestinal route, they cause septicemia in immunocompromised broilers where opportunistic pathogens cause the lysis of epiphyses of femur and/or tibia which is often termed as epiphyseolyis (McNamee & Smyth, 2000; Rojas-Núñez et al., 2020). The immunosuppressed states in broilers associated with chicken anemia virus, infectious bursal disease, Marek's disease virus or environmental stressors which allows rapid proliferation of bacteria (McNamee et al., 1999).

Multiple opportunistic pathogens have been isolated from BCO lesions with *Staphylococcus* spp., *Escherichia coli*, and *Enterococcus cecorum* are the commonly isolated bacteria (Tompkins et al., 2022). After invasion of bacteria, they undergo bacterial dependent pathways in causing lysis. Studies involving *Staphylococcus aureus* in inducing BCO when challenged by the gastrointestinal route and systemic routes are not available. Uncovering the current concern will help in establishing the experimental model for the effects of this pathogen to induce BCO through gastrointestinal and intraperitoneal routes. Furthermore, this would provide insights for therapeutic applications based on the effects of the pathogen on the broilers' bone health.

MATERIALS AND METHODS

Experimental design

The study involved five treatments and 4 replicates in each treatment with 15 birds each with a total of 300 Cobb 500 male birds. Birds were kept in 20 m^2 floor pen with saw dust as litter material. Birds were fed with basal diets (starter, grower and finisher diets) for all the treatments besides adlibitum water supply. The birds were selected based on gait scores ranging between 1 and 2 on d 40. Treatment assignment and the study started from day 40. *Staphylococcus aureus* used in this study was prepared according to protocol followed in our earlier study (Choppa, Naeini, et al., 2025). Treatment 1 (T1) was non-challenged, Treatment 2 (T2) was challenged with *Staphylococcus aureus* at 10^9 CFU per bird orally on d 42, Treatment 3 (T3) was challenged with *Staphylococcus aureus* at 10^9 CFU per bird orally on d 42, 43, and 44. Similarly, Treatment 4 (T4) was challenged with *Staphylococcus aureus* at 10^7 CFU per bird intraperitoneally on d 42 and Treatment 5 (T5) was challenged with *Staphylococcus aureus* at 10^7 CFU per bird intraperitoneally on d 42, 43, and 44 respectively. The study was conducted at Poultry Research Center, The University of Georgia following approval from Institutional Animal Care and Use Committee (A2021 12-012).

Broiler performance, sample collection, and bone health parameters

Initial body weight and feed weights were recorded on d 40 (before the start of the experiment) followed by d 49 and d 56 along with feed intake on respective d. Samples like femur bones for micro computed tomography, bone marrow for gene expression and plasma for ELISA were collected on d 49 and 56. Bone dynamic histomorphometry (calcein labeling) measurement was conducted using femur bone collected on d 56. Furthermore, on d 49 and 56, gait (Kestin et al.,

1992) and BCO (R. F. Wideman, 2016) scoring was assessed and recorded based on a previous study.

Dual-energy X-ray absorptiometry

Dual-energy X-ray absorptiometry (DEXA, GE healthcare, Chicago, IL) and lunar prodigy (GE healthcare, encore software version 12.20.023) were used for scanning and analyzing body composition which included total tissue weight, lean weight, body fat percentage, bone mineral density (BMD), and bone mineral content (BMC). DEXA machine was calibrated using phantom with a known BMD before placing the birds. On d 49 and 56, one bird per replicate was sacrificed by cervical dislocation and positioned in dorsal recumbency on the DEXA scanner and whole-body scans were performed (Chen et al., 2020). Scans were performed at a speed of 2.5 mm/s with a voxel resolution of 0.07 x 0.07 x 0.50 mm which was similar to previous studies (Chen et al., 2020; Tompkins et al., 2022).

Micro - Computed Tomography (Micro-CT)

Left femur bones were collected on d 49 and 56 and stored at -20°C before analyzing. Bones were placed in 50 mL tubes following thawing, they were immobilized in tubes using cheesecloth. Skyscan Micro-CT scanner (Skyscan 1275, Bruker microCT, Billerica, MA) was used to scan bones. 77 kV and 129 μA with pixel size of 25 μm and a 0.5 mm aluminum filter were applied for 180° scanning with a rotation of 0.4° capturing 4 images per rotation. Reconstruction of 2D image to a 3D model was achieved using N-recon (Bruker microCT) software followed by straightening with data viewer software (Bruker microCT). The region of interest (proximal metaphysis) selection was made using CTAn program (Bruker microCT). Calibration of bone mineral density was conducted using 0.25 and 0.75 g/cm^3 density phantoms with same X-ray settings applied for

bones. Further processing for cortical and trabecular separation was achieved based on previous studies where the image was converted to a binary image followed by despeckling (removal of objects around the bone) (Chen & Kim, 2020; Sharma et al., 2023; Shi et al., 2023).

Quantitative Real-Time PCR analysis (qPCR)

On d 49 and 56, Femoral bone marrow tissues (approximately 30 mg) stored at -80°C for further analyses. Messenger RNA isolation follows steps like homogenizing tissues with QiAzol for 60 seconds (Qiagen, Valencia, CA). Complementary DNA conversion was followed by measuring RNA concentration and quality with NanoDrop 2000 spectrophotometer (Thermofischer Scientific, MA, USA). cDNA synthesis kits were employed for the cDNA conversion (Applied Biosystems, Foster City, CA). Real time PCR reaction using SYBR Green Master mix was performed using Step One thermocycler (Applied Biosystems, Foster City, CA). $2^{-\Delta\Delta Ct}$ method was used to interpret target genes expression using cDNA samples ran in duplicate. Primers for housekeeping gene and target genes are listed in table 1.

Staphylococcus enumeration

Staphylococcus aureus counts in ceca and femoral head were measured on d 49 and 56. The a ceca and two (right and left) femoral heads after removal of articular cartilage were aseptically collected into sterile filter bags *(Whirl Pak®, Nasco Sampling LLC, Chicago, IL, USA)* following necropsy. The contents were diluted with 5 and 10 mL of buffered peptone water (Himedia LLC, PA, USA) to femoral head and cecal contents respectively which are then homogenized for 60 seconds using homogenizer (Neutec group Inc., Farmingdale, NY). Bone contents were collected by chopped into pieces while transferring to filter bag to quicken the process of bone homogenization. Contents were transferred to sterile tubes and serial dilutions were performed followed by transferring them

into Baird Parker agar plates (BD DIFCO, NJ, USA) with 3.5 % potassium tellurite (Sigma, St louis, MO, USA). The plates were incubated for 24-36 hours at 37°C and *S. aureus* was enumerated in the plates.

Lipopolysaccharides and Sclerostin ELISA

The plasma samples stored at -80°C were thawed for this kit-based ELISA. Lipopolysaccharides and Sclerostin levels in the plasma were measured using their respective ELISA kits (MyBioSource, Inc. San Diego, CA, USA). Sample preparation, procedure and respective analyses were conducted according to the manufacturer's instructions.

Mineral Apposition Rate (MAR)

Mineral apposition rate was conducted on the principle that calcein chelates to calcium which can be visualized as fluorescent band. Preparation and protocol for conducting MAR was based on our lab established protocols for the *Gallus gallus* (Choppa, Liu, et al., 2025; Tompkins et al., 2023). Calcein was initially dissolved in 1 M sodium hydroxide solution followed by a working solution (2%) which was prepared by mixing sterile distilled water to the above calcein dissolved solution. Calcein was given intraperitoneally to the birds at 20 mg/kg body weight as 2 doses with a 4-day interval. Femur bones were collected on d 56 and stored in 70% ethanol. The bone was carefully sliced as thin as possible at the mid diaphysis of the bone using a saw blade (Ryobi, Anderson, SC, USA). The thin slice was mounted on a glass slide with slide-mounting medium (Fischer Scientific, Fair Lawn, NJ, USA). Fluorescent microscopic images (BZ-Z800, Keyence Inc., Itasca, IL) were taken to measure distance between two fluorescent bands on the bone. The distance was measured using Image J software (National institute of Health, Bethesda, MD, USA).

Cecal and bone Microbiome analyses and functional analyses

Cecal contents and femoral head slices were collected aseptically and snap frozen with liquid nitrogen and stored at -80°C until further analysis. To reduce the surface contamination while collecting femoral heads, the cartilage cap of the femoral head was snipped off followed by collecting the piece of femoral head under it. QIAamp Fast DNA stool mini kit *(Qiagen GmbH, Hilden, Germany)* was used to extract DNA from both tissues using the manufacturer's protocol. DNA samples from bones were reprocessed again to enhance the purity. Samples were shipped to LC Sciences *(Houston, TX, USA) followed by obtaining raw data which was analyzed using QIIME.* The V3–V4 regions of the bacterial 16S rRNA gene were amplified with the primers 5′-CCTACGGGNGGCWGCAG-3′ (forward) and 5′-GACTACHVGGGTATCTAATCC-3′ (reverse). Amplicon sequencing was carried out on the Illumina NovaSeq platform (Illumina, San Diego, CA, USA) using standard protocols. Raw sequencing reads were processed through a series of steps, including demultiplexing, adapter removal, quality filtering, error correction, and chimera removal. Amplicon sequence variants (ASVs) were inferred using the DADA2 algorithm implemented in QIIME 2. Taxonomic classification was conducted based on the SILVA database (version 138.2). Alpha diversity analyses, including Chao1, Shannon, and Faith's phylogenetic diversity (Faith's PD), were performed in QIIME 2 and plotted with GraphPad Prism (version 10.4.2). Beta diversity was assessed using QIIME 2, and principal coordinate analysis (PCoA) plots were visualized in R (version 4.4.3). Taxonomic compositions at the phylum and family levels were generated using QIIME 2 and visualized with GraphPad Prism. Differences in microbial composition between groups at the phylum and family levels were analyzed using Statistical Analysis of Metagenomic Profiles (STAMP). Microbial functional profiles were predicted using PICRUSt2, based on the ASV table and representative sequences obtained from

QIIME 2. Predicted KEGG pathway functions were subsequently analyzed with STAMP to identify differences between the two groups.

Statistical Analysis

Experimental data were expressed in mean and standard errors. The data were checked for normality and homogeneity of variances. One way ANOVA and student's t test were conducted for identifying statistical significance and post hoc tests like Tukey's HSD using JMP Pro18 (SAS Institute, Inc., Cary, NC). Nonparametric data was analyzed using Kruskal Wallis test and multiple comparisons were conducted using Wilcoxon each pair and Dunn all pairs. *P*-value was set to less than 0.05 for all the data.

RESULTS

Body weight gain, feed intake

Average body weight on the d of reallocation was similar for all the treatments with minimal variations (data not shown). By d 49, treatment 2 revealed a higher body weight gain (938 g) compared to other treatments including T1 (728 g). Other treatments on d 49, revealed body weight gains of 806.3, 421.38, 382.08 g for T3, T4, and T5 respectively ($P < 0.05$) **(Figure 9.1)**. Interestingly, average feed intake did not show any significant differences between treatments from d 42-49 (data not shown) but revealed differences in average feed intake between the T5 and other treatments from d 50 to 56. The average feed intake for T1, T2, T3 and T4 were 1280.2 g, 1353.9 g, 1307.0 g, and 1076.6 g respectively but T5 which was intraperitoneally challenged for three consecutive d was only 404.6 g ($P < 0.05$) **(Figure 9.1)**.

Dual-energy X-ray absorptiometry (DEXA)

DEXA parameters on d 49, did not reveal significant differences between the treatments (data not shown). Interestingly, d 56 results for bone mineral density (BMD) and bone mineral content (BMC) were significantly lower for T4 and T5 with BMD values of 0.246 and 0.239 g/cm^2 compared to T2 which was 0.278 g/cm^2 ($P < 0.05$) **(Figure 9.2)**. T1 and T3 had a similar BMD value of 0.256 and 0.264 g/cm^2 respectively. Similarly, bone mineral content (BMC) for d 56 was significantly lower for T4 and T5 with 56.22 and 56 g respectively which was lower compared to T1, T2, and significantly lower than T3 with 66.5, 74.13, 75.225 g respectively ($P < 0.05$) **(Figure 9.2)**.

Gait and BCO scoring

On d 49, gait scores were higher for the treatments challenged on 3 consecutive days intraperitoneally (T5), than all other treatments. T1 and T2 had an average gait score of 2 respectively, which were similar to the scores during the time of reallocation (d 40). In contrast, T3 and T4 had average scores of 2.69 and 2.5 respectively but scores of T5 was even higher with an average of 4.13 ($P < 0.05$) **(Figure 9.3)**. Furthermore, on d 56, these scores were slightly higher than the averages observed on d 49 but T1 and T2 had same gait scores as d 49. T3, T4, T5 scores differed significantly from each other with averages of 3.31, 2.88, 4.38 respectively ($P < 0.05$) **(Figure 9.3)**.

BCO scores on d 49 were significantly higher for all the treatment groups when compared to T1 which were 0.3 on average. Scores for T2 were intermediate, significantly higher than T1 but significantly lower than T3, T4, having an average score of 1 and scores 0.31, 2.25, 2, 2.38 for T1, T3, T4 and T5 respectively where T3, T4, and T5 were higher than T2 and T1 ($P < 0.05$) **(Figure 9.3)**. Similarly, on d 56, average BCO scores for T1 was 0.19 which was significantly lower

compared to T2 which was 1.13. T5 was significantly higher than other treatments with 2.88. On the other hand, T3 and T4's BCO scores were higher than other treatments except T5 with 2.25 and 2 respectively **(Figure 9.3)**.

Lipopolysaccharides and Sclerostin levels

LPS levels were assessed from plasma which revealed a significant decrease in the concentrations for T2 compared to intraperitoneal challenged treatments (T4 and T5) ($P < 0.05$) **(Figure 9.4)**. Surprisingly, differences between non-challenged or naturally infected treatment (T1) and other treatments except T2 were statistically nonsignificant. The LPS concentrations for T1, T2, T3, T4, and T5 were 186.8, 108.06, 175.43, 244.65, 252.15 ng/mL respectively ($P < 0.05$) **(Figure 9.4)**.

Similarly, Sclerostin (SOST) levels measured from the same samples revealed similar findings where T2 was significantly lower than T4 and T5 with a concentration of 273.5 pg/mL compared to concentrations of 782.5 and 628.125 pg/mL respectively ($P < 0.05$) **(Figure 9.4)**. Furthermore, T1 and T3 had SOST levels at 452.81 and 550.20 respectively which were numerically higher than T2 but numerically lower than T4 and T5 **(Figure 9.4)**.

Staphylococcus aureus counts in ceca and bone

Bacterial counts from ceca and bone were determined on d 49 and 56. On d 49 cecal counts of *S. aureus* revealed non challenged treatment (T1) had significantly lower counts of 1.61 log CFU/g compared to the other treatments where the counts were 3.96 (T2), 5.02 (T3), 3.0 (T4), and 4.92 (T5) log CFU/g respectively ($P < 0.05$) **(Figure 9.5)**. Moreover, d 49 bone counts showed significantly lower *S. aureus* counts for T1 (0.61 log CFU/g). T2 had lower counts compared to T3, T5 which were 3.87, 5.02, 4.92 log CFU/g respectively ($P < 0.05$) **(Figure 9.5)**. Interestingly,

T4 bacterial count (3.9 log CFU/g) was intermediate, not being statistically different from either T2 or T3.

On d 56, Cecal bacterial counts were significantly higher only for T3 and T5 compared to other treatments with 5.46 and 5.79 log CFU/g respectively. T1, T2, and T4 had counts of 3.78, 4.1, 4.06 log CFU/g respectively ($P < 0.05$) **(Figure 9.5)**. Surprisingly in bones, these counts were significantly lower for T2 compared to T3 and T5 with 2, 3.58, and 3.98 log CFU/g respectively ($P < 0.05$) **(Figure 9.5)**. For treatments T1 and T4, *S. aureus* counts were 2.39 and 2.67 log CFU/g respectively.

Mineral apposition rate (MAR)

Bone mineral apposition rate of the treatments in the current study was measured from bones collected on d 56. T1 had highest MAR compared to other treatments with a growth of 384.57 μm ($P < 0.05$). Interestingly, T2 and T3 had MAR of 195.96 and 188.06 μm respectively which was higher than T4 and T5 which had an MAR of 86.11 and 55 μm respectively ($P < 0.05$) **(Figure 9.6)**.

Micro-computed tomography

Cortical 3-D data from micro-CT revealed that bone surface density which was the ratio between bone surface and tissue volume revealed a significant decrease for T3, T4, and T5 compared to non-challenged treatment (T1). The ratios were 3.28, 2.45, 1.9, 2.41, and 2.04 for T1 to T5 respectively ($P < 0.05$) **(Figure 9.7)**. Furthermore, bone surface to volume ratio was significantly less for T3, T4, T5 which were 1.97, 2.41, 2.04 respectively compared to T1 with a ratio of 3.28 ($P < 0.05$), T2 was not significantly different from any other treatment **(Figure 9.7)**. Additionally, total porosity percentage was significantly lower for T1, T2, and T3 compared to T5 which were

4.5, 5.06, 5.44, and 8.08 respectively **(Figure 9.7)**. In contrast, T4 was not significantly different from any other treatment with a 6.81 % ($P < 0.05$) **(Figure 9.7)**.

Microbiome analysis- Bone

On d 49, alpha diversity parameters like Chao1 index and Faith's Phylogenetic Diversity (Faith's PD) were significantly lower for T4 and T5 ($P < 0.05$) **(Figure 9.8)**. On the other hand, Shannon index was significantly lower for T5 ($P < 0.05$) **(Figure 9.8)**. Moreover, beta diversity parameters like unweighted frac revealed that T4 and T5 were distant to the other treatments ($P < 0.05$) **(Figure 9.8)**. STAMP analysis for T1 vs T2 revealed significantly higher abundance (T2) of phyla like Cyanobacteriota (9.3 %) and Actinomycetota (1.14 %). T1 had higher abundance of Bacillota (57.3 %), Pseudomonadota (8.4 %), and Bacteroidota (30.4 %) ($P < 0.05$) **(Figure 9.9)**. Furthermore, T1 vs T3 revealed a significantly higher Cyanobacteriota (5.6 %), Bacillota (58.4 %), Pseudomonadota (8.66 %) abundance in T3. In contrast, Bacteroidota (30.4 %) in T1 was significantly higher compared to T3 ($P < 0.05$) **(Figure 9.9)**. Moreover, T1 vs T4 showed a significantly higher abundance of Pseudomonadota (26.1 %), Cyanobacteriota (4.6 %) for T4 and Bacillota (57.3 %), Bacteroidota (30.4 %) for T1 ($P < 0.05$). T1 vs T5 revealed higher abundance of Pseudomonadota (37.2 %), Bacteroidota (43.8 %) for T5 and Bacillota (57.3 %), Cyanobacteriota for T1 (2.9 %) ($P < 0.05$) **(Figure 9.9)**.

On d 56, alpha diversity parameters did not show any differences (data not shown) but beta diversity parameters like unweighted UniFrac revealed a significant distance from all the challenged treatments to T1 ($P < 0.05$) **(Figure 9.10)**. Phyla comparisons for T1 vs T2 shows higher abundance of Bacillota (82.4 %) and lower abundance of Bacteroidota (16 %) in T2 ($P < 0.05$) **(Figure 9.11)**. T1 vs T3 revealed similar findings with respect to Bacillota (72.4 %) and Bacteroidota (24.9 %). Interestingly, in T1 vs T2, T1 had higher abundance of Actinomycetota

(0.68 %) and Psuedomonadota (1.07 %) ($P < 0.05$) **(Figure 9.11)**. In contrast, T3 had higher abundance of the above phyla (1.01 and 1.4 % respectively) ($P < 0.05$) **(Figure 9.11)**. Furthermore, Bacillota (67.6 %) and Actinomycetota (0.62 %) was in lower abundance besides highly abundant Bacteroidota (27.8 %) and Pseudomonadota (3.3 %) among T4 when compared to T1 ($P < 0.05$) **(Figure 9.11)**. Similar to the comparisons made between T1 vs T2 and T3, T1 vs T5 showed highly abundant Bacillota (81.1 %) and low abundance of Bacteroidota (17.36 %), Pseudomonadota (0.82 %), and Actinomycetota (0.51 %) in T5 ($P < 0.05$) **(Figure 9.11)**.

Microbiome analysis- Ceca

Cecal alpha diversity parameters did not reveal significant values (data not shown). Interestingly, cecal microbiome on d 49 revealed significant distance between the treatments for unweighted and weighted UniFrac parameters ($P < 0.05$) **(Figure 9.12)**. On D 49 and 56, Unweighted UniFrac showed treatments challenged orally (T2 & T3) were distant to T1 and intraperitoneally challenged treatments (T4 & T5) which are in turn distant to each other (T4 and T5) ($P < 0.05$) **(Figure 9.12 and 14)**. Furthermore, weighted UniFrac were distant to each other on d 49 but no significant distant was observed on d 56 (data not shown).

On d 49, relative abundances of T1 vs other treatments revealed which phyla were in higher or lower abundance ($P < 0.05$) **(Figure 9.13)**. T1 vs T2 showed highly abundant Bacillota (69.2 %), Psuedomonadota (9 %), Cyanobacteriota (1.18 %) for T2 besides low abundance of Bacteroidota (18.4 %), Actinomycetota (1.39 %) ($P < 0.05$) **(Figure 9.13)**. Moreover, T1 vs T3 revealed higher abundance of Pseudomonadota (15 %) but Bacillota (66.9 %), Cyanobacteriota (0.44 %), Bacteroidota (15.8 %), and Actinomycetota (0.92 %) were in low abundance ($P < 0.05$) **(Figure 9.13)**. Furthermore, Bacillota (38.8 %), Actinomycetota (0.91 %), and Cyanobacteriota (0.41 %) were in lower abundance besides highly abundant Bacteroidota (44 %) and

Psuedomonadota (15.2 %) in T4 (T1 vs T4) ($P < 0.05$) **(Figure 9.13)**. T1 vs T5 shows highly abundant Psuedomonadota (21.1 %) and low abundance of Bacillota (53.5 %), Bacteroidota (22.8 %), Actinomycetota (1.1 %), and Cyanobacteriota (0.44 %) ($P < 0.05$) **(Figure 9.13)**.

On d 56, Phyla comparisons made between T1, and other treatments showed that T2 had high relative abundance of Bacillota (36.1 %), Actinomycetota (0.23 %), and Cyanobacteriota (0.47 %) but lower abundance of Pseudomonadota (25.8 %), Bacteroidota (37.6 %), and Thermodesulfobacteriota (0.12 %) ($P < 0.05$) **(Figure 9.15)**. With T3, higher abundance was seen with Bacteroidota (59.3 %) and Actinomycetota (0.55 %) besides lower abundance of Bacillota (14.9 %), Pseudomonadota (24.9 %), and Thermodesulfobacteriota (0.17 %) ($P < 0.05$) **(Figure 9.15)**. Interestingly, T4 had highly abundant Bacteroidota (60.4 %), Bacillota (30.2 %), and Actinomycetota (0.28 %) besides lower abundance of Pseudomonadota (8.8 %) and Thermodesulfobacteriota 0.04 %) ($P < 0.05$) **(Figure 9.15)**. Furthermore, T5 showed high abundance of Bacteroidota (75. 2 %) and Actinomycetota (0.36 %) with low abundant phyla like Pseudomonadota (10.1 %), Bacillota (14 %), and Thermodesulfobacteriota (0.06 %) ($P < 0.05$) **(Figure 9.15)**.

Microbiome Functional analysis- Bone and Ceca

On d 49, T1 vs T4 revealed a decreased steroid biosynthesis, mRNA surveillance pathway, PPAR (Peroxisome Proliferator-Activated Receptors) signaling pathway ($P < 0.05$) **(Figure 9.16)**. T1 vs T5 revealed differences in multiple pathways including pathways affected in T4 and lipopolysaccharide biosynthesis, altered metabolic pathways, NOD like receptor (NLR) pathway, steroid hormone biosynthesis, two component system, fatty acid elongation etc., ($P < 0.05$) **(Figure 9.17)**. On d 56, T1 vs T3 showed an increased metabolic pathway (C5-branched dibasic acid metabolism, nitrogen metabolism) ($P < 0.05$) **(Figure 9.18)**. Furthermore, T1 vs T5 showed

increased Butanoate, porphyrin, and nitrogen metabolism, valine, leucine and isoleucine biosynthesis, Fatty acid biosynthesis ($P < 0.05$) **(Figure 9.19)**.

On d 49 Ceca, increased Fc gamma R-mediated phagocytosis and endocytosis for T2. Additionally, T3 showed increased fatty acid degradation, Fc gamma R-mediated phagocytosis, endocytosis, MAPK (Mitogen-activated protein kinase) signaling pathway and Calcium signaling pathway ($P < 0.05$) **(Figure 9.20)**. T4 revealed aberrations in several pathways including decreased insulin signaling pathway and increased lipopolysaccharide biosynthesis, MAPK signaling pathway, folate biosynthesis, etc. Similarly, T5 showed similar aberrations to pathways identified in T4 ($P < 0.05$) **(Figure 9.21)**.

On d 56 Ceca, functional analysis of microbiome was compared between T1 and the other treatments. T1 vs T2 revealed aberrations in pathways like decreased Wnt signaling pathway, Fatty acid degradation, Notch Signaling pathway, and Bacterial secretion system in T2 ($P < 0.05$) **(Figure 9.22)**. Furthermore, T1 vs T3 showed altered metabolic pathways besides increased MAPK signaling pathway (yeast), oxidative phosphorylation, folate biosynthesis, peroxisome. T1 vs T4 aberrations in higher number of pathways importantly increased RNA degradation, MAPK signaling pathway, decreased two component system, tryptophan metabolism etc., ($P < 0.05$) **(Figure 9.23)**. As expected T5 showed much higher alterations in pathways which revealed increased MAPK signaling pathway (yeast), Oxidative phosphorylation, folate biosynthesis, steroid hormone biosynthesis, osteoclast differentiation, and apoptosis besides decreased Wnt (Wingless-related integration) signaling pathway and Notch signaling pathway ($P < 0.05$) **(Figure 9.24)**.

DISCUSSION

Findings from this study revealed, route of inoculation and number of *S. aureus* exposure d greatly influence the BCO lesions and their severity in broiler chickens. Birds challenged orally at a single time point showed similar growth performance parameters and, interestingly, had lower inflammatory and bone pathology indicators compared to the other treatments. In contrast, repeated challenge, orally or intraperitoneally (T3 and T5), showed pronounced outcomes like poor gait, significant reductions in bone mineral density and mineral apposition rate (MAR), besides higher colonization of bone and ceca. Most importantly, intestinal and bone microbiome revealed significant alterations suggesting dysbiosis with consecutive challenge. This suggests a sustained bacteremia (consecutive doses of *S. aureus*) is key factor in inducing BCO lesions in broilers resulting in lameness and abnormalities in bone growth (Anthney et al., 2024; Rojas-Núñez et al., 2020). Early experimental models revealed that a healthy chicken developed bacteremia following by intravenous injection of *S. aureus* without any pre-existing damage, eventually colonizing metaphyses and growth plates (Daum et al., 1990). From other studies, it was known that bacteremia is needed to induce BCO with a likely source of bacteria originating from the broiler house environment which enter the host through the gastrointestinal or respiratory tract, or through the skin (Assumpcao et al., 2024; Choppa & Kim, 2023a; Rojas-Núñez et al., 2020). Some studies emphasized the potential role of opportunistic pathogens residing in the intestine (*E. coli, Staphylococcus aureus, S. agentis, Enterococcus cecorum)* that would colonize the growing regions of bone via blood circulation. When the pathogens were given via the drinking water on a wire flooring model, an incidence of lameness of 50-80 % was observed (Al-Rubaye et al., 2015). Studies have shown that broilers experiencing bacterial translocation from the intestines into the blood manifest as BCO, when they were predisposed with stress to facilitate the route of

induction (Choppa & Kim, 2023a; R. F. Wideman, 2016). Interestingly, a study revealed that BCO incidence did not increase from severe intestinal injury (subclinical necrotic enteritis) in the absence of an invasive pathogen, this suggests that the presence of a pathogen is required to induce BCO (Rojas-Núñez et al., 2020). The above statement can be supported by the observation in this study that a single oral dose was insufficient to induce BCO, but a persistent bacteremia would breach the host immune defenses and the intestinal barrier to reach the target location or to alter the bone physiology.

The oral and intraperitoneal routes used in this study gave a new insight on how bacteria reached the bones and affected bone physiology. The oral challenge or the gastrointestinal route faces a challenge where these pathogens must survive harsh intestinal environment besides competing with microbiome followed by crossing the intestinal barrier. This study, showed that one dose of *S. aureus* orally is well tolerated by the host due to bird's immune system and microbiome. Repeated oral dosing (T3), allowed recovery of *S. aureus* from bone indicating sustained bacteremia. This is possibly due to local intestinal inflammation thereby allowing the pathogens to translocate. On the other hand, the intraperitoneal route evades the intestinal tract by entering the body cavity and subsequently the blood stream. Interestingly, even a single IP injection showed a marked degree of colonization besides the systemic and microbiome changes. Furthermore, repeated doses of IP *S. aureus* produced an intense bacteremia leading to the induction of BCO. Our findings suggest that repeated or persistent bacteremia is required to induce BCO which is congruent with earlier models (Meroni et al., 2022). Previous studies using mechanical stress that enable microfractures have had success in inducing BCO (Al-Rubaye et al., 2017; Wideman Jr et al., 2012). Our study showed that the birds reared on litter developed BCO at high frequency proving that a severe infection alone can induce necrosis even without

mechanical stressor (Anthney et al., 2024). Furthermore, it is highly likely that in our treatments, routine weight bearing, in conjunction with rapid growth would serve in creating micro clefts which allows colonization of circulating bacteria in these vulnerable regions of the bone (Choppa & Kim, 2023a; Rojas-Núñez et al., 2020). Improved weight gain in T2 birds suggests a mild intestinal challenge would stimulate the immune system, without causing pathology or impaired nutrient absorption.

A major finding in the severely challenged groups (T3, T4, and T5) revealed enhanced systemic inflammation and disrupted bone homeostasis. In T5, increased LPS in the circulation was another important finding since *S. aureus* is a gram-positive bacterium. This implies that the intestinal microbiota contributes to heightened inflammation by translocating gram-negative bacteria or the release of endotoxins triggering bone turnover (Choppa et al., 2023a; Choppa, Liu, et al., 2025). Osteoclasts and Osteocytes recognize LPS followed by activating downstream cascades like MAPK pathway which enhances RANKL expression and osteoclast activation. This triggers proinflammatory mediators (IL-1 beta, TNF alpha) that indirectly increase the production of sclerostin (SOST). This increase blocks the Wnt signaling pathway thereby blocking differentiation of mesenchymal stem cells (Choppa et al., 2023b; Huang et al., 2020). This mechanism was evidently seen in our study, reflecting aberrations in bone homeostasis which are manifested by lower bone density with higher porosity (T4 and T5) representing necrotic voids in these birds. Additionally, femoral head sections with empty lacunae and increased resorption with low MAR indicates activation of bone breaking pathways while blocking bone building pathways thereby inducing BCO lesions.

Microbiome shifts in T4 and T5 reflect the severity of the infection in the T4 and T5 birds with significant changes in both ceca and bone. Furthermore, there was a marked loss in microbial

diversity among the treatments with overrepresentation of certain taxa. The control group had either sterile bone or a more diverse microbiota, while the presence of common intestinal commensals in the challenged treatment groups indicates the likelihood of intestinally originated bacteremia. Intraperitoneally challenged birds (T4 and T5) experienced intestinal barrier disruption manifested by thriving Psuedomonadota (Proteobacteria) and other opportunistic bacterial phyla representing compounded bone lesions in these treatments (Durairaj et al., 2009; Mancabelli et al., 2016). The microbiota in healthy broiler chickens is often dominated by Psuedomonadota (Proteobacteria) but dysbiosis leads to their entry into the blood circulation followed by a surge in endotoxin production in the treatments challenged intraperitoneally (Choppa & Kim, 2023a, 2023b; Durairaj et al., 2009; Mandal et al., 2020; Rath & Durairaj, 2022). Supporting evidence from our findings can be observed through a drop in alpha-diversity for T4 and T5 indicating a destabilized intestinal ecosystem, indicating systemic illness leading to changes in immunity allowing opportunistic pathogens to grow. On the other hand, repeated oral exposure (T3) maintained a reservoir of bacteria in the intestinal tract capable of translocation (Asnayanti et al., 2024; R. Wideman & Prisby, 2013). PICRUST2 analysis to predict metagenomic pathways in this study showed that severely challenged birds have differentially impacted host-relevant signaling pathways. MAPK signaling pathways enriched in challenged treatments (T3, T4, and T5) suggests possible stimulation from LPS or *S. aureus* (through its peptidoglycan and lipoteichoic acid) itself that activate MAPK cascade in the host's bone indicating the role of LPS/ *S. aureus*-driven inflammatory signaling. This indicates potential disruptions in Wnt signaling pathway and apoptosis in T3, T4, and T5 groups. Given our data, dysbiosis favors production of Sclerostin which lower/inhibits Wnt signaling and is known to interact with osteoblastogenesis (Choppa & Kim, 2023b; Durairaj et al., 2009; Rath & Durairaj, 2022). On the other hand,

Staphylococcus induces apoptosis in immune cells like neutrophils to evade pathogen clearance and causes osteomyelitis lesions (widespread apoptosis) (Packialakshmi et al., 2015; Rath et al., 2000). Additionally, enhanced oxidative phosphorylation and steroid biosynthesis pathways indicate a favorable environment for invading bacteria or an increased activated immune cellular response (Chakraborty et al., 2021; Muralidharan & Mandrekar, 2013). Although the above-mentioned inferences were functional predictions due to our limited understanding of intestinal microbiota in chickens, all the treatments challenged with the pathogen strongly suggest the same heightened inflammation (MAPK), suppressed Wnt signaling pathway, and increased apoptosis. Future studies integrating metagenomics with host transcriptomics would validate pathway interactions and specific metabolites involved in these effects (Choppa et al., 2023b; Choppa & Kim, 2023a; Rath & Durairaj, 2022).

Although modern broilers are highly susceptible to BCO with their rapid growth, T2 birds were unaffected despite the challenge, which suggests the bird's ability to avert the cascade of events leading to BCO. Additionally, mitigation strategies aiming at strengthening intestinal barrier during inflammation would greatly alleviate BCO. In some studies in which dietary supplements of organic trace minerals, probiotics, prebiotics, fermentable fiber, and phytogenic compounds (curcumin) were used, resulted in improved intestinal tight junction integrity which can be associated with likelihood of BCO occurrence (Alrubaye, Ekesi, Hasan, Elkins, et al., 2020; Alrubaye, Ekesi, Hasan, Koltes, et al., 2020; Asnayanti et al., 2024). Targeted immunoprophylaxis and vaccine development could provide a beneficial immunity to neutralize these bacteria before they invade. A recent study using an electron-beam killed *Staphylococcus* vaccine revealed a reduction in incidence of BCO by approximately 50 % by stimulating adaptive immunity against opportunistic pathogens (Assumpcao et al., 2024). This again gives insight into the development

of a multivalent vaccine targeting major opportunistic pathogens involved in BCO's pathogenesis. All of the above mitigation strategies need further investigation to use them in a commercial setting to curtail this condition.

Our study also highlights potential therapeutic targets for the infected birds. Although human studies have used monoclonal antibodies to treat osteoporosis by boosting bone formation, these are impractical in food animals. Moreover, our findings suggests the concept of maintaining bone anabolism during inflammation (Iolascon et al., 2023; Ominsky et al., 2017; Rauner et al., 2021). Additionally, nutritional strategies like supplemental Vitamin D3, antioxidants, and quorum-quenching agents could be explored to support and prevent further damage to the bone.

CONCLUSION

This study highlights that the occurrence of BCO can be modulated by the route and dose of infection along with the host responses. Although a single oral dose did not induce BCO, repeated oral doses or systemic exposures (intraperitoneal challenge) triggered BCO pathology by inducing changes in microbiome and altered inflammatory pathways. Severe outcomes were characterized by a break in intestinal integrity, bacteremia, and dysregulated immune responses induced by LPS, suppression of Wnt signaling pathway (elevated Sclerostin, altered bone homeostasis). By providing a clearer understanding of BCO pathogenesis, mitigation strategies can be developed to curtail cascading inflammation and bacteremia. These strategies would aid in modulating the host's inflammatory responses and reducing pathogen exposure, this in turn, would improve the broiler's bone health and welfare. More importantly, the productivity and food safety of broiler chickens would also be enhanced.

REFERENCES

Al-Rubaye, A. A. K., Couger, M. B., Ojha, S., Pummill, J. F., Koon, J. A., Wideman Jr, R. F., & Rhoads, D. D. (2015). Genome analysis of Staphylococcus agnetis, an agent of lameness in broiler chickens. *PloS One*, *10*(11), e0143336.

Alrubaye, A. A. K., Ekesi, N. S., Hasan, A., Elkins, E., Ojha, S., Zaki, S., Dridi, S., Wideman, R. F., Rebollo, M. A., & Rhoads, D. D. (2020). Chondronecrosis with osteomyelitis in broilers: further defining lameness-inducing models with wire or litter flooring to evaluate protection with organic trace minerals. *Poultry Science*, *99*(11), 5422–5429. https://doi.org/https://doi.org/10.1016/j.psj.2020.08.027

Alrubaye, A. A. K., Ekesi, N. S., Hasan, A., Koltes, D. A., Wideman Jr, R. F., & Rhoads, D. D. (2020). Chondronecrosis with osteomyelitis in broilers: further defining a bacterial challenge model using standard litter flooring and protection with probiotics. *Poultry Science*, *99*(12), 6474–6480.

Al-Rubaye, A. A. K., Ekesi, N. S., Zaki, S., Emami, N. K., Wideman Jr, R. F., & Rhoads, D. D. (2017). Chondronecrosis with osteomyelitis in broilers: Further defining a bacterial challenge model using the wire flooring model. *Poultry Science*, *96*(2), 332–340.

Anthney, A., Do, A. D. T., & Alrubaye, A. A. K. (2024). Bacterial chondronecrosis with osteomyelitis lameness in broiler chickens and its implications for welfare, meat safety, and quality: a review. *Frontiers in Physiology*, *15*, 1452318.

Asnayanti, A., Do, A. D. T., & Alrubaye, A. (2024). Microbiology, induction, and management practices to mitigate lameness caused by bacterial chondronecrosis with osteomyelitis in broiler chickens. *Ger. J. Vet. Res*, *4*(4), 14–30.

Assumpcao, A. L. F. V, Arsi, K., Asnayanti, A., Alharbi, K. S., Do, A. D. T., Read, Q. D., Perera, R., Shwani, A., Hasan, A., & Pillai, S. D. (2024). Electron-Beam-Killed Staphylococcus Vaccine Reduced Lameness in Broiler Chickens. *Vaccines*, *12*(11), 1203.

Chakraborty, S., Pramanik, J., & Mahata, B. (2021). Revisiting steroidogenesis and its role in immune regulation with the advanced tools and technologies. *Genes & Immunity*, *22*(3), 125–140.

Chen, C., & Kim, W. K. (2020). The application of micro-CT in egg-laying hen bone analysis: introducing an automated bone separation algorithm. *Poultry Science*, *99*(11), 5175–5183.

Chen, C., Turner, B., Applegate, T. J., Litta, G., & Kim, W. K. (2020). Role of long-term supplementation of 25-hydroxyvitamin D3 on laying hen bone 3-dimensional structural development. *Poultry Science*, *99*(11), 5771–5782.

Choppa, V. S. R., & Kim, W. K. (2023a). A Review on Pathophysiology, and Molecular Mechanisms of Bacterial Chondronecrosis and Osteomyelitis in Commercial Broilers. *Biomolecules*, *13*(7), 1032.

Choppa, V. S. R., & Kim, W. K. (2023b). A Review on Pathophysiology, and Molecular Mechanisms of Bacterial Chondronecrosis and Osteomyelitis in Commercial Broilers. *Biomolecules*, *13*(7), 1032.

Choppa, V. S. R., Liu, G., Shi, H., Sharma, M. K., Goo, D., & Kim, W. K. (2025). Effect of lipopolysaccharides and mixed Eimeria spp. challenge on performance and bone development in broilers. *Poultry Science*, 105501.

Choppa, V. S. R., Liu, G., Tompkins, Y. H., & Kim, W. K. (2023a). Altered Osteogenic Differentiation in Mesenchymal Stem Cells Isolated from Compact Bone of Chicken Treated with Varying Doses of Lipopolysaccharides. *Biomolecules*, *13*(11), 1626.

Choppa, V. S. R., Liu, G., Tompkins, Y. H., & Kim, W. K. (2023b). Altered Osteogenic Differentiation in Mesenchymal Stem Cells Isolated from Compact Bone of Chicken Treated with Varying Doses of Lipopolysaccharides. *Biomolecules*, *13*(11), 1626.

Choppa, V. S. R., Naeini, H. R. R., Lee, D. J., Katha, H. R., Ko, H., Paneru, D., Kim, Y., & Kim, W. K. (2025). Effect of Eimeria spp. and Staphylococcus aureus challenge on cecal microbiome in broilers. *Poultry Science*, 105814.

Daum, R. S., Davis, W. H., Farris, K. B., Campeau, R. J., Mulvihill, D. M., & Shane, S. M. (1990). A model of Staphylococcus aureus bacteremia, septic arthritis, and osteomyelitis in chickens. *Journal of Orthopaedic Research*, *8*(6), 804–813.

Durairaj, V., Okimoto, R., Rasaputra, K., Clark, F. D., & Rath, N. C. (2009). Histopathology and serum clinical chemistry evaluation of broilers with femoral head separation disorder. *Avian Diseases*, *53*(1), 21–25.

Gao, Y., Liu, S., Huang, J., Guo, W., Chen, J., Zhang, L., Zhao, B., Peng, J., Wang, A., & Wang, Y. (2014). The ECM-cell interaction of cartilage extracellular matrix on chondrocytes. *BioMed Research International*, *2014*(1), 648459.

Huang, X., Xie, M., Xie, Y., Mei, F., Lu, X., Li, X., & Chen, L. (2020). The roles of osteocytes in alveolar bone destruction in periodontitis. *Journal of Translational Medicine*, *18*(1), 479.

Iolascon, G., Liguori, S., Paoletta, M., Toro, G., & Moretti, A. (2023). Anti-sclerostin antibodies: a new frontier in fragility fractures treatment. *Therapeutic Advances in Musculoskeletal Disease*, *15*, 1759720X231197094.

Kestin, S. C., Knowles, T. G., Tinch, A. E., & Gregory, N. G. (1992). Prevalence of leg weakness in broiler chickens and its relationship with genotype. *The Veterinary Record*, *131*(9), 190–194.

Mancabelli, L., Ferrario, C., Milani, C., Mangifesta, M., Turroni, F., Duranti, S., Lugli, G. A., Viappiani, A., Ossiprandi, M. C., & van Sinderen, D. (2016). Insights into the biodiversity of the gut microbiota of broiler chickens. *Environmental Microbiology*, *18*(12), 4727–4738.

Mandal, R. K., Jiang, T., Wideman, R. F., Lohrmann, T., & Kwon, Y. M. (2020). Microbiota Analysis of Chickens Raised Under Stressed Conditions . In *Frontiers in Veterinary Science* (Vol. 7, p. 696). https://www.frontiersin.org/article/10.3389/fvets.2020.482637

McNamee, P. T., McCullagh, J. J., Rodgers, J. D., Thorp, B. H., Ball, H. J., Connor, T. J., McConaghy, D., & Smyth, J. A. (1999). Development of an experimental model of bacterial chondronecrosis with osteomyelitis in broilers following exposure to Staphylococcus aureus by aerosol, and inoculation with chicken anaemia and infectious bursal disease viruses. *Avian Pathology*, *28*(1), 26–35.

McNamee, P. T., & Smyth, J. A. (2000). Bacterial chondronecrosis with osteomyelitis ('femoral head necrosis') of broiler chickens: A review. *Avian Pathology*, *29*(4), 253–270. https://doi.org/10.1080/03079450050118386

Meroni, G., Tsikopoulos, A., Tsikopoulos, K., Allemanno, F., Martino, P. A., & Soares Filipe, J. F. (2022). A journey into animal models of human osteomyelitis: a review. *Microorganisms*, *10*(6), 1135.

Muralidharan, S., & Mandrekar, P. (2013). Cellular stress response and innate immune signaling: integrating pathways in host defense and inflammation. *Journal of Leukocyte Biology*, *94*(6), 1167–1184.

Ominsky, M. S., Boyce, R. W., Li, X., & Ke, H. Z. (2017). Effects of sclerostin antibodies in animal models of osteoporosis. *Bone*, *96*, 63–75.

Packialakshmi, B., Liyanage, R., Lay Jr, J. O., Okimoto, R., & Rath, N. C. (2015). Prednisolone-induced predisposition to femoral head separation and the accompanying plasma protein changes in chickens. *Biomarker Insights*, *10*, BMI-S20268.

Rath, N. C., & Durairaj, V. (2022). Chapter 22 - Avian bone physiology and poultry bone disorders. In C. G. Scanes & S. Dridi (Eds.), *Sturkie's Avian Physiology (Seventh Edition)* (pp. 549–563). Academic Press. https://doi.org/https://doi.org/10.1016/B978-0-12-819770-7.00037-2

Rath, N. C., Huff, G. R., Huff, W. E., & Balog, J. M. (2000). Factors regulating bone maturity and strength in poultry. *Poultry Science*, *79*(7), 1024–1032.

Rauner, M., Taipaleenmäki, H., Tsourdi, E., & Winter, E. M. (2021). Osteoporosis treatment with anti-sclerostin antibodies—mechanisms of action and clinical application. *Journal of Clinical Medicine*, *10*(4), 787.

Roach, H. I., & Shearer, J. R. (1989). Cartilage resorption and endochondral bone formation during the development of long bones in chick embryos. *Bone and Mineral*, *6*(3), 289–309.

Rojas-Núñez, I., Moore, A. F., & Gino Lorenzoni, A. (2020). Incidence of bacterial chondronecrosis with osteomyelitis (Femoral head necrosis) induced by a model of skeletal stress and its correlation with subclinical necrotic enteritis. *Microorganisms*, *8*(2), 205. https://doi.org/10.3390/microorganisms8020205

Sharma, M. K., Liu, G., White, D. L., Tompkins, Y. H., & Kim, W. K. (2023). Graded levels of Eimeria challenge altered the microstructural architecture and reduced the cortical bone growth of femur of Hy-Line W-36 pullets at early stage of growth (0–6 wk of age). *Poultry Science*, *102*(9), 102888.

Shi, H., Wang, J., White, D., Martinez, O. J. T., & Kim, W. K. (2023). Impacts of phytase and coccidial vaccine on growth performance, nutrient digestibility, bone development, and intestinal gene expression of broilers fed a nutrient reduced diet. *Poultry Science*, *102*(11), 103062.

Tompkins, Y. H., Chen, C., Sweeney, K. M., Kim, M., Voy, B. H., Wilson, J. L., & Kim, W. K. (2022). The effects of maternal fish oil supplementation rich in n-3 PUFA on offspring-broiler growth performance, body composition and bone microstructure. *Plos One*, *17*(8), e0273025.

Tompkins, Y. H., Choi, J., Teng, P.-Y., Yamada, M., Sugiyama, T., & Kim, W. K. (2023). Reduced bone formation and increased bone resorption drive bone loss in Eimeria infected broilers. *Scientific Reports*, *13*(1), 616.

Wideman Jr, R. F., Hamal, K. R., Stark, J. M., Blankenship, J., Lester, H., Mitchell, K. N., Lorenzoni, G., & Pevzner, I. (2012). A wire-flooring model for inducing lameness in broilers: evaluation of probiotics as a prophylactic treatment. *Poultry Science*, *91*(4), 870–883.

Wideman, R. F. (2016). Bacterial chondronecrosis with osteomyelitis and lameness in broilers: a review. *Poultry Science*, *95*(2), 325–344. https://doi.org/https://doi.org/10.3382/ps/pev320

Wideman, R., & Prisby, R. (2013). Bone Circulatory Disturbances in the Development of Spontaneous Bacterial Chondronecrosis with Osteomyelitis: A Translational Model for the Pathogenesis of Femoral Head Necrosis . In *Frontiers in Endocrinology* (Vol. 3, p. 183). https://www.frontiersin.org/article/10.3389/fendo.2012.00183

Yu, Y., Wang, S., & Zhou, Z. (2020). Cartilage homeostasis affects femoral head necrosis induced by methylprednisolone in broilers. *International Journal of Molecular Sciences*, *21*(14), 4841.

Figure 9.1 Illustrates the effects of *Staphylococcus aureus* challenge on body weight gain (d 40-49) and feed intake (d 50-56) of broiler chickens ($P < 0.05$). T1, non-challenged treatment; Treatment 2 (T2) was challenged with *Staphylococcus aureus* at 10^9 CFU orally on d 42; Treatment 3 (T3) was challenged with *Staphylococcus aureus* at 10^9 CFU orally on d 42, 43, and 44 respectively; Treatment 4 (T4) was challenged with *Staphylococcus aureus* at 10^7 CFU intraperitoneally on d 42; Treatment 5 (T5) was challenged with *Staphylococcus aureus* at 10^7 CFU intraperitoneally on d 42, 43, and 44 respectively. Columns not sharing a common letter are significantly different ($P < 0.05$, N =4).

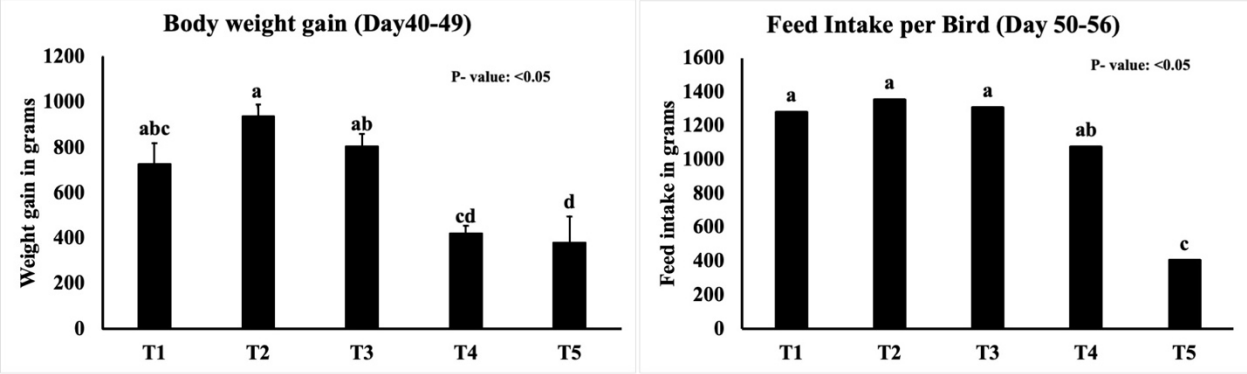

Figure 9.2 Illustrates the effects of *Staphylococcus aureus* challenge on DEXA parameters (Bone Mineral Density and Bone Mineral Content) on d 56 of broiler chickens ($P < 0.05$). DEXA= Dual Energy X-ray Absorptiometry; T1, non-challenged treatment; Treatment 2 (T2) was challenged with *Staphylococcus aureus* at 10^9 CFU orally on d 42; Treatment 3 (T3) was challenged with *Staphylococcus aureus* at 10^9 CFU orally on d 42, 43, and 44 respectively; Treatment 4 (T4) was challenged with *Staphylococcus aureus* at 10^7 CFU intraperitoneally on d 42; Treatment 5 (T5) was challenged with *Staphylococcus aureus* at 10^7 CFU intraperitoneally on d 42, 43, and 44 respectively. x

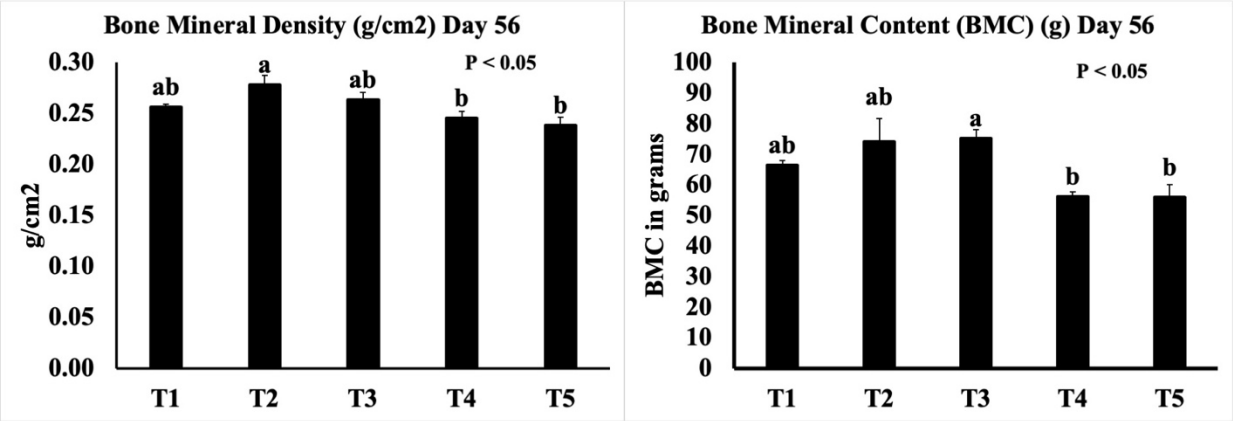

Figure 9.3 Illustrates the changes in Gait and BCO scoring of broiler chickens when challenged with *Staphylococcus aureus* ($P < 0.05$). BCO= Bacterial Chondronecrosis and Osteomyelitis; T1, non-challenged treatment; Treatment 2 (T2) was challenged with *Staphylococcus aureus* at 10^9 CFU orally on d 42; Treatment 3 (T3) was challenged with *Staphylococcus aureus* at 10^9 CFU orally on d 42, 43, and 44 respectively; Treatment 4 (T4) was challenged with *Staphylococcus aureus* at 10^7 CFU intraperitoneally on d 42; Treatment 5 (T5) was challenged with *Staphylococcus aureus* at 10^7 CFU intraperitoneally on d 42, 43, and 44 respectively. Columns not sharing a common letter are significantly different ($P < 0.05$, N =4).

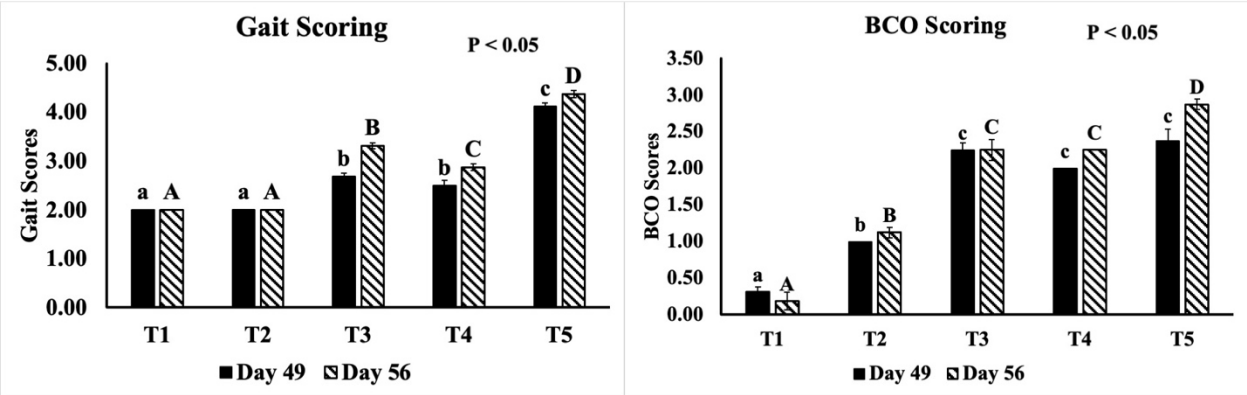

Figure 9.4 shows concentration of lipopolysaccharides (LPS) and Sclerostin (SOST) in plasma on d 49 ($P < 0.05$) of broiler chickens. T1, non-challenged treatment; Treatment 2 (T2) was challenged with *Staphylococcus aureus* at 10^9 CFU orally on d 42; Treatment 3 (T3) was challenged with *Staphylococcus aureus* at 10^9 CFU orally on d 42, 43, and 44 respectively; Treatment 4 (T4) was challenged with *Staphylococcus aureus* at 10^7 CFU intraperitoneally on d 42; Treatment 5 (T5) was challenged with *Staphylococcus aureus* at 10^7 CFU intraperitoneally on d 42, 43, and 44 respectively. Columns not sharing a common letter are significantly different ($P < 0.05$, N =4).

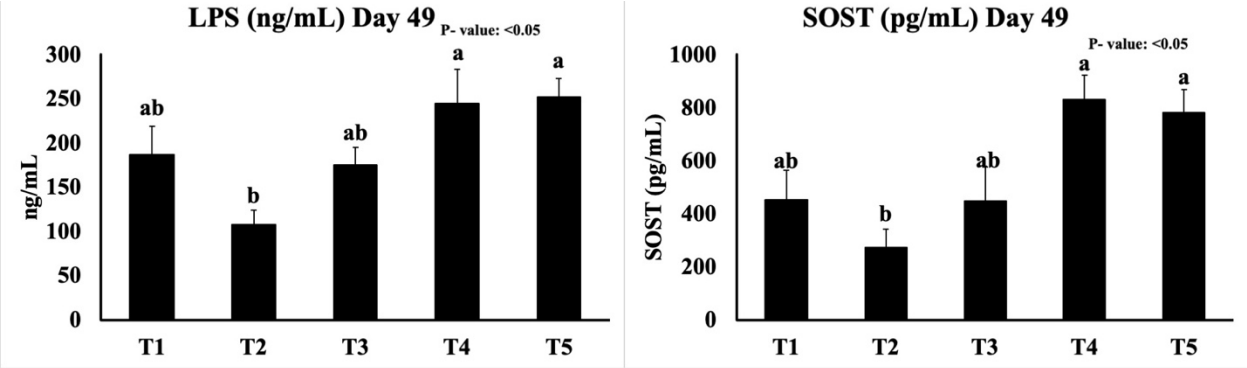

Figure 9.5 shows *Staphylococcus aureus* counts in Ceca and Bone on d 49 and 56 of broiler chickens ($P < 0.05$). T1, non-challenged treatment; Treatment 2 (T2) was challenged with *Staphylococcus aureus* at 10^9 CFU orally on d 42; Treatment 3 (T3) was challenged with *Staphylococcus aureus* at 10^9 CFU orally on d 42, 43, and 44 respectively; Treatment 4 (T4) was challenged with *Staphylococcus aureus* at 10^7 CFU intraperitoneally on d 42; Treatment 5 (T5) was challenged with *Staphylococcus aureus* at 10^7 CFU intraperitoneally on d 42, 43, and 44 respectively. Columns not sharing a common letter are significantly different ($P < 0.05$, N =4).

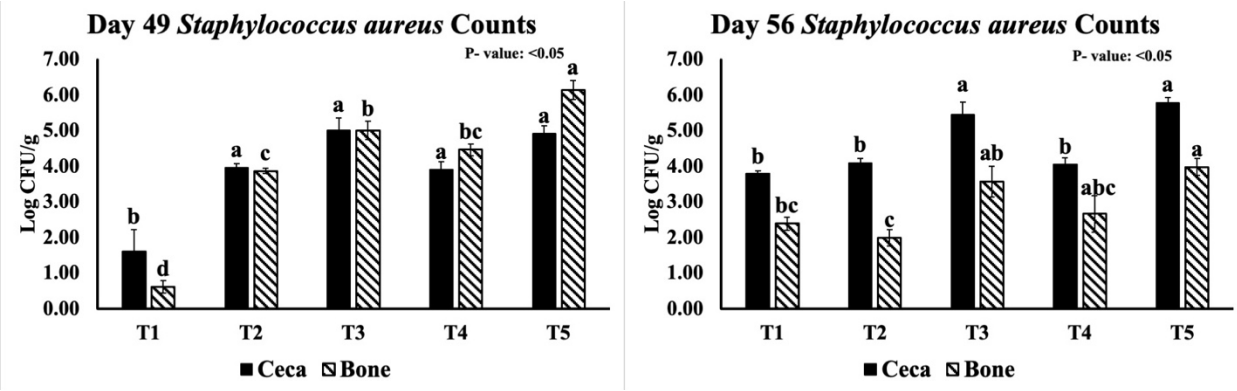

Figure 9.6 shows Mineral Apposition Rate (MAR) of broiler chickens for treatments challenged with *Staphylococcus aureus* ($P < 0.05$). T1, non-challenged treatment; Treatment 2 (T2) was challenged with *Staphylococcus aureus* at 10^9 CFU orally on d 42; Treatment 3 (T3) was challenged with *Staphylococcus aureus* at 10^9 CFU orally on d 42, 43, and 44 respectively; Treatment 4 (T4) was challenged with *Staphylococcus aureus* at 10^7 CFU intraperitoneally on d 42; Treatment 5 (T5) was challenged with *Staphylococcus aureus* at 10^7 CFU intraperitoneally on d 42, 43, and 44 respectively. Columns not sharing a common letter are significantly different ($P < 0.05$, N =4).

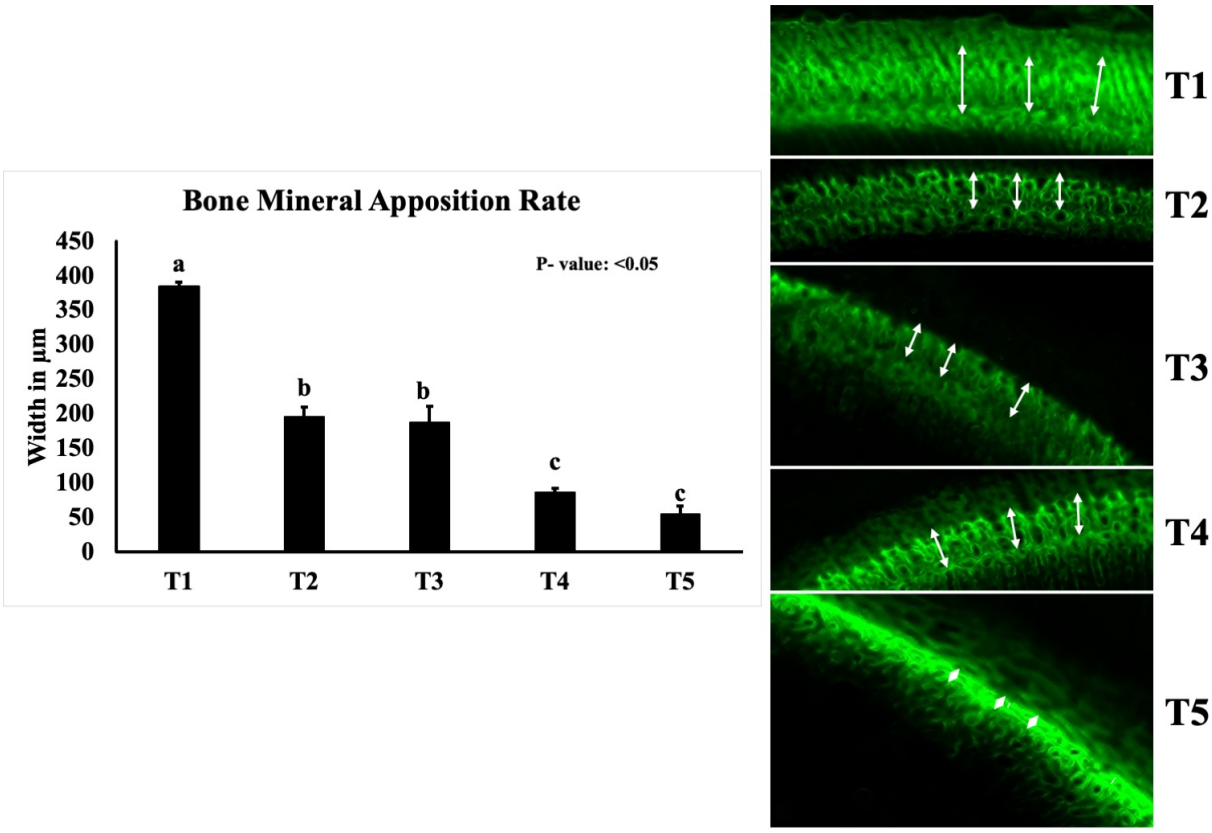

Figure 9.7 shows Micro Computed Tomography (Micro-CT) parameters like bone surface density (bone surface to tissue volume ratio), bone surface to volume ratio, and total porosity (%) of broiler chicken's treatments challenged with *Staphylococcus aureus* ($P < 0.05$). T1, non-challenged treatment; Treatment 2 (T2) was challenged with *Staphylococcus aureus* at 10^9 CFU orally on d 42; Treatment 3 (T3) was challenged with *Staphylococcus aureus* at 10^9 CFU orally on d 42, 43, and 44 respectively; Treatment 4 (T4) was challenged with *Staphylococcus aureus* at 10^7 CFU intraperitoneally on d 42; Treatment 5 (T5) was challenged with *Staphylococcus aureus* at 10^7 CFU intraperitoneally on d 42, 43, and 44 respectively. Columns not sharing a common letter are significantly different ($P < 0.05$, N =4).

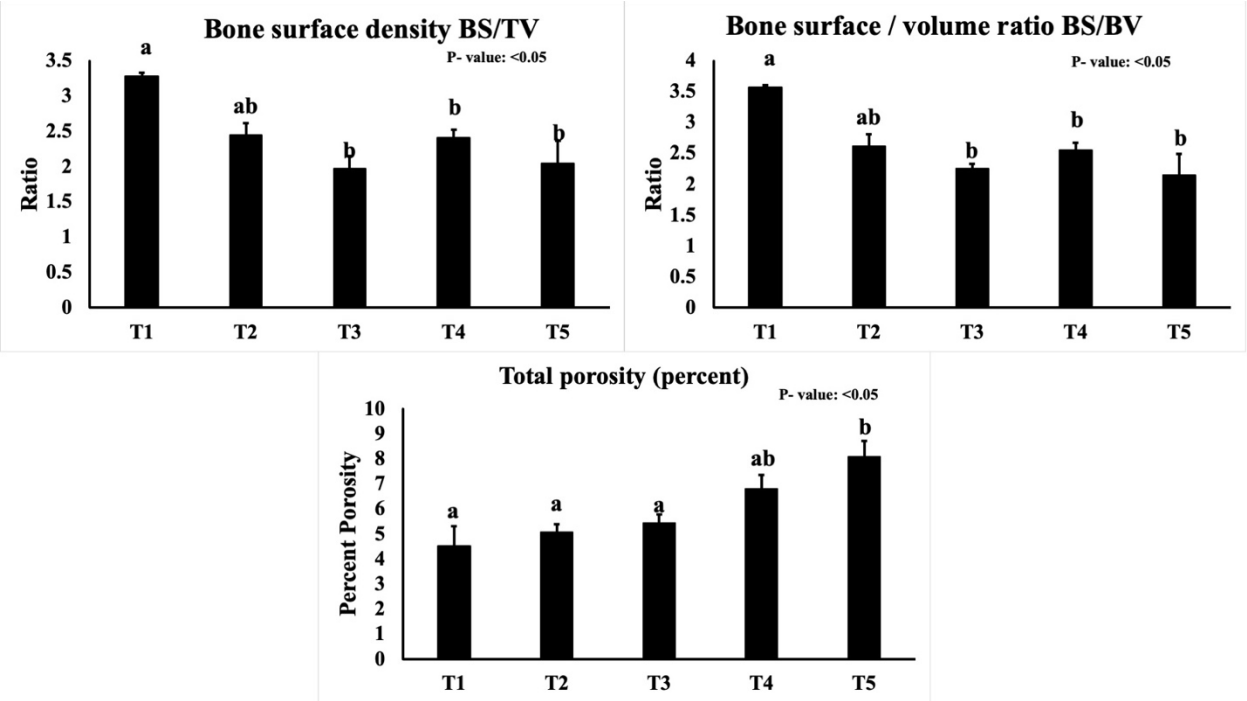

Figure 9.8 shows alpha and beta diversity parameters (shannon index, unweighted and weighted UniFrac) in bone microbiome on d 49 of broiler chicken's treatments challenged with *Staphylococcus aureus* ($P < 0.05$). T1, non-challenged treatment; Treatment 2 (T2) was challenged with *Staphylococcus aureus* at 10^9 CFU orally on d 42; Treatment 3 (T3) was challenged with *Staphylococcus aureus* at 10^9 CFU orally on d 42, 43, and 44 respectively; Treatment 4 (T4) was challenged with *Staphylococcus aureus* at 10^7 CFU intraperitoneally on d 42; Treatment 5 (T5) was challenged with *Staphylococcus aureus* at 10^7 CFU intraperitoneally on d 42, 43, and 44 respectively. Columns not sharing a common letter are significantly different ($P < 0.05$, N =4).

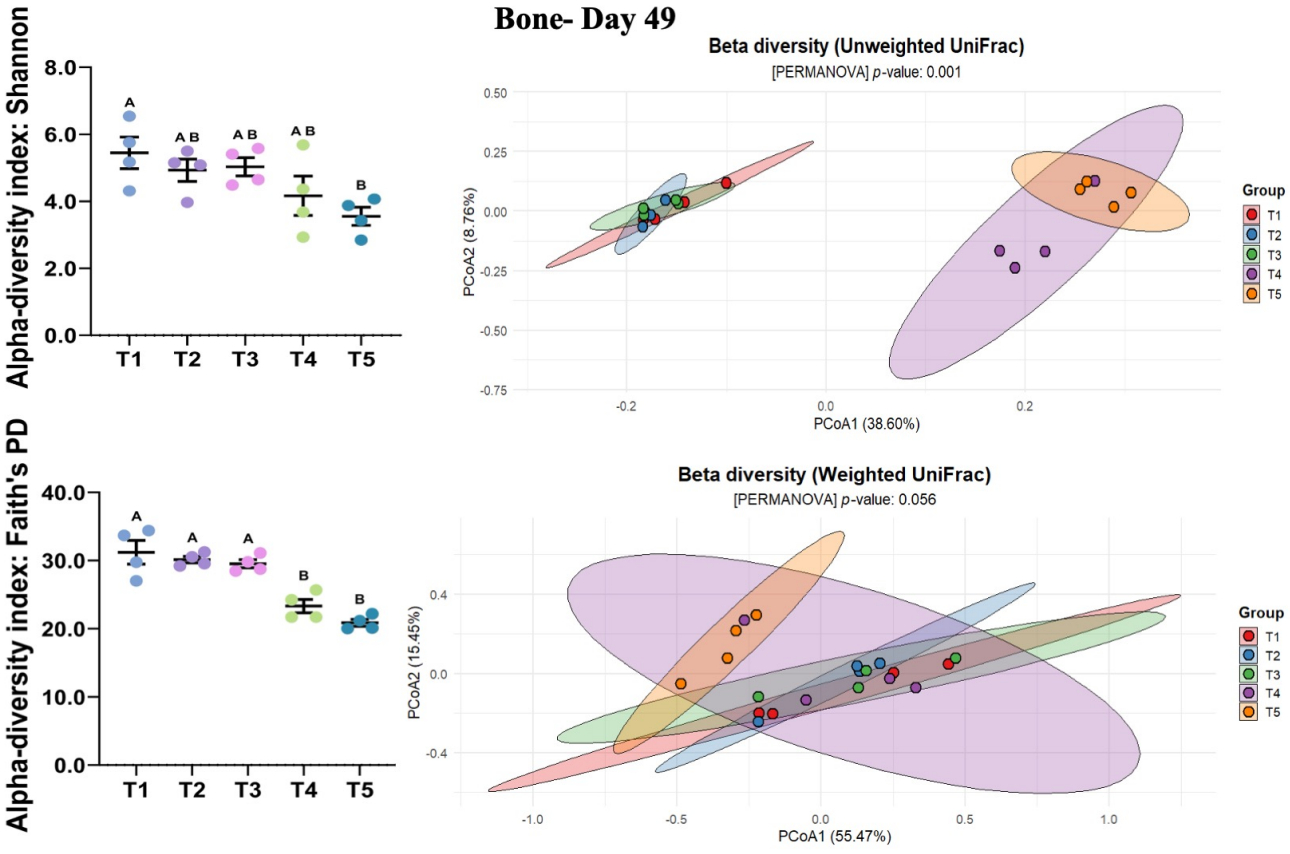

Figure 9.9 shows relative abundance of phyla in bone microbiome on d 49 of broiler chicken's treatments challenged with *Staphylococcus aureus* ($P < 0.05$). T1, non-challenged treatment; Treatment 2 (T2) was challenged with *Staphylococcus aureus* at 10^9 CFU orally on d 42; Treatment 3 (T3) was challenged with *Staphylococcus aureus* at 10^9 CFU orally on d 42, 43, and 44 respectively; Treatment 4 (T4) was challenged with *Staphylococcus aureus* at 10^7 CFU intraperitoneally on d 42; Treatment 5 (T5) was challenged with *Staphylococcus aureus* at 10^7 CFU intraperitoneally on d 42, 43, and 44 respectively ($P < 0.05$, N =4).

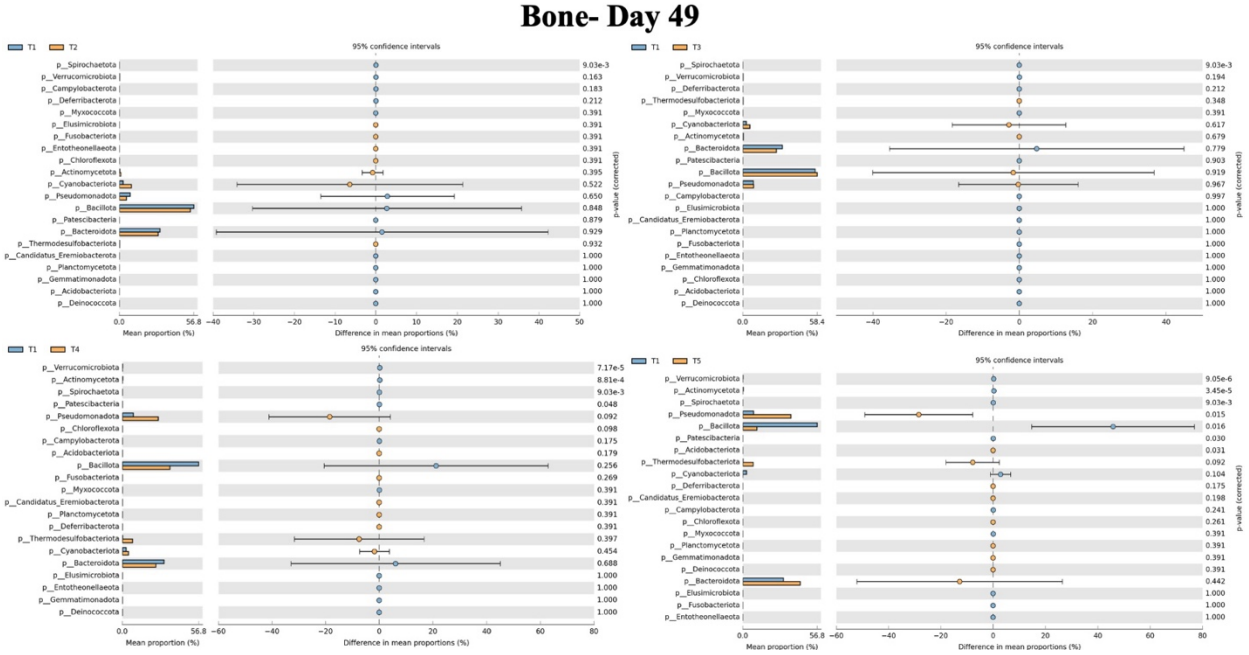

Figure 9.10 shows beta diversity parameters (unweighted and weighted UniFrac) in bone microbiome on d 56 of broiler chicken's treatments challenged with *Staphylococcus aureus* ($P < 0.05$). T1, non-challenged treatment; Treatment 2 (T2) was challenged with *Staphylococcus aureus* at 10^9 CFU orally on d 42; Treatment 3 (T3) was challenged with *Staphylococcus aureus* at 10^9 CFU orally on d 42, 43, and 44 respectively; Treatment 4 (T4) was challenged with *Staphylococcus aureus* at 10^7 CFU intraperitoneally on d 42; Treatment 5 (T5) was challenged with *Staphylococcus aureus* at 10^7 CFU intraperitoneally on d 42, 43, and 44 respectively ($P < 0.05$, N =4).

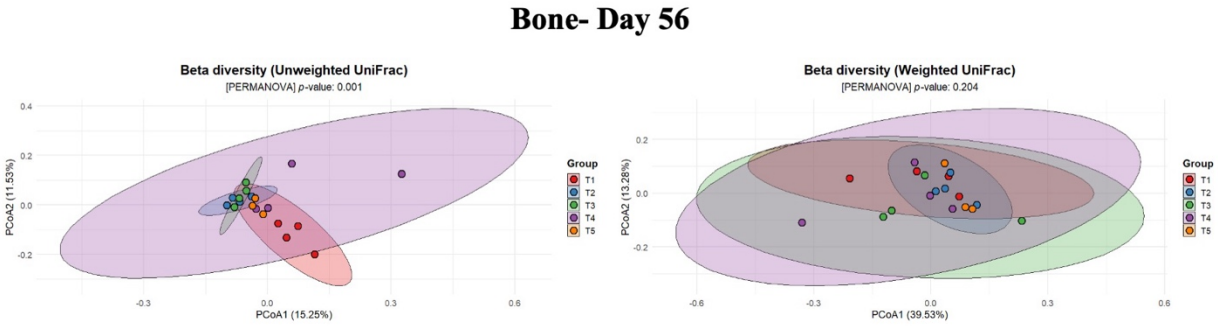

Figure 9.11 shows relative abundance of phyla in bone microbiome on d 56 of broiler chicken's treatments challenged with *Staphylococcus aureus* ($P < 0.05$). T1, non-challenged treatment; Treatment 2 (T2) was challenged with *Staphylococcus aureus* at 10^9 CFU orally on d 42; Treatment 3 (T3) was challenged with *Staphylococcus aureus* at 10^9 CFU orally on d 42, 43, and 44 respectively; Treatment 4 (T4) was challenged with *Staphylococcus aureus* at 10^7 CFU intraperitoneally on d 42; Treatment 5 (T5) was challenged with *Staphylococcus aureus* at 10^7 CFU intraperitoneally on d 42, 43, and 44 respectively ($P < 0.05$, N =4).

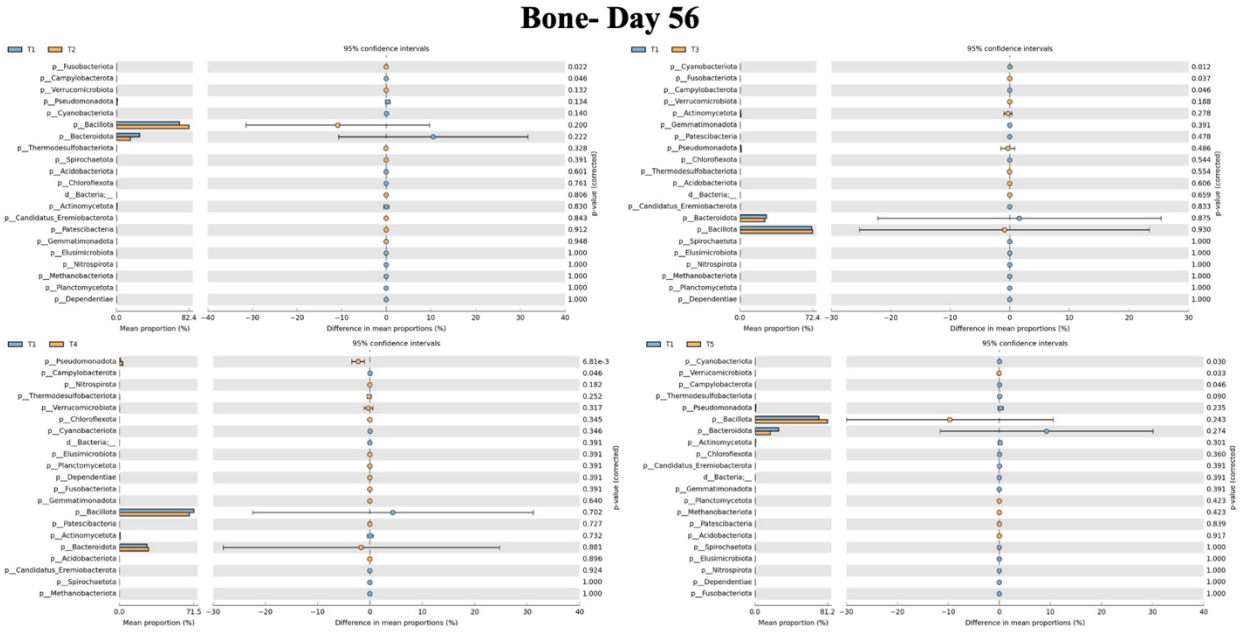

Figure 9.12 shows beta diversity parameters (unweighted and weighted UniFrac) in ceca microbiome on d 49 of broiler chicken's treatments challenged with *Staphylococcus aureus* ($P < 0.05$). T1, non-challenged treatment; Treatment 2 (T2) was challenged with *Staphylococcus aureus* at 10^9 CFU orally on d 42; Treatment 3 (T3) was challenged with *Staphylococcus aureus* at 10^9 CFU orally on d 42, 43, and 44 respectively; Treatment 4 (T4) was challenged with *Staphylococcus aureus* at 10^7 CFU intraperitoneally on d 42; Treatment 5 (T5) was challenged with *Staphylococcus aureus* at 10^7 CFU intraperitoneally on d 42, 43, and 44 respectively ($P < 0.05$, N =4).

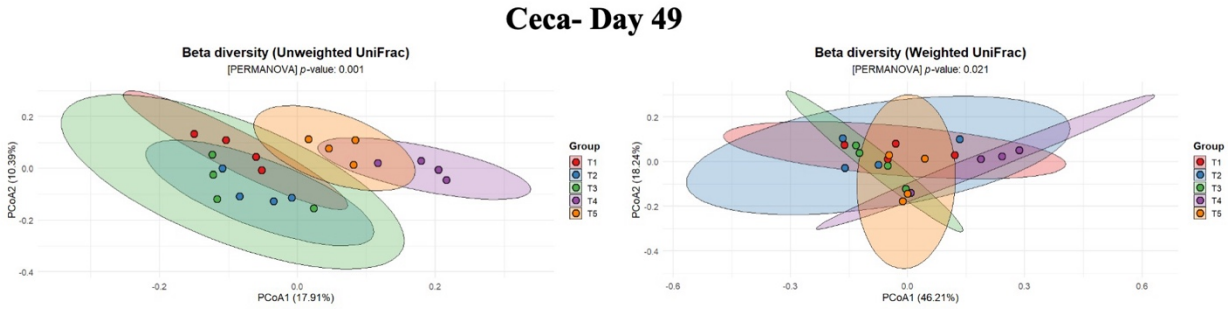

Figure 9.13 shows relative abundance of phyla in ceca microbiome on d 49 of broiler chicken's treatments challenged with *Staphylococcus aureus* ($P < 0.05$). T1, non-challenged treatment; Treatment 2 (T2) was challenged with *Staphylococcus aureus* at 10^9 CFU orally on d 42; Treatment 3 (T3) was challenged with *Staphylococcus aureus* at 10^9 CFU orally on d 42, 43, and 44 respectively; Treatment 4 (T4) was challenged with *Staphylococcus aureus* at 10^7 CFU intraperitoneally on d 42; Treatment 5 (T5) was challenged with *Staphylococcus aureus* at 10^7 CFU intraperitoneally on d 42, 43, and 44 respectively ($P < 0.05$, N =4).

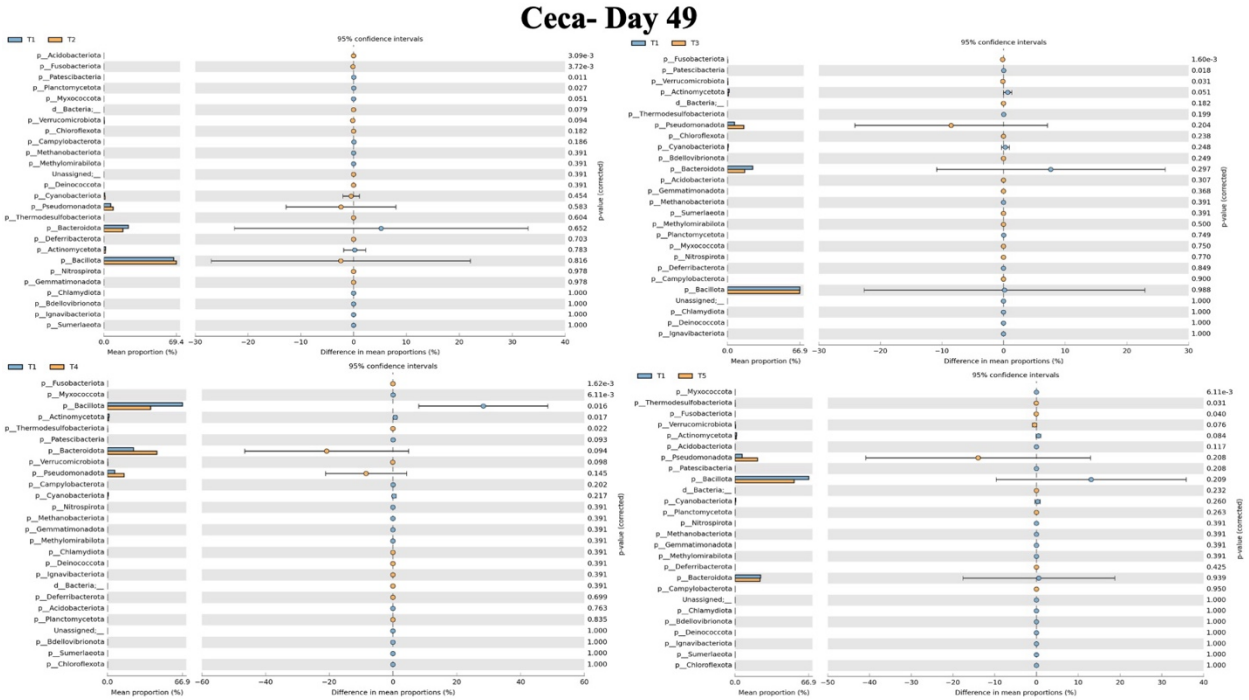

Figure 9.14 shows beta diversity parameters (unweighted and weighted UniFrac) in ceca microbiome on d 56 of broiler chicken's treatments challenged with *Staphylococcus aureus* ($P < 0.05$). T1, non-challenged treatment; Treatment 2 (T2) was challenged with *Staphylococcus aureus* at 10^9 CFU orally on d 42; Treatment 3 (T3) was challenged with *Staphylococcus aureus* at 10^9 CFU orally on d 42, 43, and 44 respectively; Treatment 4 (T4) was challenged with *Staphylococcus aureus* at 10^7 CFU intraperitoneally on d 42; Treatment 5 (T5) was challenged with *Staphylococcus aureus* at 10^7 CFU intraperitoneally on d 42, 43, and 44 respectively ($P < 0.05$, N =4).

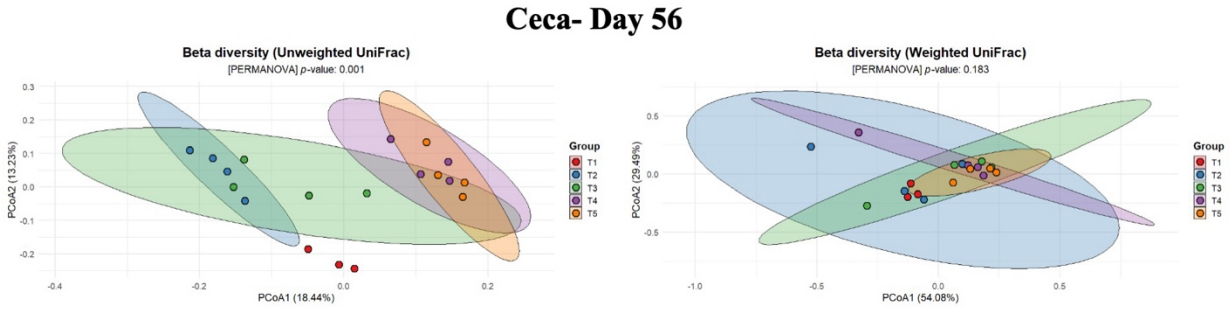

Figure 9.15 shows relative abundance of phyla in ceca microbiome on d 56 of broiler chicken's treatments challenged with *Staphylococcus aureus* ($P < 0.05$). T1, non-challenged treatment; Treatment 2 (T2) was challenged with *Staphylococcus aureus* at 10^9 CFU orally on d 42; Treatment 3 (T3) was challenged with *Staphylococcus aureus* at 10^9 CFU orally on d 42, 43, and 44 respectively; Treatment 4 (T4) was challenged with *Staphylococcus aureus* at 10^7 CFU intraperitoneally on d 42; Treatment 5 (T5) was challenged with *Staphylococcus aureus* at 10^7 CFU intraperitoneally on d 42, 43, and 44 respectively ($P < 0.05$, N =4).

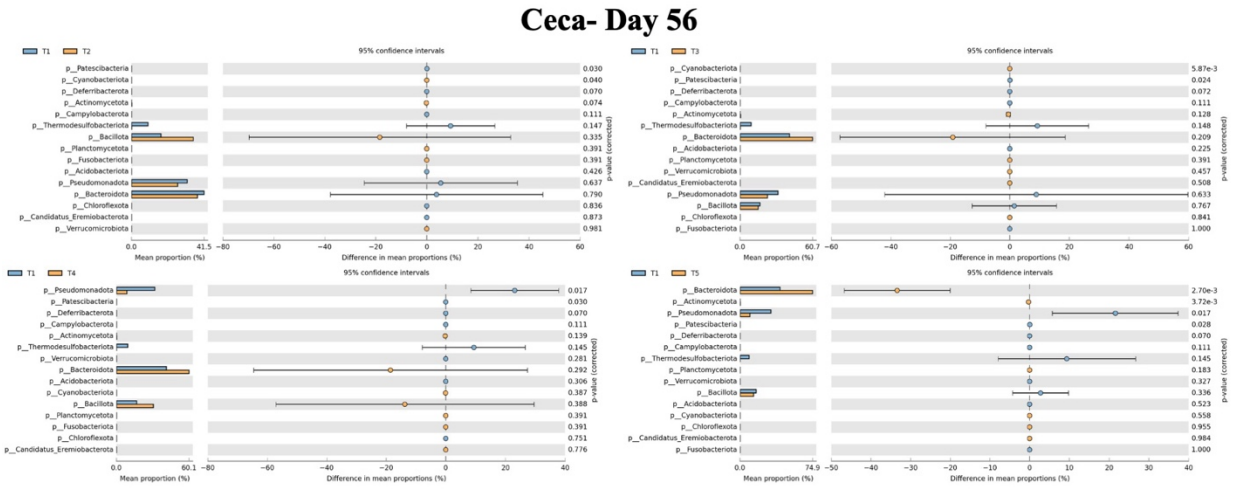

Figure 9.16 shows functional analysis of bone microbiome on d 49 of broiler chicken's treatments challenged with *Staphylococcus aureus* (T1 vs T2, T1 vs T3, T1 vs T4). T1, non-challenged treatment; Treatment 2 (T2) was challenged with *Staphylococcus aureus* at 10^9 CFU orally on d 42; Treatment 3 (T3) was challenged with *Staphylococcus aureus* at 10^9 CFU orally on d 42, 43, and 44 respectively; Treatment 4 (T4) was challenged with *Staphylococcus aureus* at 10^7 CFU intraperitoneally on d 42; Treatment 5 (T5) was challenged with *Staphylococcus aureus* at 10^7 CFU intraperitoneally on d 42, 43, and 44 respectively ($P < 0.05$, N =4).

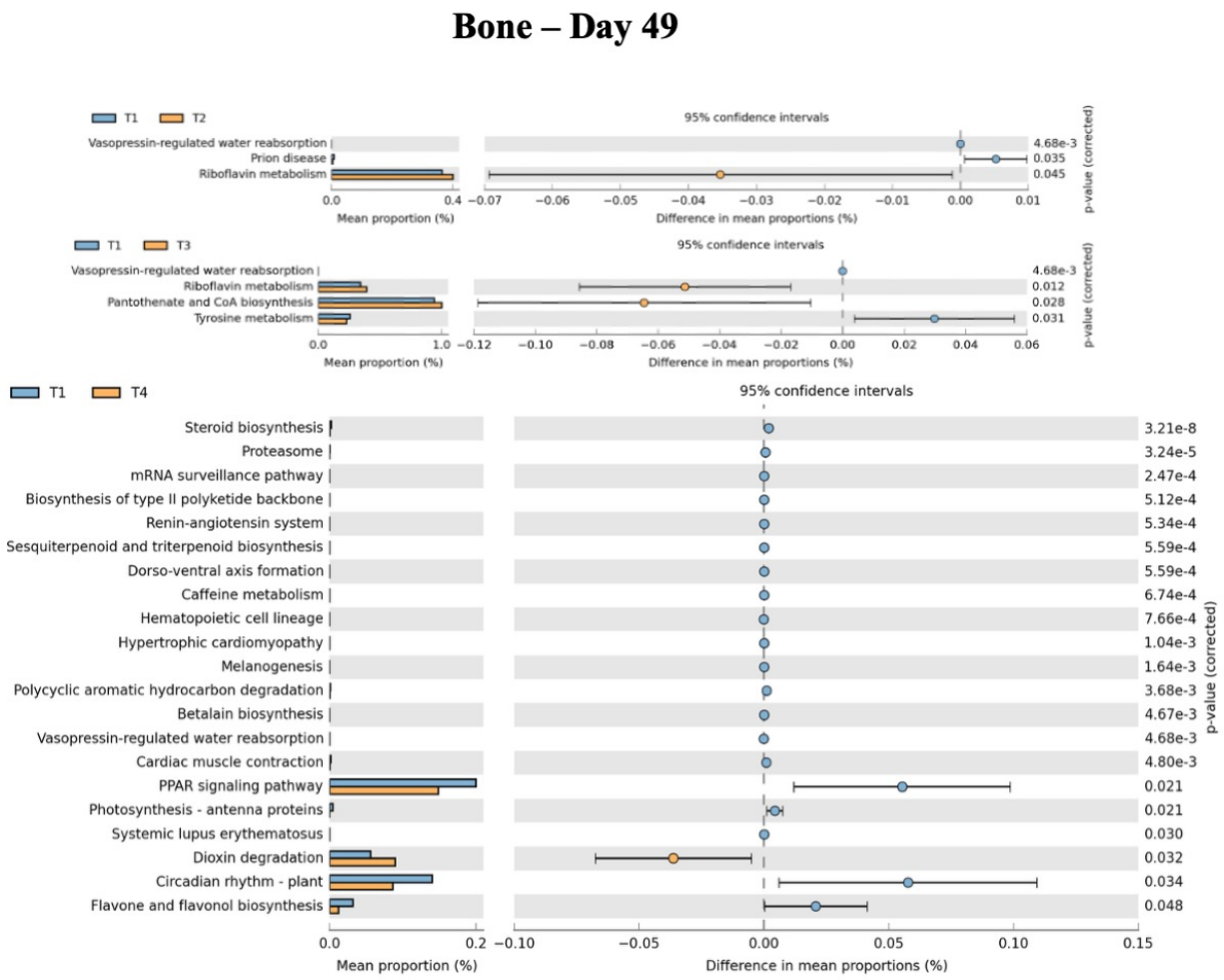

Figure 9.17 shows functional analysis of bone microbiome on d 49 broiler chicken's treatments challenged with *Staphylococcus aureus* (T1 vs T5). T1, non-challenged treatment; Treatment 2 (T2) was challenged with *Staphylococcus aureus* at 10^9 CFU orally on d 42; Treatment 3 (T3) was challenged with *Staphylococcus aureus* at 10^9 CFU orally on d 42, 43, and 44 respectively; Treatment 4 (T4) was challenged with *Staphylococcus aureus* at 10^7 CFU intraperitoneally on d 42; Treatment 5 (T5) was challenged with *Staphylococcus aureus* at 10^7 CFU intraperitoneally on d 42, 43, and 44 respectively ($P < 0.05$, N =4).

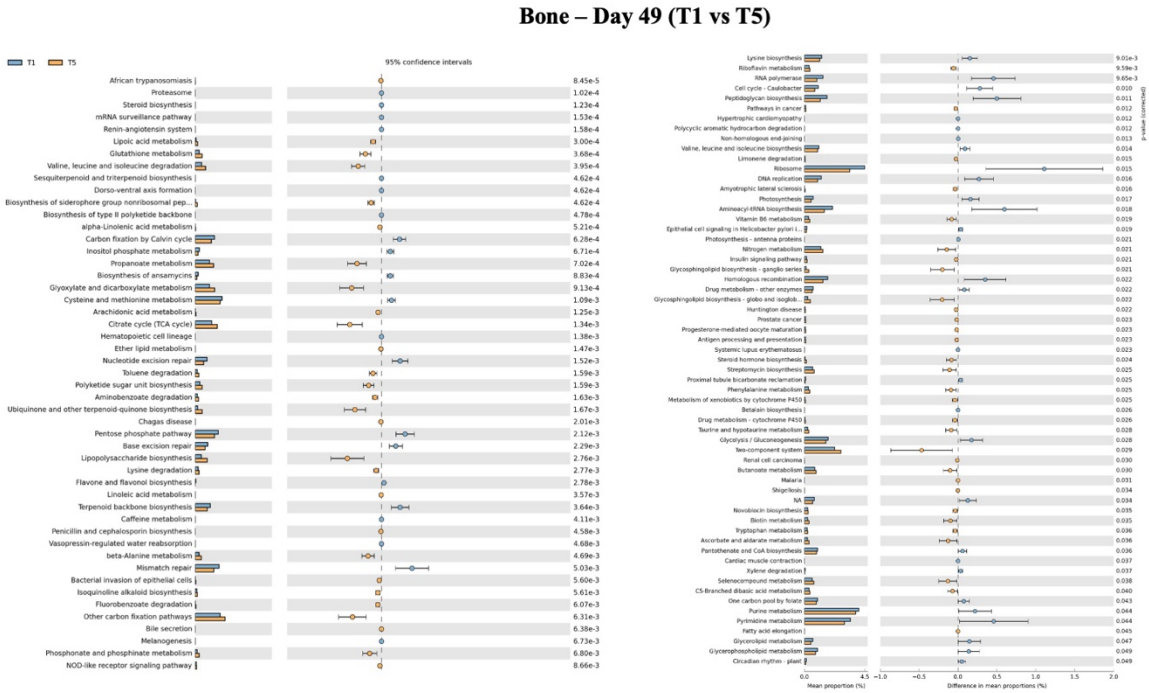

Figure 9.18 shows functional analysis of bone microbiome on d 56 broiler chicken's treatments challenged with *Staphylococcus aureus* (T1 vs T2, T1 vs T3). T1, non-challenged treatment; Treatment 2 (T2) was challenged with *Staphylococcus aureus* at 10^9 CFU orally on d 42; Treatment 3 (T3) was challenged with *Staphylococcus aureus* at 10^9 CFU orally on d 42, 43, and 44 respectively; Treatment 4 (T4) was challenged with *Staphylococcus aureus* at 10^7 CFU intraperitoneally on d 42; Treatment 5 (T5) was challenged with *Staphylococcus aureus* at 10^7 CFU intraperitoneally on d 42, 43, and 44 respectively ($P < 0.05$, N =4).

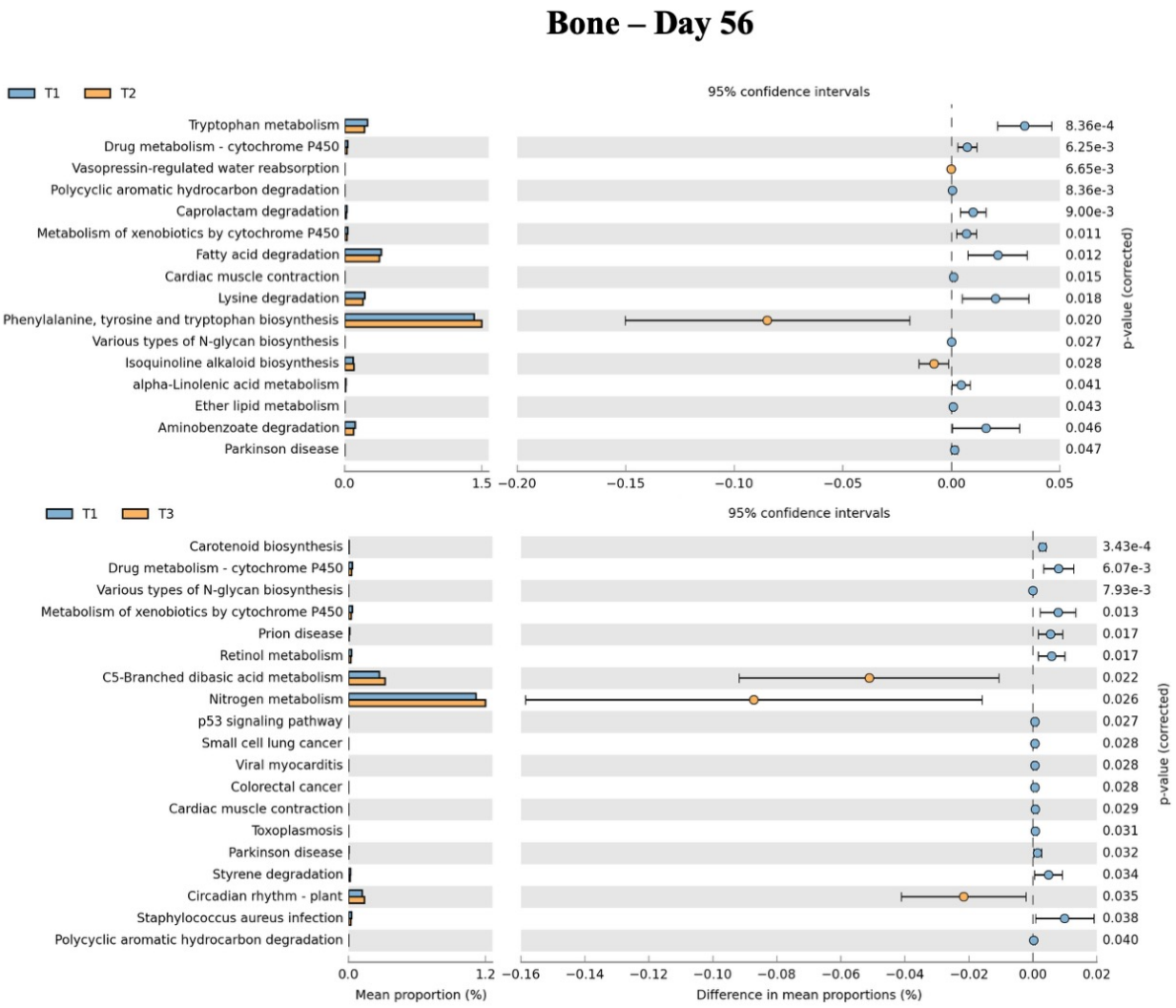

Figure 9.19 shows functional analysis of bone microbiome on d 56 broiler chicken's treatments challenged with *Staphylococcus aureus* (T1 vs T5). T1, non-challenged treatment; Treatment 2 (T2) was challenged with *Staphylococcus aureus* at 10^9 CFU orally on d 42; Treatment 3 (T3) was challenged with *Staphylococcus aureus* at 10^9 CFU orally on d 42, 43, and 44 respectively; Treatment 4 (T4) was challenged with *Staphylococcus aureus* at 10^7 CFU intraperitoneally on d 42; Treatment 5 (T5) was challenged with *Staphylococcus aureus* at 10^7 CFU intraperitoneally on d 42, 43, and 44 respectively ($P < 0.05$, N =4).

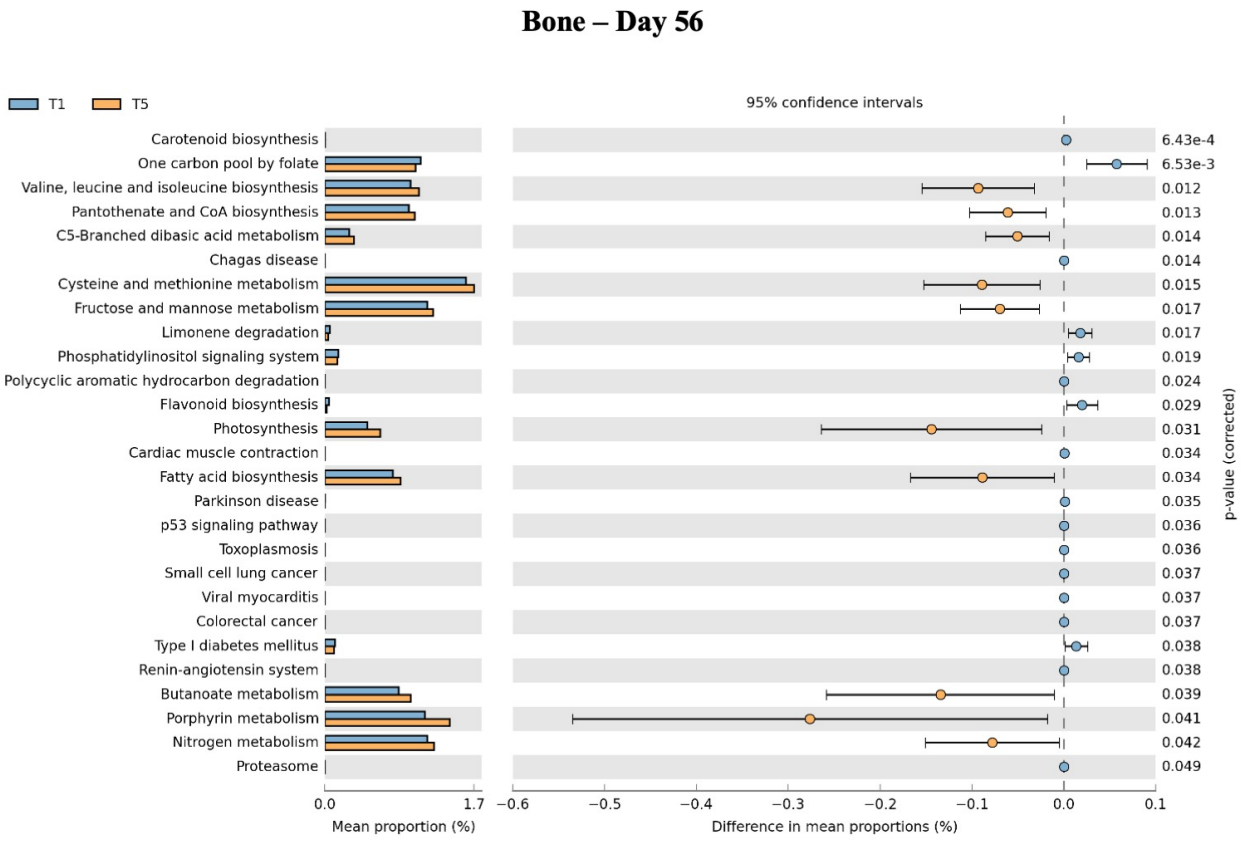

Figure 9.20 shows functional analysis of ceca microbiome on d 49 broiler chicken's treatments challenged with *Staphylococcus aureus* (T1 vs T2, T1 vs T3). T1, non-challenged treatment; Treatment 2 (T2) was challenged with *Staphylococcus aureus* at 10^9 CFU orally on d 42; Treatment 3 (T3) was challenged with *Staphylococcus aureus* at 10^9 CFU orally on d 42, 43, and 44 respectively; Treatment 4 (T4) was challenged with *Staphylococcus aureus* at 10^7 CFU intraperitoneally on d 42; Treatment 5 (T5) was challenged with *Staphylococcus aureus* at 10^7 CFU intraperitoneally on d 42, 43, and 44 respectively ($P < 0.05$, N =4).

Ceca – Day 49

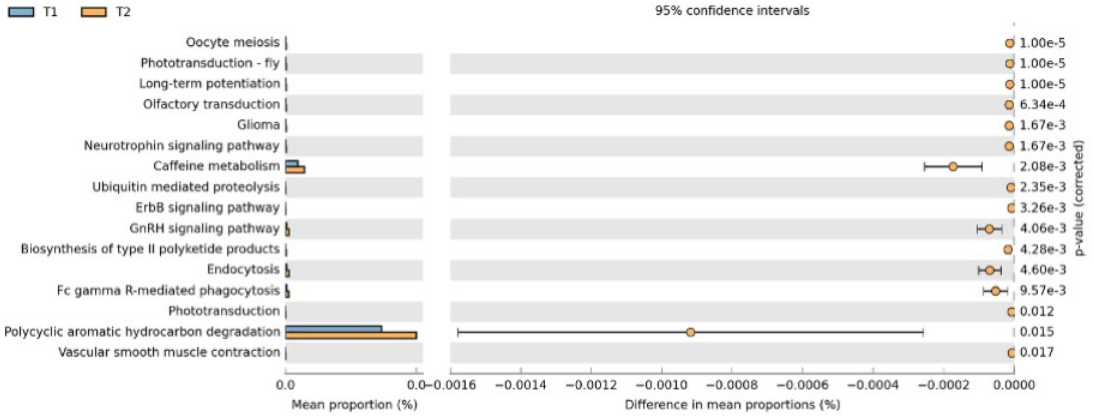
T1
T2
95% confidence intervals
Oocyte meiosis
Phototransduction - fly
Long-term potentiation
Olfactory transduction
Glioma
Neurotrophin signaling pathway
Caffeine metabolism
Ubiquitin mediated proteolysis
ErbB signaling pathway
GnRH signaling pathway
Biosynthesis of type II polyketide products
Endocytosis
Fc gamma R-mediated phagocytosis
Phototransduction
Polycyclic aromatic hydrocarbon degradation
Vascular smooth muscle contraction
1.00e-5
1.00e-5
1.00e-5
6.34e-4
1.67e-3
1.67e-3
2.08e-3
2.35e-3
3.26e-3
4.06e-3
4.28e-3
4.60e-3
9.57e-3
0.012
0.015
0.017
p-value (corrected)
0.0
0.0
−0.0016
−0.0014
−0.0012
−0.0010
−0.0008
−0.0006
−0.0004
−0.0002
0.0000
Mean proportion (%)
Difference in mean proportions (%)

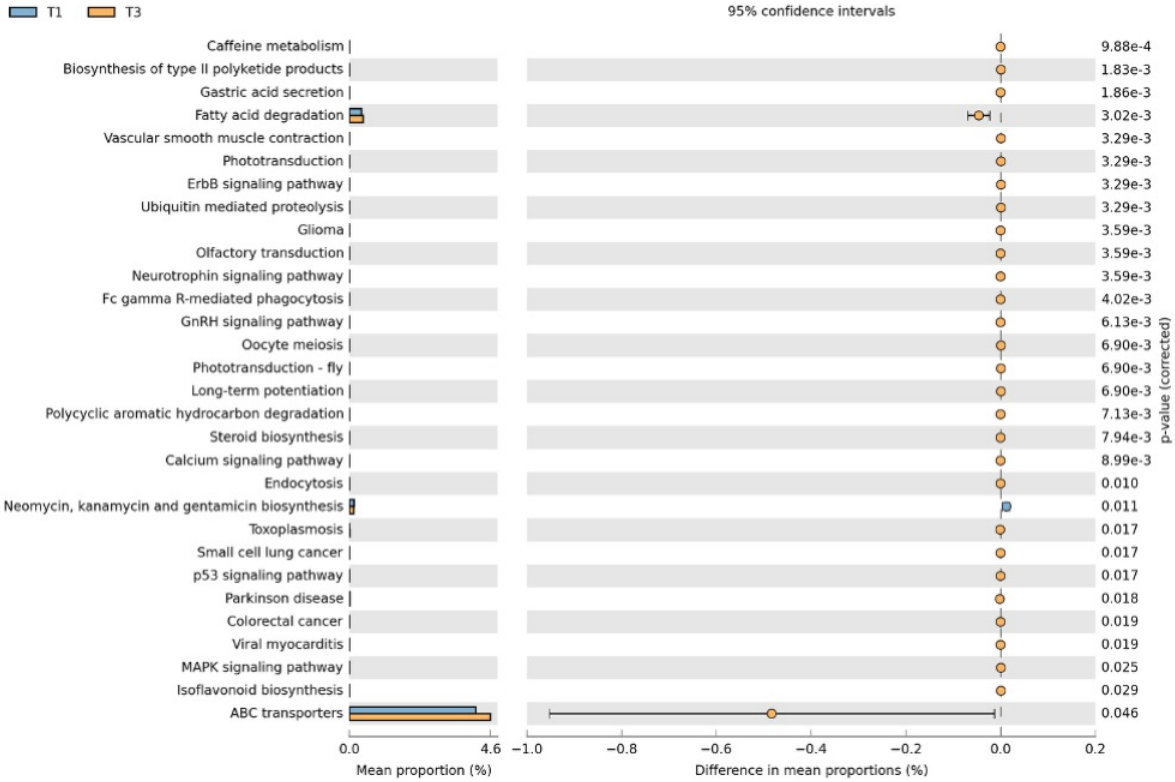
T1
T3
95% confidence intervals
Caffeine metabolism
Biosynthesis of type II polyketide products
Gastric acid secretion
Fatty acid degradation
Vascular smooth muscle contraction
Phototransduction
ErbB signaling pathway
Ubiquitin mediated proteolysis
Glioma
Olfactory transduction
Neurotrophin signaling pathway
Fc gamma R-mediated phagocytosis
GnRH signaling pathway
Oocyte meiosis
Phototransduction - fly
Long-term potentiation
Polycyclic aromatic hydrocarbon degradation
Steroid biosynthesis
Calcium signaling pathway
Endocytosis
Neomycin, kanamycin and gentamicin biosynthesis
Toxoplasmosis
Small cell lung cancer
p53 signaling pathway
Parkinson disease
Colorectal cancer
Viral myocarditis
MAPK signaling pathway
Isoflavonoid biosynthesis
ABC transporters
9.88e-4
1.83e-3
1.86e-3
3.02e-3
3.29e-3
3.29e-3
3.29e-3
3.29e-3
3.59e-3
3.59e-3
3.59e-3
4.02e-3
6.13e-3
6.90e-3
6.90e-3
6.90e-3
7.13e-3
7.94e-3
8.99e-3
0.010
0.011
0.017
0.017
0.017
0.018
0.019
0.019
0.025
0.029
0.046
p-value (corrected)
0.0
4.6
−1.0
−0.8
−0.6
−0.4
−0.2
0.0
0.2
Mean proportion (%)
Difference in mean proportions (%)

Figure 9.21 shows functional analysis of ceca microbiome on d 49 broiler chicken's treatments challenged with *Staphylococcus aureus* (T1 vs T4 and T1 vs T5). T1, non-challenged treatment; Treatment 2 (T2) was challenged with *Staphylococcus aureus* at 10^9 CFU orally on d 42; Treatment 3 (T3) was challenged with *Staphylococcus aureus* at 10^9 CFU orally on d 42, 43, and 44 respectively; Treatment 4 (T4) was challenged with *Staphylococcus aureus* at 10^7 CFU intraperitoneally on d 42; Treatment 5 (T5) was challenged with *Staphylococcus aureus* at 10^7 CFU intraperitoneally on d 42, 43, and 44 respectively ($P < 0.05$, N =4).

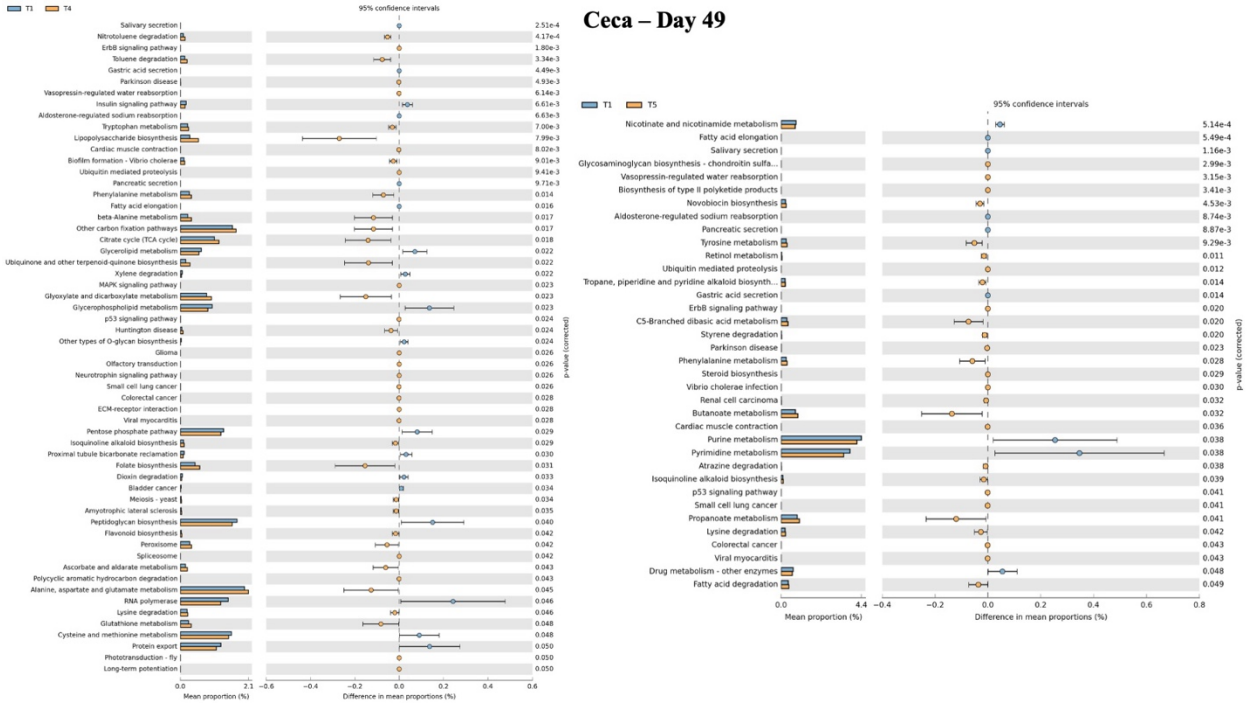

Figure 9.22 shows functional analysis of ceca microbiome on d 56 broiler chicken's treatments challenged with *Staphylococcus aureus* (T1 vs T5). T1, non-challenged treatment; Treatment 2 (T2) was challenged with *Staphylococcus aureus* at 10^9 CFU orally on d 42; Treatment 3 (T3) was challenged with *Staphylococcus aureus* at 10^9 CFU orally on d 42, 43, and 44 respectively; Treatment 4 (T4) was challenged with *Staphylococcus aureus* at 10^7 CFU intraperitoneally on d 42; Treatment 5 (T5) was challenged with *Staphylococcus aureus* at 10^7 CFU intraperitoneally on d 42, 43, and 44 respectively ($P < 0.05$, N =4).

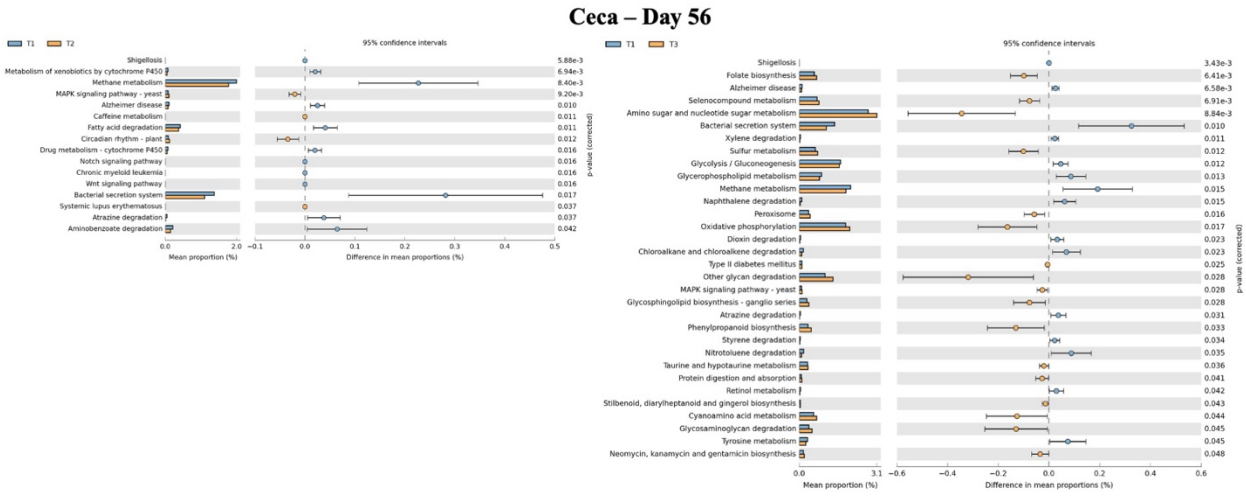

Figure 9.23 shows functional analysis of ceca microbiome on d 56 broiler chicken's treatments challenged with *Staphylococcus aureus* (T1 vs T4). T1, non-challenged treatment; Treatment 2 (T2) was challenged with *Staphylococcus aureus* at 10^9 CFU orally on d 42; Treatment 3 (T3) was challenged with *Staphylococcus aureus* at 10^9 CFU orally on d 42, 43, and 44 respectively; Treatment 4 (T4) was challenged with *Staphylococcus aureus* at 10^7 CFU intraperitoneally on d 42; Treatment 5 (T5) was challenged with *Staphylococcus aureus* at 10^7 CFU intraperitoneally on d 42, 43, and 44 respectively ($P < 0.05$, N =4).

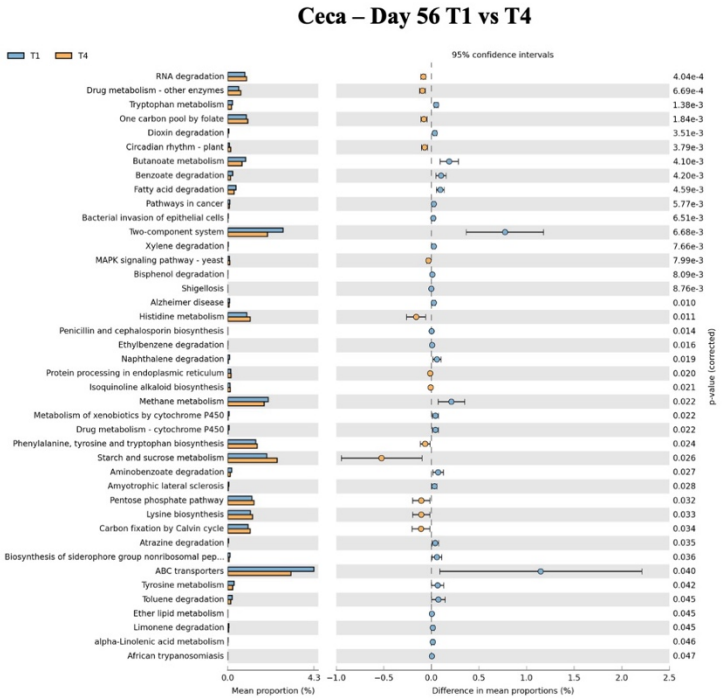

Figure 9.24 shows functional analysis of ceca microbiome on d 56 broiler chicken's treatments challenged with *Staphylococcus aureus* (T1 vs T5). T1, non-challenged treatment; Treatment 2 (T2) was challenged with *Staphylococcus aureus* at 10^9 CFU orally on d 42; Treatment 3 (T3) was challenged with *Staphylococcus aureus* at 10^9 CFU orally on d 42, 43, and 44 respectively; Treatment 4 (T4) was challenged with *Staphylococcus aureus* at 10^7 CFU intraperitoneally on d 42; Treatment 5 (T5) was challenged with *Staphylococcus aureus* at 10^7 CFU intraperitoneally on d 42, 43, and 44 respectively ($P < 0.05$, N =4).

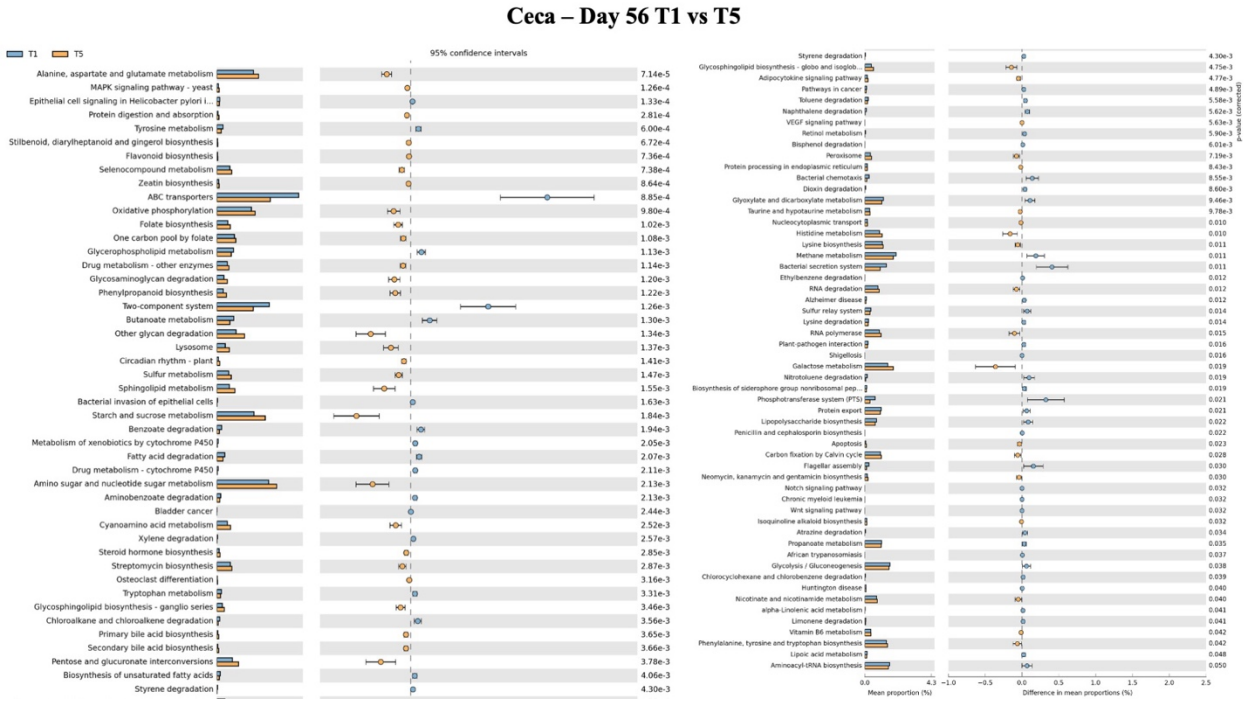

CHAPTER 10

DIETARY CURCUMIN MITIGATES BACTERIAL CHONDRONECROSIS AND OSTEOMYELITIS INDUCED BY *STAPHYLOCOCCUS AUREUS* IN MODERN-DAY BROILERS [1]

[1] Venkata Sesha Reddy Choppa, Venkata Prathap Reddy K, Sai Kumar Reddy R, Seshidhar Reddy G, Hamid Reza Rafieian Naeini, Hemanth Reddy Katha, Daniel Junpyo Lee, and Woo Kyun Kim.

To be submitted to Poultry Science.

ABSTRACT

Bacterial Chondronecrosis and Osteomyelitis (BCO) is a key cause of lameness in broilers which have economic and welfare perils. A commonly isolated pathogen which is involved in BCO pathogenesis is *Staphylococcus aureus*. For combating this global concern, phytogenic compounds like curcumin with anti-inflammatory and antimicrobial properties can be useful but the effects of this compound under bacterial challenge remain unclear. The current study focuses on the effect of dietary curcumin on bone health, systemic biomarkers, and pathogen load in broilers challenged with *S.aureus*. A total of 240 male broilers were selected on day 40 with an average gait score of 2 and were assigned to four treatments (6 replicates and 10 birds). T1 was non-challenged, other treatments (T2, T3, and T4) were challenged with 10^9 CFU *S.aureus*. Furthermore, T3 and T4 were supplemented with 200 and 400 ppm of curcumin in their respective diets. Growth performance, feed intake, BCO and gait scores, dual-energy X-ray absorptiometry (DEXA), femoral head micro-computed tomography (micro-CT), plasma lipopolysaccharides (LPS) and sclerostin (SOST), bacterial counts in femoral heads and ceca were assessed on days 49 and 56. Body weight gain and feed intake were not affected by neither challenge nor treatments ($P > 0.05$). Gait and BCO lesion scores were significantly reduced in curcumin treated groups. Micro-CT findings revealed curcumin supplementation (T3 and T4) improved trabecular microarchitecture (increased bone volume, trabecular thickness, and decreased porosity), increased bone mineral content observed from DEXA ($P < 0.05$). Plasma SOST was significantly lower in 200 ppm curcumin supplemented group. Moreover, cecal and bone *S. aureus* counts were significantly lower in curcumin-treated birds, particularly at 400 ppm ($P < 0.05$). In contrary, LPS concentrations were consistently higher on days 49 and 56 in curcumin-treated birds in 400 ppm suggesting a possible microbiota turnover which needs further studies. In summary, findings from dietary curcumin mitigate *S. aureus*-

induced bone deterioration and reduced bacterial load indicating improved welfare without affecting broiler's performance. This indicates curcumin role as cost-effective phytogenic supplement for alleviating BCO-induced lameness for a sustainable poultry production.

Keywords: broiler, *Staphylococcus aureus*, curcumin, BCO, bone health

INTRODUCTION

Bacterial chondronecrosis and osteomyelitis (BCO) is a prevalent bone disorder in modern fast-growing broilers leading to serious welfare and economic challenges (Choppa and Kim, 2023; Anthney et al., 2024). This was first observed in 1970s, which has now emerged as primary causes of lameness in broilers. Rampant genetic selection for growth and muscle yield has exceeded the skeletal development making broilers prone to microfractures (Wideman, 2016; Choppa and Kim, 2023). This allows the opportunistic pathogens to thrive, leading to necrotic bone lesions. BCO-related lameness and their associated economic losses were estimated to be $100 million in condemnations and performance losses (Anthney et al., 2024). Furthermore, field incidences were typically 1-2 % besides episodic epidemics with 15-60 % of the flock (Nääs et al., 2009; Gocsik et al., 2017). These alarming numbers underscore the need for addressing BCO to improve broilers health and poultry industry's sustainability.

Staphylococcus aureus has been predominantly implicated in BCO lesions and is considered as nidus of BCO lesions (Wideman, 2016; Cook et al., 2023). Additionally, other bacteria like *Enterococcus cecorum* and *Escherichia coli* are often recovered from infected bones (Wideman, 2016). Moreover, pathogenesis typically involves hematogenous spread where environmental or enteric bacteria translocate into bloodstream and colonize growth plate cartilage (McNamee and Smyth, 2000; Wideman, 2016). Progressive challenge often subclinical until advanced leads to osteonecrosis, inflammation, and irreversible locomotor disturbances. A comprehensive understanding of BCO requires evaluation of skeletal health besides bird's systemic inflammatory status. Invaluable tools like bone mineral density (BMD), bone mineral content (BMC), bone microarchitecture using dual-energy X-ray absorptiometry (DEXA) and micro-computed tomography (micro-CT) aids in unveiling bone health parameters (Schallier et

al., 2019; Chen and Kim, 2020). For instance, these parameters have revealed significant reductions under disease challenge conditions or models (Choppa et al., 2025a). Interestingly, advanced imaging has detected subclinical necrotic lesions in broiler femoral heads highlighting the sensitivity of these techniques for early skeletal damage (Ramser et al., 2024).

On the other hand, systemic biomarkers of inflammation and bone metabolism provide insight into BCO's pathogenesis. Furthermore, circulating lipopolysaccharides (LPS) which is an endotoxin released from gram negative bacterial flora which reflects the gut barrier dysfunction under stress or any challenge. The above phenomenon triggers systemic inflammation and potentially facilitating colonization of bone with opportunistic pathogens (Choppa and Kim, 2023; Perera et al., 2024; Choppa et al., 2025a). Furthermore, sclerostin (SOST), a protein released by osteocytes acts a marker which is involved in antagonism of Wnt signaling pathway thereby suppressing bone formation and healing (Dreyer et al., 2023; Choppa et al., 2025a). Hence, monitoring of LPS and SOST in BCO affected birds can reveal the degree of systemic inflammation and disrupted bone homeostasis following infection.

Mitigation strategies of BCO should aim at skeletal health besides alleviating strong systemic inflammatory response. One promising natural polyphenolic compound derived from *Curcuma longa* which is known for multifaceted bioactive potential is Curcumin. This compound is well documented and known for antioxidant and anti-inflammatory properties besides antimicrobial and immunomodulatory effects in poultry (Geevarghese et al., 2023; Zhang et al., 2024; Hernández-García et al., 2025; Pu et al., 2025). Dietary inclusion of curcumin has been reported to improve growth performance and favor gut microbiota and immune responses (Hernández-García et al., 2025). Additionally, antimicrobial properties of curcumin are also well recognized from the reports on broad spectrum antibacterial activity against gram-positive and

gram-negative pathogens by disrupting cell membranes and inhibiting microbial virulence factors (Dai et al., 2022). Curcumin's role in bone physiology through osteoblastogenesis and inhibition of osteoclastic activity which preserve bone mass made this bioactive compound emerge as natural bone-modulating agent (Inchingolo et al., 2022). Above properties together would suggest that curcumin can attenuate the pathophysiology of BCO.

Therapeutic potential of curcumin has been studied on poultry but research in presence of challenge or infection stress remains naïve. To elaborate, studies conducted in the absence of challenge stress revealed benefits represented in terms of improved antioxidant status, gut ecosystem, and meat quality but these results varied depending on the inclusion level (Hernández-García et al., 2025). Some studies reported a significant improvement in performance at low to moderate doses like 10-100 mg/kg feed with no additional benefit even with higher doses (200-2000 mg/kg feed) (Xie et al., 2019; Gumus et al., 2023; Guo et al., 2023; Fathi et al., 2024). In the present study, efficacy of dietary curcumin supplementation in alleviating BCO, inflammation, and bone deterioration in presence of *Staphylococcus aureus* challenge in broiler chickens is assessed. Furthermore, two inclusion levels (200 and 400 ppm) were tested to explore potential dose-dependent responses. Finally, the study aims at addressing knowledge gap on curcumin's protective role in bacterial induced lameness besides potential role of phytogenic dietary intervention's role in enhancing bone health and welfare in broiler production.

MATERIALS AND METHODS

Experimental design, broiler performance, sample collection

Current study was conducted following approval from Institutional Animal Care and Use Committee (A2024 06-021-A1) at Poultry Research Center, The University of Georgia. Four

treatments and six replicates in each treatment with 10 birds each were involved in the current study. Birds were fed with basal diets (Starter, grower and finisher diets) for all the treatments besides adlibitum water. On day 40, birds were selected based on gait scores ranging between 1 and 2 on day 40 which was followed by treatment assignment and bacterial challenge. Treatment 1 (T1) was non-challenged, Treatment 2 (T2) was challenged with *Staphylococcus aureus* at 10^9 CFU orally on day 42, 43, and 44. Treatment 3 (T3) and Treatment 4 (T4) were similarly challenged but treated with 200 ppm and 400 ppm of curcumin respectively. Current study used a commercially available preparation of curcumin (BulkSupplements, Henderson, NV, USA). *S. aureus* was isolated, prepared, and inoculated based on our previous study (Choppa et al., 2025b).

On day 40, initial body weights were recorded along with feed weights. Furthermore, on days 49 and 56 body weights and feed weights were recorded. Femur bones for micro computed tomography and plasma for ELISAs were collected on day 49 and 56. Furthermore, on day 49 and 56, gait and BCO scoring were assessed and recorded.

Dual-energy X-ray absorptiometry

Dual-energy X-ray absorptiometry (DEXA, GE healthcare, Chicago, IL) was conducted on days 49 and 56. Lunar prodigy (GE healthcare, encore software version 12.20.023) was used for analyzing total tissue weight, lean weight, body fat percentage, bone mineral density (BMD), and bone mineral content (BMC). Initially, Calibration of DEXA machine was conducted using with known BMD (Phantom). Birds were euthanized by cervical dislocation and positioned on the DEXA scanner platform with chest-up where scans were conducted similar to earlier studies at a speed of 2.5 mm/s with a voxel resolution of 0.07 x 0.07 x 0.50 mm (Chen et al., 2020; Tompkins et al., 2022).

Micro - Computed Tomography (Micro-CT)

Femur bones were collected on day 49 and 56 and stored at -20°C until analysis. After thawing, bones were placed in 50 mL tubes and secured using cheesecloth. Scanning was performed using Skyscan Micro-CT scanner (Skyscan 1275, Bruker microCT, Billerica, MA) under the following conditions like 77 kV, 129 μA, pixel size of 25 μm, and a 0.5 mm aluminum filter with a 180° scanning and a rotation at 0.4°, acquiring four images per rotation. Reconstruction of 2D images into 3D models was achieved using N-recon (Bruker microCT) software, followed by straightening with data viewer software (Bruker microCT). Region of interest (ROI) selection was performed using CTAn program (Bruker microCT). Bone mineral density calibration was performed using 0.25 and 0.75 g/cm^3 density phantoms using identical X-ray settings applied for scans. Cortical and trabecular separation was based on previous studies (Chen and Kim, 2020; Sharma et al., 2023; Shi et al., 2023).

Staphylococcus enumeration

Staphylococcus aureus counts in ceca and femur head were determined on days 49 and 56. Following necropsy, cecal and bone samples were aseptically collected into sterile filter bags *(Whirl Pak®, Nasco Sampling LLC, Chicago, IL, USA)*. The samples were diluted with 5 mL (Femoral head) and 10 mL (Ceca) of buffered peptone water (Himedia LLC, PA, USA). To facilitate bone homogenization, femoral heads were chopped into pieces prior transferring to filter bag and homogenizer (Neutec group Inc., Farmingdale, NY). Homogenized contents were transferred to sterile tubes which were serially diluted, and plated on Baird-Parker agar (BD DIFCO, NJ, USA) supplemented with 3.5 % potassium tellurite (Sigma, St louis, MO, USA) and egg yolk emulsion (Himedia laboratories, PA, USA). Plates were incubated for 24-36 hours at 37°C and *S. aureus* was enumerated in the plates.

Lipopolysaccharides and Sclerostin ELISA

Lipopolysaccharides and Sclerostin levels in plasma were measured using respective ELISA kits (MyBioSource, Inc. San Diego, CA, USA). Plasma samples were stored in -80°C until analysis and manufacturer's instructions were applied for sample processing and analysis.

Mineral Apposition Rate (MAR)

Mineral apposition rate (MAR) was based on our laboratory's established method for chickens (Tompkins et al., 2023; Choppa et al., 2025a). Calcein was first dissolved in 1 M sodium hydroxide and 2% working solution which was prepared by mixing sterile distilled water to the above calcein dissolved solution. Birds were injected with calcein intraperitoneally at 20 mg/kg body weight, administered in two doses with 4-day interval. On day 56, femur bones were collected and stored in 70% ethanol. At mid diaphysis, bones were sectioned into thin slices using a saw blade (Ryobi, Anderson, SC, USA). Sections were mounted on glass slide with slide-mounting medium (Fischer Scientific, Fair Lawn, NJ, USA). Fluorescent images (BZ-Z800, Keyence Inc., Itasca, IL) were obtained and distance between two fluorescent bands was measured using Image J software (National institute of Health, Bethesda, MD, USA).

Statistical Analysis

One way ANOVA was used to identify statistical significance among treatments and Tukey's HSD was used to separate means. Mean and standard errors were used to represent experimental data. The data analyzed was checked for normality and homogeneity of variances before applying above statistical methods on JMP Pro18 (SAS Institute, Inc., Cary, NC). Kruskal Wallis test and multiple comparisons using Steel-Dwass all pairs were applied for non-parametric data. *P*-value less than 0.05 was considered significant.

RESULTS

Body weight gain, feed intake

Average body weights recorded on the day of reallocation were made similar across the treatments. Data was not statistically different for body weight gain, feed intake. From day 40 to 49, treatments had weight gain of 1105.37, 1088.89, 1150.89, and 1170 grams for T1, T2, T3, and T4 respectively. Furthermore, from day 50 to 56, 837.78, 821.07, 944.53, and 814.59 grams for T1-T4 respectively **(Table 10.1)**. Similarly, average feed intake from day 40 to 49 was 1981.3, 1877.96, 1900.37, and 1968.52 grams for treatments (T1 to T4) respectively. Furthermore, from day 50 to 56, average feed intake for T1 to T4 were 1631.67, 1618, 1718.33, and 1708.25 grams respectively **(Table 10.1)**.

Dual-energy X-ray absorptiometry (DEXA)

No significant differences were observed for DEXA parameters on day 49 (**Table 10.2**). On day 56 results like bone mineral density (BMD), Tissue, Fat, and lean mass were not different but bone mineral contant (BMC) was 56.22, 52.07, 60.88, and 61.6 grams respectively for treatments (T1 to T4) ($P < 0.05$) **(Table 10.2)**.

Gait and BCO scoring

Gait scores on day 49 revealed a relatively higher average gait score of 2.83 for T2 compared to other treatments which had gait scores of 2.42 (T1 and T3) and 2.17 (T4). Furthermore, on day 56, T2 had highest average gait score of 2.88 compared to other treatments with gait scores of 2.29, 2.21, 2.08 for T1, T3, and T4 respectively (**Figure 10.1A)**.

On day 49, BCO scores were lower for T3 (0.33) compared to T1 (1) and T2 (0.79) ($P < 0.05$). On the other hand, treatment with higher curcumin levels (T4) had average BCO scores of

0.79 which is lower than T2 ($P < 0.05$) (**Figure 10.1B)**. Interestingly, on day 56, T1 (0.1), T3 (0.67), and T4 (0.3) had lower average BCO scores compared to T2 (1.42) ($P < 0.05$) (**Figure 10.1C)**.

Staphylococcus aureus counts in ceca and bone

On day 49, *S. aureus* counts in ceca were significantly higher for T2 and T3 compared to T4 with 2.76, 2.65, 1.6 Log10 CFU/g respectively ($P < 0.05$) (**Figure 10.2A)**. Moreover, bacterial counts in bone on day 49 were significantly lower for T1 and T4 compared to T2 with 1.39, 1.47, and 2.11 Log10 CFU/g respectively ($P < 0.05$) (**Figure 10.2B)**. Furthermore, on day 56, cecal counts for T3 (2.12 Log10 CFU/g) and T4 (1.76 Log10 CFU/g) were significantly lower compared to T2 (3.39 Log10 CFU/g) ($P < 0.05$) (**Figure 10.2C)**. On day 56, bone bacterial counts for T2 (2.76 Log10 CFU/g) were significantly higher compared to T1 (2.18 Log10 CFU/g) and T3 (2.01 Log10 CFU/g) where T4 had lowest counts with 1.49 Log10 CFU/g ($P < 0.05$) (**Figure 10.2D)**.

Lipopolysaccharides and Sclerostin levels

Day 49 plasma levels of LPS were significantly higher in T3 and T4 with levels of 153.91 and 155.82 ng/mL respectively compared to T1 (72.94 ng/mL) ($P < 0.05$) **(Figure 10.3A)**. Furthermore, LPS levels on day 56 revealed a significant decrease for T1 (107.29 ng/mL) compared to T4 (234.57 ng/mL) ($P < 0.05$) **(Figure 10.3B)**.

Sclerostin levels on day 56 for 200 ppm curcumin added treatment (T3) was significantly lower compared to T1 and T2. For T1, T2, and T3 were 453.47, 445.78, and 328 pg/mL respectively ($P < 0.05$) **(Figure 10.3C)**. Furthermore, day 49 sclerostin levels were not statistically significant but revealed a numerical decrease in levels for T1 and T3 with 464.67 and 466 pg/mL

respectively. (P > 0.05). Furthermore, T2 and T4 shown levels of 537.47 and 530 pg/mL respectively.

Micro-computed tomography

Statistically significant findings were not observed in cortical and total 3D parameters but trabecular 3d revealed interesting findings. Trabecular BMD for T2 was lesser than T1, T3, and T4 with BMD of 0.092, 0.117, 0.123, 0.117 g/cm^3 respectively (P < 0.05) (**Figure 10.4A)**. Percent bone volume which represents ratio between bone volume to tissue volume revealed a significantly lower percent for T2 (17.06 %) compared to other treatments (P < 0.05) (**Figure 10.4B)**. Furthermore, T1, T3, and T4 revealed 22.26, 21, 21.3 % respectively. Additionally, total porosity for T2 (0.47 %) was significantly greater than T1 (0.8 %), T3 (0.42 %), and T4 (0.43 %) (P < 0.05) (**Figure 10.4C)**. Moreover, trabecular thickness for T2 was significantly lower with 0.2093 μm compared to T1, T3, and T4 with 0.2273, 0.229, and 0.226 μm (P < 0.05) (**Figure 10.4D)**. In contrast, Trabecular separation for T2 was higher than T1 and T4 with a separation of 2.1917, 1.6014, and 1.4031 μm respectively (P < 0.05) (**Figure 10.4E)**.

Statistical Analyses

Data was represented in mean and standard error. Statistical significance within the treatments were analyzed with one way ANOVA and post hoc test like Tukey's HSD using JMP Pro 18 (JMP statistical discovery LLC, Cary, NC, USA). Data deviating from assumptions of ANOVA (Gait /BCO scores and non-normal data) were analyzed using Kruskal-Wallis test and Steel-Dwass all pairs. P-value was set to less than 0.05.

DISCUSSION

In the current study, *Staphylococcus aureus* challenge model and dietary inclusion of curcumin (200 and 400 ppm) aided in achieving higher body weight gains compared to unsupplemented controls. Interestingly, these body weight gains did not significantly differ among treatments suggesting curcumin doses used in the current study did not impair growth performance in the challenge conditions. These findings are similar to recent meta-analysis of 28 studies, which revealed a consistent higher growth rate and feed efficiency in broilers (Hernández-García et al., 2025). Enhanced performance with curcumin is often attributed to nutrient utilization, intestinal health. In the present study, curcumin's anti-inflammatory and antimicrobial properties likely reduced the physiological stress by allocating more energy for growth. Supportingly, curcumin supplementation overcome stress and challenge conditions like high stocking density and *Eimeria* by exhibiting responses like elevated antioxidant levels, immune status, and intestinal health (Chen et al., 2024; El-Gogary et al., 2025). Furthermore, microbial dynamics in challenged broilers will be altered in both cecal and bone tissue represented as decreased pathogen colonization and hematogenous spread. Curcumin's broad spectrum antimicrobial properties show their effect on *S. aureus* through several mechanisms like disrupting bacterial cell integrity, interference with quorum sensing mechanisms, and inhibition of virulence factors (Veselá et al., 2024). Furthermore, these actions likely alleviated domination of opportunistic pathogens thereby promoting healthier microbiota (El-Gogary et al., 2025). A study on heat-stressed broilers shown a decrease in intestinal pathogens like *E.coli* and *Proteus* with curcumin supplementation (Chen et al., 2024).

BCO-prone broilers often suffer bone loss, microfractures under infectious and inflammatory stress where improved bone density and integrity plays essential role (Choppa et al., 2025a). A major finding showing enhancement of bone mineralization was observed in curcumin

treated groups which is seen with DEXA measurements like bone mineral content compared to challenged control group. This effect was concomitantly observed with micro-CT analysis of femur head where curcumin fed broilers (T3 and T4) reveals an improved bone microstructure with higher trabecular bone volume and thickness and lower cortical porosity compared to untreated challenged birds (T2). Furthermore, curcumin treatment has been shown to regulate osteoblastogenesis and differentiation, contributing to increased bone formation besides suppressing osteoclastogenesis (Wang, 2024). Above data indicate and align with natural compounds like curcumin's role in preserving skeletal integrity in *S. aureus* infection. Importantly, bone homeostasis is associated with key regulating marker called sclerostin which was significantly reduced in 200 ppm curcumin treated group compared to control. Sclerostin is a potent osteocyte-derived Wnt/beta-catenin pathway inhibitor which is reflected as decreased bone formation and is linked to bone loss (Marini et al., 2023). In the current challenge study, control birds likely experienced inflammation induced bone aberration which is seen with elevated sclerostin. Lower sclerostin levels for 200 ppm curcumin treated birds suggests alleviated inhibitory effects on Wnt signaling, thereby promoting bone formation. Our previous study on LPS suggests decreasing sclerostin levels helps in maintaining bone homeostasis (Choppa et al., 2023, 2025a). Reduced sclerostin in curcumin (200 ppm) treated birds permit greater Wnt/beta-catenin activity, promoting mineral deposition, explaining higher BMC. Surprisingly, increasing curcumin dose to 400 ppm did not suppress sclerostin any further, which possibly indicating no additional benefit with respect to sclerostin with increasing dose. Furthermore, invitro studies on high curcumin levels suppress osteogenic differentiation via microRNAs and respective feedback mechanisms (Li et al., 2019). This could be due to hydrophobic nature and bioavailability plateaus at higher doses (Sureshbabu et al., 2023). Additionally, moderate curcumin levels (200 ppm)

optimally activate anti-inflammatory and osteogenic pathways, but additional increase might not amplify these pathways. Despite this, 200 and 400 ppm were effective, but 400 ppm did improve BMC, so this dose did not inhibit bone formation. Hence, both doses of curcumin (200 and 40 ppm) revealed a dose-related responses, but 200 ppm had greater improvement relative to control whereas effects from 400 ppm were similar or slightly exceeded the metrics of 200 ppm. This provides a valuable cost-effective information for industry application.

The improvement in bone mass can be reflected in reduction in lameness and BCO lesion severity. Curcumin-fed treatments significantly lowered gait and BCO scores than T2 (non-supplemented but challenged). These findings are particularly essential for welfare of broilers, as BCO-linked lameness is a leading cause of chronic pain and condemnations in broiler flocks (Choppa and Kim, 2023). Results from the current study is consistent with previous studies with supplements like Vitamin D3, probiotics decreased BCO incidence (Wideman Jr et al., 2015; Perera et al., 2024). LPS levels in the current study revealed 2-fold higher LPS concentrations for Curcumin treated birds (200 and 400 ppm) than unchallenged control on day 49. Interestingly, 400 ppm group has elevated endotoxin levels remained same by day 56. Curcumin generally plays dose-dependent protective roles on gut by strengthening tight junctions thereby preventing endotoxin leakage and LPS-induced intestinal damage (Ruan et al., 2022; Reisinger et al., 2024). A moderate curcumin levels (100 ppm) in a study, shows enhanced gut integrity in *Eimeria* challenged birds. Contrasting levels of LPS in the present study could be due to curcumin's antimicrobial properties which leads to massive turnover of microbiota (possible replacement of gram-negative bacteria). Additionally, curcumin could suppress early pro-inflammatory signals. Findings in the current study shows curcumin's role in gut health can become context-dependent where *S. aureus* challenge and high dose of curcumin (400 ppm) would induce microbiota and

immune shifts that increase endotoxin exposure. Further investigation might be needed to determine whether this effect is transient or because of microbiota turnover.

Future research can use findings from the current study in conducting long term trials across various management systems to determine effects under commercial conditions. Additionally, it would be beneficial to study effects with timing of supplementation and synergistic effects when combined with nutraceuticals.

CONCLUSION

Current study shows dietary supplementation of curcumin mitigates *Staphylococcus aureus* challenge induced bacterial chondronecrosis and osteomyelitis (BCO) in broiler chickens. Both levels of curcumin improved bone mineral content and trabecular microarchitecture. Furthermore, decreased bacterial colonization, gait and BCO lesion scores which indicates improved welfare. Moreover, curcumin at 200 ppm modulated bone metabolic markers which was observed with plasma concentrations of sclerostin suggesting suppression of Wnt/beta-catenin signaling. Although LPS levels were elevated in higher (400 ppm) curcumin treated groups, outcomes were not affected. In summary, these findings emphasize the role of curcumin as a considerable phytogenic strategy against challenge induced BCO. This can be extended into commercial settings when validated with studies involving dose and time dependent responses besides identifying synergistic combinations with other nutraceuticals.

REFERENCES

Anthney, A., A. D. T. Do, and A. A. K. Alrubaye. 2024. Bacterial chondronecrosis with osteomyelitis lameness in broiler chickens and its implications for welfare, meat safety, and quality: a review. Front Physiol 15:1452318.

Chen, C., and W. K. Kim. 2020. The application of micro-CT in egg-laying hen bone analysis: introducing an automated bone separation algorithm. Poult Sci 99:5175–5183.

Chen, Y., L. Liu, L. Yu, S. Li, N. Zhu, and J. You. 2024. Curcumin supplementation improves growth performance and anticoccidial index by improving the antioxidant capacity, inhibiting inflammatory responses, and maintaining intestinal barrier function in Eimeria tenella-infected broilers. Animals 14:1223.

Chen, C., B. Turner, T. J. Applegate, G. Litta, and W. K. Kim. 2020. Role of long-term supplementation of 25-hydroxyvitamin D3 on laying hen bone 3-dimensional structural development. Poult Sci 99:5771–5782.

Choppa, V. S. R., and W. K. Kim. 2023. A Review on Pathophysiology, and Molecular Mechanisms of Bacterial Chondronecrosis and Osteomyelitis in Commercial Broilers. Biomolecules 13:1032.

Choppa, V. S. R., G. Liu, H. Shi, M. K. Sharma, D. Goo, and W. K. Kim. 2025a. Effect of lipopolysaccharides and mixed Eimeria spp. challenge on performance and bone development in broilers. Poult Sci:105501.

Choppa, V. S. R., G. Liu, Y. H. Tompkins, and W. K. Kim. 2023. Altered Osteogenic Differentiation in Mesenchymal Stem Cells Isolated from Compact Bone of Chicken Treated with Varying Doses of Lipopolysaccharides. Biomolecules 13:1626.

Choppa, V. S. R., H. R. R. Naeini, D. J. Lee, H. R. Katha, H. Ko, D. Paneru, Y. Kim, and W. K. Kim. 2025b. Effect of Eimeria spp. and Staphylococcus aureus challenge on cecal microbiome in broilers. Poult Sci:105814.

Cook, J., E. S. Greene, A. Ramser, G. Mullenix, J. S. Dridi, R. Liyanage, R. Wideman, and S. Dridi. 2023. Comparative-and network-based proteomic analysis of bacterial chondronecrosis with osteomyelitis lesions in broiler's proximal tibiae identifies new molecular signatures of lameness. Sci Rep 13:5947.

Dai, C., J. Lin, H. Li, Z. Shen, Y. Wang, T. Velkov, and J. Shen. 2022. The natural product curcumin as an antibacterial agent: Current achievements and problems. Antioxidants 11:459.

Dreyer, T. J., J. A. C. Keen, L. M. Wells, and S. J. Roberts. 2023. Novel insights on the effect of sclerostin on bone and other organs. Journal of Endocrinology 257.

El-Gogary, M. R., T. M. Dorra, and I. A. El-Sayed. 2025. Impact of dietary supplementation levels of turmeric powder (curcuma longa) on performance, carcass characteristics, blood biochemical, jejunum histological and gut microflora in broiler chickens. Journal of Animal and Poultry Production 16:7–13.

Fathi, M., V. Rezaee, K. Zarrinkavyani, and P. Mardani. 2024. The impact of curcumin nanoparticles (CurNPs) on growth performance, antioxidant indices, blood biochemistry, gut morphology and cecal microbial profile of broiler chickens. Acta Agriculturae Scandinavica, Section A—Animal Science 73:10–21.

Geevarghese, A. V, F. B. Kasmani, and S. Dolatyabi. 2023. Curcumin and curcumin nanoparticles counteract the biological and managemental stressors in poultry production: An updated review. Res Vet Sci 162:104958.

Gocsik, É., A. M. Silvera, H. Hansson, H. W. Saatkamp, and H. J. Blokhuis. 2017. Exploring the economic potential of reducing broiler lameness. Br Poult Sci 58:337–347.

Gumus, R., A. Ozbilgin, G. S. Urcar, and K. Kara. 2023. Effects of Dietary Resveratrol and Curcumin Supplements on Meat Quality and Storage Time in Broilers. Brazilian Journal of Poultry Science 25:eRBCA-2023.

Guo, S., J. Hu, S. Ai, L. Li, B. Ding, D. Zhao, L. Wang, and Y. Hou. 2023. Effects of pueraria extract and curcumin on growth performance, antioxidant status and intestinal integrity of broiler chickens. Animals 13:1276.

Hernández-García, P. A., L. D. Granados-Rivera, J. F. Orzuna-Orzuna, G. Vázquez-Silva, C. Díaz-Galván, and P. B. Razo-Ortíz. 2025. Meta-Analysis of dietary curcumin supplementation in broiler chickens: growth performance, antioxidant status, intestinal morphology, and meat quality. Antioxidants 14:460.

Inchingolo, A. D., A. M. Inchingolo, G. Malcangi, P. Avantario, D. Azzollini, S. Buongiorno, F. Viapiano, M. Campanelli, A. M. Ciocia, and N. De Leonardis. 2022. Effects of resveratrol, curcumin and quercetin supplementation on bone metabolism—a systematic review. Nutrients 14:3519.

Li, H., L. Yue, H. Xu, N. Li, J. Li, Z. Zhang, and R. C. Zhao. 2019. Curcumin suppresses osteogenesis by inducing miR-126a-3p and subsequently suppressing the WNT/LRP6 pathway. Aging (Albany NY) 11:6983.

Marini, F., F. Giusti, G. Palmini, and M. L. Brandi. 2023. Role of Wnt signaling and sclerostin in bone and as therapeutic targets in skeletal disorders. Osteoporosis International 34:213–238.

McNamee, P. T., and J. A. Smyth. 2000. Bacterial chondronecrosis with osteomyelitis ('femoral head necrosis') of broiler chickens: A review. Avian Pathology 29:253–270 Available at https://doi.org/10.1080/03079450050118386.

Nääs, I. A., I. C. L. A. Paz, M. S. Baracho, A. G. Menezes, L. G. F. Bueno, I. C. L. Almeida, and D. J. Moura. 2009. Impact of lameness on broiler well-being. Journal of Applied Poultry Research 18:432–439.

Perera, R., K. Alharbi, A. Hasan, A. Asnayanti, A. Do, A. Shwani, R. Murugesan, S. Ramirez, M. Kidd, and A. A. K. Alrubaye. 2024. Evaluating the Impact of the PoultryStar® Bro Probiotic on the Incidence of Bacterial Chondronecrosis with Osteomyelitis Using the Aerosol Transmission Challenge Model. Microorganisms 12:1630.

Pu, X., Y. Liang, J. Lian, M. Xu, Y. Yong, H. Zhang, L. Zhang, and J. Zhang. 2025. Effects of dietary dihydroartemisinin on growth performance, meat quality, and antioxidant capacity in broiler chickens. Poult Sci 104:104523.

Ramser, A., E. S. Greene, R. Wideman, and S. Dridi. 2024. Potential non-invasive detection of lesions in broiler femur heads: application of the DXA imaging system. Front Physiol 15:1363992.

Reisinger, N., B. Doupovec, T. Czabany, F. Van Immerseel, S. Croubels, and G. Antonissen. 2024. Endotoxin Translocation Is Increased in Broiler Chickens Fed a Fusarium Mycotoxin-Contaminated Diet. Toxins (Basel) 16:167.

Ruan, D., S. Wu, A. M. Fouad, Y. Zhu, W. Huang, Z. Chen, Z. Gou, Y. Wang, Y. Han, and S. Yan. 2022. Curcumin alleviates LPS-induced intestinal homeostatic imbalance through reshaping gut microbiota structure and regulating group 3 innate lymphoid cells in chickens. Food Funct 13:11811–11824.

Schallier, S., C. Li, J. Lesuisse, G. P. J. Janssens, N. Everaert, and J. Buyse. 2019. Dual-energy X-ray absorptiometry is a reliable non-invasive technique for determining whole body composition of chickens. Poult Sci 98:2652–2661.

Sharma, M. K., G. Liu, D. L. White, Y. H. Tompkins, and W. K. Kim. 2023. Graded levels of Eimeria challenge altered the microstructural architecture and reduced the cortical bone growth of femur of Hy-Line W-36 pullets at early stage of growth (0–6 wk of age). Poult Sci 102:102888.

Shi, H., J. Wang, D. White, O. J. T. Martinez, and W. K. Kim. 2023. Impacts of phytase and coccidial vaccine on growth performance, nutrient digestibility, bone development, and intestinal gene expression of broilers fed a nutrient reduced diet. Poult Sci 102:103062.

Sureshbabu, A., E. Smirnova, A. Karthikeyan, M. Moniruzzaman, S. Kalaiselvi, K. Nam, G. Le Goff, and T. Min. 2023. The impact of curcumin on livestock and poultry animal's performance and management of insect pests. Front Vet Sci 10:1048067.

Tompkins, Y. H., C. Chen, K. M. Sweeney, M. Kim, B. H. Voy, J. L. Wilson, and W. K. Kim. 2022. The effects of maternal fish oil supplementation rich in n-3 PUFA on offspring-broiler growth performance, body composition and bone microstructure. PLoS One 17:e0273025.

Tompkins, Y. H., J. Choi, P.-Y. Teng, M. Yamada, T. Sugiyama, and W. K. Kim. 2023. Reduced bone formation and increased bone resorption drive bone loss in Eimeria infected broilers. Sci Rep 13:616.

Veselá, K., Z. Kejík, N. Abramenko, R. Kaplánek, M. Jakubek, and J. Petrlova. 2024. Investigating antibacterial and anti-inflammatory properties of synthetic curcuminoids. Front Med (Lausanne) 11:1478122.

Wang, K. 2024. The potential therapeutic role of curcumin in osteoporosis treatment: based on multiple signaling pathways. Front Pharmacol 15:1446536.

Wideman, R. F. 2016. Bacterial chondronecrosis with osteomyelitis and lameness in broilers: a review. Poult Sci 95:325–344 Available at https://www.sciencedirect.com/science/article/pii/S0032579119321534.

Wideman Jr, R. F., J. Blankenship, I. Y. Pevzner, and B. J. Turner. 2015. Efficacy of 25-OH vitamin D3 prophylactic administration for reducing lameness in broilers grown on wire flooring. Poult Sci 94:1821–1827.

Xie, Z., G. Shen, Y. Wang, and C. Wu. 2019. Curcumin supplementation regulates lipid metabolism in broiler chickens. Poult Sci 98:422–429.

Zhang, J., R. Zhang, S. Jin, and X. Feng. 2024. Curcumin, a plant polyphenol with multiple physiological functions of improving antioxidation, anti-inflammation, immunomodulation and its application in poultry production. J Anim Physiol Anim Nutr (Berl) 108:1890–1905.

Table 10.1 illustrates the effects of treatments (curcumin supplementation and *Staphylococcus aureus* challenge) on body performance parameters like body weight gain and feed intake for day 40-49 and day 50-56) ($P > 0.05$).

[1] T1, non-challenged treatment; Treatment 2 (T2) was challenged with *Staphylococcus aureus* at 10^9 CFU orally on days 42, 43, and 44; Treatment 3 (T3) was challenged with *Staphylococcus aureus* at 10^9 CFU orally on day 42, 43, and 44 respectively and 200 ppm of curcumin in the diet; Treatment 4 (T4) was challenged with *Staphylococcus aureus* at 10^9 CFU orally on day 42, 43, and 44 respectively and 400 ppm of curcumin in the diet.

[2] BWG= body weight gain

Treatments[1]	BWG[2] D40-49	BWG[2] D50-56	Feed intake D40-49	Feed intake D40-49
T1	1105.38 ± 29.43	837.78 ± 34.34	1981.3 ± 28.95	1631.67 ± 73.7
T2	1088.89 ± 49.74	821.07 ± 69.76	1877.97 ± 51.81	1618 ± 16.83
T3	1150.89 ± 36.69	944.54 ± 59.16	1900.38 ± 61.9	1718.34 ± 39.28
T4	1170 ± 42.77	814.6 ± 50.09	1968.52 ± 36.97	1708.25 ± 46.15

Table 10.2 illustrates the effects of treatments (curcumin supplementation and *Staphylococcus aureus* challenge) on dual-energy x-ray absorptiometry (DEXA) parameters on days 49 and 56. Letters not connected by same letter is significantly different ($P < 0.05$, N =6).

[1] T1, non-challenged treatment; Treatment 2 (T2) was challenged with *Staphylococcus aureus* at 10^9 CFU orally on days 42, 43, and 44; Treatment 3 (T3) was challenged with *Staphylococcus aureus* at 10^9 CFU orally on day 42, 43, and 44 respectively and 200 ppm of curcumin in the diet; Treatment 4 (T4) was challenged with *Staphylococcus aureus* at 10^9 CFU orally on day 42, 43, and 44 respectively and 400 ppm of curcumin in the diet.

[2] BMD= Bone mineral density in grams per square centimeter.

[3] BMC= Bone mineral content in grams.

Day 49					
Treatments[1]	BMD (g/cm2) [2]	BMC (g) [3]	Tissue (g)	Fat (g)	Lean (g)
T1	0.205 ± 0.004	55.64 ± 1.6253	3820.667 ± 53.2752	490.667 ± 27.0908	3329.834 ± 30.8669
T2	0.207 ± 0.0043	56.3 ± 1.5594	3845.667 ± 61.7008	514.167 ± 33.9327	3331.5 ± 53.7189
T3	0.198 ± 0.0048	54.75 ± 2.8277	3771.667 ± 92.3666	471.667 ± 39.3224	3300 ± 85.8037

T4	0.196 ± 0.0043	55.02 ± 1.945	3893.5 ± 80.6163	493.667 ± 11.8959	3399.834 ± 79.1402

Day 56

Treatments[1]	BMD (g/cm2) [2]	BMC (g) [3]	Tissue (g)	Fat (g)	Lean (g)
T1	0.183 ± 0.0048	56.22 ± 1.6903[ab]	4509.5 ± 104.617	425.667 ± 33.5039	4083.5 ± 97.1308
T2	0.176 ± 0.0042	52.067 ± 1.5954[b]	4428.167 ± 77.5218	499.334 ± 24.595	3928.334 ± 92.7397
T3	0.192 ± 0.0031	60.88 ± 1.609[a]	4625.5 ± 139.9357	452.667 ± 47.5119	4172.834 ± 144.2192
T4	0.187 ± 0.0076	61.6 ± 2.4443[a]	4649.334 ± 128.0864	508.834 ± 38.7526	4140.167 ± 132.4021

20

Figure 10.1 illustrates the effects of treatments (curcumin supplementation and *Staphylococcus aureus* challenge) on gait (A) and BCO scoring (B and C) on days 49 and 56. BCO= Bacterial chondronecrosis and osteomyelitis; T1, non-challenged treatment; Treatment 2 (T2) was challenged with *Staphylococcus aureus* at 10^9 CFU orally on days 42, 43, and 44; Treatment 3 (T3) was challenged with *Staphylococcus aureus* at 10^9 CFU orally on day 42, 43, and 44 respectively and 200 ppm of curcumin in the diet; Treatment 4 (T4) was challenged with *Staphylococcus aureus* at 10^9 CFU orally on day 42, 43, and 44 respectively and 400 ppm of curcumin in the diet. Letters not connected by same letter is significantly different ($P < 0.05$, N =6).

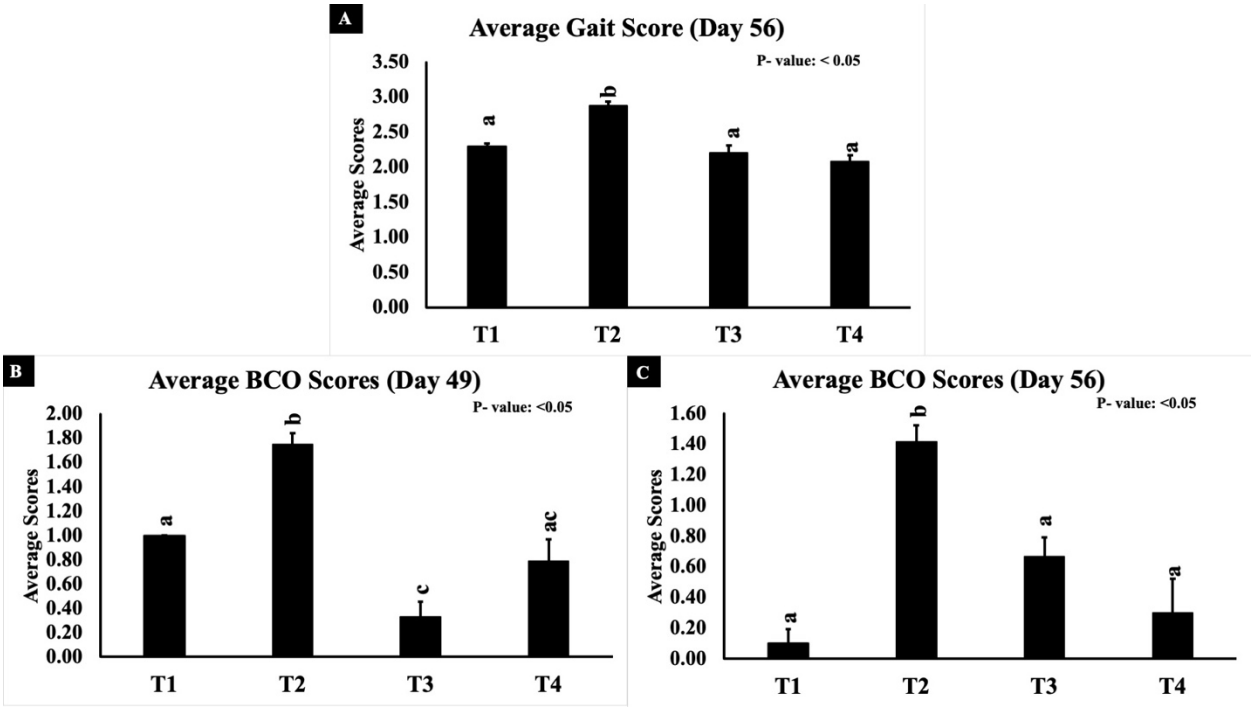

Figure 10.2 illustrates the effects of treatments (curcumin supplementation and *Staphylococcus aureus* challenge) on ceca (A, C) and bone (B, D) *Staphylococcus aureus* counts on days 49 and 56. T1, non-challenged treatment; Treatment 2 (T2) was challenged with *Staphylococcus aureus* at 10^9 CFU orally on days 42, 43, and 44; Treatment 3 (T3) was challenged with *Staphylococcus aureus* at 10^9 CFU orally on day 42, 43, and 44 respectively and 200 ppm of curcumin in the diet; Treatment 4 (T4) was challenged with *Staphylococcus aureus* at 10^9 CFU orally on day 42, 43, and 44 respectively and 400 ppm of curcumin in the diet. Letters not connected by same letter is significantly different ($P < 0.05$, N =6).

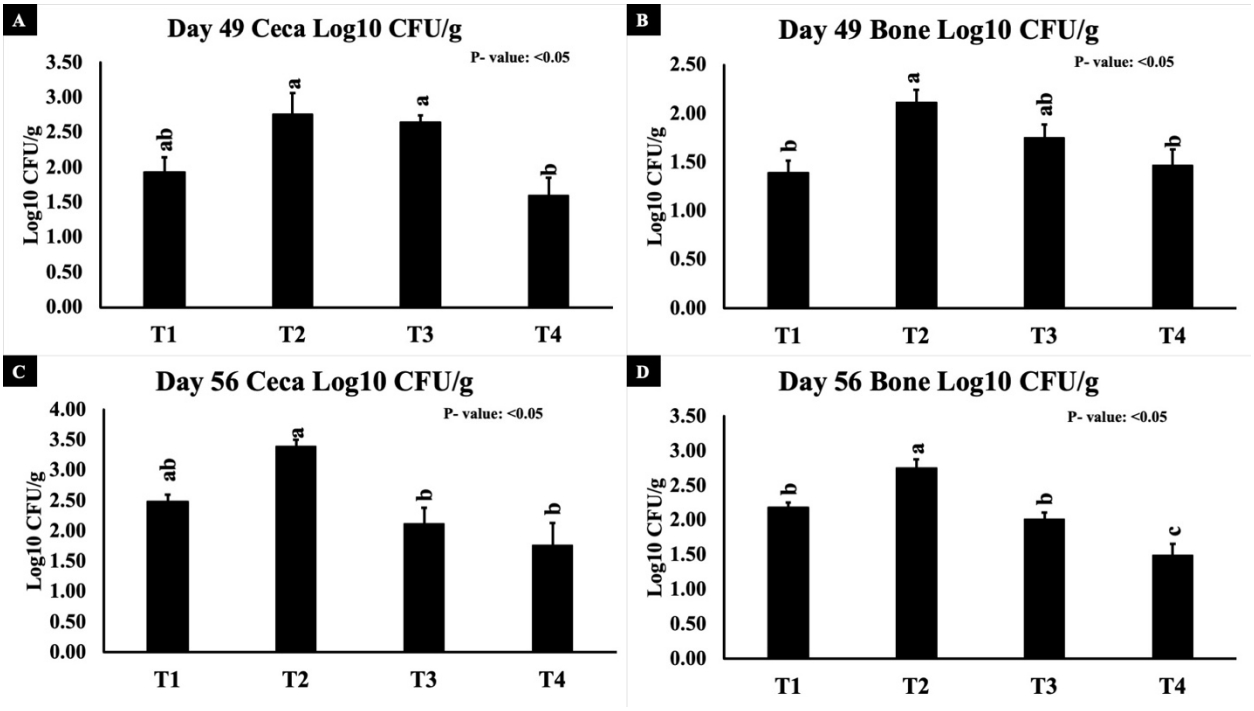

Figure 10.3 illustrates the effects of treatments (curcumin supplementation and *Staphylococcus aureus* challenge) on plasma lipopolysaccharides (LPS) (A and B) and sclerostin (SOST) (C) on days 49 and 56. T1, non-challenged treatment; Treatment 2 (T2) was challenged with *Staphylococcus aureus* at 10^9 CFU orally on days 42, 43, and 44; Treatment 3 (T3) was challenged with *Staphylococcus aureus* at 10^9 CFU orally on day 42, 43, and 44 respectively and 200 ppm of curcumin in the diet; Treatment 4 (T4) was challenged with *Staphylococcus aureus* at 10^9 CFU orally on day 42, 43, and 44 respectively and 400 ppm of curcumin in the diet. Letters not connected by same letter is significantly different ($P < 0.05$, N =6).

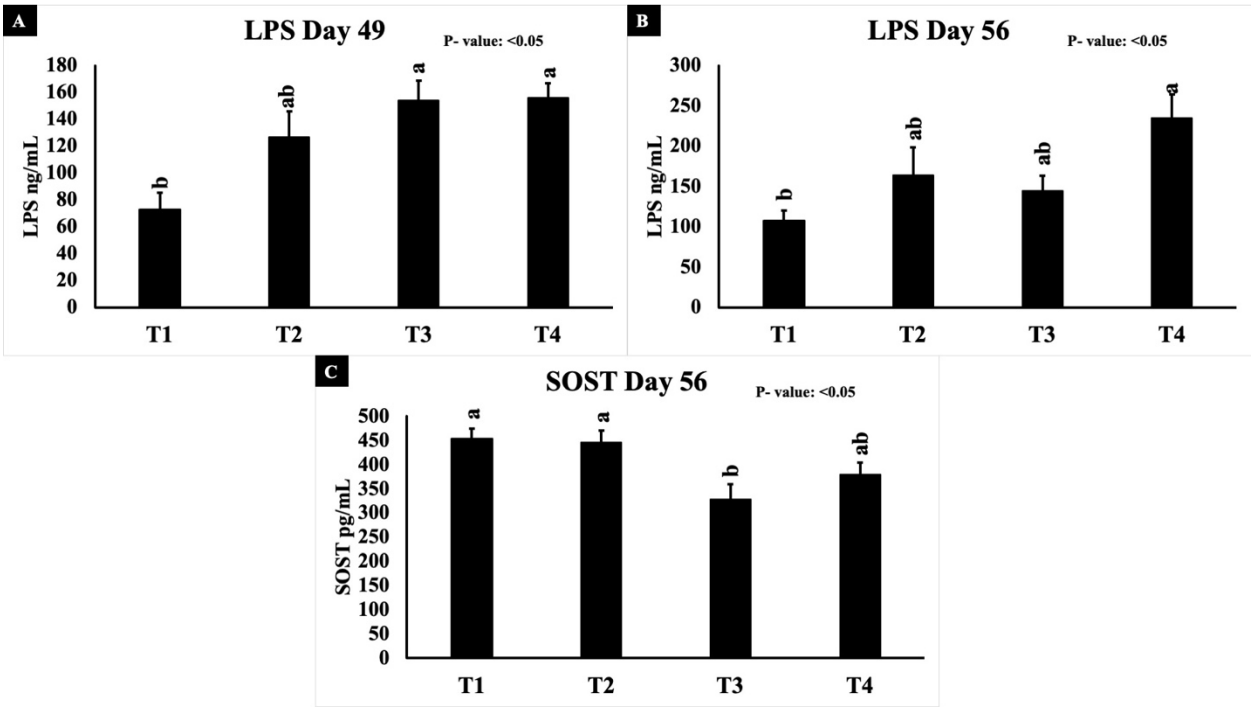

Figure 10.4 illustrates the effects of treatments (curcumin supplementation and *Staphylococcus aureus* challenge) on micro-computed tomography trabecular parameters like trabecular BMD (A), percent bone volume (B), total porosity (C), trabecular thickness (D), trabecular separation (E). BMD= bone mineral density; T1, non-challenged treatment; Treatment 2 (T2) was challenged with *Staphylococcus aureus* at 10^9 CFU orally on days 42, 43, and 44; Treatment 3 (T3) was challenged with *Staphylococcus aureus* at 10^9 CFU orally on day 42, 43, and 44 respectively and 200 ppm of curcumin in the diet; Treatment 4 (T4) was challenged with *Staphylococcus aureus* at 10^9 CFU orally on day 42, 43, and 44 respectively and 400 ppm of curcumin in the diet. Letters not connected by same letter is significantly different ($P < 0.05$, N =6).

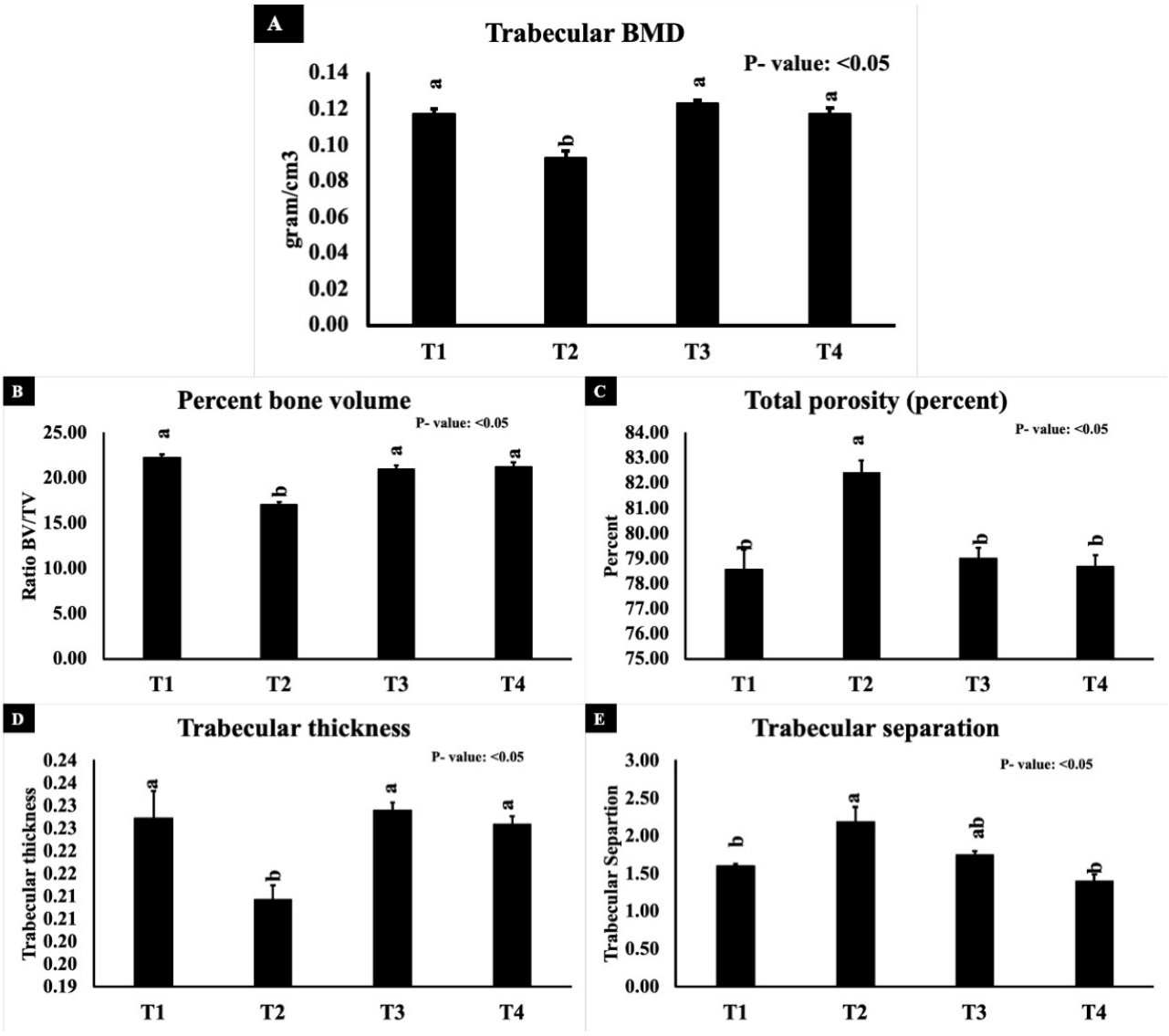
A
Trabecular BMD
P- value: <0.05
gram/cm3
0.14
0.12
0.10
0.08
0.06
0.04
0.02
0.00
a
b
a
a
T1
T2
T3
T4
B
Percent bone volume
P- value: <0.05
Ratio BV/TV
25.00
20.00
15.00
10.00
5.00
0.00
a
b
a
a
T1
T2
T3
T4
C
Total porosity (percent)
P- value: <0.05
Percent
84.00
83.00
82.00
81.00
80.00
79.00
78.00
77.00
76.00
75.00
b
a
b
b
T1
T2
T3
T4
D
Trabecular thickness
P- value: <0.05
Trabecular thickness
0.24
0.24
0.23
0.23
0.22
0.22
0.21
0.21
0.20
0.20
0.19
a
b
a
a
T1
T2
T3
T4
E
Trabecular separation
P- value: <0.05
Trabecular Separtion
3.00
2.50
2.00
1.50
1.00
0.50
0.00
b
a
ab
b
T1
T2
T3
T4

GENERAL CONCLUSION

This thesis establishes a comprehensive framework of experimental models and mechanistic insights into a leading cause of lameness, Bacterial Chondronecrosis and Osteomyelitis (BCO) in broilers. This major welfare and economic concern were deciphered using invitro and in ovo environment, where lipopolysaccharides (LPS) exposure showed inhibitory effects on osteogenic differentiation of mesenchymal stem cells (MSCs) and embryos in a dose-dependent manner. High LPS doses activated innate immune signaling and upregulated sclerostin (SOST), thereby inhibiting Wnt-signaling associated osteogenesis. In effect, disrupted bone homeostasis increasing osteoclastogenesis relative to osteoblastogenesis resulting weaker bones observed in late embryos. These invitro and embryonic LPS models provide critical mechanistic insights into systemic endotoxemia alone can trigger osteopathology following NF-κB/TNFα mediated inflammation and SOST-mediated Wnt inhibition.

Invivo co-challenge models demonstrated gut-bone axis interactions in BCO pathogenesis. Broilers given mixed *Eimeria* spp. infections and LPS suffered concerns with intestinal integrity and performance. This dual challenge also translated into disrupted skeletal development where the study revealed reduced bone mineral content, density, and trabecular bone compared to controls. Bone dynamic histomorphometry revealed elevated plasma SOST and disrupted bone formation under the combined stressors. Furthermore, TLR4 gene expression along with negative feedback modulation of NF-κB/ proinflammatory cytokine pathways, consistent with an active immune response. Synergistically, *Eimeria* infection and LPS-driven inflammation and endotoxemia, inhibited bone anabolism by increased SOST and osteoimmune mediators. These findings indicate effect of enteric disease on bone health, besides highlighting in ovo and co-challenge experiments as key tools to understand multifactorial etiology of BCO.

In vivo work on *Eimeria* and *Staphylococcus aureus* co-challenge unveiled direct link between intestinal health and BCO. Coccidial infection disrupted intestinal barrier, allowing *S. aureus* translocation and systemic endotoxemia (elevated plasma LPS) resulting in systemic inflammation, intestinal leakage, and increased sclerostin levels collectively reflected in decreased bone quality or compromised skeletal integrity. This model clearly shows that intestinal challenge and cascade of events during systemic inflammation act via loss of intestinal integrity allowing systemic entry of pathogens and LPS to activate inflammatory pathways and osteocytic SOST production, impairing bone health. The work also showed that dual infection shifts cecal microbiota. High dose of *S. aureus* with *Eimeria* exhibited marked reduction in microbial diversity besides increasing the taxa involved in inflammatory pathways with lower firmicutes to Bacteroidetes ratio.

Importantly, this thesis validated that direct *S. aureus* oral challenge or systemic inoculation induced BCO lesions and bone deficits. Repeated oral or systemic (intraperitoneal) challenge caused bacteremia and microbiome disruption along with inflammatory bone loss and suppressed Wnt signaling. This study suggests pathogen dose and route correlates with bone outcomes and highlights the relation between infection pressure and BCO risk. Together, *S. aureus* challenge models and LPS/*Eimeria* studies provided for understanding changes during induction of BCO. Importantly, mitigating inflammation and intestinal damage can preserve bone health and bird welfare.

Dietary Curcumin showed significant effects on *S. aureus* induced NCO where broilers fed with 200 and 400 ppm had higher bone mineral content and improved trabecular architecture despite challenge. Curcumin also reduced *S. aureus* colonization and gait or BCO lesion scores. This implies better welfare and productivity. Mechanistically, curcumin lowered plasma SOST

levels which reflects counteracting the Wnt-suppressive effect. This suggests that a practical intervention supports bone anabolism during infection. Collectively, it becomes clear that maintaining intestinal integrity and modulating inflammatory pathways can break infection-inflammation cycle that drives BCO. Implementing such measures in commercial settings could alleviate lameness and improve production efficiency.

In conclusion, this thesis has established and validated multiple experimental models of BCO which highlights underlying pathophysiology. MSC and embryo LPS models revealed osteoimmune mechanisms behind aberrations of bone homeostasis. *Eimeria* and *S. aureus* co-challenge models revealed a critical gut-bone axis where enteric challenge and altered microbiome that affects bone growth and facilitates colonization of *S. aureus* in the bone. Finally, the curcumin trial demonstrated an important mitigation strategy that protects bone health from threatening sequalae of BCO challenge. These contributions advance fundamental and applied poultry science by offering reproducible challenge conditions for testing interventions, molecular targets for nutritional immunology or genetics.